

Universidade de Lisboa
Faculdade de Farmácia



Dissolution of Dry Powder Inhaler formulations:
in vitro / in vivo correlations

Beatriz Noriega Fernandes

Orientadoras: Doutora Maria Luísa Teixeira de Azevedo Rodrigues Corvo
Doutora Eunice Margarida Santos Costa

Tese especialmente elaborada para a obtenção do grau de Doutor em Farmácia, Tecnologia Farmacêutica.

2022

Universidade de Lisboa
Faculdade de Farmácia



Dissolution of Dry Powder Inhaler formulations:
in vitro / in vivo correlations

Beatriz Noriega Fernandes

Orientadoras: Doutora Maria Luísa Teixeira de Azevedo Rodrigues Corvo
Doutora Eunice Margarida Santos Costa

Tese especialmente elaborada para a obtenção do grau de Doutor em Farmácia, Tecnologia Farmacêutica.

Júri:

Presidente: Doutor António José Leitão das Neves Almeida

Vogais:

- Doctor Per Gerde, Associate Professor, Institute of Environmental Medicine, Karolinska Institutet, Sweden;
- Doutora Ana Margarida Moutinho Grenha, Professora Auxiliar da Universidade do Algarve;
- Doutora Helena Isabel Fialho Florindo Roque Ferreira, Professora Associada com Agregação, Faculdade de Farmácia da Universidade de Lisboa;
- Doutora Maria Luísa Teixeira de Azevedo Rodrigues Corvo, Investigadora Auxiliar, Faculdade de Farmácia da Universidade de Lisboa, Orientadora;
- Doutora Constança Filomena Cacela Pesqueira da Silva, na qualidade de individualidade de reconhecida competência.

The research presented in this thesis was conducted at BioNanoSciences – Drug Delivery and Immunoengineering (BioNanoSci), Research Institute of Medicines (iMed.Ulisboa), Faculty of Pharmacy, University of Lisbon, Portugal, under the scientific supervision of Maria Luísa Teixeira de Azevedo Rodrigues Corvo, PhD, and at the Inhalation and Advanced Drug Delivery, Drug Product Development Group at Hovione Farmaciência SA, Loures under the scientific supervision of Eunice Margarida Santos Costa, PhD. The research was funded by Fundação para a Ciência e a Tecnologia, IP (FCT project UID/DTP/04138/2020 and UIDP/04138/2020) and Hovione Farmaciência SA.

Para a minha família.

Agradecimentos

Começo por agradecer à minha orientadora académica, Professora Luisa Corvo, e à empresarial, Eunice Costa, pela oportunidade de integrar um doutoramento em empresa com a Faculdade de Farmácia da Universidade de Lisboa em conjunto com a Hovione Farmaciência. Pelo apoio e motivação constantes, sobretudo nos momentos mais difíceis. Obrigada por não desistirem, e por serem exemplos a seguir.

I would like to thank the Inhalation Sciences team, in specific Maria Malmjöf, Mattias Nowenwik and Per Gerde, for the warm welcome to the cold Sweden and for the insightful scientific and culinary discussions.

João Henriques, obrigada pela perspetiva fresca, por tornares o desafio mais leve, e por toda a paciência.

A todos com os quais trabalhei na Hovione, agradeço tudo o que fui aprendendo nesta jornada. Aos colegas da faculdade de farmácia, o carinho com que me acolheram nas minhas visitas à sala dos bolseiros.

Agradeço a todo o (antigo) grupo do DPD, pela ciência e resolução de problemas, claro, mas sobretudo pelos vídeos de Natal.

Todos os alunos e estagiários que passaram pela Eureka, ou perto dela, obrigada pela companhia e banda sonora. Em especial, Beatriz, Cláudia, Diana, MIL, Marianna, Marina, Nuno, Lucia e Tiago, pelas aventuras em roadtrips, acampamentos, noites de jogos e de outras coisas. Por serem pilares neste caminho em conjunto.

A todos os meus amigos, um grande obrigada. Aos meus amigos de sempre – Tiago, Susana, Coxixo, Margarida e Vigas, por serem a minha companhia alentejana há tantos anos. Aos meus amigos do coração – Ana Maria, Alexandre, Rita, Eddie e Ricardo, obrigada por estarem sempre perto, mesmo do outro lado do mundo. Obrigada ao António que foi essencial para me mostrar que a vida é muito mais que o PhD, e tudo se resolve com uma viagem, um jantar e/ou um bom copo de vinho. Obrigada ao

Rodrigo, que planeou, descomplicou, apoiou, amparou e me deu a força que precisava para acreditar que era possível.

Para a minha família o maior obrigada, sem vocês nada disto era possível. Obrigada Victor, Pai e Mãe, por um amor e apoio que nunca conseguirei pagar.

Abstract

Orally inhaled drug delivery has been the preferred route to deliver locally acting drug substances (DS) to the lung for conditions such as asthma, chronic obstructive pulmonary disease (COPD) or infections, as the local delivery allows for rapid onset action while minimizing side effects. More recently, inhalation to the lung has been used as a path for systemic delivery for small and large molecules due to the large surface area of absorption and the avoidance of first path metabolism. The development of formulations for pulmonary delivery relies on aerodynamic performance *in vitro* characterization by cascade impaction, with output parameters such as the total emitted dose from the device or the dose capable of reaching the deep lung, the fine particle dose, with an aerodynamic diameter below 5 μm . It is acknowledged the DS action is dependent not only on the delivered dose, but also on dissolution and absorption kinetics of the deposited particles, nonetheless there is not a standardized globally accepted method to assess dissolution and/or absorption on the lung, mostly due the challenges of mimicking such environment – particle agglomerates deposition on an extremely large area of stagnant and thin lining fluid with a complex composition. Hence, the present research aims to develop, optimize, and explore different strategies to assess the dissolution and absorption kinetics of dry powder inhaler (DPI) formulations, from a quality control – QC – perspective, with strategies based on pre-existing compendial methodologies, and from a biorelevant performance prediction perspective, with the application of a newly developed breath simulator coupled with a biorelevant dissolution system.

Several combinations of standard cascade impactors and the United States Pharmacopeia (USP) dissolution apparatus are analyzed regarding critical method parameters. Ultimately, these resulted in reproducible methods capable of differentiating carrier-based and carrier-free DPI formulations of low and high solubility DS. In particular, the combination of the fast screening impactor with the USP apparatus II was validated by testing DS of different solubilities, and although far from mimicking the particle deposition and dissolution in the lung, was rendered suitable as a QC and formulation screening strategy at an early development stage.

Aiming for a more biorelevant approach capable to predict *in vivo* therapeutic effect more reliably, a more complex system combination, the breath simulator PreciseInhale® and the dissolution apparatus

DissolvIt® is optimized and used. This methodology proved to differentiate distinct particle engineering technologies, formulation approaches and used excipients by assessing particle deposition, dissolution, and absorption for low and high solubility DS, using a commercial product as benchmark. Moreover, the DissolvIt® system generates pharmacokinetic-like dissolution profiles which can be used as input parameters for physiologically based pharmacokinetic (PBPK) modelling. Hence, this biorelevant approach is suitable for formulation selection in later stages of pre-clinical or early clinical development and for de-risking generic development.

Overall, the present work suggests deposition and dissolution testing can be an essential tool for DPI development, but collaborative efforts of academia, pharmaceutical industry and regulatory bodies are still required to overcome remaining challenges.

Keywords: dry powder inhaler, lung dissolution, pulmonary drug delivery, in vitro dissolution method, carrier-based formulation, carrier-free formulation

Resumo

A administração de substâncias ativas (SA) pela via pulmonar tem especial interesse no tratamento de doenças respiratórias como asma, doença pulmonar obstrutiva crónica (DPOC) ou infeções, uma vez que permite uma ação rápida com efeitos secundários reduzidos. Mais recentemente, a via pulmonar tem sido utilizada para tratamentos sistémicos com moléculas de pequenas e grandes dimensões, devido à grande superfície de absorção e ao *by-pass* do metabolismo da primeira passagem. O desenvolvimento de formulações inaláveis é suportado pela caracterização do desempenho aerodinâmico *in vitro* utilizando impactores em cascata, com indicadores de desempenho tais como a dose total emitida pelo dispositivo ou a dose capaz de atingir as vias respiratórias profundas, a dose de partículas finas, com um diâmetro aerodinâmico inferior a 5 µm. Reconhece-se que a ação da SA depende não só da dose fornecida, mas também da cinética de dissolução e absorção das partículas depositadas; no entanto, não existe um método padronizado globalmente aceite para avaliar a dissolução e/ou absorção no pulmão, principalmente devido aos desafios de imitar tal ambiente - a deposição de aglomerados de partículas numa área extremamente grande de fluido de revestimento estagnado e fino com uma composição complexa. Assim, a presente investigação visa desenvolver, otimizar e explorar diferentes estratégias para avaliar a cinética de dissolução e absorção de formulações de inaladores de pó seco, de uma perspetiva de controlo de qualidade, com estratégias baseadas em metodologias compendiais pré-existentes, e de uma perspetiva de previsão de desempenho biorrelevante, com a aplicação de um simulador de respiração recentemente desenvolvido, acoplado a um sistema de dissolução biorrelevante.

Foram analisadas várias combinações de impactores padrão em cascata com *apparatus* de dissolução compendiais, avaliando os parâmetros críticos do método. Em última análise, estes resultaram em métodos reprodutíveis capazes de diferenciar formulações de pós secos para inalação compostas por SAs de baixa e alta solubilidade com diferentes excipientes, tornando-os adequados para controlo de qualidade (QC) e *screening* de formulações numa fase precoce de desenvolvimento.

Visando uma abordagem mais biorrelevante capaz de prever de forma mais fiável o efeito terapêutico *in vivo*, é otimizado e utilizado um sistema mais complexo que combina o simulador de inspiração,

PreciseInhale®, com um dissolutor, DissolvIt®. Esta metodologia mostra ser capaz de diferenciar o impacto de diferentes tecnologias de engenharia de partícula, estratégias de formulação e excipientes, avaliando a deposição, dissolução e absorção de SAs de baixa e alta solubilidade, utilizando um produto comercial como referência. Adicionalmente o sistema DissolvIt® tem como output parâmetros semelhantes aos farmacocinéticos que podem ser usados como na modelação de farmacocinética de base fisiológica (PBPK). Assim, a abordagem biorrelevante é aplicável em estágios avançados de desenvolvimento, de pré-clínico à fase inicial de ensaios clínico, assim como uma ferramenta de mitigação de risco no desenvolvimento de genéricos

Globalmente, o presente trabalho sugere que os testes de deposição e dissolução podem ser uma ferramenta essencial no desenvolvimento de inaladores de pó seco, mas ainda são necessários esforços colaborativos do meio académico, da indústria farmacêutica e dos organismos reguladores para superar este desafio.

Palavras-chave: inaladores de pó seco, dissolução no pulmão, administração de fármacos pulmonares, métodos de dissolução *in vitro*, formulação com/sem transportadores

Table of contents

| | |
|---|-------------|
| AGRADECIMENTOS | V |
| ABSTRACT | VII |
| RESUMO | IX |
| TABLE OF CONTENTS | XI |
| LIST OF FIGURES | XVI |
| LIST OF TABLES | XXII |
| LIST OF ABBREVIATIONS | XXVI |
| | |
| 1 CHAPTER 1 | 1 |
| | |
| INTRODUCTION | |
| 1.1 MOTIVATION | 2 |
| 1.2 RESEARCH AIMS AND OBJECTIVES | 4 |
| 1.3 THESIS OUTLINE | 5 |
| 1.4 REFERENCES | 7 |
| | |
| 2 CHAPTER 2 | 8 |
| | |
| DRY POWDER FOR INHALATION BACKGROUND: GATHERING FURTHER INSIGHTS THROUGH DISSOLUTION | |
| 2.1 PULMONARY DRUG DELIVERY AT A GLANCE | 9 |
| 2.1.1 Why inhalation | 9 |
| 2.1.2 Devices and inhalation products | 11 |
| 2.2 TOWARDS BIORELEVANT COLLECTION AND DISSOLUTION | 21 |
| 2.2.1 Physiological advantages of the lung as a delivery route | 21 |
| 2.2.2 Physiological disadvantages optimization requirements | 22 |

| | | |
|-------|--------------------------------------|----|
| 2.2.3 | From actuation to deposition | 26 |
| 2.2.4 | Dissolution or inhaled drug products | 34 |
| 2.3 | FORMULATION PLATFORMS | 49 |
| 2.3.1 | Carrier-based formulations | 49 |
| 2.3.2 | Engineered carrier-free particles | 55 |
| 2.4 | REFERENCES | 57 |

3 CHAPTER 3 71

PADDLE OVER DISK

DEVELOPMENT AND COMPARISON OF COLLECTION AND DISSOLUTION STRATEGIES FOR

FLUTICASONE PROPIONATE

| | | |
|-------|---|-----|
| 3.1 | SUMMARY | 73 |
| 3.2 | INTRODUCTION | 74 |
| 3.3 | FORMULATION MANUFACTURE AND CHARACTERIZATION | 77 |
| 3.3.1 | Outline | 77 |
| 3.3.2 | Materials and Methods | 77 |
| 3.3.3 | Results and discussion | 80 |
| 3.3.4 | Conclusions | 84 |
| 3.4 | PADDLE OVER DISK TO DIFFERENTIATE FORMULATIONS – PROOF OF CONCEPT | 85 |
| 3.4.1 | Outline | 85 |
| 3.4.2 | Materials and Methods | 85 |
| 3.4.3 | Results and discussion | 89 |
| 3.4.4 | Conclusions | 92 |
| 3.5 | PADDLE OVER DISK CRITICAL METHOD PARAMETERS AND LIMITATIONS | 93 |
| 3.5.1 | Outline | 93 |
| 3.5.2 | Impact of fluticasone propionate load and temperature | 93 |
| 3.5.3 | Impact deposition strategy using the next generation impactor | 98 |
| 3.5.4 | Fast screening impactor as an innovative collection strategy | 102 |

| | | |
|----------|---|------------|
| 3.5.5 | Conclusions | 109 |
| 3.6 | ANALYTICAL QUALITY BY DESIGN APPROACH FOR USP APPARATUS IV DISSOLUTION METHOD DEVELOPMENT | 111 |
| 3.6.1 | Outline | 111 |
| 3.6.2 | Rational | 111 |
| 3.6.3 | Materials and methods | 112 |
| 3.6.4 | Results and discussion | 116 |
| 3.6.5 | Conclusions | 120 |
| 3.7 | SAMPLE COLLECTION & DISSOLUTION APPARATUS BENCHMARK AND CONCLUSIONS | 121 |
| 3.8 | BIBLIOGRAPHY | 124 |
| 4 | CHAPTER 4 | 128 |

PRECISEINHALE® AND DISSOLVIT®

DRY POWDER INHALER FORMULATION COMPARISON: STUDY OF THE ROLE OF PARTICLE

DEPOSITION PATTERN AND DISSOLUTION

| | | |
|-------|---|-----|
| 4.1 | SUMMARY | 130 |
| 4.2 | INTRODUCTION | 131 |
| 4.3 | INFLUENCE OF A NEWLY DESIGNED PRE-SEPARATOR FOR PARTICLE COLLECTION | 135 |
| 4.3.1 | Outline | 135 |
| 4.3.2 | Materials and methods | 135 |
| 4.3.3 | Results and Discussion | 140 |
| 4.3.4 | Conclusions | 145 |
| 4.4.1 | Outline | 146 |
| 4.4.2 | Materials and methods | 146 |
| 4.4.3 | Results | 152 |
| 4.4.4 | Discussion | 163 |
| 4.4.5 | Conclusion | 168 |
| 4.5 | REFERENCES | 170 |

DISSOLUTION METHOD COMPARISON AND VALIDATION WITH SALMETEROL XINAFOATE

| | | |
|-------|---|-----|
| 5.1 | SUMMARY | 175 |
| 5.2 | INTRODUCTION | 176 |
| 5.3 | MATERIALS AND METHODS | 178 |
| 5.3.1 | Materials | 178 |
| 5.3.2 | Formulation manufacture | 178 |
| 5.3.3 | Solubility assessment | 179 |
| 5.3.4 | Milled salmeterol xinafoate and formulation characterization | 179 |
| 5.3.5 | Dissolution testing | 181 |
| 5.3.6 | Statistical analysis | 184 |
| 5.4 | SALMETEROL CARRIER-BASED FORMULATIONS CHARACTERIZATION | 185 |
| 5.4.1 | Particle size distribution by laser diffraction | 185 |
| 5.4.2 | Aerodynamic characterization by Next Generation Impactor | 185 |
| 5.4.3 | Aerodynamic characterization by Marple Cascade Impactor | 188 |
| 5.5 | PADDLE OVER DISK METHODOLOGY VALIDATION FOR A HIGH SOLUBILITY DRUG SUBSTANCE: SALMETEROL XINAFOATE | 191 |
| 5.5.1 | Outline | 191 |
| 5.5.2 | Experimental design | 191 |
| 5.5.3 | Results and discussion | 193 |
| 5.5.4 | Conclusions | 200 |
| 5.6 | DISSOLVIT® METHOD VALIDATION FOR A HIGH SOLUBILITY DRUG SUBSTANCE: SALMETEROL XINAFOATE | 202 |
| 5.6.1 | Outline | 202 |
| 5.6.2 | Experimental design | 202 |
| 5.6.3 | Results and discussion | 203 |
| 5.6.4 | Conclusions | 212 |

5.7 BIBLIOGRAPHY 213

6 CHAPTER 6 217

SUMMARY, FINAL REMARKS AND FUTURE WORK

List of figures

| | |
|--|----|
| Figure 2.1 - Number of published papers from 2010 to 2020 containing the words indicated in the legend as part of the title or abstract. Data obtained using linked research knowledge system Dimensions (https://app.dimensions.ai/). _____ | 14 |
| Figure 2.2 - Steps towards establishing therapeutic equivalence (TE) between a reference and a generic inhalation product according to the FDA and EMA guidelines. PD – pharmacodynamic. _____ | 19 |
| Figure 2.3 - Respiratory tract representation with lung division according to the Weibel model. GEN – generation; NR – number. _____ | 24 |
| Figure 2.4 - Schematic of the three major deposition mechanisms for inhaled particles in the respiratory tract and its relationship to particle impaction in a cascade impactor. The grey arrows show the direction of air flow. Adapted from (Dalby et al., 2009) _____ | 29 |
| Figure 2.5 - Example of an aerodynamic particle size distribution plotted as a frequency distribution (grey) or as a cumulative one (black line). Mass median aerodynamic diameter (MMAD) and fine particle fraction (FPF) are indicated in the distribution. Adapted from (S. Newman, 2009). _____ | 30 |
| Figure 2.6 - Left: Andersen cascade impactor fitted with an induction port; right: stages, plates and pre-separator. _____ | 32 |
| Figure 2.7 - Right: Next generation impactor (NGI)'s particle collection cups; Left: NGI with pre-separator and induction port. _____ | 33 |
| Figure 2.8 – Fast screening impactor (FSI) fitted with an induction port and pre-separator, including fine cut insert and filter holder. _____ | 34 |
| Figure 2.9 - Biopharmaceutical classification system. _____ | 37 |
| Figure 2.10 – Parameters considered in the inhalation biopharmaceutical classification system. ____ | 38 |
| Figure 2.11- Schematic representation of UPS apparatus I (left) and II (right). _____ | 40 |
| Figure 2.12 - Paddle dissolution apparatus used in combination with the next generation impactor. A – Securing ring of the membrane holder; B – stainless steel collector; C – Dissolution cup; D – NGI with dissolution cup after actuation. Right: Dissolution vessel with membrane holder. Adapted from (Fernandes et al., 2016a) _____ | 40 |
| Figure 2.13 - Schematic representation of the powder securing strategy used by (May et al., 2012) _____ | 42 |
| Figure 2.14 - Schematic representation of the UniDose™ collection system, from (Farias et al., 2017). _____ | 43 |
| Figure 2.15 - Schematic representation of the USP apparatus IV operating A) as an open and B) as a closed system. _____ | 43 |

| | |
|--|----|
| Figure 2.16 – Dissolution cell designed by Davies and Feddah, adapted from (Davies and Feddah, 2003). (A) stainless steel filter holders; (B) Teflon rings, (C) stainless steel screen support filters; (D) a 0.45µm pore size cellulose acetate membrane filters; (E) glass fibre filter containing the drug particles. | 44 |
| Figure 2.17 – (A) Franz cell dissolution apparatus from (May et al., 2012); (B) Transwell® system dissolution apparatus from (Arora et al., 2010). | 46 |
| Figure 2.18 – Schematic representation of the DissolvIt® system, adapted from (Gerde et al., 2017a). | 47 |
| Figure 2.19 - Schematic of PreciseInhale® actuation and glass holding. | 47 |
| Figure 2.20 - SEM images of the deposited aerosols at magnifications- (A) budesonide, (B) fluticasone propionate. From (Gerde et al., 2017a). | 48 |
| Figure 2.21 - Schematic illustration of a carrier-based formulation manufacture. | 49 |
| Figure 2.22 - Schematic representation of the spiral jet milling process. | 52 |
| Figure 2.23 - Schematic representation of the hypothesis of the occupation of areas of high adhesion by fine excipient particles. | 54 |
| Figure 2.24 – Schematic representation of the hypothesis of formation of agglomerates with drug and fine excipient particles (multiplets) during blending. | 55 |
| | |
| Figure 3.1 - SEM micrographs for carrier-based formulation FPJ1 (A and B) x300 and x1000 respectively; and for spray-dried composite formulations containing trehalose CF1 (C and D) and raffinose CF2 (E and F), x1000 and x 10 000 respectively; at 20 kV. | 81 |
| Figure 3.2 - Aerodynamic characterization of (A) the carrier-based formulation containing 1% of jet milled fluticasone propionate (FP) (white), composite particle containing trehalose (striped bars) and raffinose (dotted bars), capsules of 12.5 mg, and (B) the carrier-based formulation containing 1% of jet milled FP (white), the carrier-based formulation containing 1% of wet polished FP (striped bars), capsules of 20.0 mg, determined by Next Generation Impactor. Data expressed as mean ± SD (n=3). MPA: mouth piece adapter; IP: induction port; MOC: micro-orifice collector. Stage 1 - 7: | 82 |
| Figure 3.3 – Schematic representation of samples collection and preparation using the Next Generation Impactor prior to dissolution using the Paddle over disk apparatus. NGI schematic from Copley brochure. | 86 |
| Figure 3.4 - Dissolution profile of the carrier-free formulation of fluticasone propionate containing trehalose, CF1 (□) containing raffinose, CF2 (Δ), and of the carrier-based formulation, FPJ1 blend (○) in A) the paddle over disk apparatus and B) for the bulk formulation. Each profile is given by two replicates. Lines were fitted with Weibull model. | 90 |
| Figure 3.5 – Paddle over disk dissolution profiles of fluticasone propionate for the carrier-based formulation containing 1% of jet milled fluticasone propionate (FPJ1 blend); Weibull model fitting for 7 | |

| | |
|--|-----|
| (■, —), 10 (▲, ...) and 13 (●, - - -) actuations, with a Td of 73, 339 and 160 min, respectively. A) first 60 minutes; B) 5 hours of dissolution. n=2 | 96 |
| Figure 3.6 – Schematic representation of the proposed mechanism for particle deposition and bouncing after NGI actuation (Fernandes et al., 2016b). | 97 |
| Figure 3.7 – Dissolution profiles of fluticasone propionate showing A) Temperature influence using paddle over disk for powder collected using the next generation impactor; Weibull model fitting for 37 (○, —) and 32 (●, - - -) °C, with a Td of 339 and 1333 min, respectively. B) Temperature influence using UPS apparatus II for bulk powder; Weibull model for 37 (○, —) and 32 (●, - - -) °C, with a Td of 0.5 and 76 min respectively. n=2. | 98 |
| Figure 3.8 - Schematic representation of the powder collection procedure with the rotating disk methodology. Adapted from (Noriega et al., 2018b). | 99 |
| Figure 3.9 - Dissolution cup coupled with dissolution disk, after actuating the powder without (A), with disk rotation after 7 actuations (B), and with disk rotation after 13 actuations (C). | 100 |
| Figure 3.10 - Dissolution profiles of the carrier-based 1% (w/w) of jet milled fluticasone propionate formulation (FPJ1 blend) for 7 (full circle) and 13 (empty circle) actuations, without (black) and with (red) disk rotations. Markers represent time points of individual vessels; the line is the average of the duplicates. Comparison with normal set-up (A) and rotating disk (B); comparison between set-ups after 7 (C) and 13 (D) actuations. | 101 |
| Figure 3.11 - Schematic representation of the Fast Screening Impactor (FSI). PS – pre-separator; APSD – aerodynamic particle size distribution. | 103 |
| Figure 3.12 – Schematic representation of powder collection using the fast screening impactor (FSI) filter followed by holding with the next generation impactor (NGI) stainless still collector. | 104 |
| Figure 3.13 - Sample preparation steps from fast screening impactor to the dissolution vessel. A- filter after fast screening impactor actuation; B- filter punching to 55 mm diameter; C – punched filter and outer ring; and D – filter in dissolution vessel on the disk covered with a polycarbonate membrane. | 105 |
| Figure 3.14 - SEM images of the particles collected using the next generation impactor, at A) a low and B) high particle density area; and C) collected using the fast screening impactor. | 107 |
| Figure 3.15 – Dissolution profiles of fluticasone propionate obtained with the paddle over disk apparatus with the fast screening impactor as a collection method for FPJ2 blend (carrier-based with 1 % jet milled fluticasone propionate) and FPW blend (carrier-based with 1% wet polished fluticasone propionate). Comparison of individual dissolution profiles for FPJ2 blend (A) and FPW blend (B); total amount dissolved in the legend; (C) comparison of FPJ2 blend (---) with FPW blend (—), data expressed as mean ± SD (n=3). | 109 |
| Figure 3.16 - Schematic representation of the combination of fast screening impactor with USP Apparatus IV. | 113 |
| Figure 3.17 – Picture of powders and granulates dissolution cell and schematic representation of the tested membrane configurations. | 114 |

| | |
|--|-----|
| Figure 3.18 – Dissolution profiles of fluticasone propionate obtained with USP apparatus IV after collection with the fast screening impactor for formulation FPJ2 blend (carrier-based with 1 % jet milled fluticasone propionate) as individual dissolution profiles. Profiles generated with set-up 1, folded complete filter (●); profiles with set-up 2, folded punched filter fitted with a stopper (○); and profiles with set-up 3, punched filter folded once and rolled into a cylinder (■). | 116 |
| Figure 3.19 - Model terms effect on (1) difference between replicates (2) time of 50% of dissolution and (3) fraction dissolved at 300 min. A= volume, B= flow, C= actuations | 117 |
| Figure 3.20 - 2D Contour plots for each attribute. Top: time (min) needed to dissolve 50 % of the drug substance (DS), and bottom: fraction of DS dissolved after 300 min. | 118 |
| Figure 3.21 - Method Operable Design Region (MODR) representation. Blue: maximize dissolution at 300 min (goal minimum 0.95 min); yellow: time needed to dissolve 50% (target 20-40 min). NOR - Normal Operating Region. | 119 |
| Figure 4.1 - Schematic of the newly designed PS. From (Noriega et al., 2018a). | 136 |
| Figure 4.2 - Dissolution chamber set up. Left: coated coverslip on Preciselnhale® after actuation; right: dissolution chamber in place in the DissolvIt® equipment with zoom in to the dissolution chamber layers, from glass to perfusate. Adapted from (Noriega et al., 2019) | 138 |
| Figure 4.3 - Deposition pattern on coverslips of the Flixotide Diskus without (A) and with (B) the pre-separator (PS), and Pulmicort Flexaher without (C) and with the PS (D), after actuation using the Preciselnhale®, obtained by light microscopy with a x20 objective | 141 |
| Figure 4.4 – Scanning electron microscopy images of the deposited aerosols from Flixotide Diskus (1), with pre-separator after 5 actuations (A1,B1) and without after 1 (C2,D2); and from Pulmicort Flexhaler (2), with pre-separator after 7 actuations (A2,B2) and without after 3 actuations (C2,D2). The scale represents 30 µm for figures A1, C1, A2 and C2, and 1 µm for figures B1, D1, B2 and D2. | 142 |
| Figure 4.5 - Dissolution profiles obtained using DissolvIt® (n=3), as a fraction retained in the dissolution system for (A) the Flixotide Diskus containing fluticasone propionate (FP) and (B) the Pulmicort Flexhaler containing budesonide (BD); and as a fraction of total recovered (%/mL) for (C) the Flixotide Diskus and (D) the Pulmicort Flexhaler, with (dotted line) and without (full line) the pre-separator. All results normalized to the total deposited dose. Data expressed as mean ± SD (n=3). | 144 |
| Figure 4.6 - Schematic of Preciselnhale® actuation- and glass deposition cycles. I – the DPI is actuated with a flow rate of 40 L/min, passing through the induction port (IP) and the pre-separator (PS); II – the coarser particles impact and deposit on the IP and PS, the finer particles expand in the glass deposition chamber; III – the finer particles are collected on the coverslips. Adapted from (Noriega et al., 2018a). | 149 |
| Figure 4.7 - Aerodynamic characterization of the fluticasone propionate formulations containing jet milled particles (white) and wet polished particles (stripes), determined by Next Generation limpactor. Data expressed as mean ± SD (n=3). MPA: mouth piece adapter; MOC: micro-orifice collector. | 153 |

Figure 4.8 - Particle-size distribution as normalized mass frequency determined by Marple Cascade Impactor A –carrier-based formulations with jet milled fluticasone (FPJ blend), wet polished fluticasone (FPW blend) and commercial Flixotide Diskus; B – particle micronized by jet milling (FP JM) and wet polishing (FP WP); C – Composite formulation and the commercial Flixotide Diskus. Data expressed as mean \pm SD (n=3). MMAD - Median mass aerodynamic diameter, GSD – Geometric standard deviation _____ 155

Figure 4.9 - Deposition pattern on coverslips of the jet milled fluticasone propionate (FP) particles (A) and wet polished FP particles (B); and carrier-based formulation containing jet milled FP (C), carrier-based formulation containing wet polished FP (D), and composite formulation (E) and the commercial Flixotide Diskus (F), after actuation using the PreciseInhale[®], obtained by light microscopy with a x20 objective. _____ 156

Figure 4.10 – SEM images of the of the jet milled fluticasone propionate (FP) particles (A) and wet polished FP particles (B); and carrier-based formulation containing jet milled FP (C), carrier-based formulation containing wet polished FP (D), and composite formulation (E), and the commercial Flixotide Diskus (F), after actuation using the PreciseInhale[®]. _____ 158

Figure 4.11 - Dissolution profiles obtained using DissolvIt[®] (n=3), as a fraction of total recovered (%/mL). A – comparison of the prepared carrier-based formulations with jet milled fluticasone (FPJ blend) and wet polished fluticasone (FPW blend) with the commercial carrier-based product Flixotide Diskus; B - comparison of the micronization technologies jet milling (FP JM) and wet polishing (FP WP) with the commercial Flixotide Diskus; C – Comparison of the composite formulation with the FPJ blend formulation. All results normalized to the total deposited dose. Data expressed as mean \pm SD (n=3). _____ 160

Figure 4.12 – Dissolution performance parameters. A - Maximum concentration (C_{max}) as a fraction of total recovered (%/mL) and B – Dissolution extent (% of total recovered), for each formulation compared with the commercial Flixotide Diskus (one-way student's t-Test* $p < 0.02$ and ** $p < 0.008$). Data expressed as mean \pm SD (n=3). _____ 162

Figure 5.1 - Aerodynamic characterization of the salmeterol xinafoate formulations containing jet milled particles (white) and wet polished particles (stripes), determined by Next Generation Impactor. Data expressed as mean \pm SD (n=3). MPA: mouthpiece adapter; MOC: micro-orifice collector. _____ 186

Figure 5.2 – Particle-size distribution as normalized mass frequency determined by Marple Cascade Impactor A – jet milled salmeterol xinafoate; B - wet polished salmeterol xinafoate; C – carrier-based formulations jet milled salmeterol xinafoate; and D - carrier-based formulations with wet polished salmeterol xinafoate, n=3. _____ 189

Figure 5.3 – A: Dissolution profile (salmeterol xinafoate dissolved) determined using the paddle over disk apparatus after collection, using the fast screening impactor of the carrier-based formulations containing wet polished salmeterol xinafoate after actuation 4 capsules, $62 \pm 5 \mu\text{g}$ (□) and 5 capsules,

72 ± 1 µg (■). B is a zoom in (70 – 100% of dissolution). Each profile is given by two replicates. Lines were fitted with Weibull model, R² > 0.9. _____ 195

Figure 5.4 – Dissolution profile determined using the paddle over disk apparatus after collection using the fast screening impactor of the carrier-based formulations containing wet polished (5 capsules actuated, A) and jet milled (3 capsules actuated, C) salmeterol xinafoate in dissolution media containing 0.4% SDS (□). n=2, 0.1% SDS (■), n=3, and 0.0% SDS (■), n=3. B and D is a zoom in (70 – 100% of dissolution). _____ 195

Figure 5.5 – A: Dissolution profile determined using the paddle over disk apparatus after collection using the fast screening impactor of the carrier-based formulations containing wet polished salmeterol xinafoate after actuation 5 capsules (□) and jet milled salmeterol xinafoate after actuating 3 capsules (■). B is a zoom in (70 – 100% of dissolution). Each profile is given by three replicates. Lines were fitted with Weibull model. R² > 0.9. _____ 196

Figure 5.6 – A: Dissolution profile determined using the paddle over disk apparatus after collection using the next generation impactor, stage 4, of the carrier-based formulations containing wet polished salmeterol xinafoate after actuation 12 capsules, 78 ± 5 µg (□) and jet milled salmeterol xinafoate after actuating 7 capsules, 92 ± 1 µg (■). B is a zoom in (50 – 100% of dissolution). Each profile is given by three replicates. Lines were fitted with Weibull model. _____ 199

Figure 5.7 - Deposition pattern on coverslips of the jet milled salmeterol xinafoate (SX) particles (A) and wet polished SX particles (B); and carrier-based formulation containing jet milled SX (C), carrier-based formulation containing wet polished SX (D) after actuation using the PreciseInhale®, obtained by light microscopy with a x20 objective. 1 – agglomerates of coarse and fine particles; 2 – agglomerates of fine particles. _____ 204

Figure 5.8 - SEM images of the of the jet milled salmeterol xinafoate (SX) particles (A) and wet polished SX particles (B); and carrier-based formulation containing jet milled SX (C) and carrier-based formulation containing wet polished SX (D) after actuation using the PreciseInhale®. _____ 205

Figure 5.9 - Dissolution profiles obtained using DissolvIt®. A - Comparison of the prepared carrier-based formulations with jet milled salmeterol xinafoate (jet milled SX blend, □) and wet polished salmeterol xinafoate (wet polished SX blend, ■) as a fraction of total recovered (%/mL), B – zoom in to the first 20 minutes, C – fraction retained in the dissolution system. All results normalized to the total deposited dose. Data expressed as mean ± SD (n=3). * p-value < 0.05. _____ 208

Figure 5.10 - Dissolution profiles obtained using DissolvIt®. A - Comparison of the jet milled salmeterol xinafoate (jet milled SX, □) and wet polished salmeterol (wet polished SX, ■) as a fraction of total recovered (%/mL), B – zoom in to the first 20 minutes, C – fraction retained in the dissolution system with a zoom window in to the first 5 min. All results were normalized to the total deposited dose. Data expressed as mean ± SD (n=3). * p-value < 0.05. _____ 210

List of tables

| | |
|---|----|
| Table 2.1 - Comparison of some delivery routes with inhalation by considering advantages and disadvantages. _____ | 10 |
| Table 2.2 - Advantages and limitations of nebulization, pressurized metered dose inhalers (pMDI) and dry powder inhaler (DPI) as pulmonary delivery strategies. _____ | 12 |
| Table 2.3 – List of dry powder inhalers approved since 2010, with owner company and drug substance. Source: Pharmacircle™. (https://www.pharmacircle.com/info/) _____ | 17 |
| Table 2.4 - Summary of dissolution techniques studied for orally inhaled drugs. _____ | 36 |
| Table 2.5 - List of selected compounds delivered by the inhalation route. _____ | 38 |
| | |
| Table 3.1 - Composition of spray-dried solutions used to manufacture the composite Fluticasone Propionate (FP) formulations containing trehalose di-hydrate (CF1) and Raffinose pentahydrate (CF2) as glass formers. _____ | 78 |
| Table 3.2 - Carrier-based formulations prepared with 1% of fluticasone propionate (FP). _____ | 78 |
| Table 3.3 - Particle size distribution characterization of the spray-dried particles consisting of fluticasone propionate (FP), L-leucine and the sugar listed, as per Table 3., n=2, and jet milled and wet polished FP used for the carrier-based formulations with 1% of micronized FP (Table 3.2) _____ | 80 |
| Table 3.4 - Aerodynamic performance parameters of the carrier-based formulation containing 1% of jet milled fluticasone propionate (FP) (FPJ1 blend), composite particle containing trehalose (CF1) and raffinose (CF2), capsules of 12.5 mg, and of the carrier-based formulation containing 1% of jet milled FP (FPJ2 blend), the carrier-based formulation containing 1% of wet polished FP (FPW blend), capsules of 20.0 mg, determined by Next Generation Impactor. n=3. _____ | 84 |
| Table 3.5 - Amount of fluticasone propionate (FP) loaded in stage 4 of the next generation impactor in one actuation (m_{stage4}) and respective amount (m_{disk}) after a defined number of actuations ($N_{\text{actuations}}$) in μg , for the carrier-free formulations containing trehalose and raffinose (CF1 and CF2) and for the carrier-based formulation containing 1% of jet milled FP (FPJ1 blend). _____ | 87 |
| Table 3.6 - The dissolution performance parameters of fluticasone propionate (FP) for the carrier-free formulation containing trehalose, CF1, containing raffinose, CF2, and of the carrier-based formulation containing 1% of jet milled FP, FPJ1 blend, using the paddle over disk apparatus for the collected samples and the USP Apparatus II (USP Ap. II) for the bulk formulations. _____ | 92 |

| | |
|---|-----|
| Table 3.7 - Amount of fluticasone propionate (FP) loaded in stage 4 of the next generation impactor in each test (extrapolation in the case of tests 2 and 4) and recovered as mass and percentage of expected after adding acetonitrile and ensuring full dissolution. _____ | 94 |
| Table 3.8 - Summary of the performed <i>in vitro</i> tests using the paddle over disk apparatus (POD) and the UPS apparatus II (USP Ap. II), n=2 _____ | 95 |
| Table 3.9 - Number of actuations per disk position, illustrated on the left, for the test with the rotating disk, in the case of 7 and 13 actuations. _____ | 100 |
| Table 3.10 - Summary of FP amount collected using the fast screening impactor on the punched filter (W_{diss}), on the outer ring ($W_{outer\ ring}$) and the sum (W_{total}) for FPJ2 blend (carrier-based with 1 % jet milled fluticasone propionate) and FPW blend (carrier-based with 1% wet polished fluticasone propionate). SD – standard deviation. _____ | 108 |
| Table 3.11 - Design of experiments plan for dissolution method development using USP apparatus IV. _____ | 115 |
| Table 3.12 - Normal Operating Region (NOR) predicted by the model. _____ | 119 |
| Table 3.13 – Summary of all the tested dissolution methods including advantages, disadvantages and critical method parameters. _____ | 123 |
| | |
| Table 4.1 – Summary of the number of actuations for each collection and the obtained deposited dose for the drug substances (DS) fluticasone propionate and budesonide (M_{dep}), with and without pre-separator (PS). _____ | 140 |
| Table 4.2 - Particle-size distribution as normalized mass frequency determined by Marple Cascade Impactor for Flixotide Diskus and Pulmicor Flexhaler, with and without the pre-separator (PS). Data expressed as mean \pm SD (n=3). MMAD - Median mass aerodynamic diameter, GSD – Geometric standard deviation. _____ | 143 |
| Table 4.3 – Summary of the manufactured carrier-based formulations. FPJ blend – carrier-based formulation containing jet milled fluticasone propionate; FPW blend – carrier-based formulation containing wet polished fluticasone propionate. _____ | 147 |
| Table 4.4 - Particle size distribution characterization of the micronized material and the spray-dried particles. _____ | 152 |
| Table 4.5 - Aerodynamic performance parameters of the carrier-based formulations with jet milled fluticasone (FPJ blend) and wet polished fluticasone (FPW blend); of the composite formulation (comp. particles); and the commercial Flixotide Diskus. n=3. _____ | 154 |
| Table 4.6 - The dissolution performance parameters for the fluticasone micronized by jet milling (FP JM) and wet polishing (FP WP), for the carrier-based formulations with jet milled fluticasone (FPJ blend), wet polished fluticasone (FPW blend), for the composite formulation and for the commercial Flixotide | |

Diskusand using the Dissolv/it[®] equipment and the deposited doses using Preciselnhale[®]. Data expressed as mean \pm SD (n=3). p-value by one-way student's t-Test. _____ 161

Table 5.1 - Summary of the manufactured carrier-based formulations. SXJ blend – carrier-based formulation containing jet milled salmeterol xinafoate; SXW blend – carrier-based formulation containing wet polished salmeterol xinafoate. _____ 178

Table 5.2 - Particle size distribution characterization of the micronized salmeterol xinafoate (SX) particles. _____ 185

Table 5.3 - Aerodynamic performance parameters of the carrier-based formulations with jet milled salmeterol xinafoate (jet milled SX blend) and wet polished salmeterol (wet polished SX blend) determines by Next generation impactor (NGI), n=3. _____ 186

Table 5.4 - Particle-size distribution parameters determined by Marple Cascade Impactor. Jet milled SX blend - carrier-based formulations with jet milled salmeterol xinafoate; wet polished SX blend - carrier-based formulations with wet polished salmeterol xinafoate; jet milled SX –salmeterol; and wet polished SX – wet polished salmeterol xinafoate. Data expressed as mean \pm SD (n=3). _____ 189

Table 5.5 - Summary of dissolution tests the carrier-based formulations with jet milled salmeterol xinafoate (jet milled SX blend) and wet polished salmeterol xinafoate (wet polished SX blend) performed using the paddle over disk apparatus (POD) after collection using the fast screening impactor (FSI) and the next generation impactor (NGI). Grey lines correspond to the formulation containing jet milled SX. _____ 192

Table 5.6 - Summary of collected doses of salmeterol xinafoate (SX) and total powder (SX and lactose) for all the paddle over disk (POD) dissolution tests using fast screening impactor (FSI) as a collection method, n=3. The SX in FPF (%) is the percentage of SX in the total amount of collected powder. Grey lines (test 1, 4 and 6) correspond to the formulation containing jet milled SX. _____ 193

Table 5.7 - The dissolution performance parameters for the performed dissolution tests using the Paddle over disk apparatus couples with the fast screening impactor, for jet milled and wet polished formulations of salmeterol xinafoate (SX). _____ 196

Table 5.8 - Summary of collected doses of salmeterol xinafoate (SX) and total powder (SX and lactose) for the paddle over disk dissolution tests using next generation impactor (NGI) as a collection method, n=3. The SX in stage 4 (%) is the percentage of SX in the total amount of collected powder. Grey line correspond to the formulation containing jet milled SX. _____ 198

Table 5.9 - The dissolution performance parameters for the performed dissolution tests using the Paddle over disk apparatus coupled with the next generation impactor, for jet milled and wet polished formulations of salmeterol xinafoate (SX). _____ 199

Table 5.10 - Summary of dissolution tests of micronized salmeterol xinafoate (SX) (jet milled and wet polished) and the carrier-based formulations with jet milled SX (jet milled SX blend) and wet polished

SX (wet polished SX blend) performed using the DissolvIt® after collection using the PreciseInhale®

203

Table 5.11 - The dissolution performance parameters for the carrier-based formulations with jet milled salmeterol xinafoate (jet milled SX blend) and wet polished salmeterol xinafoate (wet polished SX blend), and for the jet milled SX and wet polished SX alone, using the DissolvIt® equipment and the deposited doses using PreciseInhale®. Data expressed as mean \pm SD (n=3). p-value by one-way student's t-Test.

212

List of abbreviations

| | |
|----------------------------|--|
| ACI | Andersen cascade impactor |
| AFM | Atomic force microscopy |
| APSD | Aerodynamic particle size distribution |
| AQbD | Analytical quality by design |
| AS | Albuterol sulfate |
| BCS | Biopharmaceutical classification system |
| BD | Budesonide |
| BET | Brunauer-Emmett-Teller |
| CI | Cascade impactor |
| C_{max} | Maximum concentration achieved by the DS during the dissolution test |
| COPD | Chronic obstructive pulmonary disease |
| Da | Aerodynamic diameter |
| DS | Drug substance |
| Dv10, Dv50 and Dv90 | Particle size below which 10 %, 50 % and 90 % of the volume of particles exist |
| EMA | European medicines agency |
| f₁ | Difference factor |
| f₂ | Similarity factor |
| FDA | Food and drug administration |
| FP | Fluticasone propionate |
| FPD | Fine particle dose |
| FPF | Fine particle fraction |
| FSI | Fast screening impactor |
| GDUFA | Generic drug user fee amendments |
| GSD | Geometric standard deviation |
| HC | Hydrocortisone |
| HFA | Hydrofluoroalkane |
| HPH | High pressure homogenization |

| | |
|---------------------------|---|
| iBCS | Inhalation biopharmaceutical classification system |
| IGC | Inverse gas chromatography |
| IP | Induction port |
| IVIVC | in vitro / in vivo correlation |
| JM | Jet milling |
| LC-MS/MS | Liquid chromatography-tandem mass spectrometry |
| M_{dep} | Amount of DS deposited on the coverslip |
| MMAD | Mass median aerodynamic diameter |
| MPA | Mouth piece adaptor |
| M_{perf} | Sum of the DS dissolved in the perfusate during the dissolution test |
| M_{system} | DS extracted from the system at the end of the dissolution experiment |
| NGI | Next generation impactor |
| OINDP | Orally inhaled and nasal drug product |
| PC | Polycarbonate |
| PD | Pharmacodynamic |
| PK | Pharmacokinetic |
| PBPK | Physiological based pharmacokinetic |
| pMDI | Pressurized metered dose inhalers |
| POD | Paddle over disk |
| PS | Pre-separator |
| PSD | Particle size distribution |
| PSG | Product specific guidance |
| QbD | Quality by design |
| Re | Reynolds number |
| SD | Standard deviation |
| SEM | Scanning electron microscopy |
| SSA | Specific surface area |
| SX | Salmeterol xinafoate |
| t_{max} | Time of C _{max} during the dissolution test |
| USP | United states pharmacopeia |
| WP | Wet polishing |

Chapter 1

Introduction



1.1 MOTIVATION

Inhalation is the preferred route of administration for the treatment of respiratory conditions such as asthma, chronic obstructive pulmonary disease (COPD) or cystic fibrosis, since the drug substance (DS) is delivered to the acting site leading to a rapid onset action while preventing the first pass metabolism of the DS minimizing systemic side effects caused by the high drug loads required by other routes. This route is also exploited as a path for systemic delivery of small to large molecules, namely for gene therapy. Due to the lungs large surface area of absorption (100 m², approximately half of a tennis court), concomitantly with the high permeability, high irrigation and less harsh enzymatic environment, the administration to the respiratory tract becomes very attractive (Labiris and Dolovich, 2003).

Nonetheless, the lung is a complex system with several defense mechanisms - the respiratory system has evolved to minimize the entry of inhaled particles and droplets in the deep lung, and to remove the ones that enter. Thus, to ensure a successful new product or generic, there is a need for formulation and device optimization to overcome these natural barriers, coupled with suitable characterization tools capable of ranking formulation/device combinations regarding their therapeutic efficacy or bioequivalence. For that, there are several factors which should be considered such as regional drug substance distribution and local dissolution, permeability, and clearance (Fröhlich, 2019). The standard characterization tools for inhaled formulations focus on aerodynamic performance, i.e, in determining the profile of particle deposition based on their aerodynamic particle size determined by cascade impaction. Cascade impactor parameters (emitted dose, fine particle dose and mass median aerodynamic diameter) show some link to the actual lung deposition, but a correlation with *in vivo* data is very often not obtained. One strategy to achieve a closer correlation is by using ways that more closely mimic clinical use, including the use of breath simulators, or of impactor inlets that simulate the human upper airway anatomy (Newman and Chan, 2008). Still, cascade impactors do not reflect on the final disposition of the DS once deposited.

Following particle deposition, the DS therapeutic action is highly dependent on its dissolution, diffusion and absorption kinetics, as well as its elimination rate. The DS dissolution is dependent on its solubility, formulation strategy (amorphous versus crystalline, or the selected excipients) or the type of microstructures generated when actuated and deposited in the lung (Forbes et al., 2015). During the last years, several efforts from the academia and industry have led to the development and comparison of collection and dissolution systems for orally inhaled products (Radivojev et al., 2019), and the first

steps towards the design of a biopharmaceutical classification system for inhalation drugs (iBCS), which besides solubility and permeation will most likely consider the regional surface area, local activity and physicochemical properties of the formulation (Gallegos-Catalán et al., 2021; Velaga et al., 2017). The development of suitable methodologies to characterize inhaled products are essential to achieve *in vitro* / *in vivo* correlations (IVIVC) for inhaled drug products, which could result in accelerated drug product development, together with reduced research and development spending (Newman and Chan, 2020). Successful IVIVC would also allow to accurately predict *in vivo* drug delivery to the lung without the need to test human subjects, to compare test and reference products in the laboratory in a clinically relevant manner, and to improve dose finding in early product development stages, among other gains. Dissolution assessment has been proven to correlate dissolution rate with system exposure for two different formulations with similar aerodynamic particle size distributions (Bäckman et al., 2014), a relationship between dissolution rate and appearance of drug in plasma has also been reported (Alayoub et al., 2021; Grainger et al., 2012a), and input parameters from biorelevant dissolution testing have been used in physiologically based pharmacokinetic (PBPK) modelling.

Nevertheless, there is not a standardized and globally accepted method to assess the dissolution and/or absorption of orally inhaled drug products which conjugates aerodynamic performance and particle characterization to deposition microstructures and dissolution in a biorelevant media (Radivojev et al., 2019). This work aims to develop and optimize collection and dissolution systems for orally inhaled drug products, both in a quality control (QC) perspective, with strategies based on pre-existing compendial methodologies, and in a biorelevant performance prediction perspective, with the application of a newly developed breath simulator couples with a biorelevant dissolution and absorption system.

1.2 RESEARCH AIMS AND OBJECTIVES

This work aims at testing, developing and optimizing technologies capable to assess the collection, dissolution and absorption of dry powder inhaler formulations, including QC and biorelevant tools.

Hence, the proposed research can be further translated into the following objectives:

- i) Evaluating the differentiation capability and applicability of dissolution compendial methods designed to other dosage forms in combination with cascade impactors as possible QC or screening tools.
- ii) Optimization and testing of a biorelevant collection and dissolution/absorption system with potential for IVIVC by differentiating micronized and formulated DS following different particle engineering and formulation approaches.

1.3 THESIS OUTLINE

This thesis is structured in 6 main chapters.

Chapter 1 conveyed the framework and research focus of this thesis. Motivation, aims, and thesis contributions were shared.

Chapter 2 presents the state-of-the-art supporting this work. The pulmonary drug delivery topic is presented at a glance, with a summary of what can be found on the market and a summary of the main advantages and challenges of the route. The underlying mechanisms of particle deposition, absorption and clearance is explored linked with the anatomy and physiology of the lungs, factors to be considered in the design of a biorelevant collection and dissolution strategy for orally inhaled products. Formulation standard characterization approaches are presented as they are essential in understanding the dose of DS deposited in the lung following inhaler actuation, and thus its bioavailability. Next, a description of the recently published dissolution systems suitable for inhalation is presented, listing the main advantages and disadvantages. Lastly, manufacturing approaches for dry powder inhalers are explained, from particle engineering to formulation development.

Chapter 3 features the development and comparison of collection and dissolution strategies for a low solubility DS, fluticasone propionate. For that, several dissolution set-ups were applied to DPI formulations aiming to assess the capability to differentiate formulations and define each system advantages, limitations and potential critical method parameters. The paddle over disk (POD) dissolution apparatus was optimized by being coupled with different cascade impactors in order to achieve a dose independent and repeatable methodology. Finally, a methodology coupling the USP apparatus IV, flow-through, with the fast screening impactor (FSI) was developed by a quality by design approach, leading to a better understanding of the impact of the dissolution method parameters such as flow-rate and dissolution medium volume on dissolution kinetics and variability.

Chapter 4 describes the optimization and application of a breath simulator as a collection method, PreciseInhale®, coupled with a biorelevant dissolution/absorption system, the DissolvIt®. Firstly, the PreciseInhale® breath simulator was optimized by the designing and testing of a novel pre-separator capable to prevent coarse particles typically retained in the upper airways when inhaled from being collected for dissolution assessment. Thus, ensuring a more biorelevant collection system. Then, the optimized system was used to compare and discriminate dry powder inhaler formulations containing

fluticasone propionate manufactured by different particle engineering technologies (spray-drying, jet milling and wet polishing) in terms of deposition structures and dissolution profile *in vitro*. The deposition and dissolution observations were compared with standard characterization results, such as aerodynamic performance and particle properties, leading to further understanding of the impact of formulation on the DPI aerosolization and deposition mechanisms in the lung.

Chapter 5 focuses on the validation of the method optimized in Chapter 3, the POD with the FSI, and Chapter 4, the PreciseInhale® and DissolvIt®, by testing different formulations and particle engineering technologies of a higher solubility DS, salmeterol xinafoate. The tested carrier-based formulations containing lactose as a carrier and salmeterol xinafoate micronized by wet polishing and jet milling were characterized regarding particle size and aerodynamic performance. For the POD the dose collection strategy repeatability was confirmed and the independence of the dissolution rate to the dose collected was proven, while for the DissolvIt®, the impact of the particle engineering technology on the generated and deposited microstructures was correlated with cohesion and adhesion forces available in the literature, and dissolution rate acceleration by the presence of lactose was confirmed, validating dissolution testing as an essential tool to both optimize an innovator DPI and de-risk generics development.

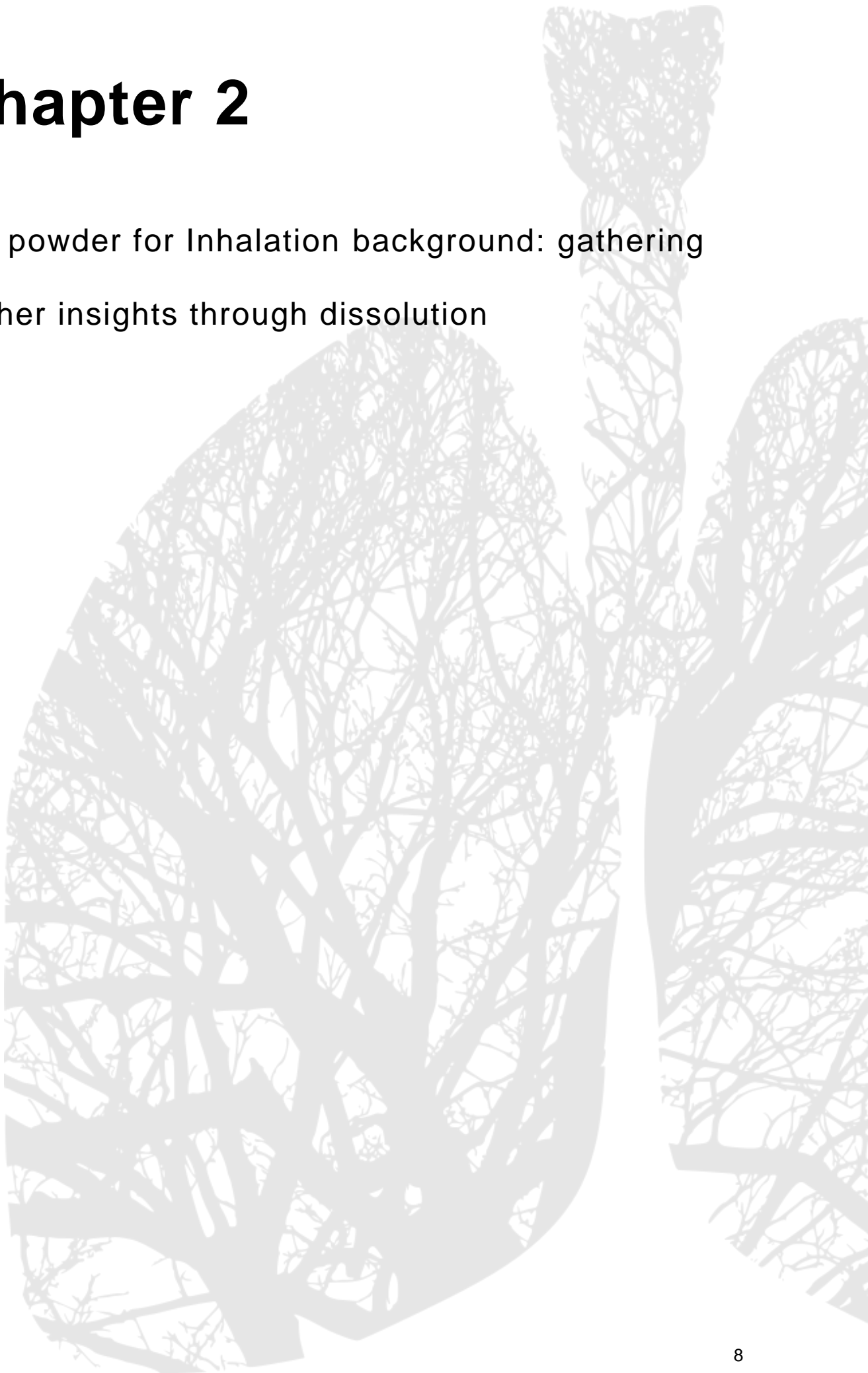
Finally, Chapter 6 presents the main conclusions of this work with recommendations to improve its outcomes and suggestions for future research.

1.4 REFERENCES

- Al ayoub, Y., Buzgeia, A., Almousawi, G., Mazhar, H.R.A., Alzouebi, B., Gopalan, R.C., Assi, K.H., 2021. In-Vitro In-Vivo Correlation (IVIVC) of Inhaled Products Using Twin Stage Impinger. *J. Pharm. Sci.* 111, 395–402. <https://doi.org/10.1016/j.xphs.2021.09.042>
- Bäckman, P., Adelman, H., Petersson, G., Jones, C.B., 2014. Advances in inhaled technologies: understanding the therapeutic challenge, predicting clinical performance, and designing the optimal inhaled product. *Clin. Pharmacol. Ther.* 95, 509–20. <https://doi.org/10.1038/clpt.2014.27>
- Forbes, B., Bäckman, P., Christopher, D., Dolovich, M., Li, B. V, Morgan, B., 2015. In Vitro Testing for Orally Inhaled Products: Developments in Science-Based Regulatory Approaches. *AAPS J.* 17, 837–52. <https://doi.org/10.1208/s12248-015-9763-3>
- Fröhlich, E., 2019. Biological Obstacles for Identifying In Vitro-In Vivo Correlations of Orally Inhaled Formulations. *Pharmaceutics* 11, 316. <https://doi.org/10.3390/pharmaceutics11070316>
- Grainger, C.I., Saunders, M., Buttini, F., Telford, R., Merolla, L.L., Martin, G.P., Jones, S.A., Forbes, B., 2012. Critical Characteristics for Corticosteroid Solution Metered Dose Inhaler Bioequivalence. *Mol. Pharm.* 9, 563–569. <https://doi.org/10.1021/mp200415g>
- Labiris, N.R., Dolovich, M.B., 2003. Pulmonary drug delivery. Part I: Physiological factors affecting therapeutic effectiveness of aerosolized medications. *Br. J. Clin. Pharmacol.* 56, 588–599. <https://doi.org/10.1046/j.1365-2125.2003.01892.x>
- Newman, S.P., Chan, H.-K., 2020. In vitro-in vivo correlations (IVIVCs) of deposition for drugs given by oral inhalation. *Adv. Drug Deliv. Rev.* 167, 135–147. <https://doi.org/10.1016/j.addr.2020.06.023>
- Newman, S.P., Chan, H.-K., 2008. In Vitro / In Vivo Comparisons in Pulmonary Drug Delivery. *J. Aerosol Med. Pulm. Drug Deliv.* 21, 77–84. <https://doi.org/10.1089/jamp.2007.0643>
- Radivojev, S., Zellnitz, S., Paudel, A., Fröhlich, E., 2019. Searching for physiologically relevant in vitro dissolution techniques for orally inhaled drugs. *Int. J. Pharm.* 556, 45–56. <https://doi.org/10.1016/j.ijpharm.2018.11.072>
- Velaga, S.P., Djuris, J., Cvijic, S., Rozou, S., Russo, P., Colombo, G., Rossi, A., 2017. Dry powder inhalers: An overview of the in vitro dissolution methodologies and their correlation with the biopharmaceutical aspects of the drug products. *Eur. J. Pharm. Sci.* 0–1. <https://doi.org/10.1016/j.ejps.2017.09.002>

Chapter 2

Dry powder for Inhalation background: gathering further insights through dissolution



2.1 PULMONARY DRUG DELIVERY AT A GLANCE

2.1.1 Why inhalation

The inhalation route has been traditionally used as a way to target the respiratory tract in the treatment of local diseases such as asthma, chronic obstructive pulmonary disease (COPD) or cystic fibrosis. In fact, inhalation is the preferred route of administration for these local conditions due to delivering the active agent to the site of action leading to a rapid clinical onset while minimizing the systemic side effect caused by the high drug loads required by other routes. Table 2.1 compares the inhalation delivery route with other available options, showcasing the rationale followed when selecting inhalation as a delivery route.

Furthermore, the inhalation route avoids the first pass metabolism by delivering the drug substance (DS) directly to the respiratory tract and a less harsh, low enzymatic environment is found. Due to its large surface area of absorption (100 m²) and highly permeable and irrigated membrane (the alveolar-capillary barrier, 0.2 – 0.7 µm thickness), this route is also a path for systemic delivery (Labiris and Dolovich, 2003). Large molecules in specific can be absorbed in significant quantities in the lung, while presenting low absorption rates by oral delivery. In point of fact, drugs such as insulin have been delivered through the inhalation route (Siekmeier and Scheuch, 2008).

However, the respiratory system is equipped with numerous strategies to hinder delivery of particles or droplets to the targeted region – the oropharynx 90 degrees bend promotes impaction and deposition of particulates at the back of the throat during inhalation, and following that, the progressive branching and narrowing of the airways generates a convoluted path for particles to navigate down to the targeted region. Tailored formulation particle size in the range 0.5 – 5 µm (2 – 3 µm for deep lung (alveolar)) is key to ensure a successful delivery to the site of action. Moreover, once the particle deposits, it needs to dissolve in the 0.1 µm layer of alveolar fluid previous to elimination - the respiratory system is equipped with defense mechanisms capable of eliminating deposited particles (such as mucociliary clearance at the upper airways and macrophage action at the alveoli), described in detail in Section 2.2.

Table 2.1 - Comparison of some delivery routes with inhalation by considering advantages and disadvantages.

| Route of administration | Advantages | Disadvantages |
|--------------------------------|---|--|
| Oral | Economical to patients; generally safe; simple and convenient for the patient (portable, easy, painless); the patient can self-administer; non-invasive; high dose possible; good permeability of the GI barrier. | Drug absorption may vary; subject to first-pass metabolism; not possible in unconscious patients or patients who are vomiting; slow onset of action; may be inefficient (low solubility). |
| Intravenous | Immediate effect; direct access to blood central compartment; does not harm mucous membranes; can be given to unconscious patients; avoids first-pass metabolism; achieves predictable and precise control over drug plasma levels compared to other routes. | Risk of infection, overdose, vein or arterial damage; inconvenient to the patient; painful; expensive; may require trained medical staff to administer; sustained release not possible. |
| Sublingual | Rapid drug absorption; can be administered for local effects; avoids first-pass metabolism; can be self-administered; convenient; can be used by people who have difficulty in swallowing tablets. | Inconvenient for some patients; small dose limit; irritation to the oral mucosa. |
| Inhalation | Rapid onset of action; systemic side effects minimised; reaches the site of action; avoids first pass metabolism; can be used for systemic delivery; large surface of absorption. | Proper inhaler technique required for efficient action; May stimulate the cough reflex; difficulty on regulating the exact amount for dosage; |

2.1.2 Devices and inhalation products

To effectively deliver the therapeutic agent and ensure its action, it is essential to consider the natural lung mechanisms in the design of the final product, regarding both delivery and absorption. There are three main strategies to deliver the active agent to the lung surface:

- Nebulizers generate droplet aerosols in the respirable size range from solutions or suspensions by utilizing (i) compressed gases, in the case of jet nebulizers; (ii) ultrasonic energy, in the case of ultrasonic nebulizers; or (iii) the vibration of a piezo element, in the case of vibrating mesh nebulizers.
- Pressurized metered dose inhalers (pMDI) use a pressurized propellant as a source of energy for expelling the drug and also as a dispersion medium, which deliver fixed volumes by the actuation of a valve.
- Dry powder inhaler (DPI) delivers the drug and formulation excipients as a dry powder, which can be present in a device container, pre-metered or metered previous to actuation, or in capsules.

A summary of the main advantages and disadvantages of each delivery strategy is presented in Table 2.2.

Table 2.2 - Advantages and limitations of nebulization, pressurized metered dose inhalers (pMDI) and dry powder inhaler (DPI) as pulmonary delivery strategies.

| Delivery strategy | Advantages | Disadvantages |
|--------------------------|---|--|
| Nebulization | <p>Straight forward product development</p> <p>Suitable for hydrophobic and hydrophobic particles (as suspensions and solutions, respectively)</p> <p>Approximately 70% of droplets are between 1-5µm</p> <p>Minimal patient cooperation and coordination needed</p> <p>Adequate for therapeutics in children, debilitated or distressed patients</p> <p>Normal breathing pattern can be used</p> | <p>Time consuming (5 to 30 min treatment time)</p> <p>Equipment is usually large and require power source</p> <p>Assembly and cleaning are required, risk of bacterial contamination</p> <p>Low efficacy with poor reproducibility</p> |
| pMDI | <p>Platform devices – small number of device types simplifies formulation development and patient compliance</p> <p>Suitable for hydrophilic and hydrophobic particles (as suspensions and solutions, respectively)</p> <p>Existence of new spacers to allow better compliance</p> | <p>Not environmentally friendly: HFA are greenhouse gases subjected to increasing regulatory constraints</p> <p>Low deposition in the lung</p> <p>Poor compliance - requires high coordination of actuation and inhalation</p> |
| DPI | <p>Propellant free</p> <p>Require little or no coordination of actuation with inhalation</p> <p>High efficacy with good reproducibility</p> <p>Stability</p> | <p>Complex product development</p> <p>Variety of devices and inhalation techniques</p> <p>Strict pharmaceutical and manufacturing standards</p> |

HFA – hydrofluoroalkane

For the DS to be able to reach the lungs through the bronchial tree, not only the formulation and inhaler must be optimized, but also the inhalation technique, i.e. the way the patient inhales must be appropriate for the device in usage. For different types of inhalers, different techniques are required. When

considering nebulizers, the normal breathing pattern is often adequate, yet that is not always the case. When using a pMDI or a DPI, the manufacturers' instructions describing the correct technique should be followed. The optimal use of pMDIs has been defined based on objective evidence (Dolovich et al., 1981; Hindle et al., 1993; Lawford and McKenzie, 1983), stating the patient must synchronize a slow and deep inhalation with the device actuation, and then hold their breath for a few seconds (allowing the particles that entered the lung to sediment). Contrasting with a similar set of instruction for the pMDIs, the instructions for DPI usage varies significantly from device to device. On the one hand, it is possible to find a wide variety of designs on the market, each one being accompanied by a detailed set of instructions comprising different number and types of steps. On the other hand, the actuation itself is instructed differently, varying from "quickly and deeply" to "steadily and deeply" or even "slowly and deeply, but at a rate sufficient to hear or feel the capsule vibrate" (Newman and Peart, 2009). All the stated variations in combination with less-than-optimal patient compliance lead to patient handling errors, and therefore to an unsuccessful pulmonary drug delivery.

Research efforts on DPIs have been significant and superior to other pulmonary delivery platforms (Figure 2.1), mostly due to the perceived limitations in pMDIs and nebulizers (Islam and Gladki, 2008), summarized on Table 2.2. However, considering the stated limitation associated with DPIs, the question arising is why to select DPIs as a strategy?

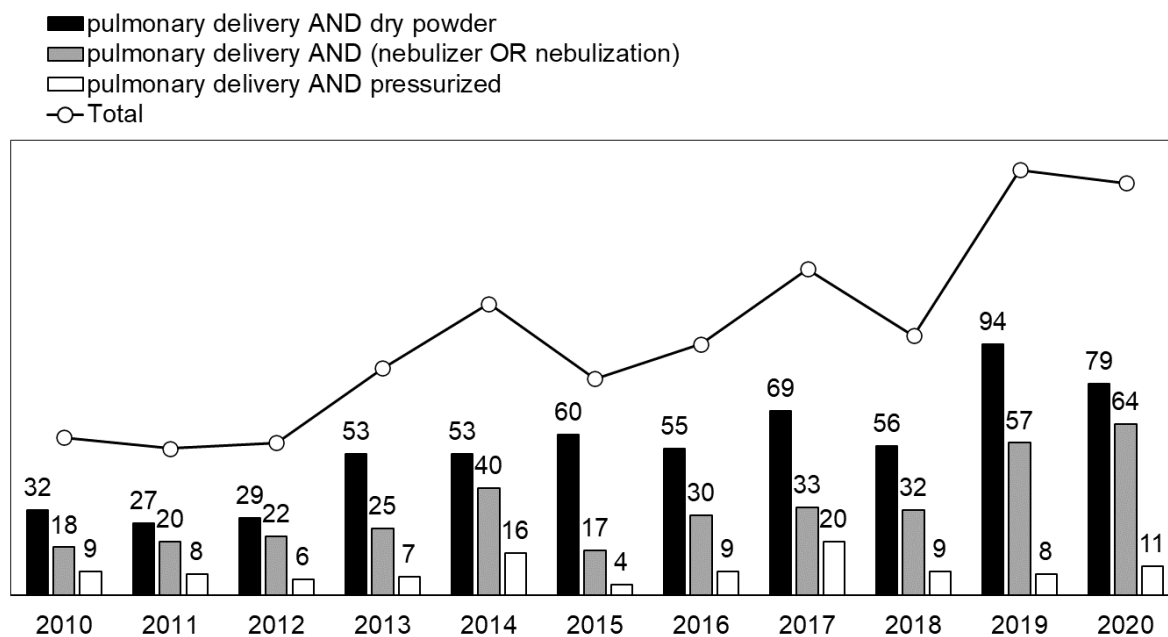


Figure 2.1 - Number of published papers from 2010 to 2020 containing the words indicated in the legend as part of the title or abstract. Data obtained using linked research knowledge system Dimensions (<https://app.dimensions.ai/>).

DPIs as a delivery platform are capable of achieving good aerosolization without a propellant with high efficiency and good reproducibility, while requiring minimum patient/device coordination during the inhalation maneuver. Additionally, DPI powder formulations with suitable packaging present superior chemical stability due to its solid form – most consist of micronized crystalline DS particles blended with larger carrier particles, or amorphous DS stabilized by an excipient matrix. Lastly, several historical reasons lead to the increased interest in DPI development – described in the following paragraphs.

The history of inhalation dates to 4000 years ago, as described before (Anderson, 2005; de Boer et al., 2017; Grossman, 1994; Sanders, 2007). It was in India that around 2000 BC inhalation therapy for asthma and other lung complications was first employed. These consisted of smoking herbal preparations through a pipe with anticholinergic bronchodilating properties (Anderson, 2005). Hippocrates (Greece, 460-377 BC) put together a pot with a reed in the lid, designing the earliest inhalation device. Following the pot-and-reed initial design, many similar devices were used, especially in the late 18th and early 19th century. Also, early atomizers and nebulizers were developed in the mid-1800s. The earliest recorded DPI is probably an apparatus patented by Newton, in London, 1864 (Sanders, 2007). In 1889, the Carbohc Smoke Ball was patented, becoming another one of the first examples of a DPI – it consisted of a squeezable hollow rubber ball with a sieve across the orifice to

disaggregate the power inside (Snell, 2001). Aerohaler was launched mid 20th century by the Abbot Laboratories to take penicillin, and was later used in the administration of norisodrine for the treatment of asthma – this inhaler served as a prototype for future capsule inhalers developed in the period of 1950-1980 (de Boer et al., 2017). It was around the same time that the first pMDI was developed at Riker (3M), being launched in late March 1956, opening the way to a future market of 400 million units of pMDIs. However, the operating difficulties found by the patients combine with the discovery that the chlorofluorocarbons (CFC) propellants contribute for the depletion of the ozone layer by early 1970 (Cutchis, 1974; Lovelock, 1977), created uncertainty about the future of this delivery strategy, and consequently became a major driver for the development of DPIs (de Boer et al., 2017). Additionally, in 1967, Fisons introduced Spinhaler, able to deliver a dose too high for pMDIs (Robson et al., 1981). Spinhaler by Fisons, the Rotahaler by Glaxo (Pover and Dash, 1985), as well the others DPIs that reach the market between 1950 and 1990 (Cocozza, 1976; Kladders, 1989), followed the same principle: gelatine capsules containing the DS formulated as a lactose-based mixture (Clark, 1995). The choice of the gelatine capsules was a result of the availability of the filling equipment at the time, avoiding this way the need for equipment development (de Boer et al., 2017). For low drug dosages, the choice of mixing the DS with lactose improved the followability of the powder, easing the capsule filling process.

The interaction between lactose and active agent was investigated by Jonas and Pilpel. They identify a strong “adsorption” (van der Waals’ and electrostatic forces) created when mixing micronized particles with larger carrier particles. Further studies endeavour on this topic (Shotton and Orr, 1971; Travers and White, 1971), and in 1975, Hersey recognized that carrier-based mixtures were not random and termed them ordered mixtures (Hersey, 1975), to be later renamed adhesive mixtures by Staniforth (Staniforth, 1987). The first studies on lactose influence on the aerosol performance were published in 1971 (Bell et al., 1971). They demonstrated the poor flow of the finest powders, and that it could be overcome by using coarse carriers in the mix. In the present, much of the research towards DPI focuses on the study of systems with a small percentage of DS (~1%) – “diluted” systems. However the performance of these systems is not always optimal, with only up to 20% reaching the deep lung (Thalberg et al., 2016), and high variability in the dose delivered to the patient due to the low DS amounts (Borgström et al., 2006). The key was the development of dry powder products within the intermediate region with regard to the drug load (2-15%), achieving higher delivered dose.

Following capsule based inhalers, multidose reservoirs inhalers and multiple UniDose™ blisters were introduced in the 1990s, however, the same type of formulation was still being used in every case, with one exception – Turbuhaler®, introduced by Astra(Zeneca) in the late 1980s. This multidose reservoir inhaler contained a carrier free formulation of DS soft aggregates (Wetterlin, 1988).

As the majority of the DPIs developed before 2010 were breath-actuated, they were categorized as passive (de Boer et al., 2017). Although it is an advantage to disperse and deliver the drug to the lungs only through patient's inhalation, with no need for external energy or propellants, it is also linked with a strong limitation: dispersion is only as efficient as the patients' forced inspiration flow (Clark, 1995). This limitation is not particularly relevant for COPD and asthma therapy, as in these cases the therapeutic windows of the drugs used are wide and the patient is allowed to take extra doses if necessary (Newman and Peart, 2009). It is however significant when considering systemic delivery through the pulmonary route, in which case a tighter control over the administered dose may be necessary (Anderson and Newman, 2009). As a solution, in the 1990s, active DPIs started to be developed (Newman and Peart, 2009), containing a mechanism besides the patient's inhalation to aerosolize the dry powder. An example of an active DPI is the Nektar Pulmonary Inhaler™, the first inhaled insulin product (Exubera®) (Dunn and Curran, 2006; Harper et al., 2007).

As of today, more than 20 DPIs are on the market for local treatments such as COPD, asthma or cystic fibrosis, and systemic treatments such as diabetes, influenza, schizophrenia/bipolar disorder. Table 2.3 lists the DPI products approved since 2010, and the DPI market is expected to keep growing for the next 10 years (Arc, n.d.).

Table 2.3 – List of dry powder inhalers approved since 2010, with owner company and drug substance.
Source: Pharmacircle™. (<https://www.pharmacircle.com/info/>)

| Product | Company | Drug substance | Date of Approval |
|---------------------------|-------------------------------------|---|-------------------------|
| Aridol® | Pharmaxis Ltd | Mannitol | 2010 |
| Inavir® TwinCaps | Daiichi Sankyo Company, Limited | Laninamivir | 2010 |
| Arcapta® NEOhaler® | Novartis International AG | Indacaterol | 2011 |
| Tudorza® Pressair/Genuair | Almirall, S.A. | acclidinium bromide | 2012 |
| Adasuve Staccato | Teva Pharmaceutical Industries Ltd. | loxapine | 2012 |
| Foster® NEXThaler | Chiesi Farmaceutici S.p.A. | budesonide/formoterol fumarate dihydrate | 2012 |
| TOBI® Podhaler® | Novartis International AG | tobramycin | 2013 |
| Breo® ELLIPTA® | GlaxoSmithKline | Fluticasone furoate/Vilanterol | 2013 |
| Anoro® ELLIPTA® | GlaxoSmithKline | Umeclidinium bromide/Vilanterol | 2013 |
| Afrezza® Dreamboat™ | MannKind Corporation | insulin | 2014 |
| Pulmoton® Elpenhaler® | ELPEN Pharmaceutical | budesonide/formoterol fumarate dihydrate | 2015 |
| ProAir® RespiClick® | Teva Pharmaceutical Industries Ltd. | salbutamol sulfate | 2015 |
| Lifsar Pulmojet | Zentiva Group, a.s. | salmeterol xinafoate/fluticasone propionate | 2015 |
| Zephyrus | SMB Laboratories | budesonide/salmeterol xinafoate | 2015 |
| AirDuo® RespiClick® | Teva Pharmaceutical Industries Ltd. | salmeterol xinafoate/fluticasone propionate | 2016 |
| Braltus® Zonda | Teva Pharmaceutical Industries Ltd. | tiotropium bromide | 2016 |
| ArmonAir® RespiClick® | Teva Pharmaceutical Industries Ltd. | fluticasone propionate | 2017 |
| ProAir® Digihaler® | Teva Pharmaceutical Industries Ltd. | salbutamol sulfate | 2018 |
| Airbufo® Forspiro® | Sandoz International | budesonide/formoterol fumarate dihydrate | 2018 |
| Inbrija® | Civitas Therapeutics, Inc. | levodopa | 2018 |
| AirDuo® Digihaler® | Teva Pharmaceutical Industries Ltd. | salmeterol xinafoate/fluticasone propionate | 2019 |
| Aectura® Breezhaler® | Novartis International AG | mometasone furoate/indacaterol acetate | 2020 |
| Sereflo® Ciphaler® | Cipla | salmeterol xinafoate/fluticasone propionate | 2020 |

Regulatory perspective on DPI development

With the expiration of product patents and with the worldwide trend of shifting from branded to generic options (pushed in part by regulatory agencies aiming for a more accessible healthcare, as generic drugs are sold at much lower prices than those of their branded counterparts), DPI generic development has gained great interest, especially for blockbuster products such as Advair® Diskus® (fluticasone propionate/salmeterol xinafoate). United States Food and Drug Administration (FDA) and European Medicines Agency (EMA) have published guidelines covering the pharmaceutical development and clinical testing for inhalation products in the USA and Europe, respectively (EMA, 2009, 2005; FDA, 2018).

There are two main guidelines covering the pharmaceutical development and clinical testing for inhalation products in Europe issued in 2005 and 2009. The 2009 document describes a stepwise approach to prove the therapeutic equivalence of two DPI products (illustrated in Figure 2.2). EMA generic development approach requires (i) the generic and reference products to have the same drug substance with an identical dosage form, safety profile and pharmaceutical performance (independently of the excipient amounts and crystalline structure); (ii) the generic device should be handled similarly and have the same resistance of the reference product; and (iii) the generic and reference products' *in vitro* equivalence should be guaranteed (delivered dose uniformity and aerodynamic particle size distribution by impactor). If the three stated pharmaceutical criteria are met, the generic product is accepted for approval. If that is not the case, pharmacokinetic or pharmacodynamic studies are required to prove equivalence - Figure 2.2.

Regarding the FDA, up until 2012 there was no bioequivalence guidance for inhalation products, resulting in almost no generic competition in the inhalation space (Lionberger, 2018). Since 2012 the Generic Drug User Fee Amendments (GDUFA) Regulatory Science Research Program aims to define critical product attributes that are relevant for *in vivo* performance of orally inhaled products, and therefore created product specific guidance's (PSG), which allow to foster drug product development, and abbreviated new drug application (ANDA) submission and approval, but, unlike EMA does not provide a general document for generic development. Since then, more than 50 generic nasal products were approved, and more than 50% of approved orally inhaled and nasal drug products (OINDP) have PSGs issued (the first DPI guidance was published on September 2013 for the fluticasone/salmeterol combination (United States Food and Drug Administration, 2013)). Since then, more than 10 draft

guidance documents have been published by the FDA to support DPI generic development: draft guidance for fluticasone furoate (Osterhout, 2016), Acridinium Bromide (Recommendations, 2015), Glycopyrrolate/Indacaterol Maleate (Recommendations, 2020a), Indacaterol Maleate (Recommendations, 2016a), fluticasone furoate/vilanterol trifenate (Recommendations, 2016b), Budesonide (Recommendations, 2016c), Fluticasone Furoate/ Umeclidinium Bromide/Vilanterol Trifenate (Recommendations, 2021), Glycopyrrolate Inhalation Powder (Recommendations, 2017a), Mometasone Furoate (Food and Drug Administration, 2017), Salmeterol Xinafoate (Recommendations, 2017b), Tiotropium Bromide (Recommendations, 2017c), Umeclidinium Bromide and Vilanterol Trifenate (Recommendations, 2020b).

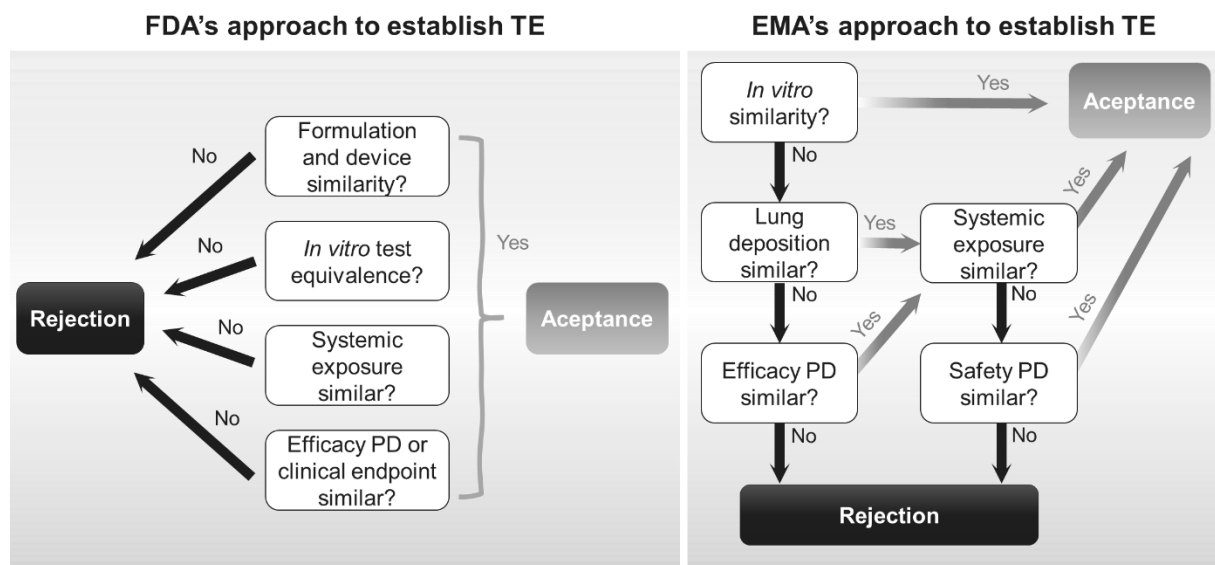


Figure 2.2 - Steps towards establishing therapeutic equivalence (TE) between a reference and a generic inhalation product according to the FDA and EMA guidelines. PD – pharmacodynamic.

The current PSGs recommend a weight of evidence approach (schematized in Figure 2.2) – it requires a battery of evidence to demonstrate pharmaceutical equivalence, bioequivalence and therapeutic equivalence, defined as:

- Pharmaceutical equivalent products contain the same active ingredient(s), are of the same dosage form and route of administration, are identical in strength or concentration. Drug products (the finished dosage form that contains a drug substance, according to the FDA) may differ in characteristics such as: shape; release mechanism; labelling (to some extent); scoring; excipients (including colors, flavors, preservatives).

- Bioequivalent products do not show a significant difference regarding the rate and extent of absorption when administered at the same molar dose of the therapeutic ingredient under similar experimental conditions in either a single dose or multiple doses; or if the difference in the rate of absorption is intentional, it is reflected in its proposed labelling, is not essential to the attainment of effective body drug concentrations on chronic use, and is considered medically insignificant for the drug.
- Therapeutic equivalent products produce the same clinical effect and safety profile as the prescribed product. Drug products are considered to be therapeutically equivalent only if they are pharmaceutical equivalents and bioequivalent.

Thus, this weight of evidence approach includes device and formulation design, comparative pharmacokinetic studies, comparative *in vitro* studies and comparative pharmacodynamics or clinical endpoint studies.

To attempt to reduce the burden of these current bioequivalence requirements, the GDUFA has launched several initiatives to develop clinically relevant *in vitro* and *in silico* tools and methodologies for prediction on *in vivo* regional drug deposition and dissolution, and to assess their applicability in the generic OINDPs development programs.

2.2 TOWARDS BIORELEVANT COLLECTION AND DISSOLUTION

2.2.1 Physiological advantages of the lung as a delivery route

When taking locally acting drug substances, the pulmonary route leads to significant clinical advantages, as previously mentioned. The main advantage of using the pulmonary route for lung locally acting DS is the direct targeting of the surfaces to be acted on, as opposed to other delivery strategies, such as oral or IV. In the latter cases, the drug will be distributed throughout the entire body and only a fraction actually reaches the targeted region (lung) (Byron and Patton, 1994; Labiris and Dolovich, 2003; Rau, 2005). With a target delivery, on the one hand, a faster onset of action is obtained, on the other hand, the drug load to be administrated is lowered. A lower administrated drug load results in a reduced plasma drug concentration, lowering the possibility of systemic adverse side effects (Jennings et al., 1991; Lipworth, 1999). Moreover, pulmonary delivery avoids the hepatic first pass metabolism oral administrated drugs go through, which may partially or totally inactivate them (Borghardt et al., 2015). Aside from the treatment of lung pathologies such as COPD or asthma, delivery of antibiotics and antivirals is of great interest when the location of initial infection and disease progression is primarily through the lungs. Some examples include de delivery of the tobramycin (TOBI® Podhaler®), antibiotic for the treatment of cystic fibrosis; or Inavir®, containing the antiviral laninamivir for treatment of influenza. More recently, the antiviral remdesivir has been studied for the treatment of Covid-19 (Sahakijpijarn et al., 2020; Vartak et al., 2021).

When considering the delivery for systemic effect, the pulmonary route is an available option for drugs which present challenges when it comes to gastrointestinal absorption. Drug delivery can be challenging due to a poor absorption and/or high metabolism in the gastrointestinal tract, or due to a variable absorption that hinder a controlled delivery. In the case of the later, parental delivery, such as subcutaneous injection, is frequently a solution (Davis, 1999). In this case, pulmonary delivery is a needle-free option, given its large surface area of contact with the systemic circulation and closer proximity to the blood flow, the rapid absorption kinetics for small molecules, and the absence of liver first pass metabolism before reaching the blood (Yadav and Lohani, 2013).

A good example of this strategy is the molecule of insulin, with products such as Exubera® (Nektar Therapeutics/Pfizer) being approved by the FDA and EMA in 2006 (Depreter et al., 2013; Santos Cavaiola and Edelman, 2014) but stopped production by 2007 due to “failing to gain the acceptance of

patients and physicians”, according to Pfizer’s CEO. Another insulin example is Afrezza®, developed by Mannkind and approved by the FDA in 2014 (“FDA Approves Afrezza to Treat Diabetes,” 2014). Other peptides and small molecules that are being studied, such as opioids for pain control (Higgins et al., 1991; Mather et al., 1998; Thippawong et al., 2003), dihydroergotamine mesylate for migraine treatment (Shrewsbury et al., 2008), interferon beta for multiple sclerosis treatment (Vallee et al., 2012), leuprolide acetate as both male and female contraception, treatment of prostate cancer, and early puberty in children (Shahiwala and Misra, 2005), parathyroid hormone and calcitonin to treat osteoporosis (Poursina et al., 2017, 2016), among others.

The pulmonary route is also a possibility for gene therapy (to deliver nucleic acids responsible for permanent expression of a gene construct, or protein coding sequence), however several challenges must be overcome before it becomes a reality (Michael Y.T. Chow et al., 2021; Laube, 2014). Being needle-free, aerosolized vaccination also presents several advantages, especially in developing countries, as it is a tool for the prevention of blood borne diseases proliferation, while requiring less medical specialized personal and medical settings for the administration, and avoiding needle disposal strategies (Laube, 2014). Some literature examples of aerosolized vaccines include the hepatitis B vaccine (Muttill et al., 2010a; Thomas et al., 2011), the diphtheria vaccine (Muttill et al., 2010b), mucosal immunity to protect against tuberculosis (Garcia Contreras et al., 2012), immunization against the human papilloma virus (Saboo et al., 2016), and the furthest along in drug development is the measles vaccine (De Swart et al., 2017). Very recently, several COVID-19 inhaled vaccine candidates in development have shown good results in pre-clinical studies (Eedara et al., 2021).

2.2.2 Physiological disadvantages optimization requirements

Throughout drug development, the natural lung defense mechanisms should be considered, as the respiratory system has evolved to minimize the entry of inhaled particles and droplets in the deep lung, and to remove the ones that enter. Considering that, pulmonary delivery requires formulation and device optimization to overcome these natural barriers. The development complexity varies depending on the delivering strategy, with nebulization being the most straight forward (limited formulation possibilities and performance mostly dependent on device used) while DPI formulations are extremely product dependent and required particle and device engineering. The formulation designed can define where the drug substance will be available and it is especially important when treating diseases confined in a

specific location, but it can also be the case the target is the lung as a whole (Stephen Newman, 2009; Ruge et al., 2013). Moreover, DPIs are subject to strict pharmaceutical and manufacturing standards by regulatory agencies, especially in regard to the demonstration of device reliability in terms of delivered dose uniformity.

To better understand the complexity of the respiratory system in regard to drug delivery and its relevance for drug delivery, in detail explanation is presented in the following paragraphs.

The respiratory system can be broken up into three main regions: the upper airways or extrathoracic region; the conducting airways or tracheobronchial region; and the alveolar airways or the respiratory region – illustrated in Figure 2.3.

The upper airways, or extrathoracic region, includes the nasal cavity, nasopharynx, mouth, oropharynx and larynx, without branching. The subsequent regions can be characterized not only by physiological attributes but also by generations based on the Weibel model. The Weibel model is one of the existing strategies to describe the arrangement of the airways branching, treating the lungs as a series of 24 airways generations, each N generation branches in 2 in generation N+1. (Weibel, 1963) It is a simplistic model, other more complex models have been described (Horsfield et al., 1971; Yeh and Schum, 1980). Models may range from empirical, not incorporating lung geometry (Rudolf et al., 1990, 1986), to mathematically complex, many-path models based on lung structure constructed from airway measurements (Anjilvel and Asgharian, 1995). However, it seems as a good way of describing the lung as a first approximation.

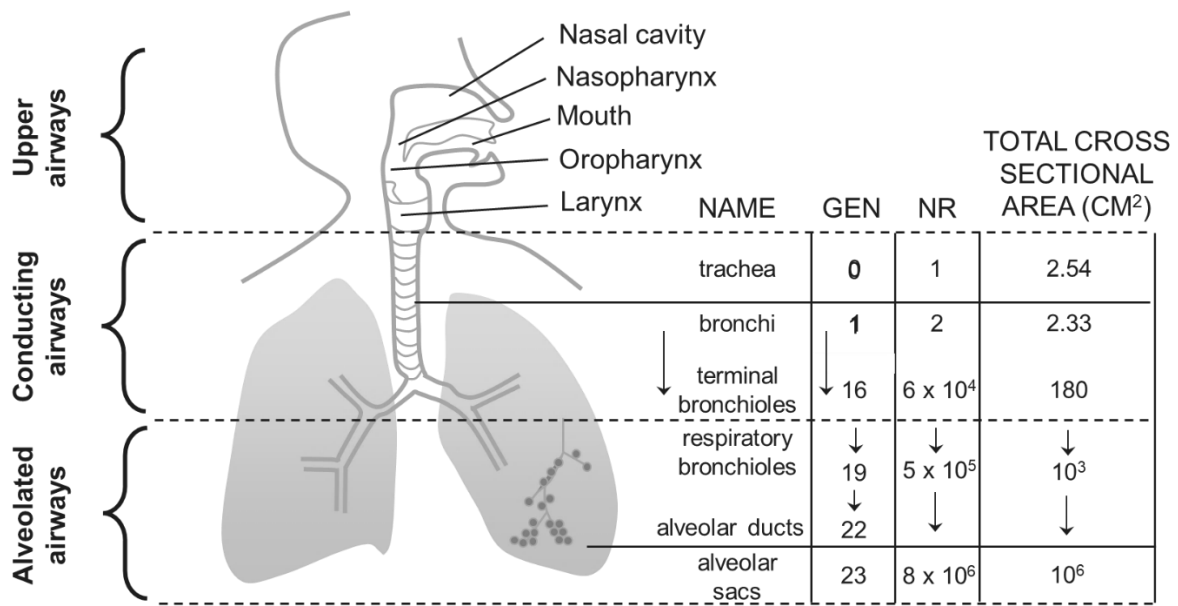


Figure 2.3 - Respiratory tract representation with lung division according to the Weibel model. GEN – generation; NR – number.

In the Weibel model, generations 0 to 16 comprise the conducting airways or tracheobronchial region. It starts in the trachea which branches at the carina into right and left main bronchi, and each main bronchus enters the lungs at the hilum. The walls of bronchi and bronchioles contain smooth muscle, but bronchi have walls supported by cartilage while bronchioles lack it. The terminal bronchioles are the smallest airway not containing alveoli. The bronchial walls are constituted by epithelial cells containing about 200 cilia per cell, and by submucosal glands and goblet cells, which are the responsible for mucus secretion (Ruge et al., 2013). The cilia drive the mucus towards the larynx (mucociliary clearance), from which it may be either swallowed or expectorated. Above the cell layer, periciliary fluid surrounds the cilia, which emerge on top to a gel layer. As the airway decreases, the mucus layer becomes discontinuous, and eventually disappears at the level of the respiratory bronchioles (Moblely and Hochhaus, 2001). Mucociliary clearance is the process of transporting mucus along the airways, and it is essential for lungs defense and health. Regarding drug action, the clearance may, on the one hand, prevent it by clearing the deposited drug, on the other hand, aid it by transporting the drug to a more central lung region, where the drug may be aimed to act on.

Weibel model's generations 17 to 23 describe the alveolated airways or respiratory region. The bronchioles have alveoli emerging from their walls, which increase in number through generations, and the region terminates in the alveolar sacs (generation 23). An acinus is the structure comprising the

alveolar ducts and the alveoli following a single bronchiole – a normal lung is constituted by approximately 25000 acini, resulting in 300-200 million alveoli, with a total volume of several liters (Stocks and Hislop, 2002), and a surface area between 100 and 190 m² (Clarke, 1984), with great variation between individual subjects. Mucus secreting cells are not present in the alveolar region, which is comprised by cells with a thickness below 1 µm, and contains pulmonary surfactant producing cells (Brain, 2007; Wolff, 1998). Once particles reach the surface of the alveolar region, they may move through the air/blood barrier, reaching the capillary – this happens by a variety of mechanisms: including passage through cells, or the paracellular transport via the tight junctions between cells (Suarez and Hickey, 2000). The mentioned transport can occur not only in the alveoli, but also in the conducting airways. Another lung defense mechanism that can be found in this lung region are the macrophages. These immune system cells absorb the deposited solid material by phagocytosis and transport it to be eliminated by the mucociliary clearance or through the lymphatic system. Moreover, the alveoli also contain esterases that alter the chemical structure of the deposited drug substances, resulting in its inactivation (Stephen Newman, 2009).

Considering the described defense mechanisms of the respiratory tract, to achieve an understanding on DPI performance two questions arise:

1. What is the real DS dose reaching the targeted region in the lung, as well as its central to peripheral distribution;
2. How long does it take for the DS to actuate (locally or systemically) or to be eliminated from the lung.

Regarding question 1, measurement and prediction of the deposited dose on the lung surface, as well as its distribution, is a fairly well studied topic. The most standard and straightforward *in vitro* method for deposition analysis is the measurement of the aerodynamic particle size distribution (APSD) by cascade impaction (described in detail in section 2.2.3), however it is well known that *in vitro* impactor results are not directly translatable to situations *in vivo* (Michael Yee Tak Chow et al., 2021). To improve the prediction value of impactor, more biosimilar mouth-throat models have been used aiming to mimic the filtering effect of the human throat (Abadelah et al., 2021; Wei et al., 2018; Zhang et al., 2007). Additionally, in recent years, novel *in silico* methods, such as Computational Fluid Dynamics capable of simulating laminar and turbulent airflow coupled with fluid-particle dynamics models were developed as useful solutions to predict particle deposition (Chen et al., 2021; Ignjatovic et al., 2021).

To predict how long a DS stays in the lung it is necessary to study its dissolution, diffusion and absorption to either the local lung tissues where it has an action, or to the systemic circulation. The dissolution and absorption of a DS depends on its molecular properties (eg. molar mass, structure, solubility, partition coefficient or dissociation constants) and on its solid state properties (eg. crystalline state, amorphous content, size or morphology). Aside from the DS properties, the wettability and dissolution profiles can be significantly impacted by the formulation strategy (used excipients and technologies), as well as the drug deposition microstructure when aerosolized, as it will affect the surface area available for dissolution as well as the local dissolution environment. However, although the literature on dissolution assessment of OINDP has been increasing, it is mostly focused on method development with a lack of data focusing on particle engineering and formulation impact (Radivojev et al., 2019).

In the following section an overview of characterization tools is presented, grouped as standard impaction apparatus and collection and dissolution/absorption systems.

2.2.3 From actuation to deposition

The application of material sciences in the characterization of the physico-chemical properties of the DS and excipients is critical to understand and optimize the performance of the final drug product. Analytical techniques used in this characterization, include optical microscopy (bright-field and cross-polarized microscopy, hot-stage microscopy); microscopy based on the use high energy electron beams (scanning electron microscopy (SEM), advanced scanning electron microscopy techniques, focused ion beam–scanning electron microscopy); microscopy based on the use of a scanning probe (atomic force microscopy, tapping mode and phase imaging, micro-thermal analysis using scanning thermal microscopy); and chemical imaging (energy-dispersive X-ray spectroscopy, raman microscopy) (Shur and Price, 2012). The listed techniques are necessary on the one hand, as a quality control tool, to identify changes on products microscopical appearance and its solid state, on the other hand, to gain information to be latter used to explain the drug product performance. For instance, SEM imaging can show, aside from real particle size, the particle porosity and shape, not attained by particle size techniques; Raman microscopy can show how the DS and excipient particles are distributed, information not obtained by other methods but highly influential on the powder performance.

Ultimately formulation development relies on the aerodynamic performance as the main characterization tool. Most pharmaceutical aerosols have particle densities different than 1 and are composed of particles

with irregular shapes, thus the aerodynamic behavior of such particles can be described by their aerodynamic diameter (D_a) or their APSD. The D_a of a particle is the diameter of a sphere of unity density that has the same settling velocity as the particle, so it is a function of particles geometric particle size, density and shape factor (Equation 2.1) (Pilcer and Amighi, 2010).

$$D_a = PS \sqrt{\frac{\rho_p}{\rho_0 \chi}} \quad \text{Equation 2.1}$$

Where PS is the geometric particle size, ρ_p and ρ_0 are the particle and unit densities, respectively, and χ is the dynamic shape factor. For example, a spherical particle with a diameter of 2.5 μm and density of 1 g/cm^3 has the same aerodynamic behaviour as a spherical particle with a diameter of 5 μm and density of 0.25 g/cm^3 .

The APSD is of the utmost importance for pulmonary drug delivery because it theoretically determines the fraction of an aerosol cloud arriving at the mouth that can penetrate into the lungs, while enabling to predict the site of the lungs where deposition is most likely to occur (Dolovich, 2000; Heyder et al., 1986). Accordingly, cascade impactors (CI) are used to classify particles according to their aerodynamic diameters, without the need to know their density or their shape (Dolovich, 1997).

In CI, particles or droplets in an aerosol plume are segregated as per their grouped characteristics that determine deposition in certain regions of the airways, considering normal human breathing. Normal breathing is defined as tidal breathing, which in a healthy adult human leads to the displacement of about 500 mL of air. While in deep breathing this volume increases to much larger volumes. The air enters the lungs because negative pressure is created by diaphragm displacement (Stephen Newman, 2009). As one moves forward through the airway generations, the cross sectional area increases immensely, due to the large number of airways (Clarke, 1984), which leads to a decrease on air velocity as it moves from the tracheobronchial to the respiratory region. With the velocity decrease, the airflow turbulence, determined by the Reynolds number (Re), is affected, as it may be turbulent in the first few airway generations, becoming laminar as it moves through (Martonen et al., 2000; Tabe et al., 2021).

Three primary mechanisms are responsible for the deposition of aerosols in the human respiratory tract (Darquenne, 2020; Martonen et al., 2000):

1. Inertial impaction – dominant mechanism in the upper airways and branching points; these are anatomic locations where the airway and airstream change direction, and if the particle has too much inertia, either because it has a large aerodynamic diameter or because it is moving too rapidly, then it may be unable to follow the airstream; it can occur during inhalation or exhalation;
2. Gravitational sedimentation – if particles penetrate to the small conducting airways and alveoli, this is generally the dominant deposition mechanism; it takes place when particles fall under gravity onto an airway wall, either during slow inhalation or during breath holding;
3. Brownian diffusion – most likely deposition mechanism for particles with diameters less than 1 μm ; these particles have insufficient inertia to deposit by inertial impaction and too low settling velocity for gravitational sedimentation to be efficient; it involves particles being deflected by molecular bombardment and hence pushed towards an airway wall; in pharmaceutical aerosols, most of the mass is composed of particles with diameters larger than 1 μm , therefore this is usually the less significant deposition mechanism.

Additionally, the three deposition mechanisms may be supplemented by electrostatic precipitation (space charge force is the repulsion between charged particles in an aerosol cloud), by the effects of turbulent air flow (flow fluctuations cause particles to change direction and to deposit on airway walls) and by interception (when a particle comes close enough to an airway wall that an edge touches its surface) (Darquenne, 2020). Due to the presence of lining liquids in the airways, once a particle has deposited on a human airway surface, it remains deposited and does not detach again.

As stated above, in the conducting airways of the lungs most aerosol deposition occurs by inertial impaction and this process is simulated in a CI. When a particle's inertia overcomes its aerodynamic drag it comes into contact with surfaces defining the air flow path in the lung, or a collection plate in a stage of a CI. Figure 2.4 illustrates the listed deposition mechanisms and how the CI simulates the pulmonary airways in order to collect particles according to their deposition mechanism – particles depositing earlier in the respiratory tract by inertial impaction will be collected in the earlier stages of the cascade impactor due to their larger D_a .

Smaller particles avoid impaction and follow the air stream either to another bifurcation in the lung or to another impaction plate in a CI (Dalby et al., 2009) - Figure 2.4.

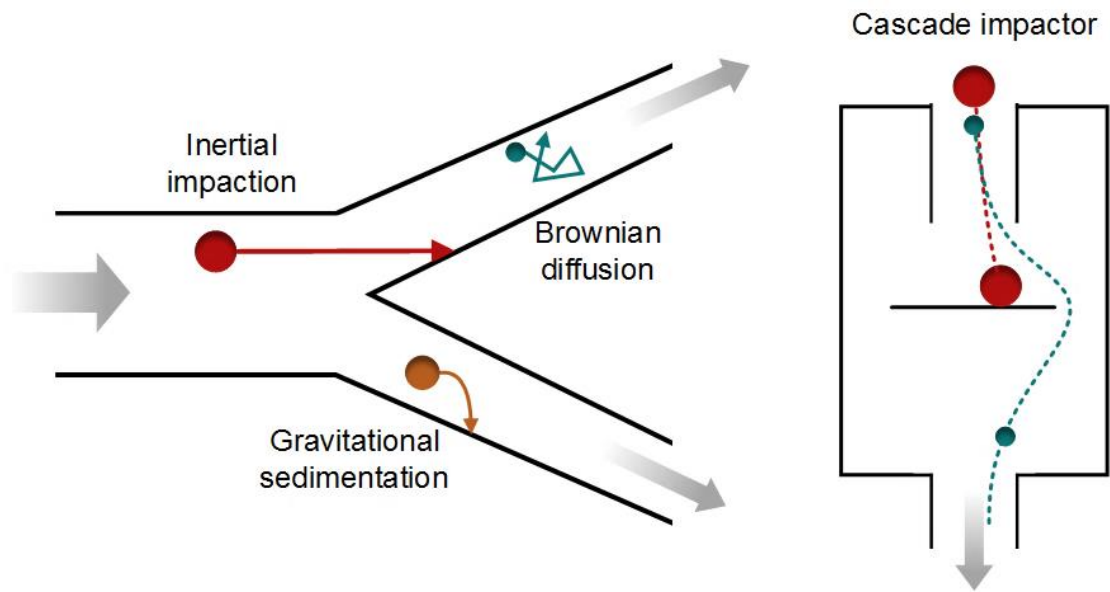


Figure 2.4 - Schematic of the three major deposition mechanisms for inhaled particles in the respiratory tract and its relationship to particle impactation in a cascade impactor. The grey arrows show the direction of air flow. Adapted from (Dalby et al., 2009)

CI consist of a series of stages, each comprising one or more jets or nozzles. Air is forced to flow through an inhaler, dragging the particles with it into the impactor at a constant volumetric flow rate. The jet or nozzle size generally decreases progressively with distance through the impactor so that the linear velocity of air flowing through successive stages increases, allowing smaller particles to impact on the collection plate or surface. (Dalby et al., 2009) While a CI should not be viewed as a model lung, it separates particles based on their aerodynamic behavior and is the most easily justified sizing method for inhalation aerosols (Mitchell et al., 2007).

The APSD is the main output of the CIs, it is most often expressed in terms of mass and this may be plotted against aerodynamic particle size as a frequency distribution or as a cumulative one, as shown in Figure 2.5 (S. Newman, 2009). Three widely used parameters that are an output of the APSD are:

- Fine particle fraction (FPF) – percentage of the aerosol drug mass constituted by particles smaller than 5 μm of aerodynamic diameter; FPF values usually correlate well with the percentage of dose which is deposited in the lungs, but systematically overestimate it (Michael Yee Tak Chow et al., 2021; Newman and Chan, 2008);
- Mass median aerodynamic diameter (MMAD) – aerodynamic diameter above and below which half of the aerosol mass resides; for heterodisperse aerosols, the use of MMAD alone is

inappropriate because its significance decreases as the geometric standard deviation increases;

- Geometric standard deviation (GSD) – a dimensionless variable, its most usual definition is: $\sqrt{D_{84.1}/D_{15.9}}$; a perfectly monodisperse aerosole has a GSD of 1; however, in practical terms, an aerosol with GSD lower than 1.22 is generally regarded as acceptably monodisperse (Fuchs and Sutugin, 1966); most pharmaceutical aerosols are heterodisperse with GSD values typically between 1.5 and 2.5.

In the example shown in Figure 2.5, the MMAD is 4.0 μm (D_{50}) and the FPF can be read from the point on the y-axis (cumulative distribution) corresponding to 5 μm on the x-axis, and it is 62%.

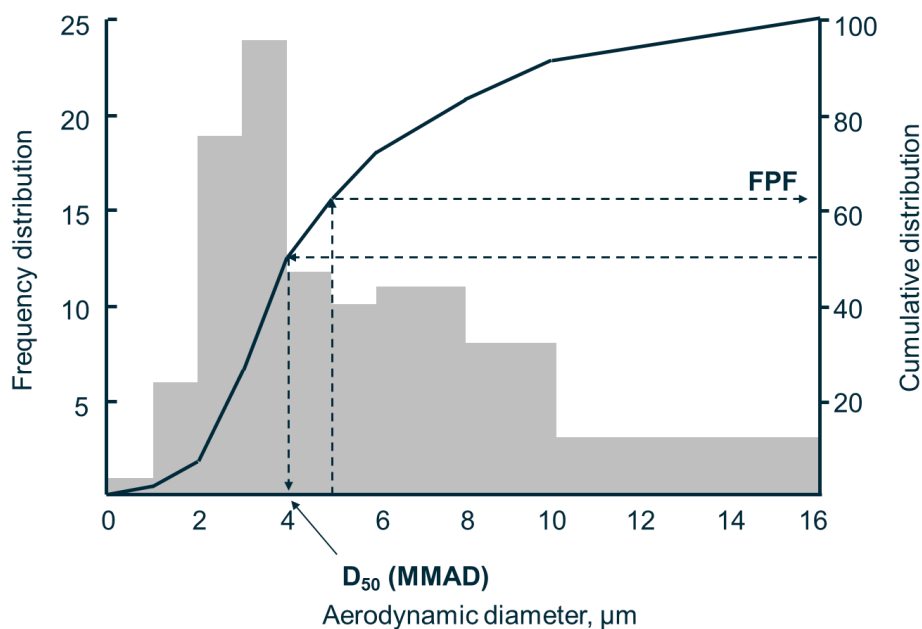


Figure 2.5 - Example of an aerodynamic particle size distribution plotted as a frequency distribution (grey) or as a cumulative on (black line). Mass median aerodynamic diameter (MMAD) and fine particle fraction (FPF) are indicated in the distribution. Adapted from (S. Newman, 2009).

Drug deposition and clinical effect have a high degree of variability between patients. For that reason, a general effort has been made to exclude biological implications from the terms used to describe *in vitro* test metrics. For example, the term “fine particle dose” (FPD, the dose of drug deposited in a CI corresponding to particles below a stated value of aerodynamic diameter) is preferred to “respirable dose”. Additionally, there is a trend away from FPF (which implies a fraction of some other value) or MMAD and GSD, both of which assume a log normal PSD and which may be insensitive to variations

in the mass of drug corresponding to smaller particles. It is now more common to report the actual mass of drug in each size fraction or CI stage (or group of stages). (S. Newman, 2009)

In the following sections some of the most commonly used impactors will be described.

2.2.3.1 Andersen Cascade Impactor

The andersen cascade impactor (ACI), presented in Figure 2.6, is a conventional cascade impactor widely used for the evaluation of inhaled products. Aerosol is introduced through the mouthpiece adaptor, which forms an inhaler specific airtight seal around the inhaler mouthpiece. The induction port, commonly known as the United States Pharmacopeia (USP) throat, is a simple cylindrical tube with a circular cross-section and a right angle (Dalby et al., 2009). Its purpose is to exclude the aerosol particles that are considered too large in aerodynamic diameter to enter the lungs. Drug deposited in the mouthpiece adaptor, the induction port and the entrance cone are not considered to have entered the ACI but it is included in the calculation of the drug that has entered the sizing apparatus. Each of the stages 0 to 7 comprises an array of jets and has a collecting plate beneath it, while stage F incorporates a filter.

CIs used to evaluate DPIs must be operated at air flow rates dictated by the resistance of the inhaler. The procedure for establishing the appropriate flow rate involves adjusting the pressure drop across the device to 4 kPa using a dose collection tube and measuring the respective flow rate. The flow rate is registered and used in all future actuations of the corresponding inhaler. When using different flow rates some of the ACI stages differ - while stages 0-7 are used for 28.3 L/min, stages -1, -0 and 1-6 are used for 60 L/min and stages -2A, -1A, -0 and 1-5 are used for 100 L/min (Roberts et al., 2020).

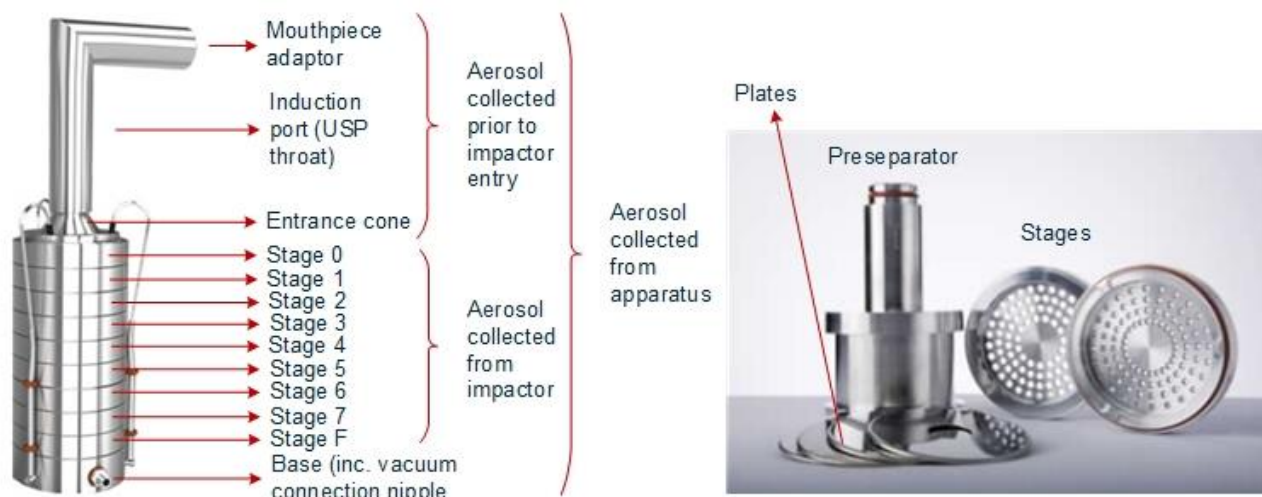


Figure 2.6 - Left: Andersen cascade impactor fitted with an induction port; right: stages, plates and pre-separator.

2.2.3.2 Next Generation Impactor

Because early ACIs showed large data variability between instruments (Stein and Olson, 1997), there was a combined effort by several companies to design the NGI as a more suitable instrument for pharmaceutical use (Dalby et al., 2009). Nonetheless, at the same time much better control has been introduced in the manufacturing of new ACIs, hence it is still very used in the pharmaceutical industry. One of the design criteria for the next generation impactor (NGI) was the potential for automation and easier recovery of drug, achieved through the use of cups, the bottom of which are the impaction surfaces Figure 2.7 (Marple et al., 1995; Virgil A. Marple et al., 2003a, 2003b). Other required features include an operating range of flow rates between 30 and 100 L/min, low wall losses and good drug recovery to ensure mass balance, being operator independent with good accuracy and precision, among others.

During operation, the aerosol is introduced into the NGI through the induction port, using a mouthpiece adaptor as a connection to the inhaler device, just like the ACI. The stages are followed by a micro-orifice collector that is 90% efficient for particles larger than or equal to 0.2 μm aerodynamic diameter. Additionally, pre-separators can be used with the ACI and the NGI during the testing of DPIs in order to eliminate an overload of their upper stages due to the capture of large drug and excipient particles (Roberts, 2000).

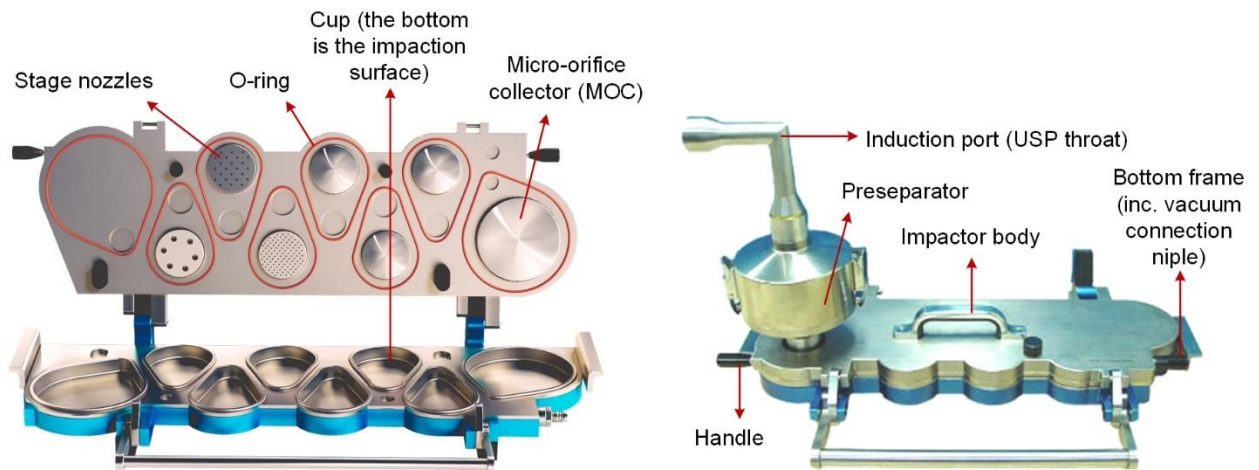


Figure 2.7 - Right: Next generation impactor (NGI)'s particle collection cups; Left: NGI with pre-separator and induction port.

2.2.3.3 Fast Screening Impactor

The fast screening impactor (FSI) - Figure 2.8 - has been designed as an abbreviated impactor to avoid the labor intensive procedures of the multi-stage cascade impactors NGI and ACI in initial screening and development studies of inhaled products and devices (Mohan et al., 2017). The FSI is not a compendial apparatus, but has been benchmarked against the ACI and NGI with results proving acceptability of the FSI as an abbreviated apparatus (Després-Gnis and Williams, 2010; Russell-Graham et al., 2010)

It is composed by an induction port similar to the used in the NGI, and a PS containing a fine cut insert with an effective cut off diameter of 5 μm . All the particle with an aerodynamic diameter lower than 5 μm , the fine particle fraction, pass on and deposit on the filter stage. The operation of the FSI is similar to the NGI apparatus, actuating the device into the induction port, using a mouthpiece adaptor as a connection to the inhaler device, at the defined flow-rate. The FSI can be used with a variety of inserts which provide a FPF cut-off at a range of flow rates, 39, 60, and 90 L/min.

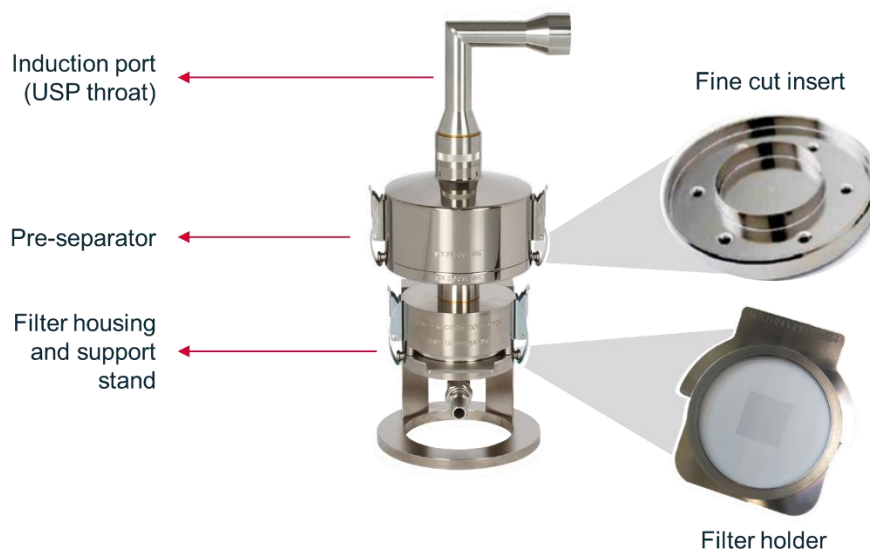


Figure 2.8 – Fast screening impactor (FSI) fitted with an induction port and pre-separator, including fine cut insert and filter holder.

2.2.4 Dissolution or inhaled drug products

There are several factors which should be considered when aiming to understand the effect of a locally acting inhaled drug substance or prove bioequivalence, such as patient-device-formulation interaction, regional DS distribution and local dissolution, permeability, and clearance. Dissolution of OINDP is challenging, but if successfully developed, may provide a link between the regional drug substance deposition and local and systemic pharmacokinetics of these products.

When developing a dissolution system for OINDP, there are several challenges to be overcome. Firstly, the selection/development of the sample collection method, as well as the design of an appropriate method for the transfer of the collected samples to dissolution apparatus (Florioiu et al., 2018); secondly, to decide between sink conditions versus physiologically relevant conditions, and if the latter is selected as the optimal choice, the challenge becomes to simulate the lung surface where the dissolution takes place, including the presence or not of mucus, its composition and its influence in the dissolution and permeation process, and the selection of an appropriate dissolution media; thirdly there is the validation of bio-predictability or of significant formulation differentiation (in the case of a quality control method); lastly, to define acceptance criteria and standardize the dissolution system.

Several dissolution systems for OINDPs have been proposed, with different sample collection strategies, dissolution set-ups, and ultimate goals (formulation differentiation versus bioequivalence tool). Examples of dissolution techniques for orally inhaled drugs are presented in Table 2.4.

As stated above, the strategies used to evaluate dissolution kinetics of inhaled DS are crucial to speed development of new drug products as well as to reduce the burden of current bioequivalence requirements. In the following sections, several of these strategies are explained and evaluated in detail.

Table 2.4 - Summary of dissolution techniques studied for orally inhaled drugs.

| Sample collection | References |
|---|--|
| No collection mechanism | (Asada et al., 2004; Buttini et al., 2018; Mezzena et al., 2009; Raula et al., 2013; Salama et al., 2008) |
| Impinger | (Grainger et al., 2012b; Haghi et al., 2012; Kumar et al., 2017) |
| Andersen Cascade Impactor | (Arora et al., 2010; May et al., 2015, 2014, 2012; Tay et al., 2018) |
| Next Generation Impactor | (Chan et al., 2013; Depreter et al., 2013; Duret et al., 2012; Fernandes et al., 2016a; Mangal et al., 2018; Noriega et al., 2018b; Pilcer et al., 2013; Rohrschneider et al., 2015a; Son and McConville, 2012, 2009; Son et al., 2010) |
| Dosage unit sampling apparatus | (Farias et al., 2017; Price et al., 2020) |
| Preciselnhale® | (Gerde et al., 2017a; Hassoun et al., 2019; Malmlöf et al., 2019; Noriega-Fernandes et al., 2021; Noriega et al., 2017) |
| Apparatus | |
| USP Apparatus I | (Asada et al., 2004) |
| USP Apparatus II | (Duret et al., 2012; Fernandes et al., 2016b, 2016a; Mangal et al., 2018; May et al., 2014, 2012; Noriega et al., 2018b; Pilcer et al., 2013; Raula et al., 2013; Salama et al., 2008; Son and McConville, 2012, 2009; Son et al., 2010) |
| Flow-through system/ USP Apparatus IV | (Davies and Feddah, 2003; Gerde et al., 2017a; Hassoun et al., 2019; Malmlöf et al., 2019; May et al., 2014, 2012; Mezzena et al., 2009; Noriega et al., 2017; Salama et al., 2008) |
| Diffusion-controlled apparatus | (Arora et al., 2010; Buttini et al., 2018; Chan et al., 2013; Grainger et al., 2012b; Haghi et al., 2012; Kumar et al., 2017; Mangal et al., 2018; May et al., 2015, 2014, 2012; Rohrschneider et al., 2015b; Salama et al., 2008) |
| Medium | |
| Phosphate buffered saline | (Arora et al., 2010; Mangal et al., 2018; May et al., 2015, 2014; Mezzena et al., 2009; Pilcer et al., 2013; Raula et al., 2013; Salama et al., 2008; Son et al., 2010) |
| Phosphate buffered saline + surfactant | (Grainger et al., 2012b; Haghi et al., 2012; May et al., 2012; Son et al., 2010) |
| Simulated lung fluid | (Chan et al., 2013; Davies and Feddah, 2003; Kumar et al., 2017; Virgil A. Marple et al., 2003b; Son and McConville, 2009) |
| Simulated lung fluid + surfactant | (Virgil A. Marple et al., 2003b; Mezzena et al., 2009; Son and McConville, 2009) |
| Artificial mucus | (Gerde et al., 2017a; Hassoun et al., 2019; Malmlöf et al., 2019; Noriega-Fernandes et al., 2021; Noriega et al., 2017) |
| Other (buffers, water, duffer + surfactant) | (Asada et al., 2004; Buttini et al., 2018; Davies and Feddah, 2003; Duret et al., 2012; Kumar et al., 2017; Son and McConville, 2012) |

But wait, is it always necessary?

Before endeavoring in the exhaustive descriptions, it is important to understand when to use these techniques, i.e., for which drugs dissolution and/or permeation tests can result in biorelevant predictions.

Employing the biopharmaceutical classification system (BCS), schematized in Figure 2.9, DS can be divided in four classes, depending on their solubility and permeability. For locally acting orally inhaled drugs, it can be said that only class II and IV molecules are good testing entities, as class I molecules are not limited by dissolution, and class III molecules present a low permeability and therefore the total residence time in the lung will depend on other factors – e.g. macrophage action.

| | | |
|--------------------------|------------------------|-----------------------|
| | High solubility | Low solubility |
| High permeability | Class I | Class II |
| Low permeability | Class III | Class IV |

Figure 2.9 - Biopharmaceutical classification system.

To focus the discussion to a list of selected compounds administered through the inhalation route and their BCS classification and application is presented in Table 2.5.

However, academia and industry have initiated the design of a BCS system for inhalation drugs (iBCS), which besides solubility and permeation will most likely consider the regional surface area, local activity (affected by the formulation and used device) and physicochemical properties of the formulation. Therefore, there is a need for the standardization of advanced characterization techniques and *in vitro* tools capable of categorizing the drug products in an inhalation classification system, conjugating aerodynamic performance and particle characterization to deposition structures and dissolution in a biorelevant media, considering the following Figure 2.10 (Gallegos-Catalán et al., 2021; Velaga et al., 2017):

Table 2.5 - List of selected compounds delivered by the inhalation route.

| Category | Name | BCS |
|------------|------------------------|----------------|
| Steroids | Hydrocortisone | I (a) |
| | Budesonide | II (a) |
| | Betamethasone | II (a) |
| | Fluticasone Propionate | II (b) |
| | Mometasone Propionate | II (b) |
| SABA | Salbutamol/albuterol | I (b) - II (a) |
| | Terbutaline | I (a) |
| LABA | Formoterol | II (a) |
| | Salmeterol | III (b) * |
| LAMA | Tiotropium | III (b) |
| Antibiotic | Amphotericin B | II (c) * |
| Antibiotic | Ciprofloxacin betaine | II (c) * |
| Antiviral | Laninamivir | III (d) |
| Hormone | Insulin | III (e) |

SABA – short-acting β 2-agonists; LABA – long-acting β 2-agonists; LAMA – long-acting muscarinic antagonist. (a) from (Eixarch et al., 2010); (b) from (Hochhaus, 2018); (c) from (Hastedt et al., 2016); (d) from (Holmes et al., 2013); (e) (Poovi and Damodharan, 2018); * dissolution limited due to the low lining fluid volume of the high dose delivered.

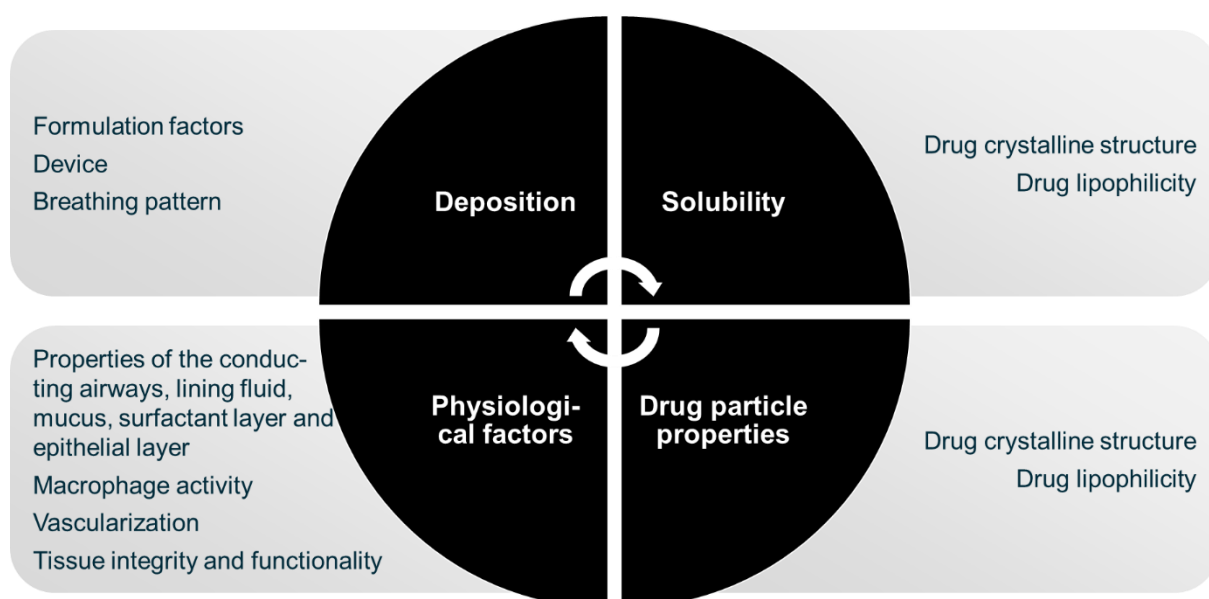


Figure 2.10 – Parameters considered in the inhalation biopharmaceutical classification system.

When developing these tools, regarding dissolution it makes sense to start by looking at the apparatus already described in the Pharmacopeia used to characterize other dosage forms intended for different delivery routes (eg. USP Apparatus II or USP Apparatus IV for oral delivery). However, these cannot be directly applied for inhalation dosage forms as per described in the pharmacopoeias – method adjustments must be implemented, such as the sample preparation by particle collection previous to dissolution testing or the dissolution medium composition. A listing of the specific similarities and differences between the two methodologies has been addressed in other reviews (Radivojev et al., 2019).

In the following sections, systems attempting to fill the required specification for an inhalation dissolution *in vitro* tool are presented, mostly focusing on the testing system, the collection method and dissolution set up (medium, temperature, stirring, volume, etc.).

2.2.4.1 Paddle dissolution (USP Apparatus I and II)

Dry powders intended for inhalation were previously widely tested using the standard paddle apparatus or a modified basket apparatus (USP Apparatus I and II represented in Figure 2.11 (Pharmacopeia United States, 2011)) (Asada et al., 2004; Jaspart et al., 2007; Learoyd et al., 2008; Sheng et al., 2008). In this system, the dissolving material is placed inside a 900-1000 mL solution and is kept resting below a smoothly rotating paddle (Forbes and Richer, Nathalie Hauet Buttini, 2015). However, these are not optimal systems to assess dissolution kinetics for dry powders for several reasons. First, the dry powders do not have an easy homogeneous dispersibility in the vessel or basket, with dispersed particles sticking into the vessel walls as well as into the basket and/or the paddle. Secondly, undissolved powder dispersed in the dissolution media can be accidentally collected during the sampling, leading to significant variability. Additionally to the functional challenges USP apparatus I and II do not provide an easy way to analyze the relevant fraction of powder which actually reaches the lungs, and therefore it completely disregards the effect of particle size on the dissolution profile, as well as powder aerosolization and deposition (the particles may deposit as agglomerates of DS, DS-excipient, and these agglomerates may present various structures) (Farias et al., 2017)f.

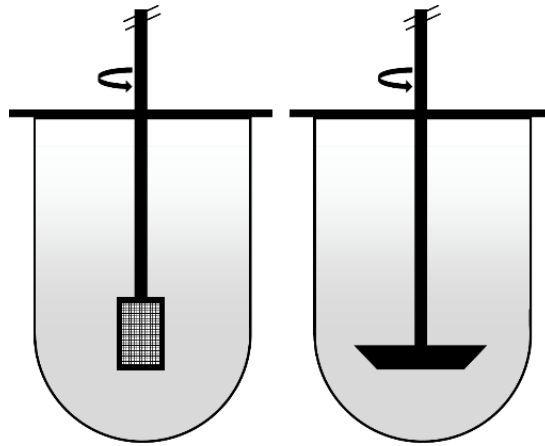


Figure 2.11- Schematic representation of UPS apparatus I (left) and II (right).

In an attempt to adapt these already standardized apparatus, the paddle over disk (POD) was tested for inhalation dry powder by combining the apparatus II with a disk containing collected powder to be tested (Figure 2.12). The POD requires very basic equipment, which is an advantage, and also allows for more complex assessments such as evaluating the impact of the particle size distribution of the sample on the dissolution profile by collecting powder fractions from different CI stages and comparing their dissolution profiles. These are relevant results to gain understanding of the dissolution of dry powders throughout the respiratory tract.

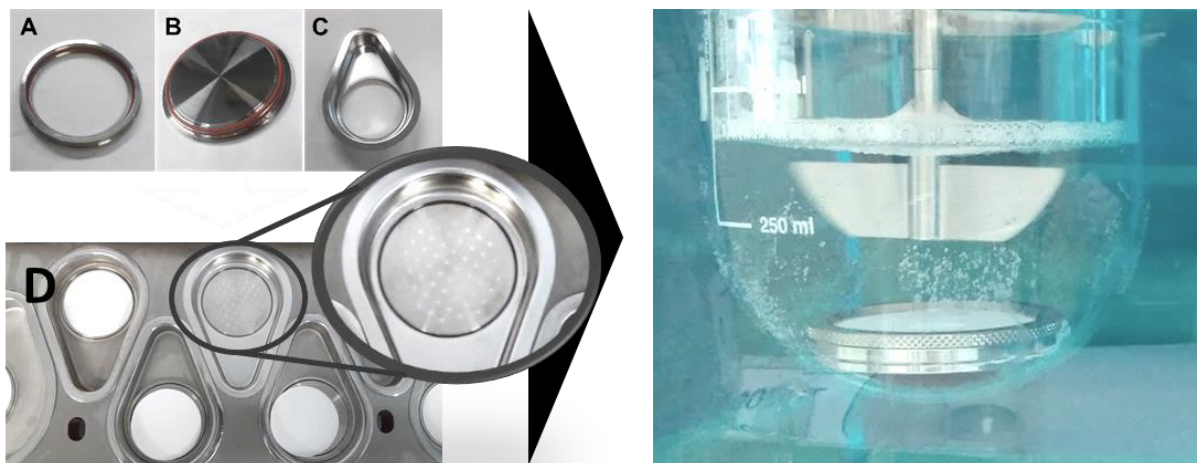


Figure 2.12 - Paddle dissolution apparatus used in combination with the next generation impactor. A – Securing ring of the membrane holder; B – stainless steel collector; C – Dissolution cup; D – NGI with dissolution cup after actuation. Right: Dissolution vessel with membrane holder. Adapted from (Fernandes et al., 2016a)

There are different renditions of this adaptation, with variations on the dissolution conditions and on the set-up, with different commercially available sample holders being used, containing themselves different collection filters and diffusion membranes.

In 2009, Son et al. (Son and McConville, 2009) developed a prototype using the POD to assess the dissolution/diffusion profile of hydrocortisone blended with lactose, in conjugation with the NGI for sample collection. In this work, polycarbonate membranes are placed on the NGI impaction stages, the powder is collected during the inhaler actuation, and the sample is then sandwiched with another polycarbonate membrane placed on top of the powder, pre-wetted, and fitted into a modified histology cassette. The cassette is then placed in the paddle apparatus. It was observed the dissolution rate could be estimated, with a significant differentiation between the dissolution profiles of particles collected in different stages - faster for smaller particles collected at later impactor stages. These results motivated the optimization of the procedure to achieve a standardizable test.

In the following works, a membrane holder assembly to be used directly in the NGI stages was designed and tested (Son et al., 2010), and it is currently commercialized by Copley Scientific. Its application is schematized in Figure 2.12. Commercial dry powder inhaler products were tested with the optimized set-up – it was observed that the amount of drug loading on the collector had a significant influence on the dissolution profile obtained, and that it was more relevant more relevant for lower solubility DS.

The profiles obtained using this system are a result not only of the dissolution rate of the product, but also of the diffusion imposed by the polycarbonate membrane. Son *et al.* observed an increase in the diffusion constant with the addition of surfactant, proposing that the surfactant may help the migration of the DS particles through the membrane (Son et al., 2010). Thus, different surfactants were tested in order to increase the migration through the membrane and avoid the dose dependency concluding that for poorly soluble drugs the type and percentage of surfactant should be optimized so that the membrane diffusion rate is not the limiting step.

May *et al.* tested a different strategy for powder collection and set-up of the POD apparatus – the powder was collected using an abbreviated ACI, so that all particles with an aerodynamic diameter smaller than 5 μm (fine particle fraction) are tested; and the membrane holder consists of a watch glass, where the particles collected on a cellulose filter are placed facing the glass, and fixed in space by a securing grid (schematized in Figure 2.13) (May et al., 2012). In this study, DS of different solubilities are tested, concluding that the POD could discriminate between all substances. A dependence on dose was

observed, however in this case there was not a diffusion membrane acting as a barrier for dissolution, suggesting that the differences observed are probably due to the wettability of the powder when deposited in greater amounts.

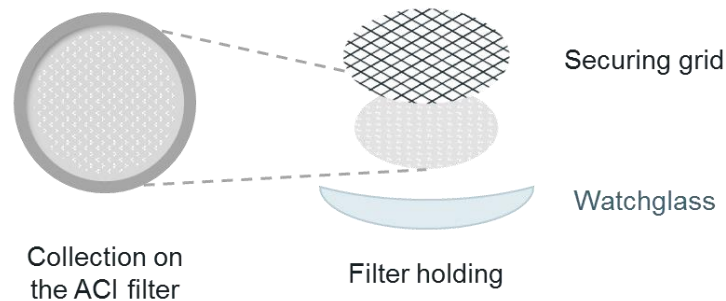


Figure 2.13 - Schematic representation of the powder securing strategy used by (May et al., 2012)

Price *et al.* (Farias et al., 2017; Price, 2018; Price et al., 2020) have developed an improved dose collecting system for the NGI, aiming to avoid the formation of powder “hotspots” and powder layers caused by the NGI stage jetnozzles (see deposition pattern in Figure 2.12, D), and consequently obtain dissolution profiles not dependent on powder sample preparation. The set-up is schematized in Figure 2.14. After powder collection on a glass microfiber filter, it is placed into a purpose-built cassette for the POD. Price *et al.* presented data during the “New Insights for Product Development and Bioequivalence Assessments of Generic Orally Inhaled and Nasal Drug Products” workshop (Price, 2018) of the low solubility DS fluticasone propionate dissolution with 1 to 10 shots, without dose influence. Moreover, the system has the capacity to differentiate between pMDI and DPI FP formulations. Later the data was published showcasing the set-up application to a range of corticosteroids with a good correlation between *in vivo* mean absorption time and *in vitro* dissolution half-life (Price et al., 2020).

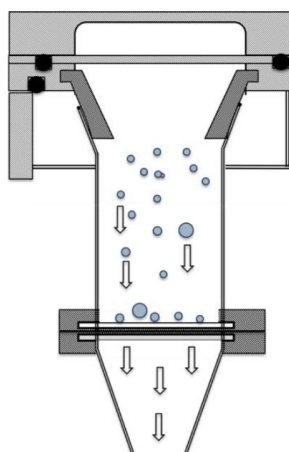


Figure 2.14 - Schematic representation of the UniDose™ collection system, from (Farias et al., 2017).

All presented configurations lack physiological relevance when considering the conditions in the lungs. For instances, even in the study where a smaller solution volume was used (Son et al., 2010), the volume is still too large to accurately represent the volume of lung fluid. Moreover, sink conditions are always maintained in these studies, which may or may not be the case when a particle dissolves in the lung (Radivojev et al., 2019).

2.2.4.2 Flow-through cell (Apparatus IV)

As the POD is an adaptation of the USP apparatus II, the various flow-through cell set-ups used in the assessment of the dissolution rates of inhalable dry powders are variations on the standard USP apparatus IV, schematized in Figure 2.15 (Pharmacopeia United States, 2011).

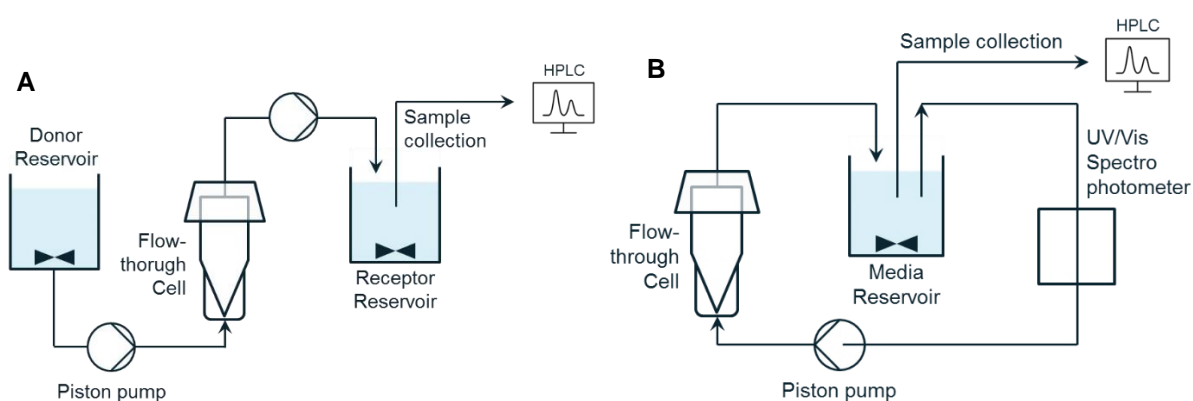


Figure 2.15 - Schematic representation of the USP apparatus IV operating A) as an open and B) as a closed system.

When using this equipment, the medium is equilibrated at a given temperature and pumped at a constant flow through the flow cell, where the formulation powder is placed. The equipment may run as an open system, with fresh medium from the reservoir continuously passing through the cell, or closed system configuration, where a fixed volume of liquid is recycled - Figure 2.15 A and B, respectively. The dissolution rate is evaluated by quantifying the DS in the receptor reservoir, in a non-cumulative form (open) or in the media reservoir, in the cumulative form (closed). The flow-through cell may be of different types depending on what is being tested, however there is not a standardized cell designed specifically to test the dissolution of inhalation forms. (Fotaki, 2011)

Thus, to use this apparatus for inhalation forms, modified versions of the flow-through cells were tested, aiming to combine the equipment with filter holders for particles within the fine particle fraction.

Davies and Feddah designed an advanced flow-through cell which consists of a modified 25 mm Millipore filter holder, schematized in Figure 2.16 (Davies and Feddah, 2003). This set-up is designed to ensure that all the particles on the collection filter experience the same flow of dissolution medium - homogeneity is achieved in the cell with very low flows, and therefore a minimum flow may be practiced. In this study, the open system set-up (Figure 2.15, A)) is used, which is stated to ensure a sink conditions' dissolution (the dissolution medium is always fresh). The lower the flow, the smaller the total dissolution volume - this is presented as one of the main advantages of using the flow-through system as a dissolution set-up for inhalation powders, usually poorly soluble: the capability to achieve sink conditions with a very small volume. However, the results showed a linear dependence between the dissolution rate and the flow-rate used, which may indicate the contrary. As pointed out by Riley *et al.*, the flat geometry of the dissolution cells has the potential to generate a higher fluid velocity at the center of the filter, and a decreasing flow gradient towards the periphery (Riley *et al.*, 2012). Another observed limitation of the flow-through cell is air entrapment, which may influence dissolution.

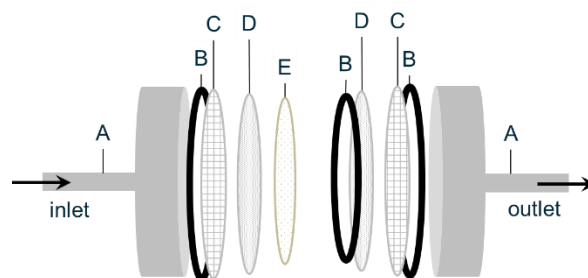


Figure 2.16 – Dissolution cell designed by Davies and Feddah, adapted from (Davies and Feddah, 2003). (A) stainless steel filter holders; (B) Teflon rings, (C) stainless steel screen support filters; (D) a 0.45µm pore size cellulose acetate membrane filters; (E) glass fibre filter containing the drug particles.

Salama *et al.* applied the described system to differentiate controlled release formulations, comparing the system with other dissolution technologies, concluding it performed worse than the paddle apparatus and the diffusion cell – no formulation differentiation was obtained (Salama et al., 2008). May *et al.* also compared the three techniques in the differentiation of DS with different solubilities, however using a cell modified by Boehringer Ingelheim to ensure uniform flow, observing an inability to differentiate between the APIs with a similar solubility (May et al., 2012).

Considering the listed results, one may completely disregard the usage of the flow-through cell, however it is important to consider that, from the presented possibilities of adapted dissolution techniques for inhalation forms, this is the only one which is not influenced by membrane diffusion, which may be the more biorelevant option for locally acting APIs. The obtained results may be a result of the lack of the diffusion resistance present in the remaining set-ups.

2.2.4.3 Diffusion-controlled cell apparatus

Diffusion-controlled cell apparatus have also been tested to assess the dissolution and diffusion of orally inhaled DS. Some examples are the Franz cell as an agitated system, presented in Figure 2.17, A (May et al., 2012), or the Transwell® system as a non-agitated, in Figure 2.17, B (Arora et al., 2010; Rohrschneider et al., 2015b). These apparatus aim to be a more biosimilar dissolution set up due to (i) the possibility of using a few milliliters of dissolution medium, and (ii) the fact the set up imposes the dissolution of the particles in a low-thickness fluid, and after that the diffusion to the receptor compartment. Diffusion-controlled systems are composed by a donor compartment above the membrane, where the solid material is placed, and a receptor compartment below the membrane. The volume of dissolution media in the donor compartment is usually low (< 1 mL), while in the acceptor compartment it can range from a few milliliters up to 1 L (Riley et al., 2012). After dissolution, there is a diffusion step through the membrane. Therefore, to compare dissolution profiles without the influence of different diffusion effects, it is necessary to determine the dissolution coefficient, its reproducibility and the affinity of the compound to the membrane before each experiment, or to eliminate the diffusion factor by adapting the membrane or medium. In terms of formulation differentiation, Salama *et al.* compared a modified Franz cell with USP apparatus II and a flow through model observing that the Franz cell provided the greatest differentiation (Salama et al., 2008). Contrariwise, May *et al.* compared the same systems and demonstrated that even though all three apparatus could discriminate between

poor and highly soluble drugs, the Franz cell could not discriminate between materials with small differences in solubility, similarly to the flow-through apparatus (May et al., 2012). Additionally, the same authors also concluded that air trapped beneath the membrane of a Franz cell leads to very low reproducibility of the results. Arora *et al.* demonstrated that with increasing sample mass the dissolution profiles obtained using the Transwell® system were decelerated due to the low volume of dissolution medium in the donor compartment which leads to undissolved particles (Arora et al., 2010).

The diffusion controlled systems are limited when it comes to prediction of DS bioavailability and release into the circulation as it is still unknown how the diffusion correlates with the *in vivo* drug behavior. Therefore, in an attempt for optimization, Rohrschneider *et al.* adapted the previously used Transwell® system to make the dissolution the rate-limiting step and not the diffusion, by incorporating a faster equilibrating membrane and using a dissolution medium with surfactant (Rohrschneider et al., 2015b). The results showed an agreement between the rank order of dissolution rates and the APIs absorption rates from pharmacokinetics studies.

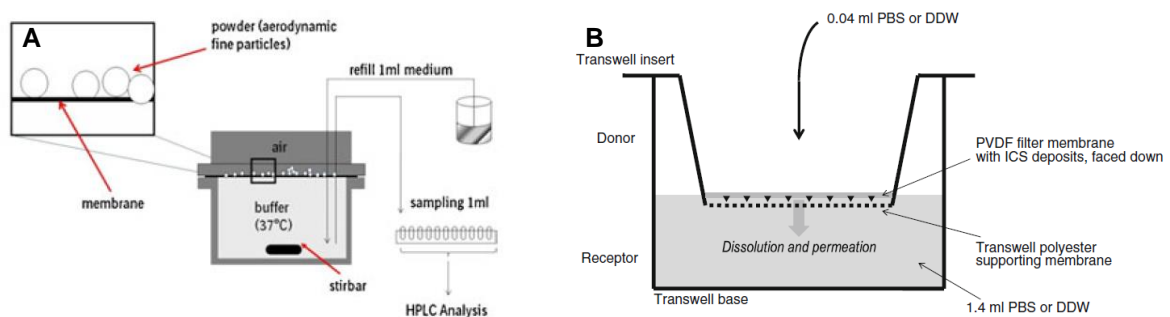


Figure 2.17 – (A) Franz cell dissolution apparatus from (May et al., 2012); (B) Transwell® system dissolution apparatus from (Arora et al., 2010).

More recently, a different diffusion system cell was developed by Gerde *et al.* aiming to achieve a more biorelevant system, including dissolution, diffusion through mucus simulant and diffusion through membrane to a blood simulant – DissolvIt® (Gerde et al., 2017a), illustrated in Figure 2.18. Moreover, unlike the flow-through systems, the medium flow is tangential to the powder particles, as it is the case for blood vessels in the alveoli.

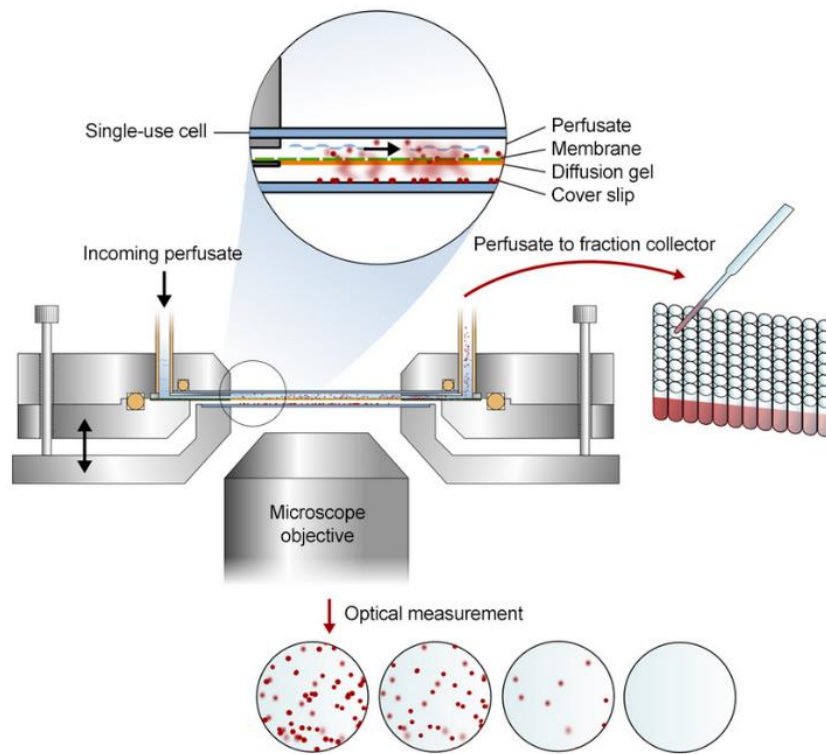


Figure 2.18 – Schematic representation of the DissolvIt® system, adapted from (Gerde et al., 2017a).

Prior to dissolution testing, the powder is collected using a breath simulator PreciseInhale® developed by the same authors (Gerde et al., 2004), schematized in Figure 2.19. PreciseInhale® includes an induction port acting as a CI induction port to account for throat impaction prior to entering the deposition chamber. However, the system does not include a pre-separator stage, meaning the particles collected for dissolution assessment may include coarser particles which do not reach the deep lung.

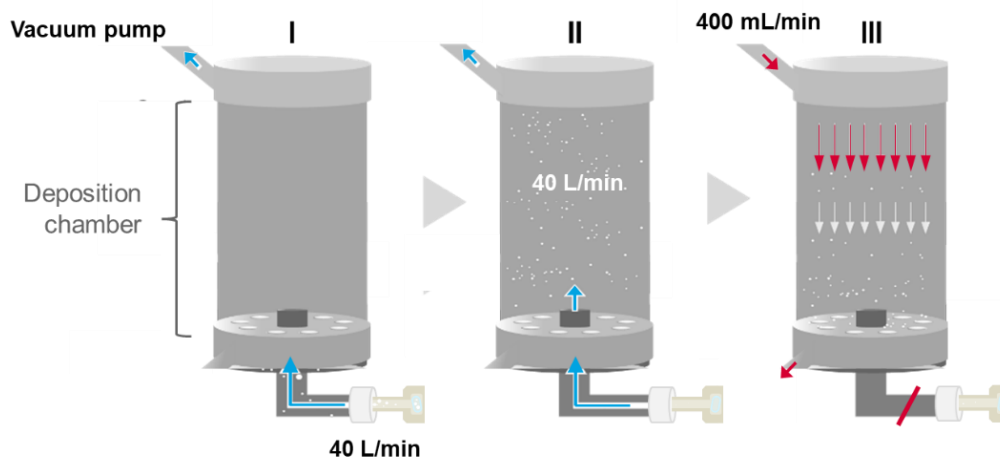


Figure 2.19 - Schematic of PreciseInhale® actuation and glass holding.

Using a breath simulator as a collection method has the advantage of ensuring particle interaction and agglomeration during collection (Figure 2.19, III), meaning the dissolution profile obtained accounts for a biorelevant particle deposition and interaction. The slow deposition is a core step as it allows the formation of powder microstructures which may have a significant influence in the dissolution behavior. In Figure 2.20 it is possible to see how budesonide and fluticasone propionate deposit forming different microstructures. The dissolution set-up includes an inverted microscope, enabling the observation not only of the structures of the deposited particles, but also its dissolution as the experiment takes place.

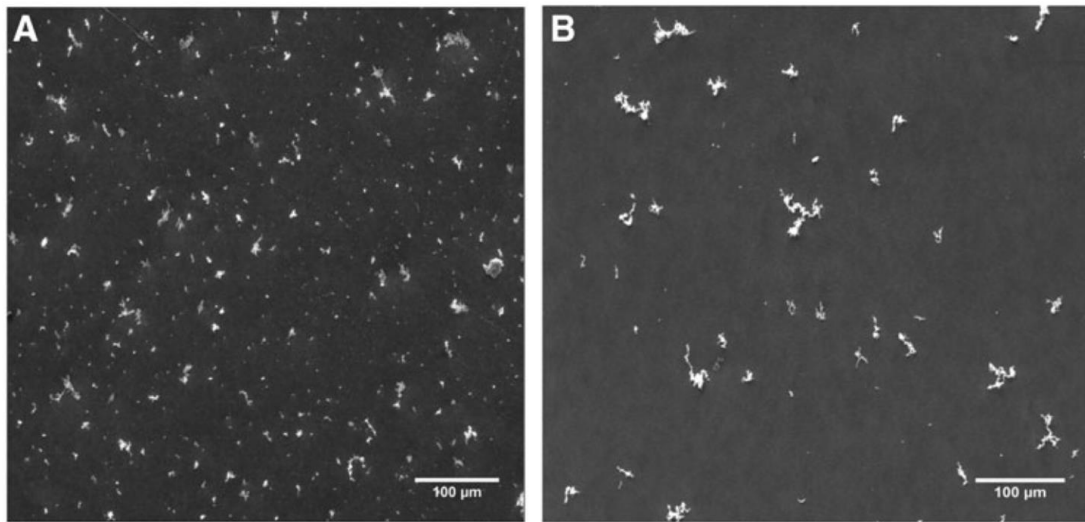


Figure 2.20 - SEM images of the deposited aerosols at magnifications- (A) budesonide, (B) fluticasone propionate. From (Gerde et al., 2017a).

Although this system is not an adaptation of standard methodologies, and therefore requires greater initial investment, as well as specific training, it appears to be the one with a stronger approximation to the *in vivo* environment.

2.3 FORMULATION PLATFORMS

There are two main strategies when developing a dry powder for inhalation:

- The carrier-based approach is the standard approach applied by most of the products on the market. A carrier-based formulation consists of a mixture of micronized DS (diameter between 0.5 and 5 μm in order to be in the inhalable range) and an excipient. The used excipient acts as a carrier and enables the micron-sized high adhesive and cohesive DS particles to reach the deep lung.
- An engineered particle approach is used when the standard approach does not meet the product requirements, which may include the delivery of higher DS doses, DS being a larger molecule not available as micronized crystalline material, solubility enhancement, drug combination etc. Spray-drying has been increasingly used to manufacture engineered particles for inhalation with the possibility to include a variety of excipients in the engineered particle and generate various morphologies depending on excipients used and process parameters.

In the present section a summary development strategy for both approaches will be presented.

2.3.1 Carrier-based formulations

As mentioned previously in this document, a possible strategy to achieve a dry powder with an optimal pulmonary delivery and good powder flow during manufacturing is to develop carrier-based formulations: a small dose of DS is blended with a large dose of excipient, and the latter will act as a carrier of the DS particles. The main goal when manufacturing a carrier-based formulation is to overcome cohesive agglomerates of the DS particles, and to distribute and establish stable adhesive interaction between drug and excipient, while enabling aerosolization.

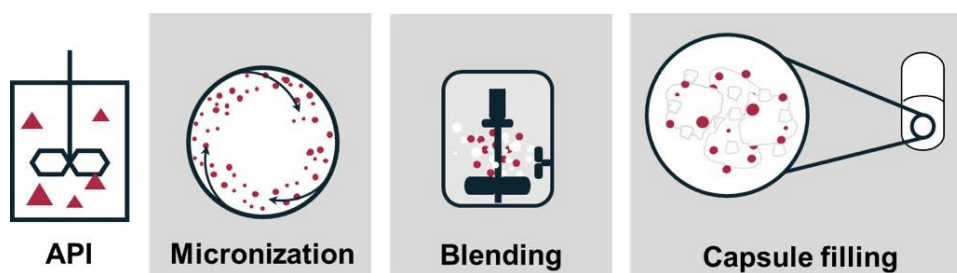


Figure 2.21 - Schematic illustration of a carrier-based formulation manufacture.

When developing a dry powder carrier-based formulation for inhalation, different steps must be understood and optimized (Figure 2.21). Firstly, the DS is usually required to have an aerodynamic particle size within 0.5 and 5 μm (Stephen Newman, 2009), which may be achieved through milling, designated as a “top-down” approach, or through controlled crystallization, the “bottom-up” approach; secondly, the DS particles are mixed into a suitable excipient or excipient combination with a blending step, using the optimal blending approach, high-shear or low-shear mixing; lastly, the manufacture blended formulation is filled into capsules, blisters or into an inhaler reservoir. Each of the listed steps have an influence on the final product performance, determining fluidization, dispersion, delivery to the lungs, and deposition in the peripheral airways, for a given inhaler device. They control the particles’ morphology, shape, size and surface properties, the DS/excipient distribution, and interaction forces such as cohesion and adhesion, and even the particle charge – discussed in detailed in the literature (Hickey, 2018).

Most of the commercialized inhalation therapies, regardless of the products type (DPI, pMDIs or nebulizers) are based on micronized DS (i.e. DS of small controlled particle size). The micronization process is especially important as it defines the size of the DS particle, the most important factor in determining the site of deposition in the respiratory airways, but is also used for the optimization of other pharmacological and physical properties of DS, including solubility, stability, and bioavailability (Chaurasiya and Zhao, 2021; S. Newman, 2009).

There are different methods to produce a drug in small particle size, they can be separated in two categories: “bottom-up” and “top-down” approaches. Following the “bottom-up” approach, the required particle size distribution of the DS particles is achieved by controlled crystallization; the “top-down” strategy is the most commonly used, in which case the optimal particle size is obtained by reduction of bigger particles, usually through milling technologies. The milling strategy allows for better control over particle size distribution while tailoring the particle surface and morphology. Moreover, milling processes tend to have a simpler process scale-up when compared with the crystallization approach.

The milling process is a unit operation in which mechanical energy is applied to physically break down coarse particle to finer ones (Loh et al., 2014), by being exposed to pressure, friction, attrition, impact, or shear. Different milling techniques produce particles with different properties, and these may have a significant influence on the optimization of the blending process, on dry powder flowability during actuation, on particles deposition pattern on the lung surface, and on dissolution kinetics (Chow et al.,

2007; Yadav and Lohani, 2013). Firstly, milling reduces the size and alters the particle size distribution, thus the milled particles present a larger specific surface area. Secondly, the milling process also transforms the surface roughness and shape of the particles. Lastly, there is an increase in free energy and decrease in thermodynamic stability due to the activation of the particle surface during the mechanical stress and the generation of amorphous regions (Loh et al., 2014). These alterations promote particle agglomeration as well as DS wettability and dissolution (Danesh et al., 2001; Ho et al., 2011).

There are a multitude of milling processes that can be used to achieve the desired size, shape and energy, and they can be categorized in two groups depending on occurring in a wet or dry basis. The milling process should be selected aiming to achieve an equilibrium between the optimal particle and the most efficient process. In any case, there is a need for process parameters optimization, which is highly material-related.

To be more specific, the spiral jet milling and wet polishing (micronization step in a wet media followed by particle isolation by spray-drying) processes will be described.

2.3.1.1 Jet milling

One of the mostly used dry milling techniques is the air jet milling, also referred to as fluid energy milling (schematized in Figure 2.22), and it has been greatly explored in the literature (Chow et al., 2007; Midoux et al., 1999; Moura et al., 2016; Wauthoz and Amighi, 2015). Shortly, the particles are loaded into a rotating chamber manually (laboratory scale) or using a feeder with a controlled flow rate. The grinding chamber is tangentially injected with high velocity compressed air streams, and once the particles enter it, they are accelerated leading to them colliding and with each other and the wall. The particles break as a combination of the impacts (particle-particle and particle-wall) while moving at high speed, and the shear forces caused by attrition at the particles' surface. The system may contain a classifier for the targeted particle size, allowing the powder to recirculate within the system while the particles within the desired range are collected.

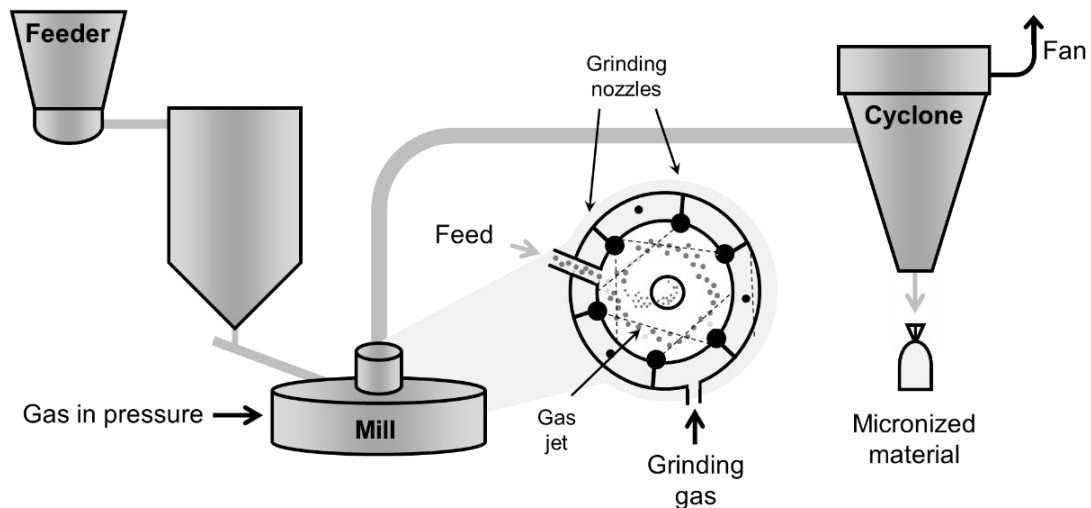


Figure 2.22 - Schematic representation of the spiral jet milling process.

The process development using a jet miller is simple, and depends mostly on two types of features:

- The mill design parameters include the diameter of the grinding chamber, which conditions the capacity of the mill; and the shape, number and angle of the grinding nozzles, which conditions the grinding gas velocity and spiral flow in the grinding chamber, and thereby determines intensity of the particle collisions (Midoux et al., 1999). The nozzle diameter is an adjustable parameter used to control the gas pressure.
- The operational conditions comprise the grinding pressure and the feed rate, the main controlled parameters to target a particle size distribution (Midoux et al., 1999).

This more in depth understanding of the process helps on the one hand a lean process development, on the other hand, a prediction of the product attributes to be expected from the milling process.

Even though jet milling is a straightforward process fairly understood and easily controlled, it presents some disadvantages. The process can be time-consuming and inefficient for some materials and shows a limited control over product parameters such as a non-homogenous particle size. Moreover, due to the high energies imposed, jet milling can promote DS amorphization and/or thermodynamically activated particle surfaces. Both effects can be responsible for a high agglomeration behavior and a decrease in DS physical and chemical stability (Moura et al., 2016).

2.3.1.2 Wet polishing

The wet polishing process is suitable to overcome the limitations listed for the jet milling process. It consists in suspending the coarse DS in an antisolvent (solvent in which the DS is considered not soluble in), followed by a size reduction step in wet media, and finally an isolation step (antisolvent evaporation) by spray-drying (Moura et al., 2016). The size reduction step can be accomplished by high pressure homogenization (HPH), with a tight and highly reproducible particle size distribution controlled by the number of milling cycles performed and the process pressure defined. Moreover, milling on a wet media results in particles with a reduced amorphization and less energetic surfaces. The main drawback of the wet polishing technology is being a two-step process.

The particle size reduction occurs due to the cavitation phenomenon, as the suspension passes from a large diameter to a very thin gap with an extremely high velocity. The liquid starts boiling, forms gas bubbles which implode after leaving the homogenization gap under normal air. Particle collision and shear forces among each other and with the equipment surfaces also promotes particle breakage through the weak points. Although the particles manufactured by the wet polishing process have been compared with particles manufactured by other technologies (Lopes et al., 2019; Moura et al., 2016), an overall analysis of the impact on final product aerodynamic performance, stability or dissolution has not yet been published.

2.3.1.3 Blending and excipient selection

Following DS micronization, a formulation step is required to obtain a powder with suitable flowability for down-stream processing, and also capable of delivering the micronized DS to the deep lung in the required amounts.

For the carrier-based systems, the research mostly focuses on diluted systems, the most common being binary, with DS and coarse lactose, or ternary, adding a small percentage of fine lactose. Other agents can also be added to improve the formulation stability or the flowability by reducing surface passivation or high energy free energy sites, such as magnesium stearate, leucine or polaxamer (Peng et al., 2016) (Shur et al., 2016). As the formulation is mostly composed by coarse lactose, the particle interactions are greatly dependent on the carrier surface characteristics (Chan et al., 2003; Farizhandi et al., 2021; Heng et al., 2000; Islam et al., 2004a, 2004b; Larhrib et al., 2003a, 2003b). For instance, an increase on lactose carrier surface rugosity has been shown to result in an increase of the emitted dose but a

decrease of drug availability on stage 2 of the cascade impactor (Heng et al., 2000), and machine learning approaches suggest aerodynamic performance prediction with regression models based on carrier design (Farizhandi et al., 2021). This points towards a need to find the optimum balance between adherence and detachment of DS from the carrier surface when selecting the optimal carrier coarse lactose. The selection of a fine excipient type, grade and concentration should also be considered carefully. Moreover, it has been observed that the removal of intrinsic fines from a lactose carrier can worsen the formulation performance, while the addition of fines of different materials to the formulation boosts it (Jones and Price, 2006). The mechanism of action of ternary components within dry powder aerosols has been well investigated (Jones and Price, 2006; Shalash and Elsayed, 2017) and several hypothesis have been proposed to explain the effect of fine addition on the formulation performance:

The hypothesis of the occupation of areas of high adhesion by fine excipient particles, schematized in Figure 2.23, proposes that the fine excipient particles preferentially attach to the carrier surface in areas with stronger binding forces, forcing the DS article to attach to less strong binding site. On actuation, the DS particles are more easily liberated from the carrier and free to flow to the deeper lung areas, optimizing performance. This hypothesis can be used to explain experimental observations of various studies (Jones and Price, 2006), however this is not the case for all the observed behaviors, possibly to the overly simplistic assumption the carrier surface can be divided into areas of strong and weak adhesion forces, which has been showed not to be the case (Louey et al., 2001).

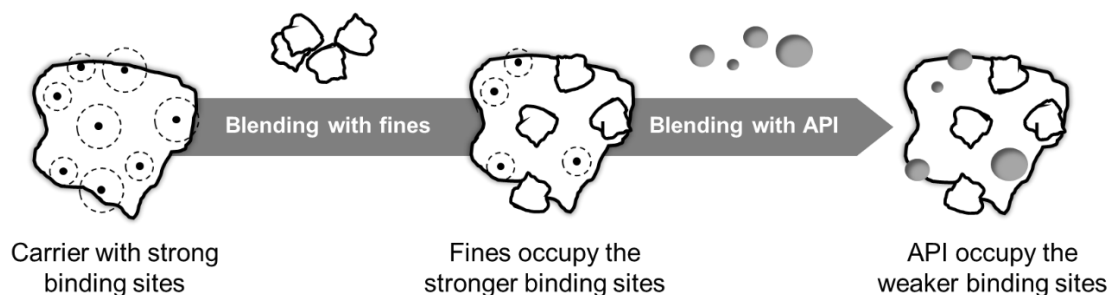


Figure 2.23 - Schematic representation of the hypothesis of the occupation of areas of high adhesion by fine excipient particles.

A second hypothesis to explain fine influence on the DPI performance suggests the formation of agglomerates of drug and fine excipient particles during the blending process (multiplets), from which the DS particles more easily detach during actuation (Figure 2.24). This would be because the surface of the fine lactose is smoother, resulting in a weaker force of adhesion between lactose and DS particles.

Additionally, it is also theorized that the formed multiplets adhere to the carrier lactose particle, but the detachment is easier due to the greater detachment mass.



Figure 2.24 – Schematic representation of the hypothesis of formation of agglomerates with drug and fine excipient particles (multiplets) during blending.

Similarly, to the previously presented hypothesis, the multiplets theory does not explain the totality of experimental observations. The actual description of the particles interaction within the formulation is possibly a combination of the two presented hypothetical mechanisms.

Possibly, the strategy to understand the mechanism by which fines influence the formulation performance is to fundamentally understand particle interaction with advanced characterization techniques such as colloid probe atomic force microscopy (AFM) or inverse gas chromatography (IGC), which have been used to achieve some insight regarding the interaction of DPI binary mixtures and its relation to the DPI performance in several works (Jones and Price, 2006; Lee et al., 2018), and more recently for ternary mixtures (Bungert et al., 2021; Jones et al., 2008b).

2.3.2 Engineered carrier-free particles

Although the carrier-based approach is standard and well understood, drug deposition in the deep lung with this approach can be insufficient to enhance therapeutic activity – in fact, Boer *et al.* estimated from *in vivo* deposition studies with radiolabel drugs in various marketed DPIs that only 14% of the DS on a carrier-based formulation is available to deposit in the deep lung, while 21% is lost in the high oropharyngeal region and about 65% of the DS is not released from the carrier (de Boer et al., 2017). Particle engineering as a formulation approach for carrier-free particles is an innovative strategy to increase pulmonary deposition by designing particles with optimized aerodynamic performance, while improving uniformity. Several DPI containing engineered particles are already on the market such as Aridol® (spray-dried mannitol powder), TOBI® Podhaler® (low density porous particles of tobramycin

with PulmoSpheres® technology), or Pulmicort® (agglomerated fine particles of budesonide). Aside from optimizing aerodynamic performance enables the formulation and delivery of large molecules, for instance Exubera® (removed from the market) and Afrezza® Dreamboat™ are commercial products containing spray-dried and lyophilized insulin, respectively. Other carrier-free DPI formulations include corrugated particles, particles with surface modified by force control agents, particle surface modified by hydrophobic barriers, particles containing hygroscopic excipients capable of excipient-enhanced growth, co-formulations of two or more DS having synergistic combinations, and excipient-free formulations produced by crystallization, spray-drying, milling and supercritical fluid process (Das et al., 2018).

Spray-drying is commonly used in the manufacture of carrier-free engineered particles for inhalation as it is a single step and rapid process, easily scalable, suitable for the production of crystalline or amorphous materials of micro and nano-particles (Vehring, 2008). Lastly, it offers significant economic and processing advantages compared to comparable techniques such as lyophilization/freeze-drying and it is well established in the pharmaceutical industry (Lechanteur and Evrard, 2020).

Fundamentally, spray-dried particles are produced by the atomization of the liquid feed into a hot drying gas that leads to solvent evaporation. The formed particles will be carried by the drying gas and collected using a recovery system which can be a cyclone or a bag filter (Lechanteur and Evrard, 2020).

Particle design is highly dependent of process conditions such as temperatures, atomization or feed solution solids concentration, and on particle composition defined by the excipients used and their proportions. It is common to include sugars with high glass transition temperature values (important to ensure powder stability) such as lactose, trehalose or raffinose, and amino acids to reduce the powder hygroscopicity, improve the aerodynamic performance and/or protect the DS, especially proteins against thermal stress, and denaturation (Pilcer and Amighi, 2010). Other excipients such as DSPC (intrinsic lung lipid) are used to design porous particles (Pulmopheres® technology); or chitosan to provide a higher transmucosal bioavailability when delivered as a powder (Li and Birchall, 2006).

2.4 REFERENCES

- Abadelah, M., Abdalla, G., Chrystyn, H., Larhrib, H., 2021. Gaining an insight into the importance of each inhalation manoeuvre parameter using altered patients' inhalation profiles. *J. Drug Deliv. Sci. Technol.* 61, 102181. <https://doi.org/10.1016/j.jddst.2020.102181>
- Anderson, P., 2005. History of Aerosol Therapy : Liquid Nebulization to MDIs to DPIs Ceramic Inhalers (19th Century) 50, 1139–1149.
- Anderson, P., Newman, S., 2009. Drugs by the Pulmonary Route, in: Newman, S. (Ed.), *Respiratory Drug Delivery: Essential Theory and Practice*. Respiratory Drug Delivery Online, Richmond, Virginia, pp. 337–382.
- Anjilvel, S., Asgharian, B., 1995. A Multiple-Path Model of Particle Deposition in the Rat Lung. *Toxicol. Sci.* 28, 41–50. <https://doi.org/10.1093/toxsci/28.1.41>
- Arc, I., n.d. Dry Powder Inhaler Devices Market - Forecast(2021 - 2026) [WWW Document]. URL <https://www.industryarc.com/Report/16963/dry-powder-inhaler-devices-market.html>
- Arora, D., Shah, K.A., Halquist, M.S., Sakagami, M., 2010. In Vitro aqueous fluid-capacity-limited dissolution testing of respirable aerosol drug particles generated from inhaler products. *Pharm. Res.* 27, 786–795. <https://doi.org/10.1007/s11095-010-0070-5>
- Asada, M., Takahashi, H., Okamoto, H., Tanino, H., Danjo, K., 2004. Theophylline particle design using chitosan by the spray drying. *Int. J. Pharm.* 270, 167–174. <https://doi.org/10.1016/j.ijpharm.2003.11.001>
- Bell, J.H., Hartley, P.S., Cox, J.S.G., 1971. Dry powder aerosols I: A new powder inhalation device. *J. Pharm. Sci.* 60, 1559–1564. <https://doi.org/10.1002/jps.2600601028>
- Borghardt, J.M., Weber, B., Staab, A., Kloft, C., 2015. Review Article Pharmacometric Models for Characterizing the Pharmacokinetics of Orally Inhaled Drugs 17. <https://doi.org/10.1208/s12248-015-9760-6>
- Borgström, L., Olsson, B., Thorsson, L., 2006. Degree of Throat Deposition Can Explain the Variability in Lung Deposition of Inhaled Drugs. *J. Aerosol Med.* 19, 473–483. <https://doi.org/10.1089/jam.2006.19.473>
- Brain, J.D., 2007. Inhalation, Deposition, and Fate of Insulin and Other Therapeutic Proteins. *Diabetes Technol. Ther.* 9, S-4-S-15. <https://doi.org/10.1089/dia.2007.0228>
- Bungert, N., Kobler, M., Scherließ, R., 2021. Surface energy considerations in ternary powder blends for inhalation. *Int. J. Pharm.* 609, 121189. <https://doi.org/10.1016/j.ijpharm.2021.121189>
- Buttini, F., Balducci, A.G., Colombo, G., Sonvico, F., Montanari, S., Pisi, G., Rossi, A., Colombo, P., Bettini, R., 2018. Dose administration maneuvers and patient care in tobramycin dry powder inhalation therapy. *Int. J. Pharm.* 548, 182–191. <https://doi.org/10.1016/j.ijpharm.2018.06.006>
- Byron, P.R., Patton, J.S., 1994. Drug Delivery via the Respiratory Tract. *J. Aerosol Med.* 7, 49–75. <https://doi.org/10.1089/jam.1994.7.49>
- Chan, J.G.Y., Chan, H.-K., Prestidge, C.A., Denman, J.A., Young, P.M., Traini, D., 2013. A novel dry powder inhalable formulation incorporating three first-line anti-tubercular antibiotics. *Eur. J. Pharm. Biopharm.* 83, 285–292. <https://doi.org/10.1016/j.ejpb.2012.08.007>
- Chan, L.W., Lim, L.T., Heng, P.W.S., 2003. Immobilization of fine particles on lactose carrier by precision

- coating and its effect on the performance of dry powder formulations. *J. Pharm. Sci.* 92, 975–984. <https://doi.org/10.1002/jps.10372>
- Chaurasiya, B., Zhao, Y.Y., 2021. Dry powder for pulmonary delivery: A comprehensive review. *Pharmaceutics* 13, 1–28. <https://doi.org/10.3390/pharmaceutics13010031>
- Chen, W.-H., Chang, C.-M., Mutuku, J.K., Lam, S.S., Lee, W.-J., 2021. Aerosol deposition and airflow dynamics in healthy and asthmatic human airways during inhalation. *J. Hazard. Mater.* 416, 125856. <https://doi.org/10.1016/j.jhazmat.2021.125856>
- Chow, A.H.L., Tong, H.H.Y., Chattopadhyay, P., Shekunov, B.Y., 2007. Particle engineering for pulmonary drug delivery. *Pharm. Res.* 24, 411–437. <https://doi.org/10.1007/s11095-006-9174-3>
- Chow, Michael Y.T., Chang, R.Y.K., Chan, H.-K., 2021. Inhalation delivery technology for genome-editing of respiratory diseases. *Adv. Drug Deliv. Rev.* 168, 217–228. <https://doi.org/10.1016/j.addr.2020.06.001>
- Chow, Michael Yee Tak, Tai, W., Chang, R.Y.K., Chan, H.-K., Kwok, P.C.L., 2021. In vitro-in vivo correlation of cascade impactor data for orally inhaled pharmaceutical aerosols. *Adv. Drug Deliv. Rev.* 177, 113952. <https://doi.org/10.1016/j.addr.2021.113952>
- Clark, A.R., 1995. Medical Aerosol Inhalers: Past, Present, and Future. *Aerosol Sci. Technol.* 22, 374–391. <https://doi.org/10.1080/02786829408959755>
- Clarke, S.W., 1984. Anatomy and physiology of the human lung, in: Clarke, S.W., Pavia, D. (Eds.), *Aerosols and the Lung: Clinical and Experimental Aspects*. Butterworth-Heinemann, London, pp. 1–18.
- Cocozza, S., 1976. Inhaler for powdered medicaments. US patent 3991761.
- Cutcher, P., 1974. Stratospheric Ozone Depletion and Solar Ultraviolet Radiation on Earth. *Science* (80-). 184, 1161–1161. <https://doi.org/10.1126/science.184.4142.1161-b>
- Dalby, R., Byron, P., Newman, S., Anderson, P., 2009. In vitro assessment of inhaled products., in: River, G. (Ed.), *Respiratory Drug Delivery: Essential Theory and Practice*. Respiratory Drug Delivery Online/VCU, Richmond. Davis Healthcare International Publishing, pp. 59–96.
- Danesh, A., Connell, S.D., Davies, M.C., Roberts, C.J., Tendler, S.J.B., Williams, P.M., Wilkins, M.J., 2001. An in situ dissolution study of aspirin crystal planes (100) and (001) by atomic force microscopy. *Pharm. Res.* 18, 299–303. <https://doi.org/10.1023/A:1011046728622>
- Darquenne, C., 2020. Deposition Mechanisms. *J. Aerosol Med. Pulm. Drug Deliv.* 33, 181–185. <https://doi.org/10.1089/jamp.2020.29029.cd>
- Das, S.C., Stewart, P.J., Tucker, I.G., 2018. The respiratory delivery of high dose dry powders. *Int. J. Pharm.* 550, 486–487. <https://doi.org/10.1016/j.ijpharm.2018.09.014>
- Davies, N.M., Feddah, M.R., 2003. A novel method for assessing dissolution of aerosol inhaler products. *Int. J. Pharm.* 255, 175–187. [https://doi.org/10.1016/S0378-5173\(03\)00091-7](https://doi.org/10.1016/S0378-5173(03)00091-7)
- Davis, S.S., 1999. Delivery of peptide and non-peptide drugs through the respiratory tract. *Pharm. Sci. Technol. Today* 2, 450–456. [https://doi.org/10.1016/S1461-5347\(99\)00199-6](https://doi.org/10.1016/S1461-5347(99)00199-6)
- de Boer, A.H., Hagedoorn, P., Hoppentocht, M., Buttini, F., Grasmeyer, F., Frijlink, H.W., 2017. Dry powder inhalation: past, present and future. *Expert Opin. Drug Deliv.* 14, 499–512. <https://doi.org/10.1080/17425247.2016.1224846>
- De Swart, R.L., De Vries, R.D., Rennick, L.J., Van Amerongen, G., McQuaid, S., Verburgh, R.J., Yüksel,

- S., De Jong, A., Lemon, K., Nguyen, D.T., Ludlow, M., Osterhaus, A.D.M.E., Duprex, W.P., 2017. Needle-free delivery of measles virus vaccine to the lower respiratory tract of non-human primates elicits optimal immunity and protection. *npj Vaccines* 2, 1–10. <https://doi.org/10.1038/s41541-017-0022-8>
- Depreter, F., Pilcer, G., Amighi, K., 2013. Inhaled proteins: Challenges and perspectives. *Int. J. Pharm.* 447, 251–280. <https://doi.org/10.1016/j.ijpharm.2013.02.031>
- Després-Gnis, F., Williams, G., 2010. Comparison of next generation impactor and fast-screening impactor for determining fine particle fraction of dry powder inhalers., in: EPAG-Sponsored Workshop on Abbreviated Impactor Measurement (AIM) and Efficient Data Analysis (EDA) Concepts in Inhaler Testing: Overview of AIM-EDA.
- Dolovich, M., Ruffin, R.E., Roberts, R., Newhouse, M.T., 1981. Optimal delivery of aerosols from metered dose inhalers. *Chest* 80, 911–915.
- Dolovich, M.A., 2000. Influence of inspiratory flow rate, particle size, and airway caliber on aerosolized drug delivery to the lung. *Respir. Care* 45, 597–608.
- Dolovich, M.B., 1997. Aerosols, in: Barnes, P., Grunstein, M. (Eds.), . *Asthma*. Philadelphia: Lippincott-Raven, pp. 1349–1365.
- Dunn, C., Curran, M.P., 2006. Inhaled Human Insulin (Exubera??). *Drugs* 66, 1013–1032. <https://doi.org/10.2165/00003495-200666070-00019>
- Duret, C., Wauthoz, N., Sebti, T., Vanderbist, F., Amighi, K., 2012. Solid dispersions of itraconazole for inhalation with enhanced dissolution, solubility and dispersion properties. *Int. J. Pharm.* 428, 103–113. <https://doi.org/10.1016/j.ijpharm.2012.03.002>
- Eedara, B.B., Alabsi, W., Encinas-Basurto, D., Polt, R., Ledford, J.G., Mansour, H.M., 2021. Inhalation Delivery for the Treatment and Prevention of COVID-19 Infection. *Pharmaceutics* 13, 1077. <https://doi.org/10.3390/pharmaceutics13071077>
- Eixarch, H., Haltner-Ukomadu, E., Beisswenger, C., Bock, U., 2010. Drug Delivery to the Lung: Permeability and Physicochemical Characteristics of Drugs as the Basis for a Pulmonary Biopharmaceutical Classification System (pBCS). *J. Epithel. Biol. Pharmacol.* 3, 1–14. <https://doi.org/10.2174/1875044301003010001>
- EMA, 2009. Guideline on the Requirements for Clinical Documentation for Orally Inhaled Products (OIP) Including the Requirements for Demonstration of Therapeutic Equivalence Between Two Inhaled Products for use in the Treatment of Asthma and Chronic Obstructive Pulm. <https://doi.org/10.2165/00128415-200912820-00006>
- EMA, 2005. GUIDELINE ON THE PHARMACEUTICAL QUALITY OF INHALATION AND NASAL PRODUCTS. <https://doi.org/10.1136/bmj.333.7574.873-a>
- Farias, G., Ganley, W., Deddie, H.-J., Kippax, P., Shur, J., Price, R., 2017. Investigating the microstructure of dry powder inhalers using orthogonal analytical approaches, in: *Drug Delivery to the Lungs*. The Aerosol Society, Edinburg, UK, pp. 262–265.
- Farizhandi, A.A.K., Alishiri, M., Lau, R., 2021. Machine learning approach for carrier surface design in carrier-based dry powder inhalation. *Comput. Chem. Eng.* 151, 107367. <https://doi.org/10.1016/j.compchemeng.2021.107367>
- FDA, 2018. Guidance for Industry: Metered Dose Inhaler Inhaler (DPI) Products - (MDI) and Dry Powder

Quality Considerations Guidance.

- FDA Approves Afrezza to Treat Diabetes [WWW Document], 2014. URL <https://www.drugs.com/newdrugs/fda-approves-afrezza-diabetes-4050.html> (accessed 1.19.21).
- Fernandes, B., Maia, F., Paiva, A., Corvo, M., Costa, E., 2016a. Paddle over disk as a dissolution test for orally inhaled drugs: discriminating composite from carrier-based formulations., in: Drug Delivery to the Lungs. The Aerosol Society, Bristol, UK, pp. 308–312.
- Fernandes, B., Paiva, A.M., Corvo, M.L., Costa, E., Maia, F.M., 2016b. Paddle Over Disk as a Dissolution Test for Orally Inhaled Fluticasone Propionate: Impact of Temperature, Dose and Formulation, in: Respiratory Drug Delivery Europe 2017 Book 2. Nice, France, p. 215.
- Floroiu, A., Klein, M., Krämer, J., Lehr, C.M., 2018. Towards standardized dissolution techniques for in vitro performance testing of dry powder inhalers. *Dissolution Technol.* 25, 6–18. <https://doi.org/10.14227/DT250318P6>
- Food and Drug Administration, 2017. Draft Guidance on Mometasone Furoate. Fda.
- Forbes, B., Richer, Nathalie Hauet Buttini, F., 2015. Dissolution: A Critical Performance Characteristic of Inhaled Products?, in: Pulmonary Drug Delivery: Advances and Challenges. pp. 223–240.
- Fotaki, N., 2011. Flow-Through Cell Apparatus (USP Apparatus 4): Operation and Features. *Dissolution Technol.* 18, 46–49. <https://doi.org/10.14227/DT180411P46>
- Fuchs, N.A., Sutugin, A.G., 1966. Generation and use of monodisperse aerosols. *Aerosol Sci.* 1–30.
- Garcia Contreras, L., Awashthi, S., Hanif, S., Hickey, A., 2012. Inhaled Vaccines for the Prevention of Tuberculosis. *J. Mycobacterial Dis.* 03, 1–13. <https://doi.org/10.4172/2161-1068.S1-002>
- Gerde, P., Ewing, P., Låstbom, L., Ryrfeldt, Å., Waher, J., Lidén, G., 2004. A Novel Method to Aerosolize Powder for Short Inhalation Exposures at High Concentrations: Isolated Rat Lungs Exposed to Respirable Diesel Soot. *Inhal. Toxicol.* 16, 45–52. <https://doi.org/10.1080/08958370490258381>
- Gerde, P., Malmlöf, M., Havsborn, L., Sjöberg, C.-O., Ewing, P., Eirefelt, S., Ekelund, K., 2017. Dissolvt: An In Vitro Method for Simulating the Dissolution and Absorption of Inhaled Dry Powder Drugs in the Lungs. *Assay Drug Dev. Technol.* 15, 77–88. <https://doi.org/10.1089/adt.2017.779>
- Grainger, C.I., Saunders, M., Buttini, F., Telford, R., Merolla, L.L., Martin, G.P., Jones, S.A., Forbes, B., 2012. Critical characteristics for corticosteroid solution metered dose inhaler bioequivalence. *Mol. Pharm.* 9, 563–569. <https://doi.org/10.1021/mp200415g>
- Grossman, J., 1994. The evolution of inhaler technology. *J. Asthma* 31, 55–64. <https://doi.org/10.3109/02770909409056770>
- Haghi, M., Traini, D., Bebawy, M., Young, P.M., 2012. Deposition, Diffusion and Transport Mechanism of Dry Powder Microparticulate Salbutamol, at the Respiratory Epithelia. *Mol. Pharm.* 9, 1717–1726. <https://doi.org/10.1021/mp200620m>
- Harper, N.J., Gray, S., Groot, J. De, Parker, J.M., Sadzadeh, N., Schuler, C., Schumacher, J.D., Seshadri, S., Smith, A.E., Steeno, G.S., Stevenson, C.L., Taniere, R., Wang, M., Bennett, D.B., 2007. The Design and Performance of the Exubera® Pulmonary Insulin Delivery System. *Diabetes Technol. Ther.* 9, S-16-S-27. <https://doi.org/10.1089/dia.2007.0222>
- Hassoun, M., Malmlöf, M., Scheibelhofer, O., Kumar, A., Bansal, S., Selg, E., Nowenwik, M., Gerde, P., Radivojevic, S., Paudel, A., Arora, S., Forbes, B., Hassoun, M., Bansal, S., Scheibelhofer, O., Forbes, B., Paudel, A., Malmlof, M., Nowenwik, M., Kumar, A., Gerde, P., Arora, S., 2019. Use of

- PBPK modelling to evaluate the performance of DissolvIt, a biorelevant dissolution assay for orally inhaled drug products. *Mol. Pharm.* 16, 1245–1254. <https://doi.org/10.1021/acs.molpharmaceut.8b01200>
- Hastedt, J.E., Bäckman, P., Clark, A.R., Doub, W., Hickey, A., Hochhaus, G., Kuehl, P.J., Lehr, C., Mauser, P., McConville, J., Niven, R., Sakagimi, M., Weers, J.G., 2016. Scope and relevance of a pulmonary biopharmaceutical classification system AAPS/FDA/USP Workshop March 16-17th, 2015 in Baltimore, MD. *AAPS Open* 2, 1. <https://doi.org/10.1186/s41120-015-0002-x>
- Heng, P.W.S., Chan, L.W., Lim, L.T., 2000. Quantification of the Surface Morphologies of Lactose Carriers and Their Effect on the in Vitro Deposition of Salbutamol Sulphate. *Chem. Pharm. Bull. (Tokyo)*. 48, 393–398. <https://doi.org/10.1248/cpb.48.393>
- Hersey, J.A., 1975. Ordered Mixing: a New Concept in Powder Mixing Practice. *Powder Technol.* 11, 41–44. [https://doi.org/10.1016/0032-5910\(75\)80021-0](https://doi.org/10.1016/0032-5910(75)80021-0)
- Heyder, J., Gebhart, J., Rudolf, G., Schiller, C.F., Stahlhofen, W., 1986. Deposition of particles in the human respiratory tract in the size range 0.005–15 μm . *J. Aerosol Sci.* 17, 811–825. [https://doi.org/10.1016/0021-8502\(86\)90035-2](https://doi.org/10.1016/0021-8502(86)90035-2)
- Hickey, A.J., 2018. Fundamentals of Dry Powder Inhaler Technology, in: *AAPS Advances in the Pharmaceutical Sciences Series*. Springer International Publishing, pp. 213–232. https://doi.org/10.1007/978-3-319-94174-5_5
- Higgins, M.J., Asbury, A.J., Brodie, M.J., 1991. Inhaled nebulised fentanyl for postoperative analgesia. *Anaesthesia* 46, 973–976. <https://doi.org/10.1111/j.1365-2044.1991.tb09862.x>
- Hindle, M., Newton, D.A., Chrystyn, H., 1993. Investigations of an optimal inhaler technique with the use of urinary salbutamol excretion as a measure of relative bioavailability to the lung. *Thorax* 48, 607–610. <https://doi.org/10.1136/thx.48.6.607>
- Ho, R., Dilworth, S.E., Williams, D.R., Heng, J.Y.Y., 2011. Role of Surface Chemistry and Energetics in High Shear Wet Granulation. *Ind. Eng. Chem. Res.* 50, 9642–9649. <https://doi.org/10.1021/ie2009263>
- Hochhaus, G., 2018. Predictive Dissolution Methods for OINDPs - Development of an Optimized Dissolution Test System for OINDPs.
- Holmes, E.H., Devalapally, H., Li, L., Perdue, M.L., Ostrander, G.K., 2013. Permeability Enhancers Dramatically Increase Zanamivir Absolute Bioavailability in Rats: Implications for an Orally Bioavailable Influenza Treatment. *PLoS One* 8, e61853. <https://doi.org/10.1371/journal.pone.0061853>
- Horsfield, K., Dart, G., Olson, D.E., Filley, G.F., Cumming, G., 1971. Models of the human bronchial tree. *J. Appl. Physiol.* 31, 207–217. <https://doi.org/10.1152/jappl.1971.31.2.207>
- Ignjatovic, J., Austersic, T., Cvijic, S., Bodic, A., Duris, J., Ibric, S., Filipovic, N., 2021. Comparative Assessment of Computational vs. In Vitro Methods for the Estimation of Dry Powders for Inhalation Emitted Fraction, in: *2021 IEEE 21st International Conference on Bioinformatics and Bioengineering (BIBE)*. IEEE, pp. 1–5. <https://doi.org/10.1109/BIBE52308.2021.9635217>
- Islam, N., Gladki, E., 2008. Dry powder inhalers (DPIs)—A review of device reliability and innovation. *Int. J. Pharm.* 360, 1–11. <https://doi.org/10.1016/j.ijpharm.2008.04.044>
- Islam, N., Stewart, P., Larson, I., Hartley, P., 2004a. Lactose surface modification by decantation: Are

- drug-fine lactose ratios the key to better dispersion of salmeterol xinafoate from lactose-interactive mixtures? *Pharm. Res.* 21, 492–499. <https://doi.org/10.1023/B:PHAM.0000019304.91412.18>
- Islam, N., Stewart, P., Larson, I., Hartley, P., 2004b. Effect of carrier size on the dispersion of salmeterol xinafoate from interactive mixtures. *J. Pharm. Sci.* 93, 1030–1038. <https://doi.org/10.1002/jps.10583>
- Jaspart, S., Bertholet, P., Piel, G., Dogné, J.-M., Delattre, L., Evrard, B., 2007. Solid lipid microparticles as a sustained release system for pulmonary drug delivery. *Eur. J. Pharm. Biopharm.* 65, 47–56. <https://doi.org/10.1016/j.ejpb.2006.07.006>
- Jennings, B.H., Andersson, K.-E., Johansson, S.♦, 1991. Assessment of systemic effects of inhaled glucocorticosteroids: comparison of the effects of inhaled budesonide and oral prednisolone on adrenal function and markers of bone turnover. *Eur. J. Clin. Pharmacol.* 40, 77–82. <https://doi.org/10.1007/BF00315143>
- Jones, M.D., Hooton, J.C., Dawson, M.L., Ferrie, A.R., Price, R., 2008. An Investigation into the Dispersion Mechanisms of Ternary Dry Powder Inhaler Formulations by the Quantification of Interparticulate Forces. *Pharm. Res.* 25, 337–348. <https://doi.org/10.1007/s11095-007-9467-1>
- Jones, M.D., Price, R., 2006. The influence of fine excipient particles on the performance of carrier-based dry powder inhalation formulations. *Pharm. Res.* 23, 1665–1674. <https://doi.org/10.1007/s11095-006-9012-7>
- Kladders, H., 1989. Powdered pharmaceutical inhaler. US patent 4889114.
- Kumar, A., Terakosolphan, W., Hassoun, M., Vandera, K.-K., Novicky, A., Harvey, R., Royall, P.G., Bicer, E.M., Eriksson, J., Edwards, K., Valkenborg, D., Nelissen, I., Hassall, D., Mudway, I.S., Forbes, B., 2017. A Biocompatible Synthetic Lung Fluid Based on Human Respiratory Tract Lining Fluid Composition. *Pharm. Res.* 34, 2454–2465. <https://doi.org/10.1007/s11095-017-2169-4>
- Labiris, N.R., Dolovich, M.B., 2003. Pulmonary drug delivery. Part I: Physiological factors affecting therapeutic effectiveness of aerosolized medications. *Br. J. Clin. Pharmacol.* 56, 588–599. <https://doi.org/10.1046/j.1365-2125.2003.01892.x>
- Larhrib, H., Martin, G.P., Marriott, C., Prime, D., 2003a. The influence of carrier and drug morphology on drug delivery from dry powder formulations. *Int. J. Pharm.* 257, 283–296. [https://doi.org/10.1016/S0378-5173\(03\)00156-X](https://doi.org/10.1016/S0378-5173(03)00156-X)
- Larhrib, H., Martin, G.P., Prime, D., Marriott, C., 2003b. Characterisation and deposition studies of engineered lactose crystals with potential for use as a carrier for aerosolised salbutamol sulfate from dry powder inhalers. *Eur. J. Pharm. Sci.* 19, 211–221. [https://doi.org/10.1016/S0928-0987\(03\)00105-2](https://doi.org/10.1016/S0928-0987(03)00105-2)
- Laube, B.L., 2014. The expanding role of aerosols in systemic drug delivery, gene therapy and vaccination: an update. *Transl. Respir. Med.* 2, 3. <https://doi.org/10.1186/2213-0802-2-3>
- Lawford, P., McKenzie, D., 1983. Pressurized aerosol inhaler technique: How important are inhalation from residual volume, inspiratory flow rate and the time interval between puffs? *Br. J. Dis. Chest* 77, 276–281. [https://doi.org/10.1016/0007-0971\(83\)90054-2](https://doi.org/10.1016/0007-0971(83)90054-2)
- Learoyd, T.P., Burrows, J.L., French, E., Seville, P.C., 2008. Chitosan-based spray-dried respirable powders for sustained delivery of terbutaline sulfate. *Eur. J. Pharm. Biopharm.* 68, 224–234. <https://doi.org/10.1016/j.ejpb.2007.04.017>

- Lechanteur, A., Evrard, B., 2020. Influence of composition and spray-drying process parameters on carrier-free DPI properties and behaviors in the lung: A review. *Pharmaceutics* 12. <https://doi.org/10.3390/pharmaceutics12010055>
- Lee, H.-J., Lee, H.-G., Kwon, Y.-B., Kim, J.-Y., Rhee, Y.-S., Chon, J., Park, E.-S., Kim, D.-W., Park, C.-W., 2018. The role of lactose carrier on the powder behavior and aerodynamic performance of bosentan microparticles for dry powder inhalation. *Eur. J. Pharm. Sci.* 117, 279–289. <https://doi.org/10.1016/j.ejps.2018.03.004>
- Li, H.-Y., Birchall, J., 2006. Chitosan-Modified Dry Powder Formulations for Pulmonary Gene Delivery. *Pharm. Res.* 23, 941–950. <https://doi.org/10.1007/s11095-006-0027-x>
- Lionberger, R., 2018. New Tools for Generic ODPs to Maximize Prospects of FDA Approval.
- Lipworth, B.J., 1999. Systemic Adverse Effects of Inhaled Corticosteroid Therapy. *Arch. Intern. Med.* 159, 941. <https://doi.org/10.1001/archinte.159.9.941>
- Loh, Z.H., Samanta, A.K., Sia Heng, P.W., 2014. Overview of milling techniques for improving the solubility of poorly water-soluble drugs. *Asian J. Pharm. Sci.* 10, 255–274. <https://doi.org/10.1016/j.ajps.2014.12.006>
- Lopes, A., Barros, R., Silva, S., 2019. Inhalation Drug Delivery: The Impact of Particle Size Reduction. *Pharm. Technol. Eur.* 43, 25–28.
- Louey, M.D., Mulvaney, P., Stewart, P.J., 2001. Characterisation of adhesional properties of lactose carriers using atomic force microscopy. *J. Pharm. Biomed. Anal.* 25, 559–567. [https://doi.org/10.1016/S0731-7085\(00\)00523-9](https://doi.org/10.1016/S0731-7085(00)00523-9)
- Lovelock, J.E., 1977. Halogenated hydrocarbons in the atmosphere. *Ecotoxicol. Environ. Saf.* 1, 399–406. [https://doi.org/10.1016/0147-6513\(77\)90030-6](https://doi.org/10.1016/0147-6513(77)90030-6)
- Malmlöf, M., Nowenwik, M., Meelich, K., Rådberg, I., Selg, E., Burns, J., Mascher, H., Gerde, P., 2019. Effect of particle deposition density of dry powders on the results produced by an in vitro test system simulating dissolution- and absorption rates in the lungs. *Eur. J. Pharm. Biopharm.* 139, 213–223. <https://doi.org/10.1016/j.ejpb.2019.03.005>
- Mangal, S., Nie, H., Xu, R., Guo, R., Cavallaro, A., Zemlyanov, D., Zhou, Q., 2018. Physico-Chemical Properties, Aerosolization and Dissolution of Co-Spray Dried Azithromycin Particles with L-Leucine for Inhalation. *Pharm. Res.* 35, 28. <https://doi.org/10.1007/s11095-017-2334-9>
- Marple, V.A., Olson, B.A., Miller, N.C., 1995. A Low-Loss Cascade Impactor with Stage Collection Cups: Calibration and Pharmaceutical Inhaler Applications. *Aerosol Sci. Technol.* 22, 124–134. <https://doi.org/10.1080/02786829408959732>
- Marple, V.A., Olson, B.A., Santhanakrishnan, K., Mitchell, J.P., Hudson-Curtis, B.L., Murray, S.C., Hudson-Curtis, B.L., 2003a. Next Generation Pharmaceutical Impactor (a new impactor for pharmaceutical inhaler testing). Part II: Archival calibration. *J. Aerosol Med. Depos. Clear. Eff. Lung* 16, 301–324. <https://doi.org/10.1089/089426803769017668>
- Marple, V.A., Roberts, D.L., Romay, F.J., Miller, N.C., Truman, K.G., Van Oort, M., Olsson, B.O., Holroyd, M.J., Mitchell, J.P., Hochrainer, D., Ph, D., Roberts, D.L., Ph, D., Romay, F.J., Ph, D., Miller, N.C., Ph, D., Truman, K.G., Sc, B., Oort, M.V.A.N., Ph, D., Olsson, B.O., Ph, D., Hochrainer, D., Phil, D., 2003b. Next generation pharmaceutical impactor (a new impactor for pharmaceutical inhaler testing). Part I: Design. *J. Aerosol Med.* 16, 283–299.

<https://doi.org/10.1089/089426803769017659>

- Martonen, T.B., Musante, C.J., Segal, R.A., Schroeter, J.D., Hwang, D., Dolovich, M.A., Burton, R., Spencer, R.M., Fleming, J.S., 2000. Lung models: strengths and limitations. *Respir. Care* 45, 712–36.
- Mather, L.E., Woodhouse, A., Ward, M.E., Farr, S.J., Rubsamen, R.A., Eltherington, L.G., 1998. Pulmonary administration of aerosolised fentanyl: Pharmacokinetic analysis of systemic delivery. *Br. J. Clin. Pharmacol.* 46, 37–43. <https://doi.org/10.1046/j.1365-2125.1998.00035.x>
- May, S., Jensen, B., Weiler, C., Wolkenhauer, M., Schneider, M., Lehr, C.-M.M., 2014. Dissolution Testing of Powders for Inhalation: Influence of Particle Deposition and Modeling of Dissolution Profiles. *Pharm. Res.* 31, 3211–3224. <https://doi.org/10.1007/s11095-014-1413-4>
- May, S., Jensen, B., Wolkenhauer, M., Schneider, M., Lehr, C.M., 2012. Dissolution Techniques for In Vitro Testing of Dry Powders for Inhalation. *Pharm. Res.* 29, 2157–2166. <https://doi.org/10.1007/s11095-012-0744-2>
- May, S., Kind, S., Jensen, B., Wolkenhauer, M., Schneider, M., Lehr, C.-M., 2015. Miniature In Vitro Dissolution Testing of Powders for Inhalation. *Dissolution Technol.* 22, 40–51. <https://doi.org/10.14227/DT220315P40>
- Mezzena, M., Scalia, S., Young, P.M., Traini, D., 2009. Solid Lipid Budesonide Microparticles for Controlled Release Inhalation Therapy. *AAPS J.* 11, 771–778. <https://doi.org/10.1208/s12248-009-9148-6>
- Midoux, N., Hošek, P., Pailleres, L., Authelin, J.R., 1999. Micronization of pharmaceutical substances in a spiral jet mill. *Powder Technol.* 104, 113–120. [https://doi.org/10.1016/S0032-5910\(99\)00052-2](https://doi.org/10.1016/S0032-5910(99)00052-2)
- Mitchell, J., Newman, S., Chan, H.-K., 2007. In vitro and in vivo aspects of cascade impactor tests and inhaler performance: A review. *AAPS PharmSciTech* 8, 237–248. <https://doi.org/10.1208/pt0804110>
- Mobley, C., Hochhaus, G., 2001. Methods used to assess pulmonary deposition and absorption of drugs. *Drug Discov. Today* 6, 367–375. [https://doi.org/10.1016/S1359-6446\(01\)01691-9](https://doi.org/10.1016/S1359-6446(01)01691-9)
- Mohan, M., Lee, S., Guo, C., Peri, S.P., Doub, W.H., 2017. Evaluation of Abbreviated Impactor Measurements (AIM) and Efficient Data Analysis (EDA) for Dry Powder Inhalers (DPIs) Against the Full-Resolution Next Generation Impactor (NGI). *AAPS PharmSciTech* 18, 1585–1594. <https://doi.org/10.1208/s12249-016-0625-9>
- Moura, C., Neves, F., Costa, E., 2016. Impact of jet-milling and wet-polishing size reduction technologies on inhalation API particle properties. *Powder Technol.* 298, 90–98. <https://doi.org/10.1016/j.powtec.2016.05.008>
- Muttill, P., Prego, C., Garcia-Contreras, L., Pulliam, B., Fallon, J.K., Wang, C., Hickey, A.J., Edwards, D., 2010a. Immunization of guinea pigs with novel hepatitis B antigen as nanoparticle aggregate powders administered by the pulmonary route. *AAPS J.* 12, 330–7. <https://doi.org/10.1208/s12248-010-9192-2>
- Muttill, P., Pulliam, B., Garcia-Contreras, L., Fallon, J.K., Wang, C., Hickey, A.J., Edwards, D.A., 2010b. Pulmonary Immunization of Guinea Pigs with Diphtheria CRM-197 Antigen as Nanoparticle Aggregate Dry Powders Enhance Local and Systemic Immune Responses. *AAPS J.* 12, 699–707.

<https://doi.org/10.1208/s12248-010-9229-6>

- Newman, Stephen, 2009. Background to Pulmonary Drug Delivery, in: *Respiratory Drug Delivery: Essential Theory and Practice*. Respiratory Drug Delivery Online, Richmond, Virginia, pp. 1–28. <https://doi.org/1933722266>
- Newman, S., 2009. Aerosol properties and deposition principles., in: Grove, R. (Ed.), *Respiratory Drug Delivery: Essential Theory & Practice*. Davis Healthcare International Publishing, pp. 29–58.
- Newman, S., Peart, J., 2009. Dry Powder Inhalers, in: Newman, S. (Ed.), *Respiratory Drug Delivery: Essential Theory and Practice*. Respiratory Drug Delivery Online, R, pp. 257–307.
- Newman, S.P., Chan, H.-K., 2008. In Vitro / In Vivo Comparisons in Pulmonary Drug Delivery. *J. Aerosol Med. Pulm. Drug Deliv.* 21, 77–84. <https://doi.org/10.1089/jamp.2007.0643>
- Noriega-Fernandes, B., Malmjöf, M., Nowenwik, M., Gerde, P., Corvo, M.L., Costa, E., 2021. Dry powder inhaler formulation comparison: Study of the role of particle deposition pattern and dissolution. *Int. J. Pharm.* 607. <https://doi.org/10.1016/j.ijpharm.2021.121025>
- Noriega, B., Malmjöf, M., Costa, E., Corvo, M.L., Gerde, P., Maia, F.M., 2017. Dissolution of Orally Inhaled Drugs using DissolvIt®: Influence of a Newly Designed Pre-Separator for Particle Collection, in: *Drug Delivery to the Lungs 28*. Aerosol Society, Bristol, UK, p. 190.
- Noriega, B., Paiva, A.M., Corvo, M.L., Costa, E., 2018. Dissolution of Orally Inhaled Drugs Using Paddle Over Disk Apparatus A Deposition Study, in: *Respiratory Drug Delivery*. Tucson, Arizona, pp. 411–416. <https://doi.org/10.15713/ins.mmj.3>
- Osterhout, J.L., 2016. Draft Guidance on Fluticasone Furoate 1–7.
- Peng, T., Lin, S., Niu, B., Wang, X., Huang, Y., Zhang, X., Li, G., Pan, X., Wu, C., 2016. Influence of physical properties of carrier on the performance of dry powder inhalers. *Acta Pharm. Sin. B* 6, 308–318. <https://doi.org/10.1016/j.apsb.2016.03.011>
- Pharmacopeia United States, 2011. USP General Chapter (711) Dissolution. US Pharmacopeial Conv. United B. Press 1.
- Pilcer, G., Amighi, K., 2010. Formulation strategy and use of excipients in pulmonary drug delivery. *Int. J. Pharm.* 392, 1–19. <https://doi.org/10.1016/j.ijpharm.2010.03.017>
- Pilcer, G., Rosière, R., Traina, K., Sebti, T., Vanderbist, F., Amighi, K., 2013. New Co-Spray-Dried Tobramycin Nanoparticles-Clarithromycin Inhaled Powder Systems for Lung Infection Therapy in Cystic Fibrosis Patients. *J. Pharm. Sci.* 102, 1836–1846. <https://doi.org/10.1002/jps.23525>
- Poovi, G., Damodharan, N., 2018. Lipid nanoparticles: A challenging approach for oral delivery of BCS Class-II drugs. *Futur. J. Pharm. Sci.* 4, 191–205. <https://doi.org/10.1016/j.fjps.2018.04.001>
- Poursina, N., Vatanara, A., Rouini, M.R., Gilani, K., Najafabadi, A.R., 2016. The effect of excipients on the stability and aerosol performance of salmon calcitonin dry powder inhalers prepared via the spray freeze drying process. *Acta Pharm.* 66, 207–218. <https://doi.org/10.1515/acph-2016-0012>
- Poursina, N., Vatanara, A., Rouini, M.R., Gilani, K., Rouholamini Najafabadi, A., 2017. Systemic delivery of parathyroid hormone (1–34) using spray freeze-dried inhalable particles. *Pharm. Dev. Technol.* 22, 733–739. <https://doi.org/10.3109/10837450.2015.1125924>
- Pover, G.M., Dash, C.H., 1985. A new, modified form of inhaler ('Rotahaler') for patients with chronic obstructive lung disease. *Pharmatherapeutica* 4, 98–101.
- Price, R., 2018. New Insights for Product Development and Bioequivalence Assessments of Generic

- Orally Inhaled and Nasal Drug Products (OINDPs) - Dissolution and Beyond: The Use of Advanced Characterization Tools for Demonstrating Pharmaceutical Equivalence of Orally Inha.
- Price, R., Shur, J., Ganley, W., Farias, G., Fotaki, N., Conti, D.S., Delvadia, R., Absar, M., Saluja, B., Lee, S., 2020. Development of an Aerosol Dose Collection Apparatus for In Vitro Dissolution Measurements of Orally Inhaled Drug Products. *AAPS J.* 22, 1–9. <https://doi.org/10.1208/s12248-020-0422-y>
- Radivojev, S., Zellnitz, S., Paudel, A., Fröhlich, E., 2019. Searching for physiologically relevant in vitro dissolution techniques for orally inhaled drugs. *Int. J. Pharm.* 556, 45–56. <https://doi.org/10.1016/j.ijpharm.2018.11.072>
- Rau, J.L., 2005. The inhalation of drugs: advantages and problems. *Respir. Care* 50, 367–382.
- Raula, J., Rahikkala, A., Halkola, T., Pessi, J., Peltonen, L., Hirvonen, J., Järvinen, K., Laaksonen, T., Kauppinen, E.I., 2013. Coated particle assemblies for the concomitant pulmonary administration of budesonide and salbutamol sulphate. *Int. J. Pharm.* 441, 248–254. <https://doi.org/10.1016/j.ijpharm.2012.11.036>
- Recommendations, C.N., 2021. Draft Guidance on Fluticasone Furoate/ Umeclidinium Bromide/Vilanterol Trifenatate.
- Recommendations, C.N., 2020a. Draft Guidance on Glycopyrrolate/ Indacaterol Maleate 2–7.
- Recommendations, C.N., 2020b. Draft Guidance on Umeclidinium Bromide/Vilanterol Trifenatate 2–8.
- Recommendations, C.N., 2017a. Draft Guidance on Glycopyrrolate Inhalation Powder 1–7.
- Recommendations, C.N., 2017b. Draft Guidance on Salmeterol Xinafoate. *Cent. Drug Eval. Res. Food Drug Adm.*
- Recommendations, C.N., 2017c. Draft Guidance on Tiotropium Bromide. *Cent. Drug Eval. Res. Food Drug Adm.*
- Recommendations, C.N., 2016a. Draft Guidance on Indacaterol Maleate 2–7.
- Recommendations, C.N., 2016b. Draft Guidance on Fluticasone Furoate/Vilanterol Trifenatate 2–8.
- Recommendations, C.N., 2016c. Draft Guidance on Budesonide 2–8.
- Recommendations, C.N., 2015. Draft Guidance on Acclidinium Bromide 1–2.
- Riley, T., Christopher, D., Arp, J., Casazza, A., Colombani, A., Cooper, A., Dey, M., Maas, J., Mitchell, J., Reiners, M., Sigari, N., Tougas, T., Lyapustina, S., 2012. Challenges with Developing In Vitro Dissolution Tests for Orally Inhaled Products (OIPs). *AAPS PharmSciTech* 13, 978–989. <https://doi.org/10.1208/s12249-012-9822-3>
- Roberts, D.L., 2000. A high-capacity pre-separator for cascade impactors., in: Raleigh, N. (Ed.), *Respiratory Drug Delivery VII*. Serentec Press, pp. 443–445.
- Roberts, D.L., Chambers, F., Copley, M., Mitchell, J.P., 2020. Internal Volumes of Pharmaceutical Compendial Induction Port, Next-Generation Impactor With and Without Its Pre-separator, and Several Configurations of the Andersen Cascade Impactor With and Without Pre-separator. *J. Aerosol Med. Pulm. Drug Deliv.* 33, 214–229. <https://doi.org/10.1089/jamp.2019.1590>
- Robson, R., Taylor, B.J., Taylor, B., 1981. Sodium cromoglycate: spincaps or metered dose aerosol. *Br. J. Clin. Pharmacol.* 11, 383–384. <https://doi.org/10.1111/j.1365-2125.1981.tb01136.x>
- Rohrschneider, M., Bhagwat, S., Krampe, R., Michler, V., Breitkreutz, J., Hochhaus, G., 2015a. Evaluation of the Transwell System for Characterization of Dissolution Behavior of Inhalation

- Drugs: Effects of Membrane and Surfactant. *Mol. Pharm.* 12, 2618–2624. <https://doi.org/10.1021/acs.molpharmaceut.5b00221>
- Rohrschneider, M., Bhagwat, S., Krampe, R., Michler, V., Breitzkreutz, J., Hochhaus, G., 2015b. Evaluation of the Transwell System for Characterization of Dissolution Behavior of Inhalation Drugs: Effects of Membrane and Surfactant. *Mol. Pharm.* 12, 2618–2624. <https://doi.org/10.1021/acs.molpharmaceut.5b00221>
- Rudolf, G., Gebhart, J., Heyder, J., Schiller, C.F., Stahlhofen, W., 1986. An empirical formula describing aerosol deposition in man for any particle size. *J. Aerosol Sci.* 17, 350–355. [https://doi.org/10.1016/0021-8502\(86\)90103-5](https://doi.org/10.1016/0021-8502(86)90103-5)
- Rudolf, G., Köbrich, R., Stahlhofen, W., 1990. Modelling and algebraic formulation of regional aerosol deposition in man. *J. Aerosol Sci.* 21, S403–S406. [https://doi.org/10.1016/0021-8502\(90\)90266-Z](https://doi.org/10.1016/0021-8502(90)90266-Z)
- Ruge, C.C., Kirch, J., Lehr, C.M., 2013. Pulmonary drug delivery: From generating aerosols to overcoming biological barriers-therapeutic possibilities and technological challenges. *Lancet Respir. Med.* 1, 402–413. [https://doi.org/10.1016/S2213-2600\(13\)70072-9](https://doi.org/10.1016/S2213-2600(13)70072-9)
- Russell-Graham, D., Cooper, A., Stobbs, B., McAulay, E., Bogard, H., Heath, V., Monsallier, E., 2010. Further evaluation of the fast-screening impactor for determining fine particle fraction of dry powder inhalers, in: Mitchell, J., Nichols, S.C. (Eds.), *Drug Delivery to the Lungs-21*. The Aerosol Society, Edinburgh, pp. 374–377.
- Saboo, S., Tumban, E., Peabody, J., Wafula, D., Peabody, D.S., Chackerian, B., Muttill, P., 2016. Optimized Formulation of a Thermostable Spray-Dried Virus-Like Particle Vaccine against Human Papillomavirus. *Mol. Pharm.* 13, 1646–1655. <https://doi.org/10.1021/acs.molpharmaceut.6b00072>
- Sahakijpipjarn, S., Moon, C., Koleng, J.J., Christensen, D.J., Williams, R.O., 2020. Development of Remdesivir as a Dry Powder for Inhalation by Thin Film Freezing. *Pharmaceutics* 12, 1002. <https://doi.org/10.3390/pharmaceutics12111002>
- Salama, R.O., Traini, D., Chan, H.K., Young, P.M., 2008. Preparation and characterisation of controlled release co-spray dried drug-polymer microparticles for inhalation 2: Evaluation of in vitro release profiling methodologies for controlled release respiratory aerosols. *Eur. J. Pharm. Biopharm.* 70, 145–152. <https://doi.org/10.1016/j.ejpb.2008.04.009>
- Sanders, M., 2007. Inhalation therapy: An historical review. *Prim. Care Respir. J.* 16, 71–81. <https://doi.org/10.3132/pcrj.2007.00017>
- Santos Cavaiaola, T., Edelman, S., 2014. Inhaled insulin: A breath of fresh air? a review of inhaled insulin. *Clin. Ther.* 36, 1275–1289. <https://doi.org/10.1016/j.clinthera.2014.06.025>
- Shahiwala, A., Misra, A., 2005. A preliminary pharmacokinetic study of liposomal leuprolide dry powder inhaler: A technical note. *AAPS PharmSciTech* 6, E482–E486. <https://doi.org/10.1208/pt060360>
- Shalash, A.O., Elsayed, M.M.A., 2017. A New Role of Fine Excipient Materials in Carrier-Based Dry Powder Inhalation Mixtures: Effect on Deagglomeration of Drug Particles During Mixing Revealed. *AAPS PharmSciTech* 18, 2862–2870. <https://doi.org/10.1208/s12249-017-0767-4>
- Sheng, J.J., Sirois, P.J., Dressman, J.B., Amidon, G.L., 2008. Particle diffusional layer thickness in a USP dissolution apparatus II: A combined function of particle size and paddle speed. *J. Pharm. Sci.* 97, 4815–4829. <https://doi.org/10.1002/jps.21345>
- Shotton, E., Orr, N.A., 1971. Studies on mixing cohesive powders. *J. Pharm. Pharmacol.* 23, 260S-

- 260S. <https://doi.org/10.1111/j.2042-7158.1971.tb08852.x>
- Shrewsbury, S.B., Cook, R.O., Taylor, G., Edwards, C., Ramadan, N.M., 2008. Safety and Pharmacokinetics of Dihydroergotamine Mesylate Administered Via a Novel (Tempo™) Inhaler. *Headache J. Head Face Pain* 48, 355–367. <https://doi.org/10.1111/j.1526-4610.2007.01006.x>
- Shur, J., Price, R., 2012. Advanced microscopy techniques to assess solid-state properties of inhalation medicines. *Adv. Drug Deliv. Rev.* 64, 369–382. <https://doi.org/10.1016/j.addr.2011.11.005>
- Shur, J., Price, R., Lewis, D., Young, P.M., Woollam, G., Singh, D., Edge, S., 2016. From single excipients to dual excipient platforms in dry powder inhaler products. *Int. J. Pharm.* 514, 374–383. <https://doi.org/10.1016/j.ijpharm.2016.05.057>
- Siekmeier, R., Scheuch, G., 2008. Inhaled insulin - does it become reality? *J. Physiol. Pharmacol.* 59, 81–113.
- Snell, N.J.C., 2001. The Carbolic Smoke Ball. *Int. J. Pharm. Med.* 15, 195–196. <https://doi.org/10.2165/00124363-200108000-00006>
- Son, Y.-J., McConville, J.T., 2012. Preparation of sustained release rifampicin microparticles for inhalation. *J. Pharm. Pharmacol.* 64, 1291–1302. <https://doi.org/10.1111/j.2042-7158.2012.01531.x>
- Son, Y.J., Horng, M., Copley, M., McConville, J.T., 2010. Optimization of an in vitro dissolution test method for inhalation formulations. *Dissolution Technol.* 17, 6–13. <https://doi.org/10.14227/DT170210P6>
- Son, Y.J., McConville, J.T., 2009. Development of a standardized dissolution test method for inhaled pharmaceutical formulations. *Int. J. Pharm.* 382, 15–22. <https://doi.org/10.1016/j.ijpharm.2009.07.034>
- Staniforth, J.N., 1987. British Pharmaceutical Conference Science Award Lecture 1986: Order out of chaos. *J. Pharm. Pharmacol.* 39, 329–334. <https://doi.org/10.1111/j.2042-7158.1987.tb03393.x>
- Stein, S.W., Olson, B.A., 1997. Variability in size distribution measurements obtained using multiple Andersen Mark II cascade impactors. *Pharm. Res.* 14, 1718–1725. <https://doi.org/10.1023/A:1012175612193>
- Stocks, J., Hislop, A.A., 2002. Structure and function of the respiratory system: Developmental aspects and their relevance to aerosol therapy, in: Bisgaard, H., Chris, O., C. Smaldone, G. (Eds.), *Drug Delivery to the Lung*. Marcel Dekker, New York, pp. 47–104.
- Suarez, S., Hickey, A.J., 2000. Drug properties affecting aerosol behavior. *Respir. Care* 45, 652–66.
- Tabe, R., Rafee, R., Valipour, M.S., Ahmadi, G., 2021. Investigation of airflow at different activity conditions in a realistic model of human upper respiratory tract. *Comput. Methods Biomech. Biomed. Engin.* 24, 173–187. <https://doi.org/10.1080/10255842.2020.1819256>
- Tay, J.Y.S., Liew, C.V., Heng, P.W.S., 2018. Dissolution of fine particle fraction from truncated Anderson cascade impactor with an enhancer cell. *Int. J. Pharm.* 545, 45–50. <https://doi.org/10.1016/j.ijpharm.2018.04.048>
- Thalberg, K., Åslund, S., Skogevall, M., Andersson, P., 2016. Dispersibility of lactose fines as compared to API in dry powders for inhalation. *Int. J. Pharm.* 504, 27–38. <https://doi.org/10.1016/j.ijpharm.2016.03.004>
- Thippahawong, J.B., Babul, N., Morishige, R.J., Findlay, H.K., Reber, K.R., Millward, G.J., Otulana, B.A.,

2003. Analgesic efficacy of inhaled morphine in patients after bunionectomy surgery. *Anesthesiology* 99, 693–700. <https://doi.org/10.1097/00000542-200309000-00026>
- Thomas, C., Rawat, A., Hope-Weeks, L., Ahsan, F., 2011. Aerosolized PLA and PLGA Nanoparticles Enhance Humoral, Mucosal and Cytokine Responses to Hepatitis B Vaccine. *Mol. Pharm.* 8, 405–415. <https://doi.org/10.1021/mp100255c>
- Travers, D.N., White, R.C., 1971. The mixing of micronized sodium bicarbonate with sucrose crystals. *J. Pharm. Pharmacol.* 23, 260S-261S. <https://doi.org/10.1111/j.2042-7158.1971.tb08853.x>
- United States Food and Drug Administration, 2013. Guidance on Fluticasone Propionate; Salmeterol Xinafoate. *US Food Drug Adm.* 2–8.
- Vallee, S., Rakhe, S., Reidy, T., Walker, S., Lu, Q., Sakorafas, P., Low, S., Bitonti, A., 2012. Pulmonary Administration of Interferon Beta-1a-Fc Fusion Protein in Non-Human Primates Using an Immunoglobulin Transport Pathway. *J. Interf. Cytokine Res.* 32, 178–184. <https://doi.org/10.1089/jir.2011.0048>
- Vartak, R., Patil, S.M., Saraswat, A., Patki, M., Kunda, N.K., Patel, K., 2021. Aerosolized nanoliposomal carrier of remdesivir: an effective alternative for COVID-19 treatment in vitro. *Nanomedicine* 16, 1187–1202. <https://doi.org/10.2217/nnm-2020-0475>
- Vehring, R., 2008. Pharmaceutical particle engineering via spray drying. *Pharm. Res.* 25, 999–1022. <https://doi.org/10.1007/s11095-007-9475-1>
- Velaga, S.P., Djuris, J., Cvijic, S., Rozou, S., Russo, P., Colombo, G., Rossi, A., 2017. Dry powder inhalers: An overview of the in vitro dissolution methodologies and their correlation with the biopharmaceutical aspects of the drug products. *Eur. J. Pharm. Sci.* 0–1. <https://doi.org/10.1016/j.ejps.2017.09.002>
- Wauthoz, N., Amighi, K., 2015. Formulation strategies for pulmonary delivery of poorly soluble drugs, in: Nokhodchi, A., Martin, G.P. (Eds.), *Pulmonary Drug Delivery Advances and Challenges*. John Wiley & Sons, Ltd, Chichester, pp. 87–122.
- Wei, X., Hindle, M., Kaviratna, A., Huynh, B.K., Delvadia, R.R., Sandell, D., Byron, P.R., 2018. In Vitro Tests for Aerosol Deposition. VI: Realistic Testing with Different Mouth–Throat Models and In Vitro—In Vivo Correlations for a Dry Powder Inhaler, Metered Dose Inhaler, and Soft Mist Inhaler. *J. Aerosol Med. Pulm. Drug Deliv.* 31, 358–371. <https://doi.org/10.1089/jamp.2018.1454>
- Weibel, E.R., 1963. Geometric and Dimensional Airway Models of Conductive, Transitory and Respiratory Zones of the Human Lung. *Morphometry Hum. Lung* 136–142. https://doi.org/10.1007/978-3-642-87553-3_11
- Wetterlin, K., 1988. Turbuhaler: A New Powder Inhaler for Administration of Drugs to the Airways. *Pharm. Res.* 5, 506–508.
- Wolff, R.K., 1998. Safety of Inhaled Proteins for Therapeutic Use. *J. Aerosol Med.* 11, 197–219. <https://doi.org/10.1089/jam.1998.11.197>
- Yadav, N., Lohani, A., 2013. Dry powder inhalers: A review. *Indo Glob. J. Pharm. Sci.* 3, 142–155.
- Yeh, H.-C., Schum, G.M., 1980. Models of human lung airways and their application to inhaled particle deposition. *Bull. Math. Biol.* 42, 461–480. [https://doi.org/10.1016/S0092-8240\(80\)80060-7](https://doi.org/10.1016/S0092-8240(80)80060-7)
- Zhang, Y., Gilbertson, K., Finlay, W.H., 2007. In Vivo—In Vitro Comparison of Deposition in Three Mouth–Throat Models with Qvar® and Turbuhaler® Inhalers. *J. Aerosol Med.* 20, 227–235.

<https://doi.org/10.1089/jam.2007.0584>

Chapter 3

Paddle over disk

Development and comparison of collection and dissolution strategies for fluticasone propionate



This chapter has been published as:

Fernandes B., Maia F.M., Paiva A.M., Corvo M.L., Costa E., 2016. Paddle over disk as a dissolution test for orally inhaled drugs: discriminating composite from carrier based formulations. In Drug Delivery to the Lungs 27. The Aerosol Society. Bristol. pages 308-12.

Fernandes B., Paiva A.M., Corvo M.L., Costa E., Maia F.M., 2016. Paddle. Over Disk as a Dissolution Test for Orally Inhaled Fluticasone Propionate: Impact of Temperature, Dose and Formulation. In Respiratory Drug. Delivery Europe 2017 Book 2. page 215.

Noriega B., Paiva A.M., Corvo M.L., Costa E., 2016. Dissolution of orally inhaled drugs using Paddle Over Disk Apparatus: a deposition study. In Respiratory Drug Delivery Europe 2018: page 411.

Noriega B., Sousa L.V., Chaves R., Corvo M.L., Paiva M., Costa E., An Analytical Quality by Design (AQbD) approach to predict dissolution of dry powders inhalers with Apparatus IV In Respiratory Drug Delivery Europe 2019. Volume 2: pages 301-6.

3.1 SUMMARY

There is not a performance characterization test for orally inhaled drugs aside from the impaction test, which is limited to aerosolization performance. Most of the under-development dissolution apparatus for inhalation found in the literature combine a collection step with a dissolution step aiming to assess the dissolution profile of powder within the inhalable particle size range.

In the present chapter, the paddle over disk (POD) strategy is presented, combining cascade impactors (fast screening impactor (FSI) and next generation impactor (NGI) as a collection step with standard dissolution paddle apparatus (UPS apparatus II). The USP apparatus II was adapted to dissolve the powder after its aerosolization and collection with both impactors. A disk is placed inside of the dissolution vessel, with the stirring paddle over it, holding the previously collected fraction of powder that might be able to reach the deep lung, separated from the dissolution medium by a polycarbonate membrane.

To implement this strategy, three differentiated formulations were used: a carrier-based formulation containing the drug substance (DS) fluticasone propionate (FP) produced by two different particle size engineering technologies (jet milling and wet polishing), and carrier free formulation produced by spray-drying. Additionally to formulation comparison, method parameters were studied, such as the influence of the amount of DS collected in the impactor and thus present in the dissolution vessel, or the influence of medium temperature on the dissolution kinetics. The impact of sample collection methods (NGI vs FSI) combined with in the UPS apparatus II was assessed by comparing the dissolution profile obtained for the same formulations.

Finally, a quality by design analysis was applied to a combination of a flow-through dissolution system (UPS apparatus IV) with the FSI for dose collection.

3.2 INTRODUCTION

One of the most important steps with *in vitro* performance testing of inhalation products is the characterization of the delivery of a given drug substance (DS) from a specified inhaler using a pharmaceutical impactor/impinger, to estimate the actual dose that can potentially deposit on the lung. However, aerodynamic characterization does not completely describe the particles behavior once inhaled. It completely misses the assessment of the drug absorption profile, which depends in great extent on the dissolution of the pharmaceutical dosage form. An ideal dissolution test procedure for inhaled formulations would involve particle aerodynamic classification followed by an evaluation of the dissolution behavior for the classified drug particles that may deposit at various sites in the respiratory tract (Radivojev et al., 2019).

Although dissolution testing for oral drugs is widespread and routinely used for both quality control and R&D to identify the influence of critical manufacturing parameters on dissolution profiles and for establishing *in vitro* / *in vivo* correlations, none of the standard USP apparatus I, II, III and IV are readily adapted for assessing inhaled products. Few reports of powder or nanoparticle dissolution testing are based on apparatus suited for oral drugs, and studies failed to discriminate between formulations (Heng et al., 2008; Raula et al., 2013; Sievens-Figueroa et al., 2012), as the dry powders are difficult to disperse homogeneously and tend to adhere to the walls and paddles.

When developing a dissolution system for orally inhaled drugs, there are several challenges to be overcome. Firstly, the selection/development of the sample collection method, as well as the design of an appropriate method for the transfer of the collected samples to dissolution apparatus (Floroiu et al., 2018). The collection method becomes relevant not only because it allows to select the fraction of powder to be tested, either the fine particle fraction or a smaller fraction which reaches a specific lung region, achieving a more target specific methodology. Moreover, for DS with lower solubility, the particles disposition when collected (powder microstructure) can have a significant impact on the dissolution rate, either due to the dissolution area available being altered when particles deposit separately or as agglomerates; or due to the presence or lack of excipients in the agglomerate, which when dissolved will alter the dissolution media composition, and therefore may affect the dissolution rate (Farias et al., 2017; Price et al., 2020).

Secondly, a decision must be made between sink conditions versus physiologically relevant conditions, and if the latter is selected as the optimal choice, the challenge becomes to simulate the lung surface where dissolution takes place, including the presence or not of mucus, its composition and its influence in the dissolution and permeation process, and the selection of an appropriate dissolution media. This decision should come with a validation of the bio-predictability or of significant formulation differentiation (in case of a quality control method).

The last step to achieve a suitable methodology is to define the acceptance criteria (e.g. target maximum variability, sensibility to formulation variations due to changes on process parameters known to impact *in vivo* observations (quality control perspective), formulation differentiation capability (product development perspective)) and standardize the dissolution system. System standardization and commercial availability are crucial to ensure comparable results throughout industry and academia, acceptance by the regulatory agencies and an overall better understanding the dissolution and absorption of inhaled products, and their impact on clinical efficacy – similarly to what occurred for other dosage forms (Grady et al., 2018).

Several authors have attempted to develop systems capable of overcoming the mentioned drawbacks (Cook et al., 2005; Davies and Feddah, 2003; Kwon et al., 2007; Sdraulig et al., 2008). Son et al. (Son et al., 2010; Son and McConville, 2009) developed a potential standardized test method applicable to various formulations, as a variation of USP Apparatus II (paddle), designated paddle over disk apparatus (POD). A stainless-steel support disc is placed under the paddle to hold the test sample at a precise distance from the bottom edge of the paddle. This method is amenable for inhaled products as particles with a known aerodynamic diameter can be collected using an aerosol impactor such as the NGI or FSI and can be directly positioned inside the vessel, guaranteeing that the tested powder is within the respirable fraction.

To pursue the objective to elucidate some of the demands specified above, the present chapter intends to study selected methodologies and is divided in three main studies using FP differentiated model formulations. Firstly, a section focusing on a proof of concept of the POD apparatus is presented. Here, the set-up as per used in the literature and commercialized is applied by collecting the formulation on an NGI stage is tested with carrier-based formulation (micronized DS mixed with lactose as a carrier), and advanced formulations manufactured by spray-drying, containing DS distributed in particles containing a bulking agent and a force control agent. The next study aims to optimize the set-up

parameters and define the main limitation while upgrading the set-up to obtain an enhanced procedure. Finally, the optimized particle collection set-up is used in combination with other standard dissolution equipment – USP apparatus IV (flow-through) – which is tested regarding the impact of the method critical parameters on the formulation dissolution profile, using an analytical quality by design approach.

Overall, this chapter attempts to propose a number of dissolution methodology possibilities for orally inhaled dry powders, listing each advantage and draw back.

3.3 FORMULATION MANUFACTURE AND CHARACTERIZATION

3.3.1 Outline

Prior to dissolution assessment, formulations containing FP were manufactured, including carrier-based formulations containing jet milled and wet polished FP, and carrier-free formulations with different sugars as glass forming agents. The manufactured powders were characterized as per standard approaches: geometric particle size distribution by laser diffraction, morphology by scanning electron microscopy (SEM) and aerodynamic performance by next generation impactor (NGI).

The characterization is relevant, on the one hand, to plan the dissolution methodology regarding the collection strategy – to select an NGI stage, maximize the sample collection amount and number of actuations required for the target dose. On the other hand, particle size and morphology information is helpful in the understanding of the dissolution kinetics.

3.3.2 Materials and Methods

3.3.2.1 Materials

Lactose micronized powders Lactohale 230 and Respitose SV003 were purchased from DHE Pharma (Germany), and Inhalac 400 was purchased from Meggle Pharma (Germany). Capsules number 3 were purchased from Capsugel (USA). Crystalline fluticasone propionate (FP; C₂₅H₃₁F₃O₅S; Mw = 500.6) micronized by jet milling (JM) and wet polishing (WP) was supplied by Hovione S.A. (Portugal). Raffinose pentahydrate was purchased from Amresco (USA). Trehalose di-hydrated was purchased from Pfanstiehl (USA). L-Leucine was purchased from Merck KGaA (Germany). All other chemicals were of analytical grade.

3.3.2.2 Methods

3.3.2.2.1 Formulation manufacture

To produce carrier-free powders, a solution with 2% (w/w) of solids in a water/ethanol (50/50, % (w/w)) solvent mixture was prepared, with 20% L-leucine to act as a force control agent, 79% sugar (trehalose or raffinose) as a bulking agent, and 1% FP as indicated in Table 3.1. The formulations were spray-dried at an outlet temperature of 95 °C (inlet temperature of 145 °C), a solution feed flow of 7 g/min,

atomization pressure of 8 bar and atomization gas flow at 50 mm in the rotameter, using a Büchi model B-290 unit equipped with a two fluid nozzle with a 1.4 mm cap and 0.7 mm orifice. The manufactured formulations were hand-filled in HPMC size 3 capsules with a target fill weight of 12.5 mg, with acceptance limits of +/- 0.5 mg.

Table 3.1 - Composition of spray-dried solutions used to manufacture the composite Fluticasone Propionate (FP) formulations containing trehalose di-hydrate (CF1) and Raffinose pentahydrate (CF2) as glass formers.

| Component | CF1 (g) | CF2 (g) |
|--|----------------|----------------|
| Solvent - Water/Ethanol (50/50% (w/w)) | 392 | 392 |
| Trehalose di-hydrated | 7.01 | - |
| Raffinose pentahydrate | - | 7.47 |
| L-Leucine | 1.58 | 1.58 |
| Fluticasone Propionate (FP) | 0.08 | 0.08 |

To obtain the carrier-based blend powders, homogeneous mixtures of 150 g of coarse and fine lactose with 1% (w/w) micronized FP were prepared in a high shear mixer from Diosna model P1-6 (Germany), following geometric dilution of FP in a 0.5 L bowl. Content of fine excipient in the prepared blends is described in Table 3.2. The carrier-based formulations were filled in HPMC size 3 capsules with a target fill weight of 12.5 mg for FPJ1 blend, for the proof-of-concept study, and 20 mg of FPJ2 blend and FPW blend for the optimization studies (with acceptance limits of +/- 0.5 mg) using a semi-automatic Quantos unit from Mettler Toledo AG (Spain).

Table 3.2 - Carrier-based formulations prepared with 1% of fluticasone propionate (FP).

| Formulation | Micronization technology | Fine lactose | Coarse lactose | % of fine lactose | Fill weight (mg) |
|--------------------|---------------------------------|---------------------|-----------------------|--------------------------|-------------------------|
| FPJ1 blend | Jet Milling | Lactohale | Respitose SV003 | 5 | 12.5 ± 0.6 |
| FPJ2 blend | Jet Milling | 230 | | 5 | 20.0 ± 1.0 |
| FPW blend | Wet Milling | Inhalac400 | | 10 | 20.0 ± 1.0 |

3.3.2.2.2 Scanning electron microscopy and particle size analysis

The manufactured formulations CF1, CF2 and FPJ1 blend were visualized by scanning electron microscope (SEM - JEOL JSM-7001/Oxford INCA Energy 250/HKL, Japan) in high vacuum mode was used with a typical accelerating voltage between 5 and 20 kV. The samples attached to adhesive carbon tapes (Ted Pella, Inc., CA, USA), exposed to vacuum for 2 hours and coated with a 15 nm gold layer (South Bay Technologies, former Polaron, model E5100, San Clement, CA). The images were captured at different magnifications.

The particle size distribution of spray-dried formulation was measured as dry powder by laser diffraction using a HELOS laser diffraction instrument (Sympatec GmbH, Germany). The particle size distribution data was presented as Dv10, Dv50 and Dv90 (particle size below which 10 %, 50 % and 90 % of the volume of particles exist).

3.3.2.2.3 Aerodynamic particle size distribution by next generation impactor

The carrier-based formulations were assessed by NGI (n=3) with chemical recovery (HPLC, (section 3.3.2.2.4) with 5 capsules per replicate, using the Plastiapne Monodose inhaler (40L/min at 4 kPa pressure drop). The carrier-free formulations were actuated with the PowdAir inhaler (40L/min at 4 kPa pressure drop) and its deposition profile determined with a gravimetric analysis of collected NGI deposits (n=3), using one capsule per replicate.

3.3.2.2.4 Quantification of Fluticasone propionate (FP)

To quantify the FP deposited in the NGI, a Waters HPLC system with UV detection was used. The system consisted of a Waters 717 plus autosampler, a Waters 1525 binary HPLC Pump and a Waters Jet Stream 2 Plus incubator. Dissolution samples were filtered using 0.45 µm GHP Acrodisc® syringe filters before injection (Merck KGaA, Germany). Chromatography was performed using a Symmetry C18 5 µm, 4.6 mm × 250 mm column (Waters, USA). The mobile phase which consisted of methanol, acetonitrile and acetate buffer solution 0.01M, pH 4 in a ratio of 35:35:30 (v/v/v) respectively, a flow rate of 1.0 mL/min was used and the detection was made using an UV detector set to a wavelength of 240 nm. The column temperature was maintained at 35 °C and the volume of each sample injected was 20 µL.

3.3.3 Results and discussion

For this study, the development and characterization of formulations prior dissolution assessment are crucial steps to be performed. Therefore, formulations manufactured by FP blending with coarse and fine lactose, as well as manufactured by spray-drying were prepared and characterized in terms of particle size distribution, morphology, and aerodynamic particle size distribution. These parameters are important to understand the impact of particle and formulation characteristics on the dissolution profiles obtained.

3.3.3.1 Particle size distribution and morphology

The PSD analysis of the spray-dried composite aerosols containing trehalose and raffinose showed a similar particle size distribution, with 90% of particles having a diameter below 3.3 and 3.2 μm , and a span of 2.0 and 2.1, respectively. These results indicate the generated particles are suitable for inhalation as their particle size is within the inhalation range (0.5 to 5 μm). Additionally, the SEM analysis (Figure 3., C-F) confirm the PSD results and show how both formulations have a similar morphology – spherical slightly corrugated particles – a typical morphology for spray-dried particles containing L-leucine and a sugar (Moura et al., 2015). Spherical corrugated particles with a particle size in the respirable range are typically optimal for inhalation delivery as good aerodynamic performance is ensured while minimizing particle cohesion due to reduced number of contact points. As the particle size distribution and morphology are very similar for the carrier-free formulations, differences on dissolution profiles should not be related with these parameters.

Table 3.3 - Particle size distribution characterization of the spray-dried particles consisting of fluticasone propionate (FP), L-leucine and the sugar listed, as per Table 3., n=2, and jet milled and wet polished FP used for the carrier-based formulations with 1% of micronized FP (Table 3.2)

| | Dv10 (μm) | Dv50 (μm) | Dv90 (μm) | Span |
|--------------------------|------------------------|------------------------|------------------------|------|
| Composite with trehalose | 0.5 | 1.4 | 3.3 | 2.0 |
| Composite with raffinose | 0.5 | 1.3 | 3.2 | 2.1 |
| Jet milled FP | 0.9 | 1.9 | 3.6 | 1.4 |
| Wet polished FP | 1.1 | 1.9 | 3.2 | 1.1 |

Dv10, Dv50 and Dv90: Particle size below which 10 %, 50 % and 90 % of the volume of particles exist.

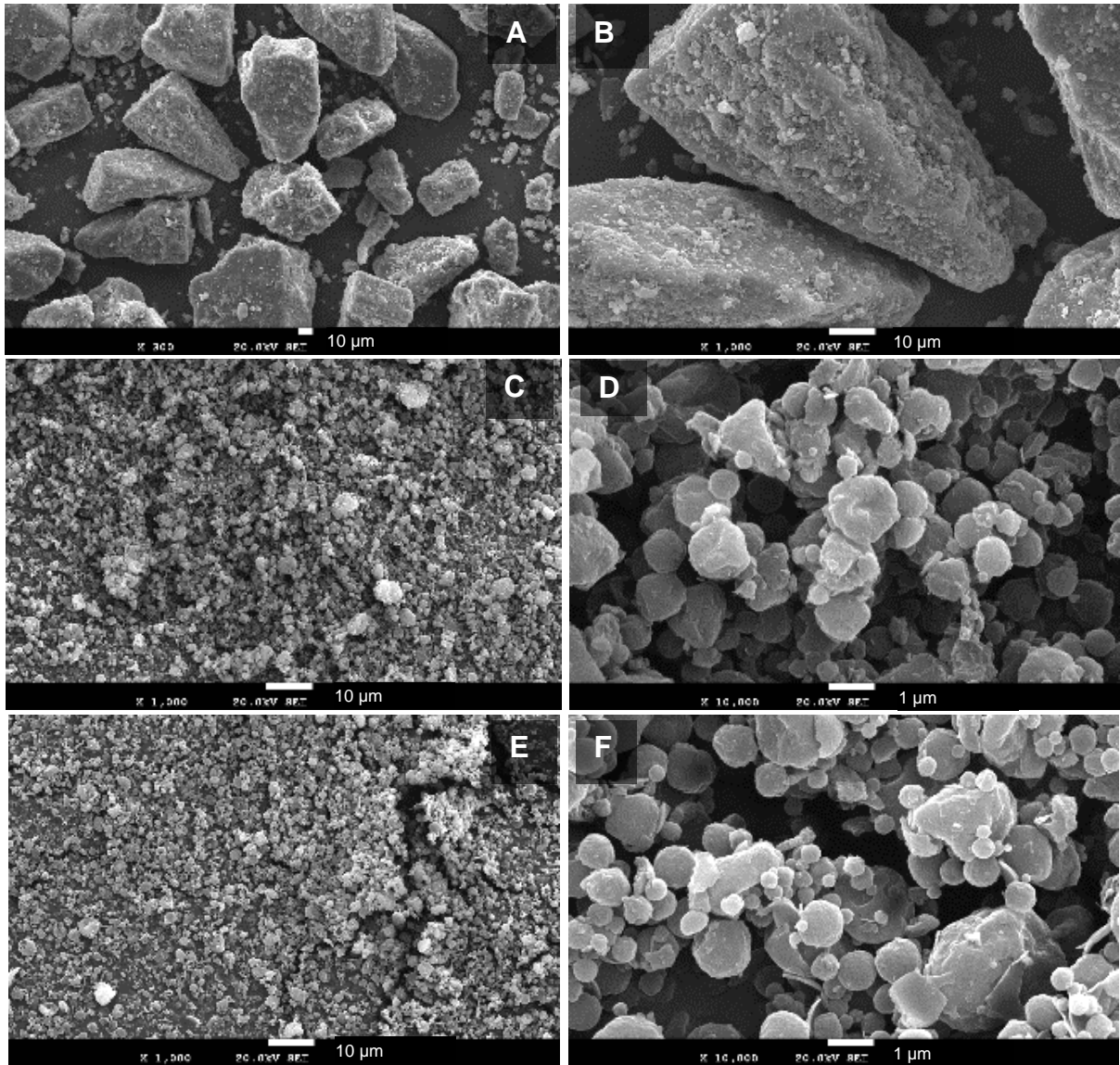


Figure 3.1 - SEM micrographs for carrier-based formulation FPJ1 (A and B) x300 and x1000 respectively; and for spray-dried composite formulations containing trehalose CF1 (C and D) and raffinose CF2 (E and F), x1000 and x 10 000 respectively; at 20 kV.

For the carrier-based formulation the SEM images are presents in Figure 3., A-B. This formulation presents a typical particle disposition - smaller agglomerates of fines ($\approx 10 \mu\text{m}$), and fines attached to the carrier lactose particles. Upon actuation a release the fine particles from the coarse lactose surface is expected as well as a deagglomeration of the larger globules of particles, freeing the FP particles to reach the deep lung surface. As the SEM analysis presented show the structures previous to actuation the disposition of the DS and excipient particles during dissolution assessment cannot the predicted at the present stage.

3.3.3.2 Aerodynamic particle size distribution

The aerodynamic performance of the formulations FPJ1 blend, CF1 and CF2 determined by NGI is illustrated in Figure 3.2.A, and of the formulations FPJ2 blend and FPW blend in Figure 3.2.B. The performance parameters are summarized in Table 3.4.

Formulation FPJ1 blend, CF1 and CF2 were compared in the proof of concept study (section 3.4) and during method development using the NGI as a collection strategy (sections 3.5.2 and 3.5.3), while formulations FPJ2 blend and FPW blend were compared using the FSI as a collection strategy (section 3.5.4). The pre-separator (PS) was included for the carrier-based formulation to collect the FP adhered to the coarse lactose particles, and it was not required for the carrier-free particles.

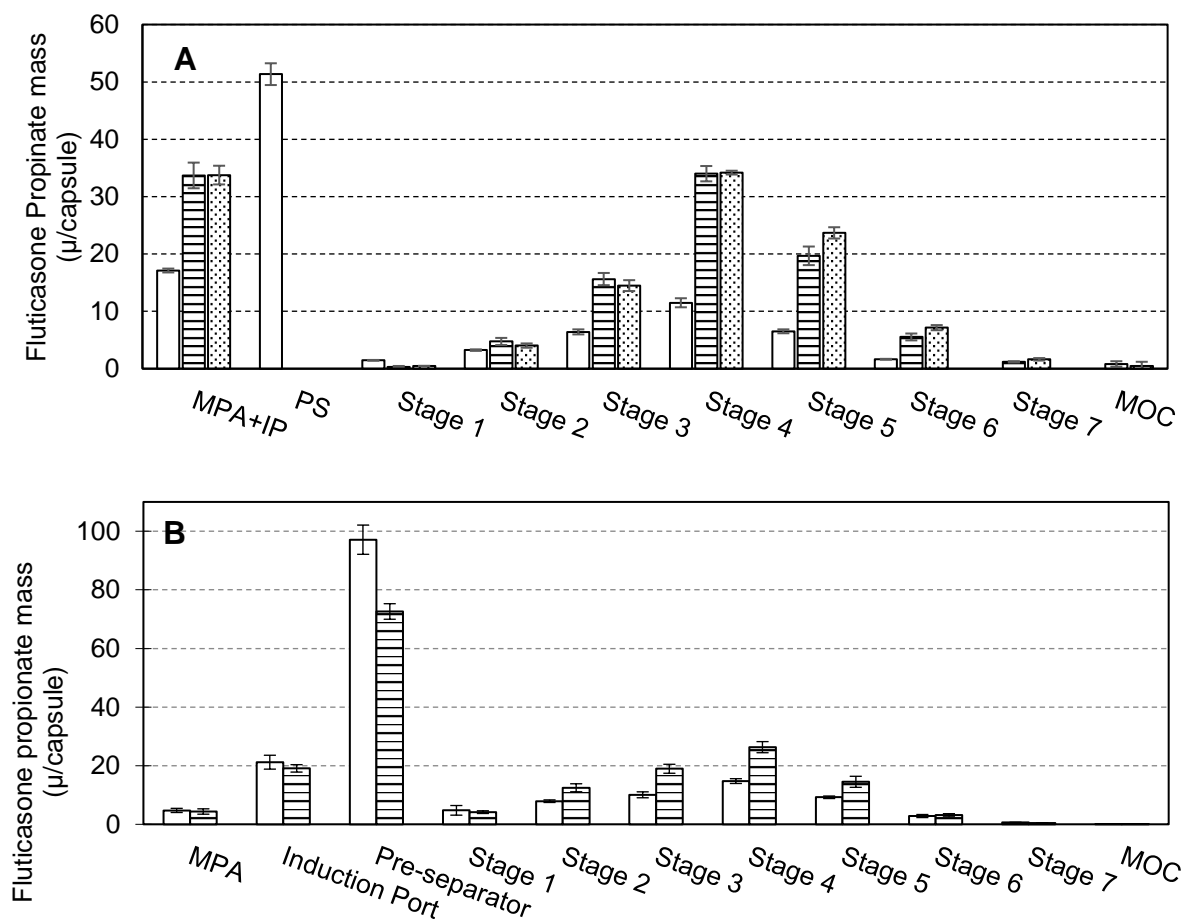


Figure 3.2 - Aerodynamic characterization of (A) the carrier-based formulation containing 1% of jet milled fluticasone propionate (FP) (white), composite particle containing trehalose (striped bars) and raffinose (dotted bars), capsules of 12.5 mg, and (B) the carrier-based formulation containing 1% of jet milled FP (white), the carrier-based formulation containing 1% of wet polished FP (striped bars), capsules of 20.0 mg, determined by Next Generation Impactor. Data expressed as mean \pm SD (n=3). MPA: mouth piece adapter; IP: induction port; MOC: micro-orifice collector. Stage 1 - 7:

As expected, the carrier-based formulation presented a significant worse aerodynamic performance with a mass median aerodynamic diameter almost doubled (2.9 to 3.2 μm) compared with the carrier-free formulations (1.5 \pm 0.1 μm and 1.4 \pm 0.1 μm , for the particle containing trehalose and raffinose, respectively). The differences can also be quantified by comparing the emitted dose and the fine particle dose parameters, significantly larger for the carrier-free formulations. These results were not surprising as the carrier-free formulations were optimized for both composition and process to ensure the maximum lung delivery (Moura et al., 2015). Also, each formulation was actuated using different devices (PowdAir for carrier-based and Plastiaple RS01 40L/min for carrier-free) which also have an impact on the aerodynamic performance.

When comparing the carrier-free formulations containing trehalose and raffinose, the raffinose formulations appears to have a slightly higher fine particle dose (77 \pm 2 $\mu\text{g}/\text{cap}$ and 82 \pm 2 $\mu\text{m}/\text{cap}$), however when considering mass median aerodynamic diameter (MMAD), geometric standard deviation (GSD) and fine particle fraction (FPF) no significant difference is observed.

Finally, the carrier-based formulations containing jet milled (FPJ2 blend) and wet polished (FPW blend) FP, filled with a 20.0 mg fill-weight, show a significantly different performance, with the wet polished formulation presenting an almost double fine particle dose (FPD) - 36 \pm 1 $\mu\text{m}/\text{dose}$ and 60 \pm 7 $\mu\text{m}/\text{dose}$, for the formulation containing jet milled and wet polished FP, respectively, in spite of the PSD of the micronized FP being similar. These results indicate the formulation strategy (the particle engineering technology, blending mechanism and the amount of fine lactose) has a decisive impact on drug product final performance, which is in accordance with the literature (Jones et al., 2010; Kaialy, 2016; Kinnunen et al., 2014).

Table 3.4 - Aerodynamic performance parameters of the carrier-based formulation containing 1% of jet milled fluticasone propionate (FP) (FPJ1 blend), composite particle containing trehalose (CF1) and raffinose (CF2), capsules of 12.5 mg, and of the carrier-based formulation containing 1% of jet milled FP (FPJ2 blend), the carrier-based formulation containing 1% of wet polished FP (FPW blend), capsules of 20.0 mg, determined by Next Generation Impactor. n=3.

| Parameter | FPJ1 blend | CF1 | CF2 | FPJ2 blend | FPW blend |
|-----------------------|-------------|----------------|----------------|----------------|----------------|
| Device | PowdAir | Plastiape RS01 | Plastiape RS01 | Plastiape RS01 | Plastiape RS01 |
| ED (µg/dose) | 93 ± 2 | 115 ± 1 | 119 ± 2 | 173 ± 8 | 176 ± 10 |
| FPD (µg/dose) | 25 ± 2 | 77 ± 2 | 82 ± 2 | 36 ± 1 | 60 ± 7 |
| FPF _{ED} (%) | 27 ± 1 | 67 ± 2 | 69 ± 2 | 18 ± 1 | 30 ± 1 |
| MMAD (µm) | 2.9 ± 0.1 | 1.5 ± 0.1 | 1.4 ± 0.1 | 3.2 ± 0.2 | 3.2 ± 0.1 |
| GSD - | 1.91 ± 0.02 | 1.81 ± 0.02 | 1.79 ± 0.01 | 1.99 ± 0.02 | 2.40 ± 0.20 |

ED: emitted dose; FPD: fine particle dose; FPF_{ED}: fine particle fraction over emitted dose; MMAD: mass median aerodynamic diameter; GSD: geometric standard deviation.

3.3.4 Conclusions

A range of formulations were manufactured to support POD dissolution method proof-of concept, and optimization, as well as USP apparatus IV method development. The formulations have significantly different morphologies (spray-dried carrier-free particles are corrugated spheres, with carrier-based formulations are a mixture of crystalline material), compositions and aerodynamic performances. Considering this, the next questions are 1) will the formulation strategy also influence dissolution kinetics, and 2) can the POD dissolution system identify that influence, or is a more discriminative approach required.

3.4 PADDLE OVER DISK TO DIFFERENTIATE FORMULATIONS – PROOF OF CONCEPT

3.4.1 Outline

POD is available commercially and tested in the literature for commercial DPI formulations. Herein, POD was applied to compare newly developed formulations with FP (model drug with low solubility and high permeability) manufactured as both a carrier-based and a carrier-free formulation.

The prepared formulations and previously characterized formulations FPJ1 blend (carrier-based), CF1 and CF2 (carrier-free) dissolution profiles were compared using the UPS apparatus II and the POD apparatus after collection using the NGI. To minimize the impact of drug load in the dissolution kinetics and ensure comparable dissolution conditions, a similar drug load in the dissolution media was targeted. For that, the number of actuated capsules was determined to collect approximately 100 µg on the disk for each formulation.

The main goal of the present section is to evaluate the differentiation capabilities of the POD methodology.

3.4.2 Materials and Methods

3.4.2.1 Materials

Beyond the materials used in sections 3.3.2.1, sodium dodecyl sulfate (SDS) was purchased from Sigma-Aldrich (USA), 0.01 M phosphate buffer saline tablets from Sigma-Aldrich (USA) and polycarbonate membranes with a 76 mm diameter and 0.05 µm pore size from Whatman (USA).

3.4.2.2 Methods

3.4.2.2.1 Next Generation Impactor set-up for sample collection

As a first iteration, the NGI equipped with a dissolution cup was used to collect samples of the different formulations, at the same stage (similar aerodynamic particle size).

The DPI formulations were actuated in an NGI following the conditions previously described for aerodynamic profile determination (Section 3.3.2.2.3) in order to obtain particle separation and collect a

known amount of FP and a powder with a narrow and known aerodynamic particle size distribution. The collection was conducted by placing a dissolution cup assembled with an impactor insert in stage 4 of the NGI - stage with greater amount of powder – as schematized in Figure 3.3

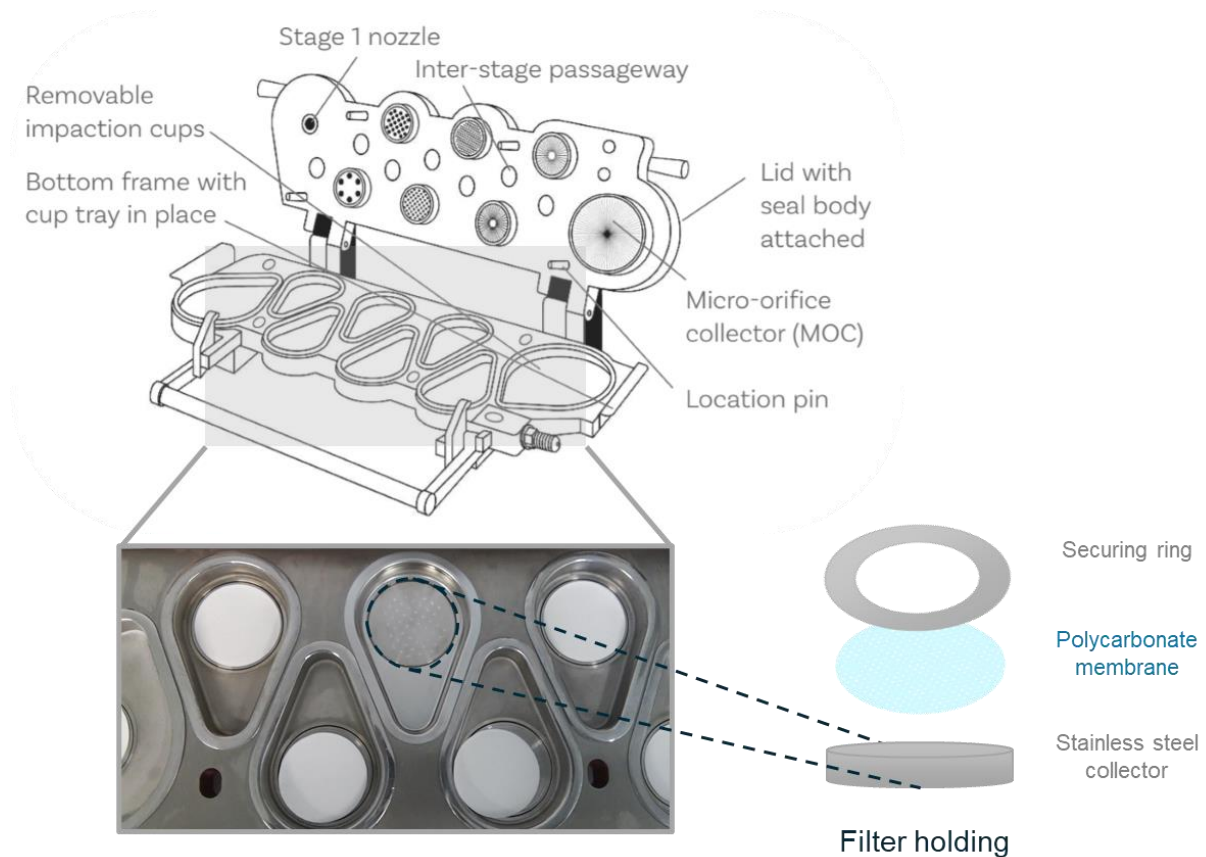


Figure 3.3 – Schematic representation of samples collection and preparation using the Next Generation Impactor prior to dissolution using the Paddle over disk apparatus. NGI schematic from Copley brochure.

Plate 4 was selected for powder collection for all formulations as it consistently displayed the maximum deposition of FP and the collected particles are within the respirable fraction (aerodynamic cutpoint, $D_{50} \approx 3.5 < 5 \mu\text{m}$ for a flow rate of 40 L/min (Virgil A. Marple et al., 2003a)). Considering the amount of FP collected in stage 4 for each formulation, the number of actuations was defined in order to obtain approximately 100 μg of FP in said stage. The amount of FP collected for each formulation, as well as the number of actuations required are summarized in Table 3.5.

For the dissolution of the bulk powder, the fraction dissolved was calculated considering 100% as the plateau of the dissolution profile, as it was maintained for several hours, indicating the total amount of FP was dissolved. This amount was not all the FP expected to be in the 12.5 mg of formulation, and the

difference is possibly related to the variability of the capsule fill-weight (5%) and the FP retained in the capsule when poured. For the test performed in the present section with the powder collected on the disk, the calculated collected amount was used as the 100% FP available for dissolution when calculating the dissolved fraction for the carrier-based formulation, as the total amount of FP did not dissolve, while for the carrier-free formulation the total amount of dissolver FP was considered as 100%, as the dissolution profile presented a plateau for the last timepoints. This methodology is optimized in the following sections by recovering the non-dissolved FP after dissolution assessment.

Table 3.5 - Amount of fluticasone propionate (FP) loaded in stage 4 of the next generation impactor in one actuation (m_{stage4}) and respective amount (m_{disk}) after a defined number of actuations ($N_{\text{actuations}}$) in μg , for the carrier-free formulations containing trehalose and raffinose (CF1 and CF2) and for the carrier-based formulation containing 1% of jet milled FP (FPJ1 blend).

| Disk | m_{stage4} (μg) | $N_{\text{actuations}}$ | m_{disk} (μg) |
|-------------|--|---|--|
| CF1 | 34.0 | 3 | 102.0 |
| CF2 | 34.2 | 3 | 102.6 |
| FPJ1 blend | 11.5 | 10 | 115.0 |

3.4.2.2.2 Sample preparation for dissolution studies

Sampling of the formulation for dissolution studies need to ensure the collected powder fraction is retained on the collection disk to avoid powder dispersion in the dissolution medium – this would lead to powder adhesion to the vessel or paddle surfaces, or to the sampling of undissolved FP. Hence, the collected powder was covered and sealed previous to the dissolution test.

Thus, following the impaction, the stainless steel collector was removed from the NGI dissolution cup and covered with a pre-soaked polycarbonate membrane with a 76 mm diameter and 0.05 μm pore size (Whatman (USA)), which was sealed in place with the securing ring of the membrane holder (Figure 3.3), to be finally placed inside a dissolution vessel with the membrane facing up. To assess the dissolution profiles, a Tablet Dissolution Tester DIS 6000 from Copley Scientific (UK) was employed as USP apparatus II with and without a membrane holder. The apparatus consists of vessels containing 350 mL of dissolution medium (0.01 M phosphate buffer saline, pH of 7,4), containing 0.4% (w/v) SDS. The medium composition is frequently used in the literature in a range of SDS percentages (Grainger et

al., 2012b; Price et al., 2020; Rohrschneider et al., 2015b) and was selected considering it is easily to prepare in reproducible and stable form while maintaining a pH similar or the lung extracellular fluid (Radiojevic et al., 2019) and containing a surfactant to simulate the lung surfactant. Moreover, it is a simple matrix and thus interference with the analysis is avoided. The system was maintained at 32 ± 0.5 °C and stirred with paddles at 75 rpm, placed 25 ± 2 mm above the bottom of the vessel or the membrane holder. The described disposition allows for a complete submersion of the paddle, securing an effective drug dispersion after membrane release and continuous circulation of the medium in the vessel.

As a comparison, the dissolution profile of the hand filled capsules was also assessed by opening and pouring a capsule content (12.5 ± 0.5 mg) into the dissolution apparatus. The goal of these tests was to assess the impact of analysing the bulk formulation versus the actuated and collected powder, as well as the membrane impact. Aliquots of 3 mL of dissolution medium (~1 % of the dissolution volume) were withdraw manually and filtrated, then replaced with pre-warmed medium

3.4.2.2.3 Quantification of Fluticasone propionate

To quantify the dissolution samples using the POD apparatus, the methods used is described in section 3.3.2.4

3.4.2.2.4 Data analysis

To interpret the dissolution rate data, the obtained dissolution profiles were fitted to the Weibull model, a general mathematical expression used to describe the curve in terms of mathematical parameters (Langenbucher, 1972). The Weibull model (Equation 3.) expresses the accumulated fraction of the material in a solution, m , at time t , and a and b define the time scale and curve. It has been reported in the literature as a reasonable description of the dissolution of orally inhaled drugs (Riley et al., 2012). The dissolution time (Equation 3.2), T_d , corresponds to the time necessary to dissolve 63.2% of the totally released drug.

$$m = 1 - \exp\left[\frac{-t^b}{a}\right] \quad \text{Equation 3.1}$$

$$a = (T_d)^b \quad \text{Equation 3.2}$$

To compare dissolution profiles, two model-independent approaches are used based on a difference factor (f_1) and a similarity factor (f_2), calculates as presented in Equation 3. and Equation 3.4. For that, all timepoints were considered for a given dissolution profile (T_i) and a reference one (R_i) (Shah et al., 1999).

$$f_1 = \frac{\sum_{j=1}^n |R_j - T_j|}{\sum_{j=1}^n R_j} \quad \text{Equation 3.3}$$

$$f_2 = 50 \times \log \left\{ \left[1 + \frac{1}{n} \sum_{t=1}^n (R_t - T_t)^2 \right]^{-0.5} \times 100 \right\} \quad \text{Equation 3.4}$$

The difference factor, f_1 , determines if there is evidence of significant difference between the two profiles by measuring the percent error over all time points. By contrast, the similarity factor, f_2 , determines if there is sufficient evidence of similarity between the two profiles by using an equivalence approach based on mean squared differences. The accepting criteria suggested for solid oral doses by both FDA and EMA are considered in this work: f_1 values lower than 15 indicate no difference and f_2 values higher than 50 indicate similarity.

3.4.3 Results and discussion

The release profiles of the collected powders using the NGI were assessed and are presented in Figure 3.4, A). To better compare the diffusion phenomenon through the membrane in each formulation, the dissolution profile of 12.5 mg of bulk powder was also assessed (Figure 3.4, B). The release profiles were fitted to the Weibull model (Equation 3. and Equation 3.2) and compared by the similarity factor (f_2). A summary of the dissolution parameters is presented in Table 3.6. All the Weibull models fitted to the data present a R^2 larger than 0.9, indicating a good fit. In the Weibull model a denotes a scale parameter that describes the time dependence, while b describes the shape of the dissolution curve progression. The curves generated with the POD apparatus fit a curve with $b < 1$, indicating a steeper increase than the shape of an exponential profile ($b=1$), while the USP apparatus II profiles with bulk powder fit curves with $b > 1$, showing a sigmoidal curve with a turning point.

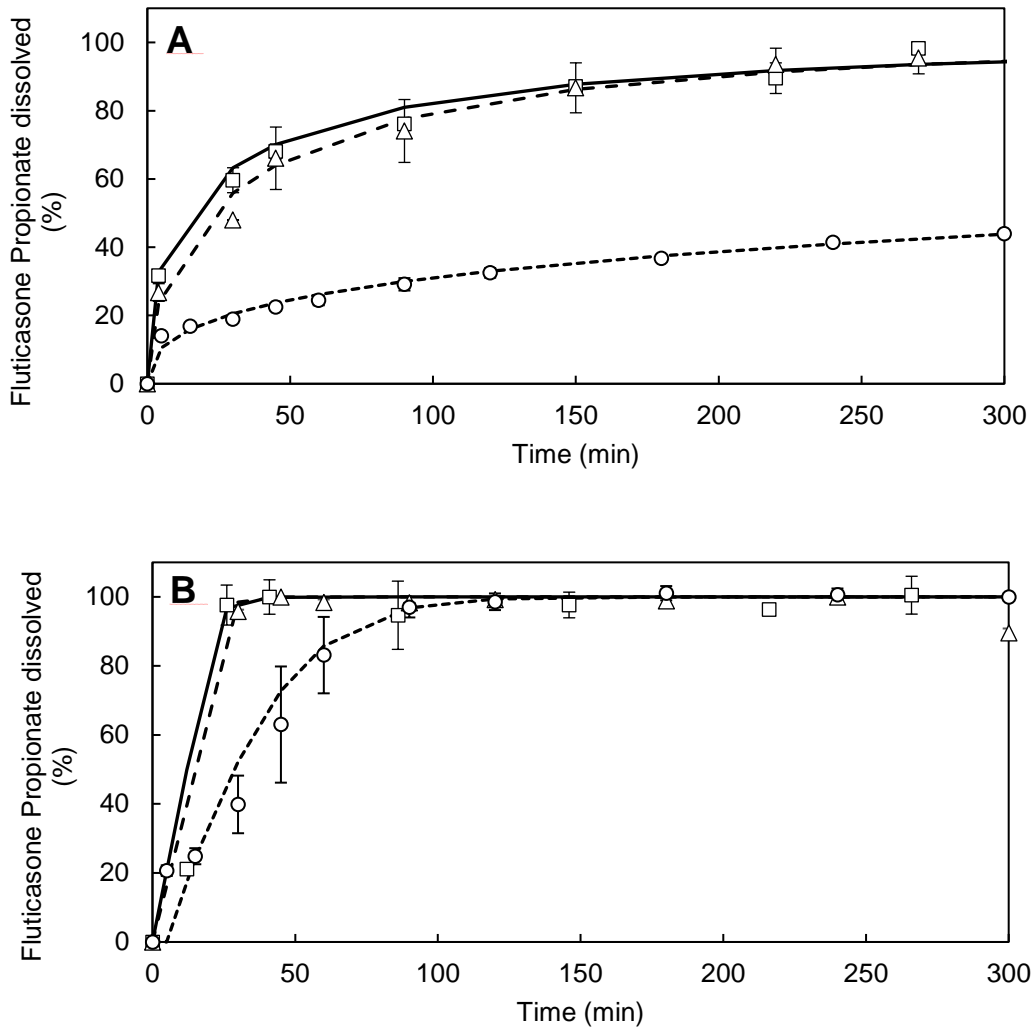


Figure 3.4 - Dissolution profile of the carrier-free formulation of fluticasone propionate containing trehalose, CF1 (□) containing raffinose, CF2 (Δ), and of the carrier-based formulation, FPJ1 blend (○) in A) the paddle over disk apparatus and B) for the bulk formulation. Each profile is given by two replicates. Lines were fitted with Weibull model.

When comparing the two carrier-free formulations tested in the paddle over disk apparatus, the presence of trehalose appears to lead to a faster dissolution (T_d of 30 min < 43 min), which can be related with the differences on dissolution of the two sugars having an impact on the dissolution of the FP due to local medium composition changes - trehalose solubility in water is 689 g/L (Jain and Roy, 2008) while raffinose solubility in water is 203 g/L (Human Metabolome Database, n.d.), or to differences on the amorphous solid dispersion generated in the particle core, although this cannot be confirmed by the applied analytical methodologies due to the low FP content not being detected by X-Ray Powder Diffraction methods. Nonetheless, there is not a meaningful discrimination when considering the

similarity factor, $f_2=64.1 > 50$. Moreover, when considering the individual timepoints it is clear most of the release profile is similar.

When comparing formulation strategies, a significant difference is observable between the dissolution profiles of carrier-based and carrier-free formulations ($f_2= 19.8/18.1 < 50$) using the paddle over disk apparatus. In fact, for the carrier-based formulation profile (Figure 3.4.A)) dissolution is not complete after the 5 h of dissolution, unlike the carrier-free formulations. It is expected that the crystalline micronized FP present in the carrier-based formulations dissolves slower than the FP contained in the carrier-free particles due to the solid state of the particles, as the crystalline state is more stable than the likely amorphous state in the carrier-free formulations, which has been known to influence solubility (Murdande et al., 2010).

Considering the bulk powder dissolution profiles, it is clear that the presence of the polycarbonate membrane leads to a significant diffusion barrier, as the total amount of FP was dissolved 30 min after dissolution start for both carrier-free formulation in the absence of membrane while only 43% of FP was released from the disk during that time. For the carrier-based formulation, a significant impact of the membrane was also observed. Thus, the presence of membrane delayed the FP release more than twice. In the application of the paddle over disk technology, the observed delay indicates the presence of the membrane could be helpful in the discrimination of formulations with a fast dissolution rate. Aside from improved discrimination, the presence of a polycarbonate membrane minimizes result variability, more significantly for the carrier-based formulation, which is related with poor control over powder wetting, adherence to the dissolution vessel walls or paddle, as well as the structures of FP and excipients being dissolved, which can be impacted by the powder handling previous to the dissolution start. Thus, a polycarbonate membrane is considered essential for a dissolution system suitable for inhalation dry powder assessment, and will be maintained in the next development steps.

It should be highlighted that the presented results have an approximation: the total amount of FP considered for the calculation of the percentage of dissolved FP was not confirmed by recovery of the undissolved FP at the end of the dissolution test – this is corrected in the next presented trials.

To further develop the methodology, it is also relevant to understand the impact of the FP amount on the collecting disk on the dissolution performance, and if the sink conditions are maintained in this set up.

Table 3.6 - The dissolution performance parameters of fluticasone propionate (FP) for the carrier-free formulation containing trehalose, CF1, containing raffinose, CF2, and of the carrier-based formulation containing 1% of jet milled FP, FPJ1 blend, using the paddle over disk apparatus for the collected samples and the USP Apparatus II (USP Ap. II) for the bulk formulations.

| | FPJ1 blend | CF1 | CF2 | FPJ1 bulk | CF1 bulk | CF1 bulk |
|-----------------------------------|------------------------|------------|------------|------------------------|-----------------|-----------------|
| Set-up | POD | POD | POD | USP Ap. II | USP Ap. II | USP Ap. II |
| f ₂ (%) | 19.8/18.1 ¹ | | 64.1 | 27.5/31.0 ¹ | | 48.6 |
| a ² | - 1.23 | - 0.90 | - 0.68 | - 1.80 | - 1.30 | - 1.00 |
| b ² | 0.40 | 0.55 | 0.46 | 1.20 | 1.30 | 1.20 |
| T _d (min) ² | 1189 | 43 | 30 | 32 | 10 | 7 |
| R ² | 0.981 | 0.990 | 0.992 | 0.945 | 0.990 | 0.948 |

¹ Calculated according to Equation 4, compared with formulation with trehalose/raffinose

² Calculated according to Equations 1 and 2

3.4.4 Conclusions

The paddle over disk apparatus can be successfully employed to discriminate between different formulations of dry powders, and although the present results do not show the discriminating power regarding composite particles with similar morphology, an improvement was reached when comparing to the paddle apparatus, inspiring next steps to achieve system optimization and better system understanding:

- Evaluate temperature impact on the paddle over disk dissolution profile.
- Evaluate the impact of the FP dose on the dissolution profile.
- Quantify the total amount of FP collected and used for dissolution assessment, to avoid approximations in the dissolution percentage calculation.

3.5 PADDLE OVER DISK CRITICAL METHOD PARAMETERS AND LIMITATIONS

3.5.1 Outline

In the previous section the discriminative power of the POD on carrier-free and carrier-based formulations was evaluated for the poorly soluble drug FP. The next sections aim to assess the influence of temperature and amount of FP collected for dissolution testing.

The evaluation of the temperature is relevant as the value used in the previous studies (32 °C) is below the lung surface temperature and depending on the criticality of the parameter it may be a factor to consider in future *in vivo* / *in vitro* correlations. The FP collected dose impact on the dissolution kinetics may indicate if the dissolution system in contact with the FP sample (below the membrane) is in sink conditions, and if not, how relevant it is to ensure a similar collected dose in future studies.

It was hypothesized the dissolution dependence on amount of DS collected could be related with the “hot spots” generated on NGI actuation. To test this hypothesis a study was performed rotating the collection surface in order to deposit the DS as a larger area.

Lastly, a novel collection strategy with the FSI was tested in order to achieve a uniform powder distribution and collect the fine particle fraction, and not be limited to one NGI stage.

3.5.2 Impact of fluticasone propionate load and temperature

One of the more discussed limitations of the paddle over disk apparatus is the impact of the DS dose on the collecting disk on the dissolution profile, as it has been observed the increase of dose leads slower dissolution profiles (Price et al., 2020; Son and McConville, 2009). It is theorized the powder wetting and dissolution are limited by the local high concentration of DS in the neighborhood of the powder hotspots generated by the NGI air jets, demonstrated by SEM (Floroiu et al., 2018). A number of strategies have been developed and published, including a modified ACI with a stage extension which showed the formation of a homogenous-particle layer on the collection membrane (May et al., 2014, 2012), and the UniDose™ device designed for separating and collecting the fine particle dose for dissolution testing with an extension in the stage 2 of the NGI, with a similar effect (Farias et al., 2017; Price et al., 2020; Price and Shur, 2017). The developed equipment led to dissolution profiles without

impact of the dose collected, overcoming one of the limitations of the paddle over disk apparatus. However, they require the acquisition of additional equipment pieces, or might not even be available for acquisition, as is the case for UniDose™. Therefore, an additional advantage could be attained by applying equipment readily available. One possibility is the use of the NGI attempting to spread the powder throughout the collecting stage; while another is the use of the FSI, designed to collect the total amount of fine particle fraction on a filter in a uniform powder layer. Both strategies were attempted in the present section.

The temperature has an impact on the solubility; therefore, it is expected to be significant in the dissolution profile. Previous dissolution trials were performed following USP indications for USP apparatus V – paddle over disk apparatus designed to assess dissolution and permeation upon topic delivery. For that reason, a temperature of 32 °C was used. Considering the lung has a temperature of 37°C (D'Amato et al., 2018), the impact of this parameter was also studied in the present section.

3.5.2.1 Experimental design

All the Materials and Methods used were described in previous Materials and Methods sections previous presented in this chapter. Formulation FPJ1 blend (1 % (w/w) FP, 5 % (w/w) of fine lactose LH230 and 94 % (w/w) of coarse lactose SV003) was used with the Plastiaple Monodose inhaler (40L/min at 4 kPa pressure drop). Similarly to the previous trials, stage 4 was selected for powder collection as it displayed the maximum deposition of DS within the respirable fraction (aerodynamic cut-point, $D_{50} \approx 3.5 < 5 \mu\text{m}$ for 40 L/min) – NGI deposition per stage presented in Figure 3.2. The expected amount of FP per test and the actual collected determined by recovering the total amount of FP in the dissolution vessel is shown in Table 3.7.

Table 3.7 - Amount of fluticasone propionate (FP) loaded in stage 4 of the next generation impactor in each test (extrapolation in the case of tests 2 and 4) and recovered as mass and percentage of expected after adding acetonitrile and ensuring full dissolution.

| Test | Number of actuations | Theoretical FP in stage 4 (ug) | FP recovered (ug) | % of theoretical |
|------|----------------------|--------------------------------|-------------------|------------------|
| 2 | 7 | 80.5 | 57.6 | 77 |
| 3 | 10 | 115.0 | 114.1 | 99 |
| 4 | 13 | 149.4 | 107.8 | 72 |

The prepared samples with different FP loads were used for dissolution assessment as per the previously described method (section 3.4.2.2.2). A summary of all the performed test is presented in Table 3.8. Three parameters were varied as previously discussed – the number of actuations and therefore FP load, the dissolution media temperature, and the dissolution apparatus set-up – USP apparatus II and paddle over disk.

Table 3.8 - Summary of the performed *in vitro* tests using the paddle over disk apparatus (POD) and the UPS apparatus II (USP Ap. II), n=2

| Test | Apparatus | Temperature (°C) | Number of actuations |
|------|------------|------------------|----------------------|
| 1 | POD | 32 ± 0.5 | 10 |
| 2 | POD | 37 ± 0.5 | 7 |
| 3 | POD | 37 ± 0.5 | 10 |
| 4 | POD | 37 ± 0.5 | 13 |
| 5 | USP Ap. II | 32 ± 0.5 | - |
| 6 | USP Ap. II | 37 ± 0.5 | - |

3.5.2.2 Dissolution results and discussion

The profiles obtained after 7, 10 and 13 actuations, as well as the fitted Weibull curves are presented in Figure 3.5. The total mass recovered in Test #3 (10 actuations) corresponded to 99 % of the expected mass; however, only 70 % of the expected mass was recovered after 7 and 13 actuations (tests #1 and #3, respectively). This mass variability is addressed by expressing the dissolution profile as a percentage of total recovered powder, attending that the tests were performed under sink conditions (solubility of FP in the used medium is 12 ± 2 µg/ml). From the profiles in Figure 3.5, a relationship between the mass of deposited FP and its release can be observed – higher amounts of deposited FP result in a slower dissolution rate (drug load↑ lead to Td↑ - time necessary to dissolve 63.2% of the totally released drug, Equation 3.2). Similar results have been reported (May et al., 2012; Son et al., 2010; Son and McConville, 2009) possibly due to a decrease of exposed surface area (in accordance with the Noyes-Whitney equation for dissolution (Cabrera et al., 2006)) following agglomeration in hotspots during powder collection (visible in Figure 3.3).

Figure 3.5.A presents a zoom-in of the first 60 min of dissolution, and contrary to later time points, the test with a higher amount of deposited DS shows a faster initial dissolution, which may be related with the dissolution of dispersed powder on the disk surface caused by particle bouncing on the created agglomerates – schematized in Figure 3.6.

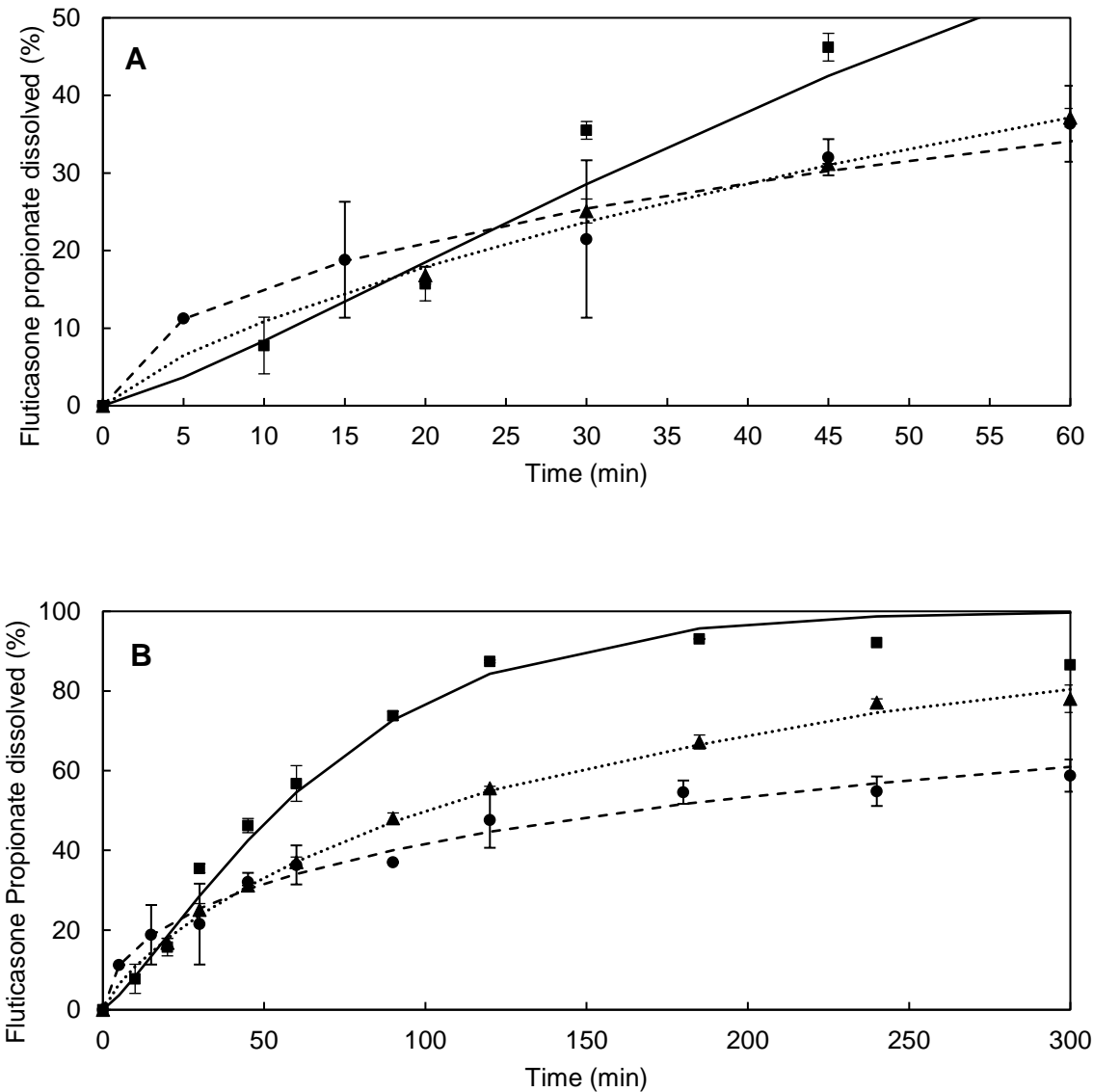


Figure 3.5 – Paddle over disk dissolution profiles of fluticasone propionate for the carrier-based formulation containing 1% of jet milled fluticasone propionate (FPJ1 blend); Weibull model fitting for 7 (■, —), 10 (▲, ...) and 13 (●, - - -) actuations, with a Td of 73, 339 and 160 min, respectively. A) first 60 minutes; B) 5 hours of dissolution. n=2

Fundamentally, the increased size of the agglomerates decreases the contact area, which can explain the differences in dissolution rates for experiments with varying amounts of powder. What is

hypothesized is that the first minutes of the dissolution curve depict the dissolution of the FP particles that bounce from the agglomerated during actuation, depositing on the surface of the disk (Figure 3.6), which would be more significant for bigger agglomerates.

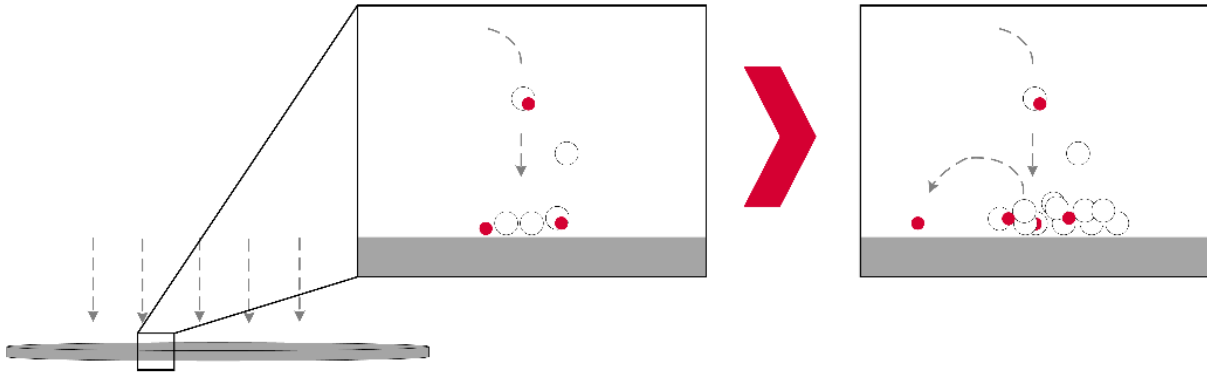


Figure 3.6 – Schematic representation of the proposed mechanism for particle deposition and bouncing after NGI actuation (Fernandes et al., 2016b).

Considering this, a powder collection procedure that avoids powder agglomeration on the disk would better simulate the lung deposition. A strategy for that is presented in later sections of the present chapter.

The influence of temperature of the medium using the POD and UPS apparatus II is shown in Figure 3.7, with a comparison of the dissolution rate for both bulk powder and the fraction collected at the stage 4 of the NGI. In both setups, a higher temperature is associated with an FP faster dissolution, which highlights the importance of this parameter when simulating FP *in vivo* dissolution and diffusion after inhalation.

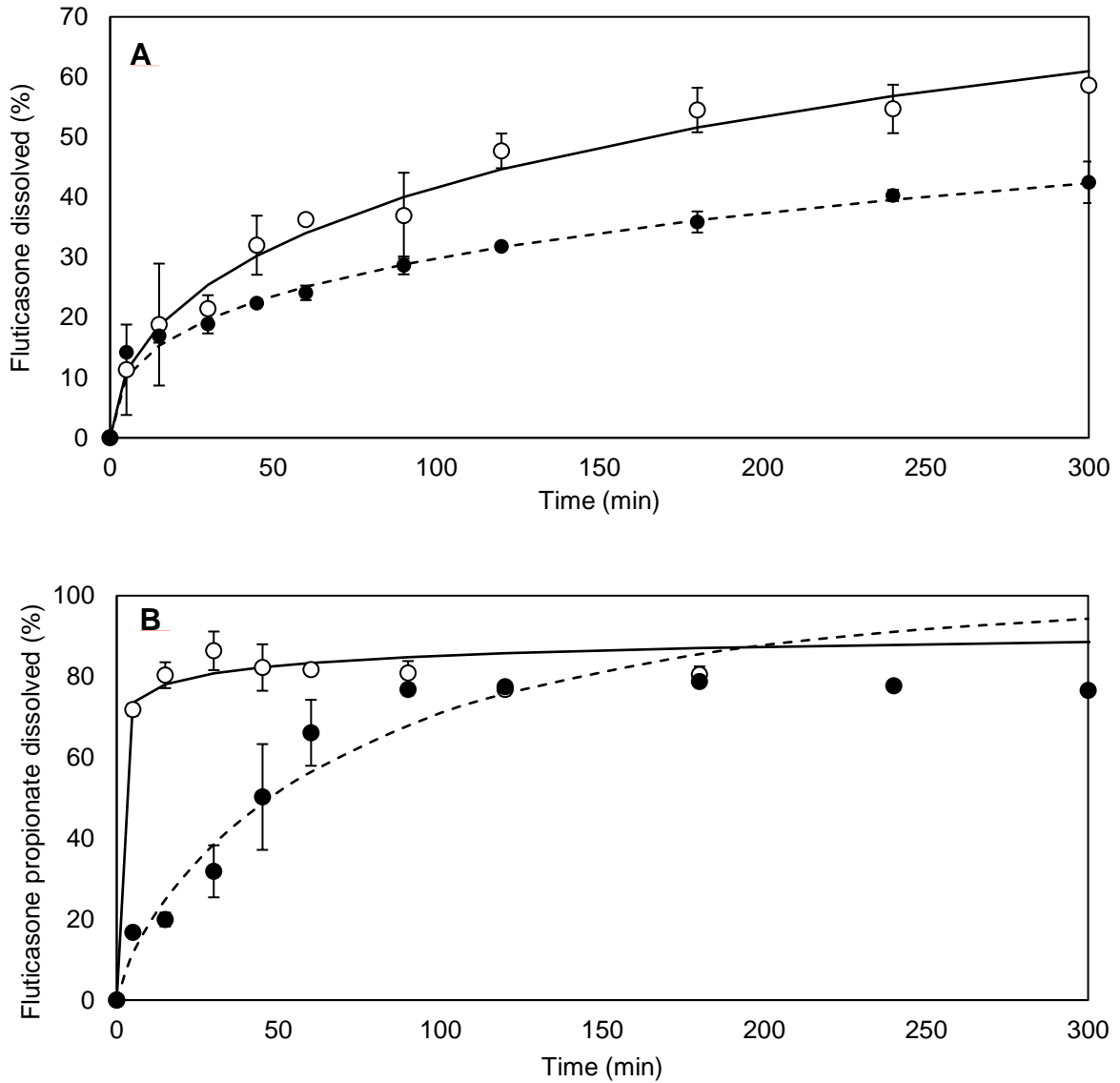


Figure 3.7 – Dissolution profiles of fluticasone propionate showing A) Temperature influence using paddle over disk for powder collected using the next generation impactor; Weibull model fitting for 37 (○, —) and 32 (●, - - -) °C, with a Td of 339 and 1333 min, respectively. B) Temperature influence using UPS apparatus II for bulk powder; Weibull model for 37 (○, —) and 32 (●, - - -) °C, with a Td of 0.5 and 76 min respectively. n=2.

3.5.3 Impact deposition strategy using the next generation impactor

Following the previously presented hypothesis, the aim of the work presented next is to study the influence of powder agglomeration in hotspots during collection. For that, the carrier-based FP formulation was collected on the dissolution disk by rotating it between NGI actuations (Figure 3.8),

aiming at distributing the powder throughout the disk surface and therefore decreasing the particle layering.

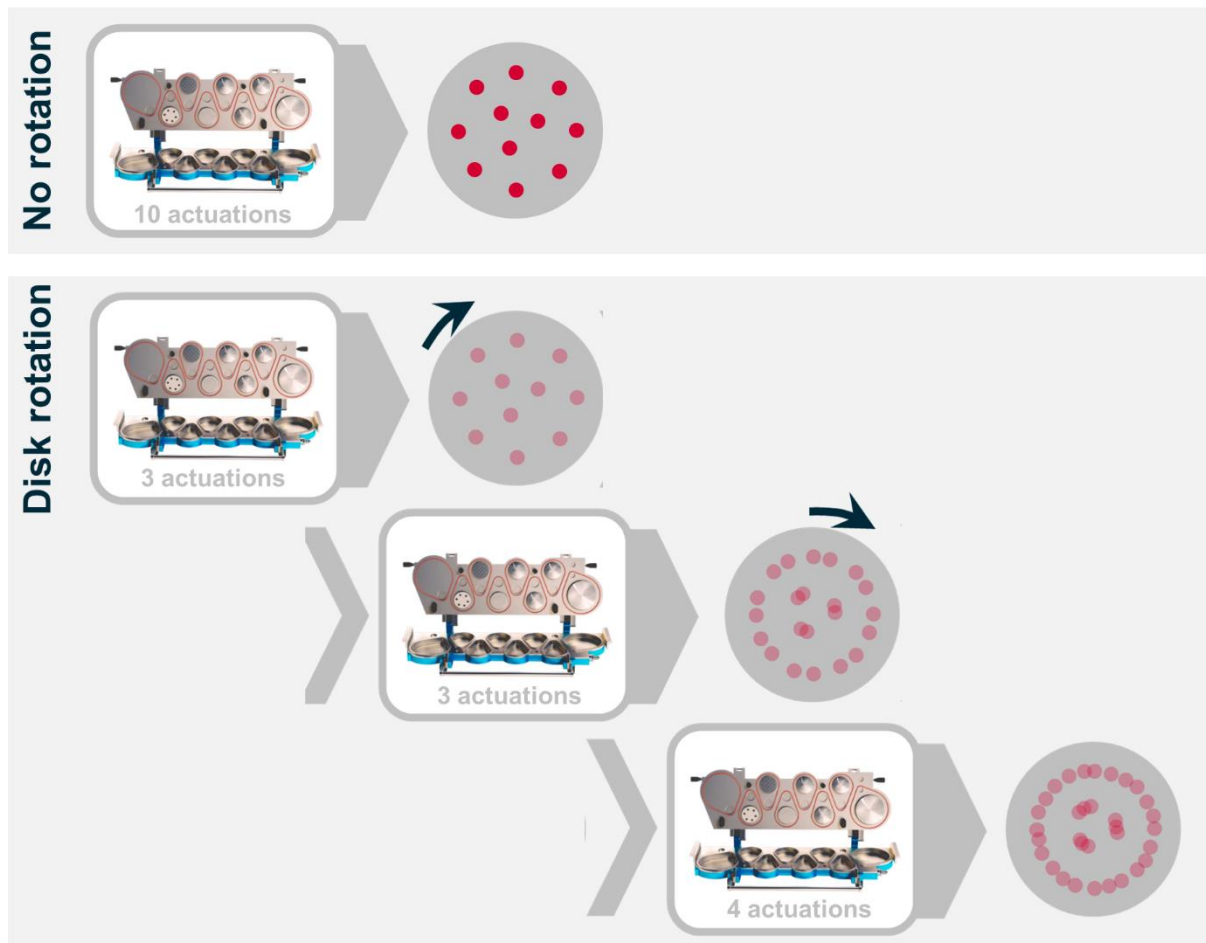
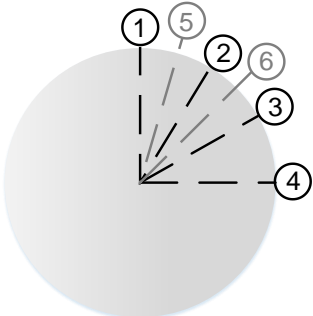


Figure 3.8 - Schematic representation of the powder collection procedure with the rotating disk methodology. Adapted from (Noriega et al., 2018b).

3.5.3.1 Experimental design

The NGI was opened between each actuation and the disk was manually rotated to pre-defined positions. The positions and number of actuations were defined in order to minimize powder handling while maximizing the powder distribution area on the disk surface as evenly as possible. Considering that, six disk positions were defined for actuations, and a maximum of 3 actuations per position, resulting in a maximum of 3 layers of powder on the disk surface, summarized in Table 3.9.

Table 3.9 - Number of actuations per disk position, illustrated on the left, for the test with the rotating disk, in the case of 7 and 13 actuations.

|  | 1 (0°) | 2 (30°) | 3 (60°) | 4 (90°) | 5 (15°) | 6 (24°) | Total |
|---|--------|---------|---------|---------|---------|---------|-------|
| | 2 | 2 | 3 | - | - | - | 7 |
| | 2 | 2 | 2 | 2 | 2 | 3 | 13 |

3.5.3.2 Deposition and dissolution results and discussion

Figure 3.9 shows the powder collected on the disk with and without disk rotation, for 7 and 13 actuations. It can be observed how the powder has an improved distribution on the surface of the disk when it is rotated. Hotspots can still be seen, however these represent two or three layers of powder, instead of seven or thirteen, resulting in less packed particles. Also, the surface of contact between powder and medium increased, which may have an influence on the dissolution profile obtained.

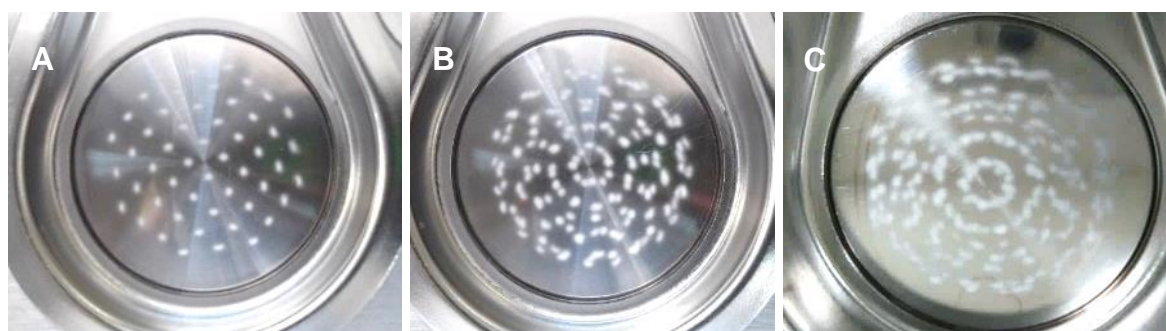


Figure 3.9 - Dissolution cup coupled with dissolution disk, after actuating the powder without (A), with disk rotation after 7 actuations (B), and with disk rotation after 13 actuations (C).

The dissolution profiles for FP formulations obtained after 7 and 13 actuations, with and without disk rotation are presented in Figure 3.10. For each test, the results obtained in the two replicates are presented (circle markers) as well as the average (line). The top figures (A and B) compare results for 7 and 13 actuations in each set-up; the bottom ones (C and D) the comparison between the two set-ups with the same number of actuations. The top results indicate that collecting the powder by disk rotation

did not influence significantly the dissolution profiles. In both set-ups, actuating 7 times results in a profile that reaches maximum concentration at approximately 100 min; actuating 13 times leads to profiles that did not present a plateau of maximum concentration even after 300 min, as the curve ends on a slope. The equilibrium solubility of the micronized FP on the dissolution medium was determined as 12 ± 2 $\mu\text{g/mL}$ (Fernandes et al., 2016b), 50-times higher than the total dissolved after 5 h, ensuring sink conditions in the dissolution vessel for both 7 and 13 actuations. However, a local saturation may be happening between the deposited powder and the covering membrane, decreasing the dissolution rate of the FP when a greater amount of powder is present.

Evaluating the dissolution profiles, it is evident that a lower amount of powder was present on the disk when collecting it with the rotating disk procedure, possibly due to powder loss during the manual rotation. However, even though the average curves are shifted down, the overall profile tendency is similar.

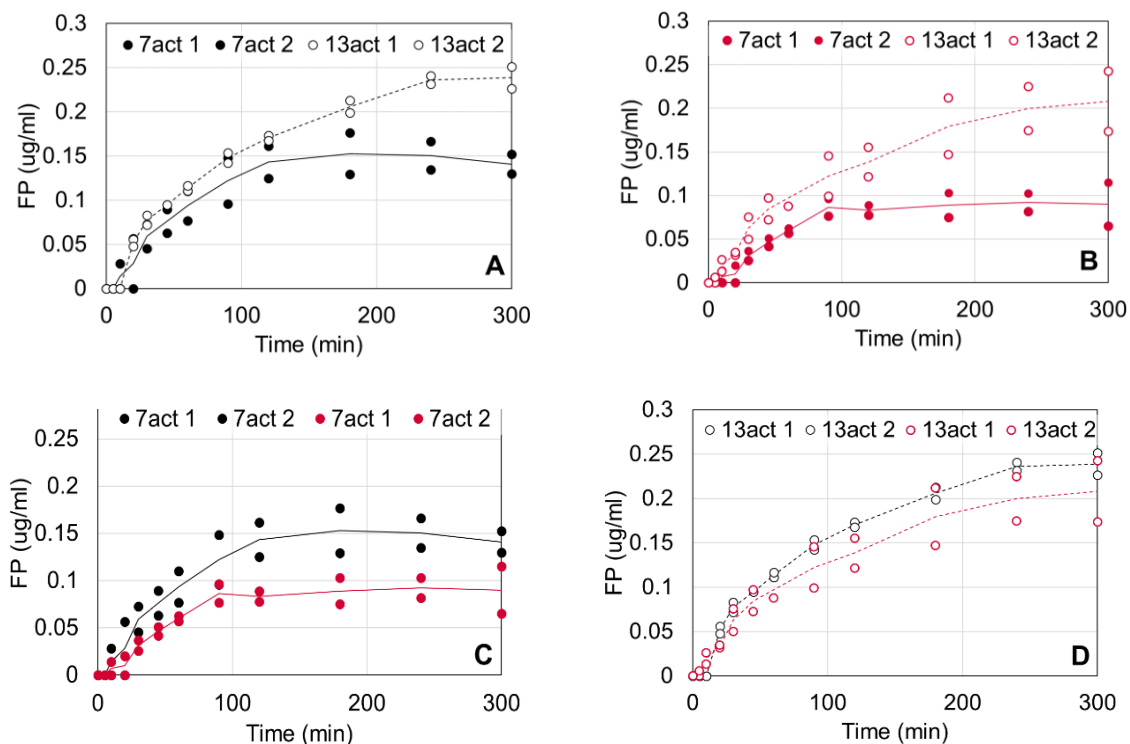


Figure 3.10 - Dissolution profiles of the carrier-based 1% (w/w) of jet milled fluticasone propionate formulation (FPJ1 blend) for 7 (full circle) and 13 (empty circle) actuations, without (black) and with (red) disk rotations. Markers represent time points of individual vessels; the line is the average of the duplicates. Comparison with normal set-up (A) and rotating disk (B); comparison between set-ups after 7 (C) and 13 (D) actuations.

In conclusion, it was observed that the POD apparatus employed to assess the dissolution of a FP formulation delivers similar results when depositing the powder with or without the rotations of the collecting disk, i.e., with visually different powder distributions. Considering these results, a novel collection strategy was tested – presented in the following section.

3.5.4 Fast screening impactor as an innovative collection strategy

3.5.4.1 Rational

The use of the NGI as a collection strategy, although simple and easily implemented with a UPS apparatus, presents several disadvantages. Firstly, to ensure the dissolution is initiated upon dissolution media contact, the collection stage is not coated as per standard (to minimized particle bouncing), leading to collected dose variability, especially when a large number of actuations is required. As confirmed in the previous section, the dissolution profile is highly impacted by the collected dose, therefore, as a consequence, the method variability is increased. Secondly, the collection strategy, as it is designed commercially, limits the powder being tested to an aerodynamic particle size fraction which does not include the totality of the respirable fraction (APSD < 5 μm), but just one NGI stage. On the one end this allows to test particles deposited at different lung levels for a more targeted analysis, on the other end, a full respirable fraction analysis requires a much larger number of tests (3, 4 of 5 times more, depending on the flowrate used). Finally, particle deposition is nothing like the lung surface deposition, where particles deposit falling into a large area separated from each other. In the NGI, as previously discussed and studied, particles deposit in hotspots (high density particles) surrounded by areas of low particle density, according to the NGI stage nozzles.

Considering these limitations, the next step on the POD method development was to test a different collection mechanism capable of collecting the totality of the respirable fraction without generating the hotspots observed in the NGI collection. For that, another commercially available method was used – the FSI. This is an impactor generally used in the screening phase of formulation development to quantify the amount of DS with an APSD below 5 μm (Nichols et al., 2016; Russell-Graham et al., 2010). The FSI is composed by the NGI induction port, and a pre-separator equipped with an impaction plate with a cut-off diameter of 5 μm (available for 40, 60 and 100 L/min flowrates). The particles with an aerodynamic particle size below 5 μm are collected on a micro glass fiber filter as illustrated in Figure 3.11.

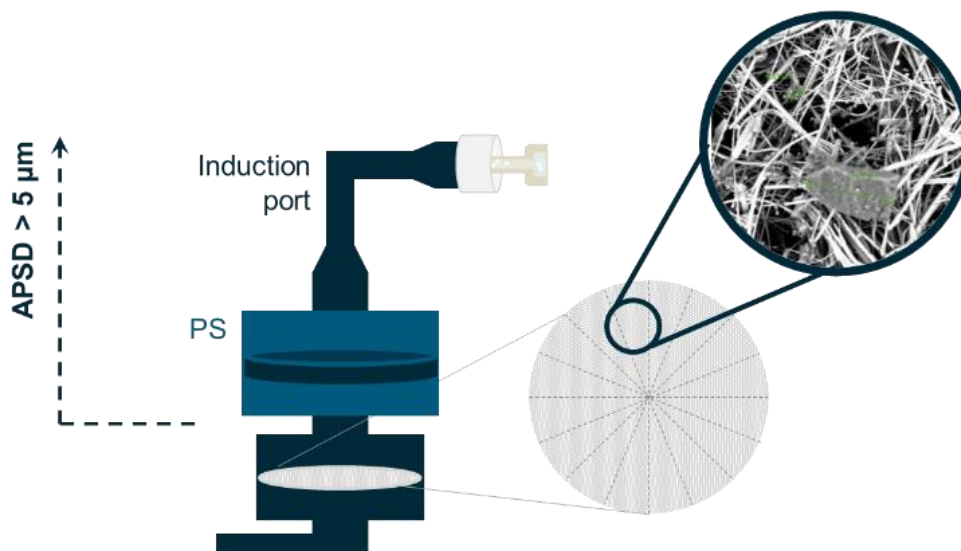


Figure 3.11 - Schematic representation of the Fast Screening Impactor (FSI). PS – pre-separator; APSD – aerodynamic particle size distribution.

Considering the stated equipment characteristics, the FSI presents a number of upsides for particle collection for dissolution:

- As the FSI system collects the size-fractionated portion into a filter, all particles are retained on the filter without losses with no need for stage coating. The particle bouncing from the pre-separator is prevented by including 15 mL of dissolution mixture on the pre-separator center (similar procedure to the NGI method).
- The totality of the respirable fraction is collected onto the filter stage, eliminating the need to test different stages.
- The particles deposit as a visually homogeneous powder layer, avoiding NGI stages hotspots, and therefore this collection strategy is one step closer to *in vivo* powder deposition.

Based on these, the FSI was adapted to collect aerosol particles for dissolution testing. The following section describes the adaptation steps.

3.5.4.2 Methods

3.5.4.2.1 Method development for sample collection with the fast screening impactor

The FSI is not standardly applied as a collection method for further particle use aside from DS recovery with dissolution mixture for quantification of the fine particle fraction. Thus, unlike the dissolution cup for

the NGI collection approach, there is not a straightforward sample passage from the FSI to the dissolution vessel. To overcome that limitation, and in order to maintain dissolution vessel distances between bottom, sample and paddle, as well as volumes, the stainless-steel collector and securing ring used for the NGI collection was employed. The main challenge of the adaptation is the difference in dimensions between the NGI collection disk (55 mm, designed to fit the NGI stage) and the FSI collection filter (76 mm, designed to fit the FSI stage). To overcome this limitation a 55 mm punch is used to cut the FSI filter with minimum handling previous to transfer to the stainless-steel collector. Finally, the filter is covered with a pre-wet polycarbonate filter and secured with a stainless-steel ring – schematized in Figure 3.12.

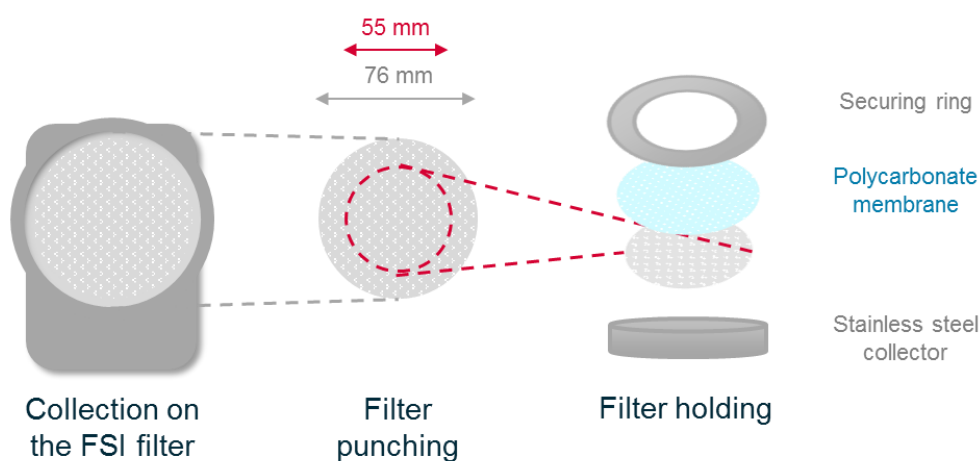
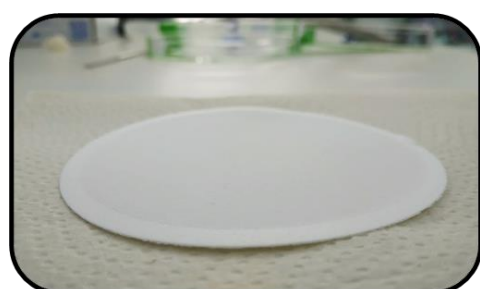


Figure 3.12 – Schematic representation of powder collection using the fast screening impactor (FSI) filter followed by holding with the next generation impactor (NGI) stainless still collector.

To optimize FSI collection and samples preparation for dissolution, two FP formulations were used – FPJ2 blend (1 % (w/w) jet milled fluticasone propionate, 5 % (w/w) fine lactose LH230 and 94 % (w/w) coarse lactose SV003) and FPW blend (1 % (w/w) wet polished fluticasone propionate, 5 % (w/w) fine lactose LH230 and 94 % (w/w) coarse lactose SV003 fine lactose (w/w) LH230 and 94 % (w/w) coarse lactose SV003) - Table 3.2. For each formulation, 5 capsules were actuated at 40 L/min with a Plastiape Monodose inhaler (as per NGI actuation described in section 3.4.2.2.1). The resulting filter was punched and the filter holding prepared as represented in Figure 3.13, covered with a pre-wet membrane. Dissolution was carried out as previously described (Section 3.4.2.2.2), with two replicates from each formulation.

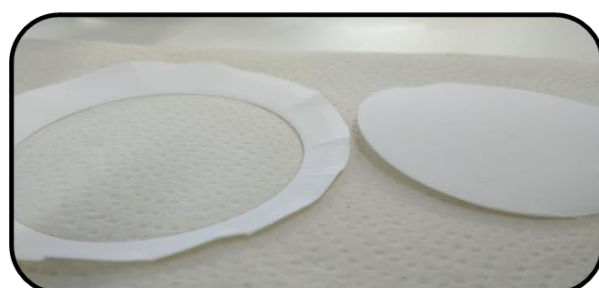
Taking into account the pictures presented in Figure 3.13, some observations to the sample preparation method can be highlighted. Firstly, the filter surface after actuation presented a visually uniform powder deposition without clear areas of particle accumulation, as expected (Figure 3.13, A)). Secondly, filter punching ensures 100 % of filter area is coated with powder as the punch diameter is smaller than the powder deposition diameters (slightly smaller than the filter diameter (Figure 3.13 B) and C)). Lastly, Figure 3.13 D shows air is entrapped between the filter holder and the polycarbonate membrane, which is present throughout the dissolution. Following the presented observations, the sample preparation procedure was optimized to avoid the generation of air pockets by adding 1 mL of dissolution media directly on the stainless-steel holder, prior to the filter placement, ensuring the filter was completely adhered to the holder surface. The described procedure was followed for the remaining tests after FSI sample collection, and air pocket presence/size was considered a critical process parameter – any test presenting an air pocket was not considered.



A: Powder collected on filter



B: Filter punching



C: Filter punched



D: Filter in stainless-steel holder

Figure 3.13 - Sample preparation steps from fast screening impactor to the dissolution vessel. A- filter after fast screening impactor actuation; B- filter punching to 55 mm diameter; C – punched filter and outer ring; and D – filter in dissolution vessel on the disk covered with a polycarbonate membrane.

3.5.4.2.2 Particle morphology and deposition pattern

To assess the morphology of the particles being dissolved as well as their microscopic deposition pattern, fractions of powder were prepared for SEM by being collected using the NGI and the FSI. In the first case, the particles were directly collected on to a double coated carbon tape.

3.5.4.3 **Deposition and dissolution results and discussion**

Taking a closer look at the particles after collection using the NGI and the FSI (Figure 3.14), a significant difference on particle distance and disposition was observed, with powder collected using the NGI showing packed particles with a tighter particle size distribution. This is in accordance with the used methods, as in the case of the NGI the stage 4 with a 40 L/min flow rate corresponds to particles with an aerodynamic diameter between 2.00 and 3.45 μm collected in a powder hotspot generated by the stage nozzle, while in case of the FSI filter, all particles have an aerodynamic diameter lower than 5 μm and are collected as a uniformly distributed powder layer, as observed in Figure 3.13. Moreover, in the microscopic image it can be seen how they are disposed far for each other, and at different depths of the filter (Figure 3.14). Lastly, coarse lactose with FP particles attached on the surface can be seen on the FSI filter, while on the NGI stage there is no coarse lactose, so the FP can only be attached to itself and to fine lactose, having an impact on the FP and lactose concentrations on the media surrounding the particle upon dissolution. These differences can have a significant impact on the wetting, dissolution and diffusion of the excipient and DS particles.

To assess if the FSI as a sample collection methodology for dissolution could overcome the dose dependency limitation observed with the NGI collection methodology, the two FP carrier-based formulations were tested – FPJ2 blend (1 % (w/w) jet milled fluticasone propionate, 5 % (w/w) fine lactose LH230 and 94 % (w/w) coarse lactose SV003) and FPW blend (1 % (w/w) wet polished fluticasone propionate, 5 % (w/w) fine lactose LH230 and 94 % (w/w) coarse lactose SV003). The recovery and quantification of the FP deposited on the filter outer ring (after punching) was included as an additional control analysis to evaluate deposition repeatability and uniformity. The total amount of FP deposited on the 55 mm punched filter (w_{diss}), on the outer ring ($w_{outer\ ring}$) and the sum (w_{powder} - Equation 3.5) for all the performed tests is summarized in Table 3.10.

$$W_{total} = W_{diss} + W_{outer\ ring}$$

Equation 3.5

Following sample collection, the dissolution profiles with the different collected doses were compared for both studied formulation and are presented in Figure 3.15.

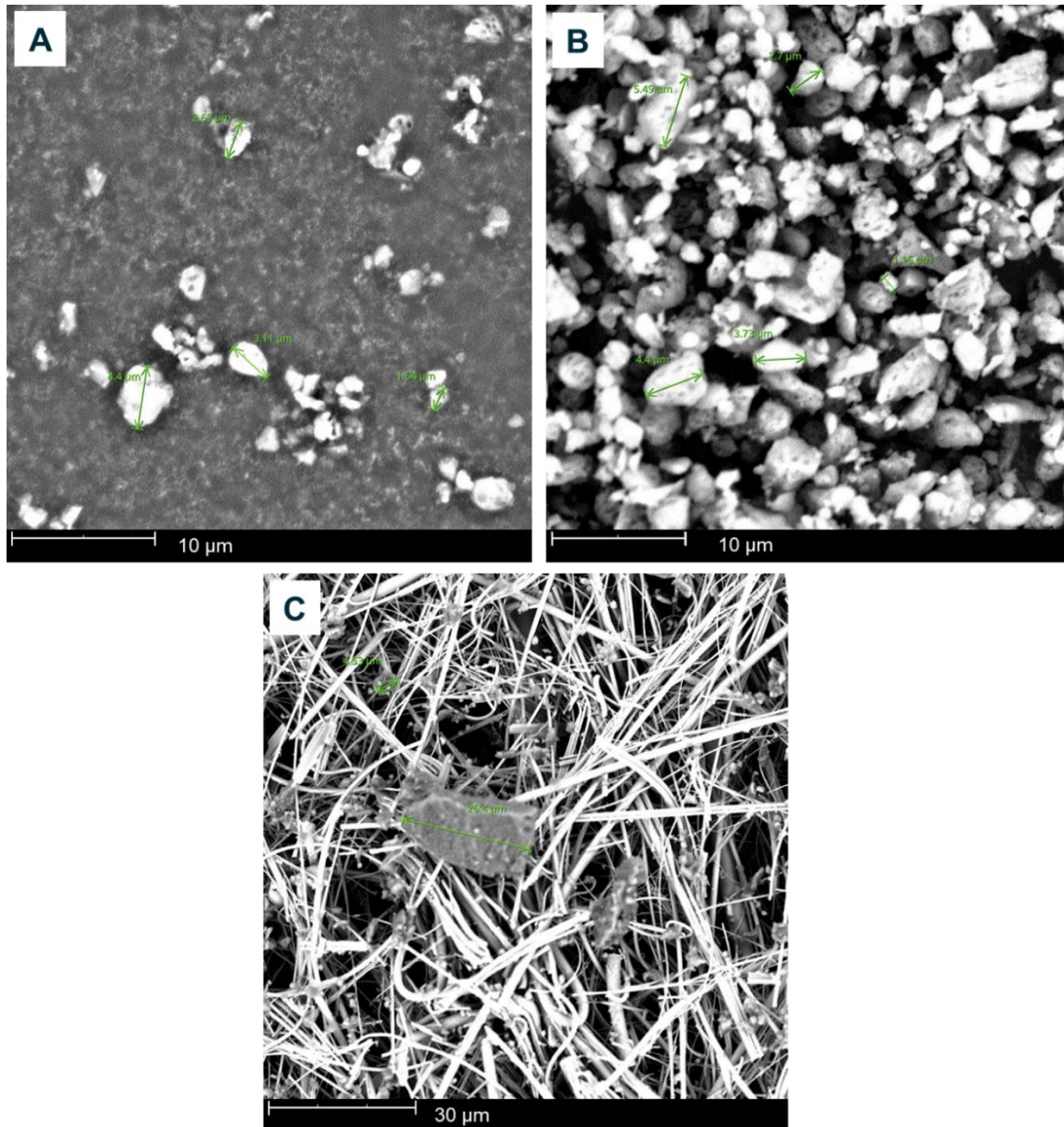


Figure 3.14 - SEM images of the particles collected using the next generation impactor, at A) a low and B) high particle density area; and C) collected using the fast screening impactor.

Table 3.10 - Summary of FP amount collected using the fast screening impactor on the punched filter (W_{diss}), on the outer ring ($W_{outer\ ring}$) and the sum (W_{total}) for FPJ2 blend (carrier-based with 1 % jet milled fluticasone propionate) and FPW blend (carrier-based with 1% wet polished fluticasone propionate). SD – standard deviation.

| Formulation | Vessel | W_{diss} (μg) | $W_{outer\ ring}$ (μg) | W_{total} (μg) |
|------------------|--------|------------------------------|-------------------------------------|-------------------------------|
| FPJ2 blend | 1 | 153 | 68 | 222 |
| | 2 | 159 | 83 | 241 |
| | 3 | 159 | 80 | 239 |
| Average \pm SD | | 157 \pm 3 | 77 \pm 6 | 234 \pm 9 |
| FPW blend | 1 | 203 | 99 | 302 |
| | 2 | 186 | 88 | 274 |
| | 3 | 297 | 91 | 388 |
| Average \pm SD | | 229 \pm 49 | 93 \pm 5 | 321 \pm 49 |

The generated results show no correlation between the collected amount and the dissolution rate - Figure 3.15.A and B. In specific, for FPJ2 blend formulation which presents more significant dose variations (from 186 μg to 297 μg), there is not a negative effect of the dose on the dissolution profile rate. When comparing both formulations (formulation FPJ2 containing jet milled FP, and formulation FPW containing wet polished FP), there is not a significant difference in the dissolution profiles after almost 23 h, even with a dose increase of almost 50 % from FPJ2 blend to FPW blend. Overall, the results suggest the use of the FSI as a method collection strategy can overcome the main limitations of the use of the NGI, namely the powder accumulation in hotspots, the aerodynamic particle size range limitation of each stage, and dose dependency.

The optimized method was validated by being applied to a high solubility drug substance salmeterol xinafoate presented in Chapter 5.

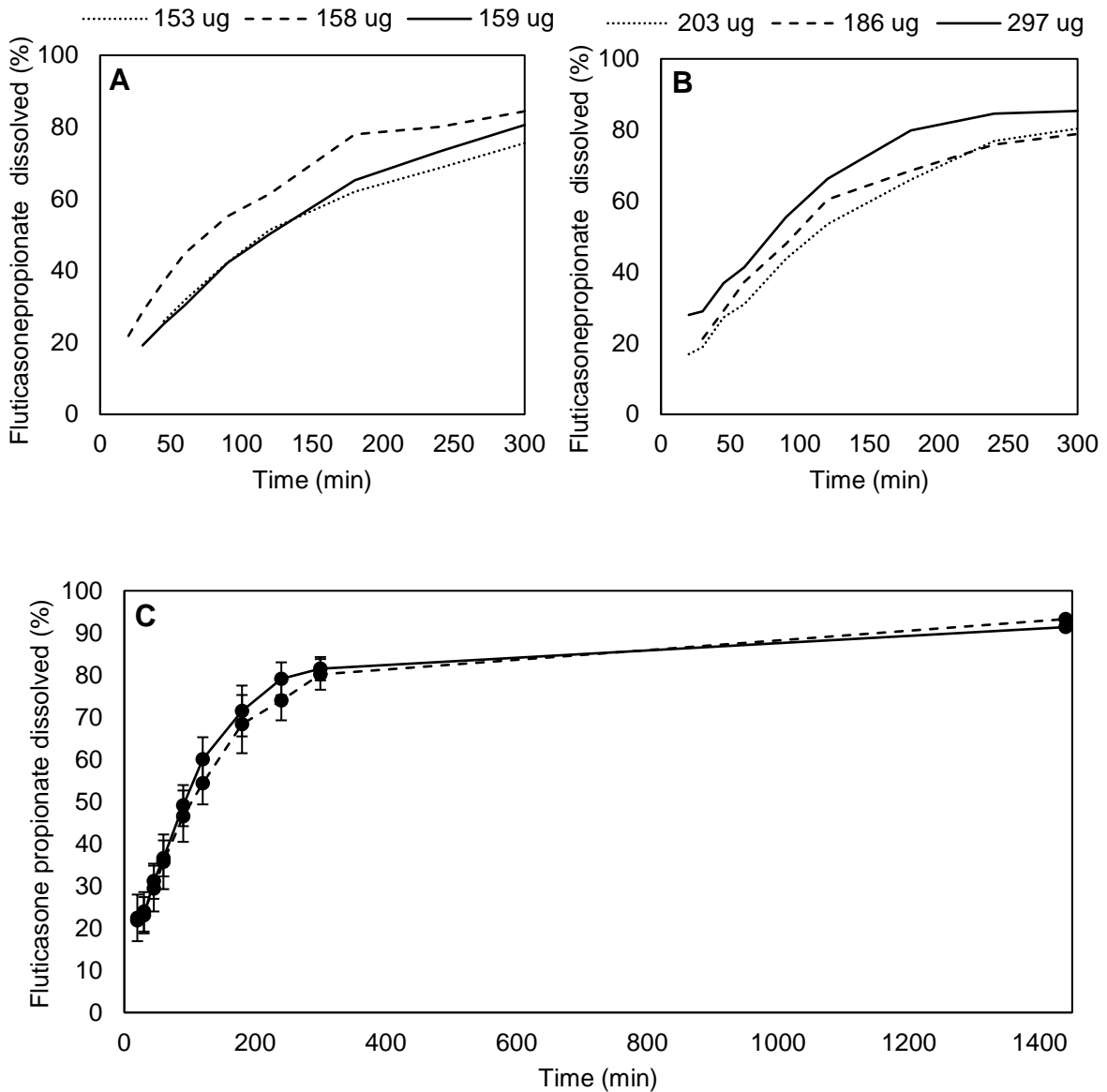


Figure 3.15 – Dissolution profiles of fluticasone propionate obtained with the paddle over disk apparatus with the fast screening impactor as a collection method for FPJ2 blend (carrier-based with 1 % jet milled fluticasone propionate) and FPW blend (carrier-based with 1% wet polished fluticasone propionate). Comparison of individual dissolution profiles for FPJ2 blend (A) and FPW blend (B); total amount dissolved in the legend; (C) comparison of FPJ2 blend (---) with FPW blend (—), data expressed as mean \pm SD (n=3).

3.5.5 Conclusions

The paddle over disk apparatus as per presented in the literature (NGI used for sample collection combined with USP apparatus II for dissolution) was successfully used to differentiate dissolution

kinetics of carrier-free from carrier-based formulations of FP, with the carrier-free formulation showing a significantly faster dissolution rate. The method critical parameters were identified and evaluated proving a significant dependency on dissolution temperature (32 versus 37 °C, suggesting that this may be an important factor to control for *in vivo* / *in vitro* correlations) and on total dose being dissolved, showing an inverse relationship between the amount of FP and its dissolution rate. The dose dependency was further studied using the NGI by increasing powder dispersion in the dissolution surface, without significant impact. Hence, dose dependency is a limitation of the POD methodology when combined with the NGI for dose collection, possibly due to the powder hotspots generated that increase local FP concentration. In order to overcome this limitation, a novel strategy was investigated and optimized - the POD was combined with the FSI, capable of uniformly dispersing the total fine particle fraction of the DPI on a filter. This was a successful approach as it led to repeatable results independent of the collected dose.

3.6 ANALYTICAL QUALITY BY DESIGN APPROACH FOR USP APPARATUS IV DISSOLUTION METHOD DEVELOPMENT

3.6.1 Outline

The USP apparatus IV, unlike the remaining systems, is not diffusion dependent, allowing the determination of the true dissolution, which is particularly relevant for locally acting DS. Since this is a new approach that has many variables to be taken into consideration during development (e.g., how much DS should be considered, what should be the dissolution system volume, what flow enables a lower variability between replicates, among others), an Analytical Quality by Design (AQbD) approach was applied in the development of a dissolution methodology for orally inhaled drug products using the UPS apparatus IV in combination with the FSI for particle collection. As an output, a design space (known as Method Operable Design Region, MODR) can be defined for a given formulation target performance.

The objective of this section is to develop an understanding of the critical parameters of a novel dissolution system. If successful, a general screening method to predict dissolution for new formulations could be used to support pre-clinical development.

3.6.2 Rational

The Quality by Design (QbD) approach was initially applied in the pharmaceutical industry to enhance the development of robust manufacturing processes, allowing for a better process understanding and its impact on product quality. QbD is defined as a systematic approach to development that begins with predefined objectives and emphasizes process and product understanding and process control, based on sound science and quality-risk-management. This concept was recognized by regulatory agencies and industries and it is well described in ICH Q8-Q12 (International Conference Harmonisation, 2020, 2012, 2005; International Council for Harmonisation, 2015, 2009). AQbD is a systematic approach to obtain an increased scientific understanding and improved confidence in the final method developed, beginning with predefined objectives followed by continuous verification and improvement throughout the method lifecycle (Musters et al., 2013; Peraman et al., 2015).

A DoE was used to evaluate the impact of potentially critical method parameters in the system, carefully selected by a risk assessment exercise:

- Flow rate impact on dissolution was selected as a critical method parameter as it is expected to have an impact on dissolution rate as well as variability. Dissolution rate is expected to increase with flow rate as the dissolution cell local DS concentration decreases with the faster media substitution. However, lower flow rate can lead to increased variability due to more heterogeneous filter wetting and media path in the dissolution cell. A more biorelevant dissolution method for inhaled drugs should be achieved with the minimum flow rate achieved by the equipment (2 mL/min), but the increase of method flow rate could be required to ensure reproducibility (16 L/min).
- Dissolution medium volume in the reservoir was studied from the minimum possible to fill the dissolution system sections (50 mL) with a maximum concentration of approximately 2 µg/mL (sink conditions), to 90 mL with a maximum concentration of ~1 µg/mL (sink conditions), in order to assess the impact of the DS concentration in the media on the dissolution profile.
- Lastly, the number of actuations was varied to assess the impact of the amount of available DS on the dissolution profile as well as on the results variability, as previously assessed for the paddle over disk apparatus.

3.6.3 Materials and methods

3.6.3.1 Preliminary assessment

To our knowledge, the use of the USP apparatus IV for inhalation dry powder dissolution assessment collected on the FSI filter (Figure 3.16) has not been tested previously.

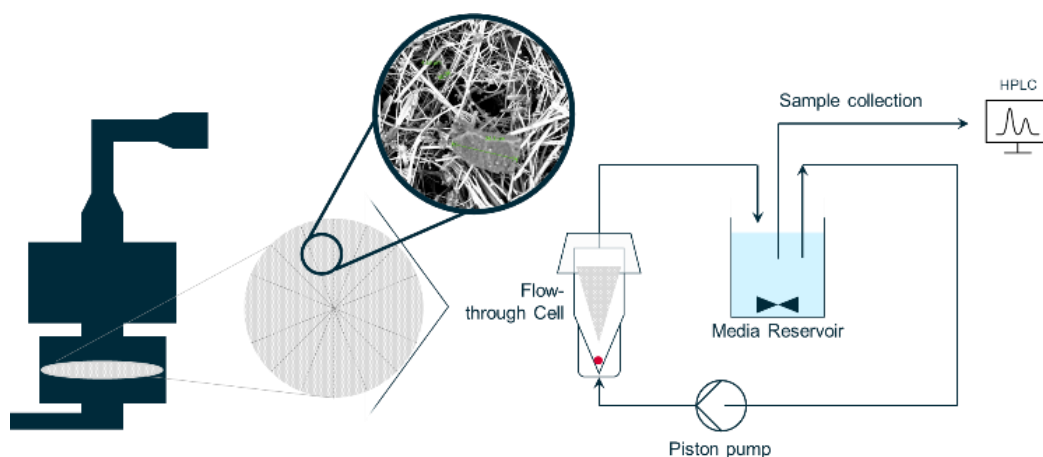


Figure 3.16 - Schematic representation of the combination of fast screening impactor with USP Apparatus IV.

Considering the impact of FSI filter configuration in the dissolution cell was unknown, preliminary tests were performed to assess the best strategy to place the collection filter in the USP apparatus IV dissolution cell by evaluating the dissolution profile variability and well as preparation complexity. For that, after sample collection the glass fiber filter was folded and placed inside an USP apparatus IV dissolution cell with three different configurations (Figure 3.17): (1) folded complete filter; (2) folded punched filter (55 mm) fitted inside the dissolution cell with a stopper to maximize filter wetting; and (3) punched filter folded once and rolled into a cylinder, to allow for media passage inside the created cylinder.

For the preliminary assessment, the system comprised a fraction collector CG1X, a dissolution testing unit CE7 smart, and a piston pump CP7-35 (Sotax AG, Switzerland). Sotax offers a range of dissolution cells compatible to different dosage forms such as different size tablets, suppositories and soft gelatin capsules, implants or large medical devices. The cell designed for powders and granulates (EP 2.9.43 "Apparent Dissolution") was selected for the present set-up (Figure 3.17, left). The dissolution medium contained 0.01M PBS buffer, pH 7.4 and 0.4% (w/v) SDS (similarly to the previous studies) and pumped at 9 mL/min at 37 °C, with a closed system, in duplicates. Samples of 1.0 mL were automatically collected at 1, 10, 20, 30, 45, 60, 90, 120, 180, 240, 300 and 1440 min. A more in detail description of the closed loop configuration can be found in Chapter 2, section 2.2.4.2. Formulation FPJ2 blend (1 % (w/w) jet milled fluticasone propionate, 5 % (w/w) fine lactose LH230 and 94 % (w/w) coarse lactose SV003) was used for the preliminary tests, with one capsule actuation.

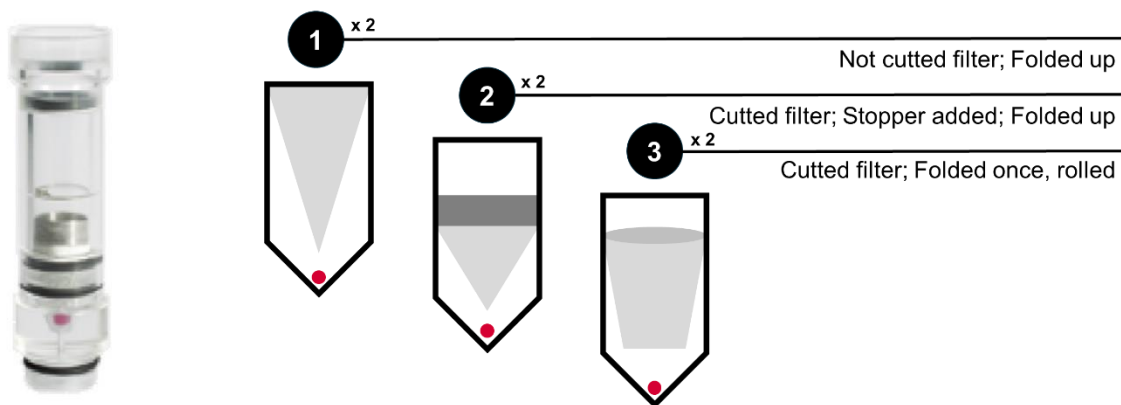


Figure 3.17 – Picture of powders and granulates dissolution cell and schematic representation of the tested membrane configurations.

3.6.3.2 Analytical quality by design experimental design

Following the generated preliminary results, the system dissolution variables, volume, dose and flow-rate, were evaluated using the selected set-up, following a QbD approach. Fusion QbD® from S-Matrix version 9.8.1 was used to plan the optimization Central Composite Face-Centered Design presented in Table 3.11.

Samples of 1.0 mL were automatically collected at 1, 10, 20, 30, 45, 60, 90, 120, 180, 240, 300 and 1440 min. The 24 h release was considered as the total amount of collected DS, based on previous results

Table 3.11 - Design of experiments plan for dissolution method development using USP apparatus IV.

| Experiment | Volume (mL) | Flow (mL/min) | Number of actuations |
|------------|-------------|---------------|----------------------|
| 1 | 90 | 9 | 2 |
| 2 | 70 | 16 | 2 |
| 3 | 50 | 16 | 3 |
| 4 | 50 | 2 | 3 |
| 5 | 90 | 16 | 3 |
| 6 | 90 | 2 | 1 |
| 7 | 90 | 2 | 3 |
| 8 | 70 | 9 | 2 |
| 9 | 70 | 9 | 1 |
| 10 | 50 | 16 | 1 |
| 11 | 70 | 9 | 3 |
| 12 | 50 | 9 | 2 |
| 13 | 90 | 16 | 1 |
| 14 | 50 | 2 | 1 |
| 15 | 70 | 2 | 2 |

3.6.3.3 Data analysis

The targeted attributes studied were selected in order to have an optimized dissolution method capable of identifying the impact of the different formulation characteristics on the dissolution profile. For that, (i) the difference between the replicates curves was calculated – aiming to minimize variability (Equation 3.6), (ii) the time needed to dissolve 50% of the DS was considered – to assess dissolution rate as well as (iii) the fraction of DS dissolved at 300 min – to assess dissolution extent. By minimizing variability and controlling dissolution rate and extent with method parameter control (flow-rate, volume and DS dose), the USP apparatus IV dissolution set-up could be adjusted to maximize differentiation independently of the formulation and DS.

$$Dif = \frac{\sum_{i=1}^{12} (A_i - B_i) / Average(A_i, B_i)}{12} \quad \text{Equation 3.6}$$

Where Dif is the difference between the replicates curves, A_i and B_i are the fraction of DS dissolved at i = (1... 1440 min).

Fusion QbD® from S-Matrix version 9.8.1 was used to perform the correspondent statistical analysis.

3.6.4 Results and discussion

The dissolution profiles of fluticasone propionate generated during the preliminary tests with the three described set-ups are presented in Figure 3.18. A significant difference can be observed between the three set-ups: set-up 1 results in a higher concentration at the dissolution media due to the higher amount of powder on the filter and thus more FP is available for dissolution (total amount of powder collected using the FSI), dissolved in a higher amount because more FP is available; set-up 3 appears to be repeatable, but requires an additional step for filter cutting; set-up 2 leads to a higher variability, possibly due to the handling required to add an additional piece to the dissolution cell.

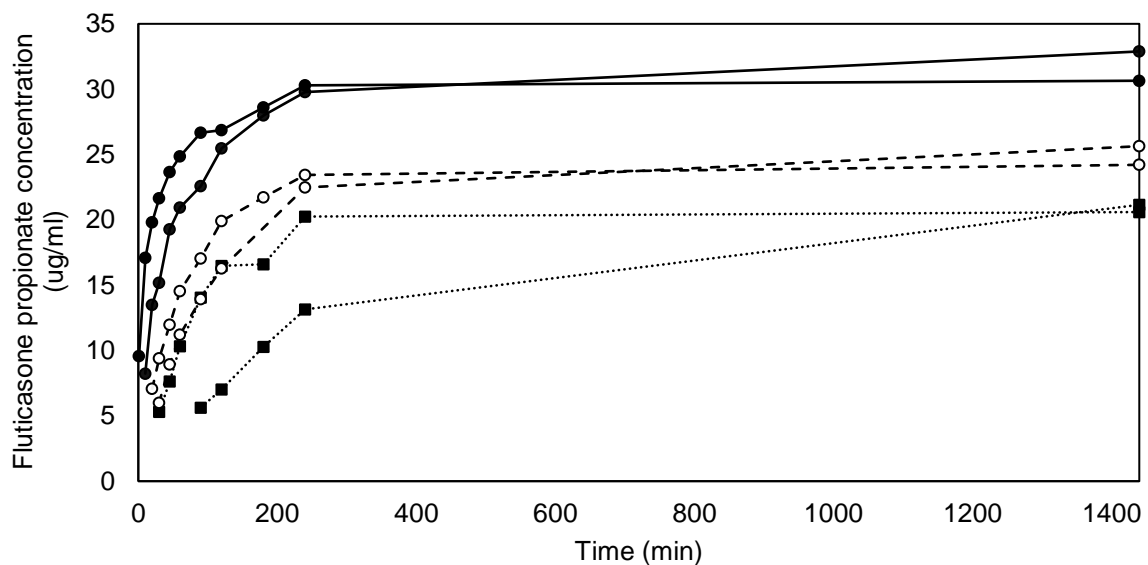


Figure 3.18 – Dissolution profiles of fluticasone propionate obtained with USP apparatus IV after collection with the fast screening impactor for formulation FPJ2 blend (carrier-based with 1 % jet milled fluticasone propionate) as individual dissolution profiles. Profiles generated with set-up 1, folded complete filter (●); profiles with set-up 2, folded punched filter fitted with a stopper (○); and profiles with set-up 3, punched filter folded once and rolled into a cylinder (■).

The results indicate the best set-up to move on with is 1 due to:

- Does not require filter punching (one less step on sample preparation);

- Tests the total amount of powder collected with the FSI;
- Lower variability as less samples handling is required.

Following the preliminary assessment, the DoE listed tests were performed and the difference between replicates calculated (Equation 3.6). After calculation of the *Dif* for all the DoE points, and prior to statistical analysis, dissolution runs were selected according to experimental observations where one of the replicates from six runs was excluded when the dissolution cell failed to meet the set-up criteria (not completely filled). However, all the *Dif* results were used as model input, attempting to determine the set up in which this observation had lower impact.

With the selected runs, the regression models illustrated in Figure 3.19 were obtained, where the importance of the mathematical model terms for each attribute is represented.

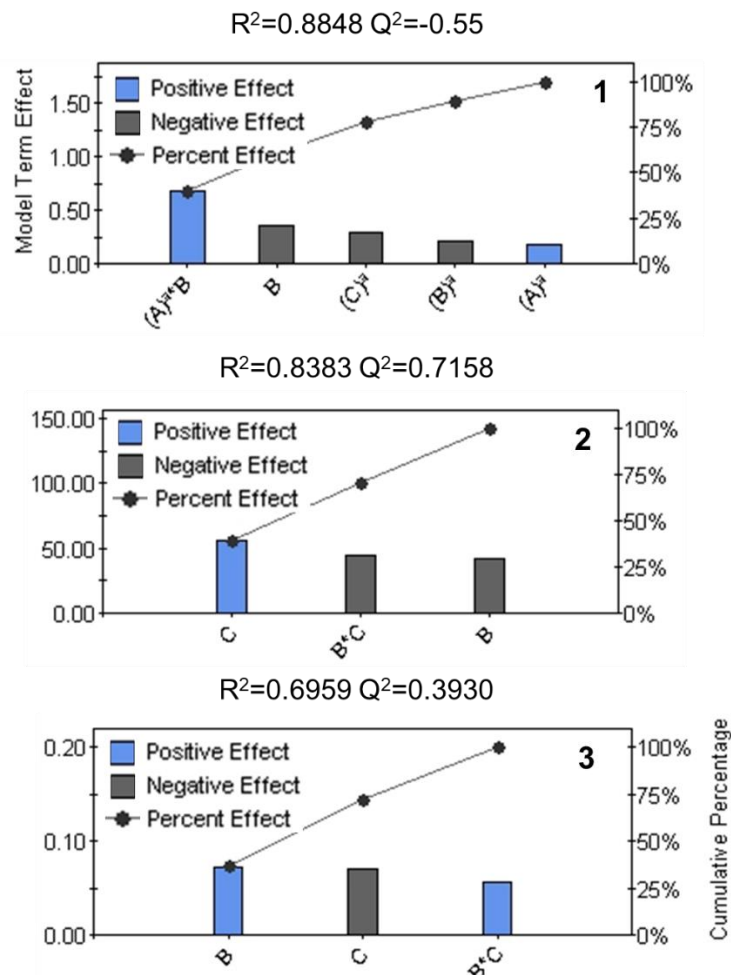


Figure 3.19 - Model terms effect on (1) difference between replicates (2) time of 50% of dissolution and (3) fraction dissolved at 300 min. A= volume, B= flow, C= actuations

A predictive model for the variability could not be found, possibly due to the differences between runs being strongly related to the dissolution cell preparation. One reason could be due to the folding and insertion of the filter, which was not considered in the current model. However, a regression with a dependence on all the parameters was found. The flow and number of actuations have an impact on the remaining evaluated responses, resulting in a model with predictive capability; thus, these two should be considered during method development.

Analyzing the contour plots, Figure 3.20, it can be observed that with a lower flow the dissolution rate decreases. However, this effect is mitigated for lower number of actuations. These suggest that, even though the system is in sink conditions, a local saturation around the filter could be occurring, due to insufficient mixing around it. Additional tests will be performed ensuring a better homogeneity in the dissolution cell and evaluating again these dependencies.

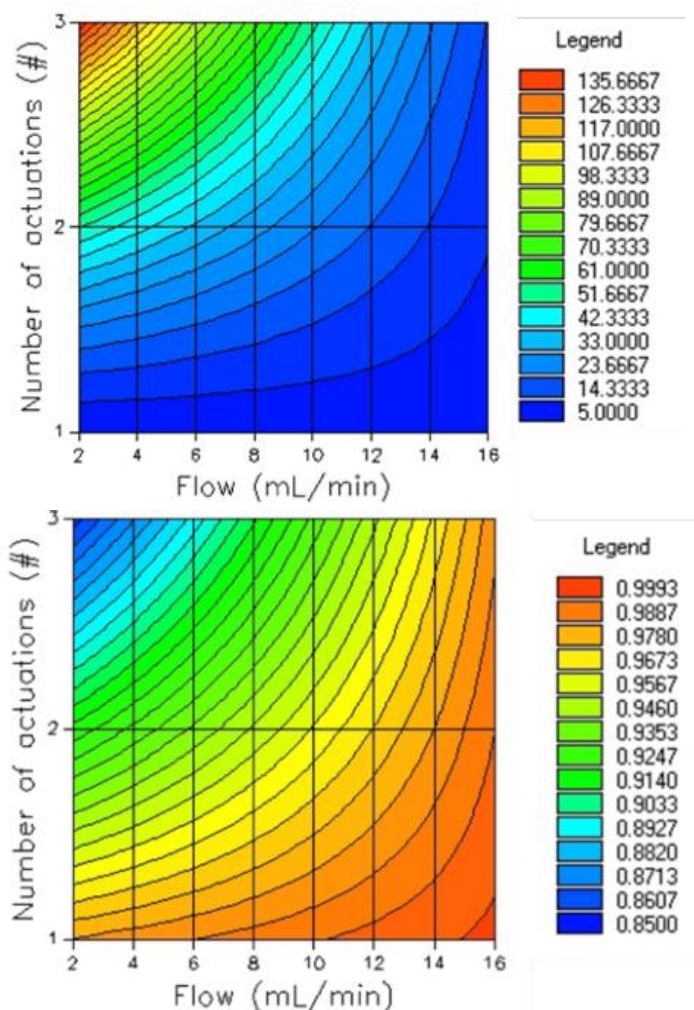


Figure 3.20 - 2D Contour plots for each attribute. Top: time (min) needed to dissolve 50 % of the drug substance (DS), and bottom: fraction of DS dissolved after 300 min.

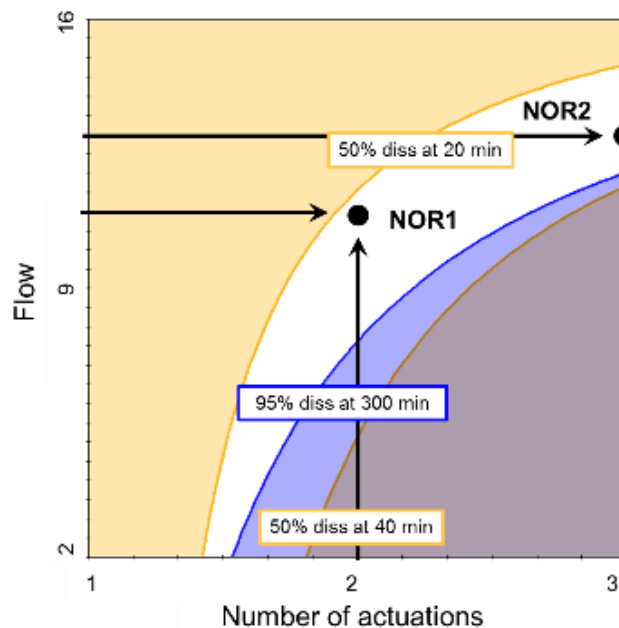


Figure 3.21 - Method Operable Design Region (MODR) representation. Blue: maximize dissolution at 300 min (goal minimum 0.95 min); yellow: time needed to dissolve 50% (target 20-40 min). NOR - Normal Operating Region.

Finally, taking into consideration the selected set of criteria for the target attributes: (1) to achieve a 50% dissolution rate between minute 20 and 40; and (2) to maximize the dissolution at 300 minutes, a MODR can be obtained by the combination and interaction between variables (the white color in Figure 3.21) where the main goal for each attribute was met. The MORD is used for the establishment of a multidimensional space with suitable method performance based on method factors and settings. Based on MODR, the optimal operating conditions can be defined, as NOR (Normal Operable Range). In Table 3.12 examples of possible NORs are presented where 1 or 2 actuations are used with varying flow rates. The MODR also illustrates that for 1 actuation, it is not possible to achieve the goal dissolution rate as a complete dissolution is not ensured at 300 min.

Table 3.12 - Normal Operating Region (NOR) predicted by the model.

| | Flow (mL/min) | Act. | Fraction dissolved at 300 min | Time to diss. 50% |
|-------|---------------|------|-------------------------------|-------------------|
| NOR 1 | 11 | 2 | 0.97 | 21 min |
| NOR 2 | 13 | 3 | 0.96 | 31 min |

3.6.5 Conclusions

In conclusion, a novel dissolution system for orally inhaled drug products was successfully assessed using an AQbD approach, comprising a powder collection stage using the FSI, and a dissolution stage using the USP Apparatus IV. The obtained model showed the influence of the number of actuations, and the flow of the dissolution system, on the dissolution rate and extent, defining the NOR for a target profile. However, local saturation phenomena might be impacting some of the dependencies observed, and the sample preparation can be further improved in order to ensure the dissolution cell is completely filled upon dissolution initiation.

The AQbD approach allowed a deeper and structured understanding of the system variables' impact on dissolution for a complex apparatus.

3.7 SAMPLE COLLECTION & DISSOLUTION APPARATUS BENCHMARK AND CONCLUSIONS

In the present section, a number of dissolution set-ups was applied to DPI formulations aiming to assess the capability to differentiate formulations and define each system advantages, limitations and potential critical method parameters. A summary of the main observations and conclusions is presented in Table 3.13.

The POD apparatus coupled with an impactor apparatus for inhalable fraction sample collection has been greatly studied for the assessment of dissolution kinetics of orally inhaled drug products (Duret et al., 2012; Mangal et al., 2018; May et al., 2014, 2012; Pilcer et al., 2013; Raula et al., 2013; Salama et al., 2008; Son and McConville, 2012, 2009; Son et al., 2010). Moreover, some studies have attained *in vivo* / *in vitro* correlations using the POD system. In fact, some set-up solutions are currently commercially available (dissolution cup by Copley) or being commercialized as analytical services (UniDose™ by Nanopharm). Hence, further investigation and development on the POD system is of great interest. The results of the present thesis show how the system can differentiate between carrier-based and carrier-free formulations of FP, but also showcase the limitations of the system that should be subject to future system optimization.

The POD system coupled with the NGI is an easy to implement and straightforward method, but it is not a lung-like collection system, and the results of the present section confirmed the literature suggestion of a dose dependency limitation. Thus, the FSI was used to overcome the dose dependency while ensuring a more biorelevant powder collection – homogenous distribution of the respirable fraction. A repeatable method was developed without dose dependency for the studied range, yet it requires significant sample handling. Future work should include equipment design to minimize sample preparation steps, such as automation of filter punching or membrane coverage. Moreover, tests with a second drug substance with different characteristics should be performed to validate the observed results – this is presented in Chapter 5. Comparing with the literature and the commercially available options, the use of the FSI as a sample collection strategy bring the great benefit of using an already available and tested impactor equipment without the need for additional equipment design.

The development of the POD was a step-by-step approach, mostly due to the lack of available knowledge regarding the equipment. However, an AqBD approach (in this case, a strategic process for

development meant to ensure that the intended performance of a final method is as expected), can bring significant advantages to the development such as identifying and minimizing sources of variability that may lead to poor method robustness and ensuring that the method meets its intended performance requirements throughout the product and method lifecycle. Accordingly, AQB approach was followed for the testing and optimization of the combination of the FSI with the USP apparatus IV as a dissolution strategy for orally inhaled products: the last strategy to be tested and optimized in the present chapter. The AQB approach allowed a deeper and structured understanding of the system variables' impact on dissolution, as well as identification of needed improvements (such as sample preparation method) allowing for a straightforward application for other formulations and DS. As the test with USP apparatus IV focused on method understanding, the next step should be to evaluate the system capability to differentiate formulations or as a quality control strategy by identifying the impact of critical manufacturing process parameters.

Each method has its advantages and limitations, for instance with USP apparatus IV there is a direct contact between the dissolution medium and the dry powder, and thus the measured profile does not have the impact of membrane diffusion obtained with the POD apparatus, and allows for the use of smaller volumes; however it is far from simulating *in vivo* environment, where particles are dissolved in a stagnant fluid. Thus, the flow-through system is a better quality control solution, with easily controlled method parameters with a clear impact on dissolution profiles, and the POD system a better strategy for formulation development and ranking. Both can be suitable for *in vivo* / *in vitro* correlations as both dissolution and diffusion constants can be used and pharmacokinetic model inputs (Borghardt et al., 2015).

Finally, aside from the tested systems, there are many other varying collection systems and dissolution mechanism available, and there is still no obvious selection for the best dissolution system for orally inhaled products leading to a lack of standardization. Collaborative efforts of academia, pharmaceutical industry and regulatory bodies are still required to overcome this challenge.

Table 3.13 – Summary of all the tested dissolution methods including advantages, disadvantages and critical method parameters.

| Method | Advantage | Disadvantage | Critical method parameters |
|--------------------------|---|--|---|
| UPS apparatus II | <p>Standard methodology used for other dosage forms.</p> <p>Sample preparation is not required (time saving).</p> <p>Capable to differentiate formulations.</p> | <p>Dissolution of powder as a bulk independent of respirable fraction, including coarse particles and not aerosolized agglomerates.</p> <p>Variability due to powder segregation to the medium surface and vessel and paddle surfaces.</p> | <ul style="list-style-type: none"> • Temperature • Stirring speed • Medium |
| NGI and POD | <p>Evaluation of specific aerodynamical size fractions – possibility to assess dissolution at various lung stages.</p> <p>Minimal sample collection handling (collection disk used for NGI collection and dissolution).</p> <p>Commercial sample collection set-up.</p> <p>Capable to differentiate formulations.</p> | <p>Powder deposition in hotspots, unlike <i>in vivo</i> deposition, with impact on dissolution kinetics. Need to ensure similar collected dose for comparison.</p> <p>Limited to a short range particle size fraction per dissolution trial – time consuming to assess the totality of the FPF.</p> <p>Minimum dissolution medium of 350 mL (to ensure paddle submersion).</p> | <ul style="list-style-type: none"> • Temperature • Stirring speed • Medium • Dose |
| FSI and POD | <p>Evaluation of all the FPF.</p> <p>Visually uniform powder deposition without clear areas of particle accumulation.</p> <p>No dose dependency observed for the studied range.</p> | <p>Complex sample preparation – additional equipment design should be considered.</p> <p>Minimum dissolution medium of 350 mL (to ensure paddle submersion).</p> | <ul style="list-style-type: none"> • Temperature • Stirring speed • Medium • Sample prep. |
| FSI and USP apparatus IV | <p>Evaluation of all FPF without membrane diffusion.</p> <p>Dissolution rate correlated with equipment parameters.</p> <p>Possibility to use lower volumes.</p> <p>No need for filter punching.</p> | <p>Variability due to the filter position in cell and complex sample preparation – additional dissolution cell should be considered.</p> | <ul style="list-style-type: none"> • Temperature • Medium • Flowrate • Volume • Dose • Sample prep. |

FSI – fast screening impactor; USP – united states pharmacopeia; FPF – fine particle fraction;

3.8 BIBLIOGRAPHY

- Borghardt, J.M., Weber, B., Staab, A., Kloft, C., 2015. Review Article Pharmacometric Models for Characterizing the Pharmacokinetics of Orally Inhaled Drugs 17. <https://doi.org/10.1208/s12248-015-9760-6>
- Cabrera, M.I., Luna, J.A., Grau, R.J.A., 2006. Modeling of dissolution-diffusion controlled drug release from planar polymeric systems with finite dissolution rate and arbitrary drug loading. *J. Memb. Sci.* 280, 693–704. <https://doi.org/10.1016/j.memsci.2006.02.025>
- Cook, R.O., Pannu, R.K., Kellaway, I.W., 2005. Novel sustained release microspheres for pulmonary drug delivery. *J. Control. Release* 104, 79–90. <https://doi.org/10.1016/j.jconrel.2005.01.003>
- D'Amato, M., Molino, A., Calabrese, G., Cecchi, L., Annesi-Maesano, I., D'Amato, G., 2018. The impact of cold on the respiratory tract and its consequences to respiratory health. *Clin. Transl. Allergy* 8, 20. <https://doi.org/10.1186/s13601-018-0208-9>
- Davies, N.M., Feddah, M.R., 2003. A novel method for assessing dissolution of aerosol inhaler products. *Int. J. Pharm.* 255, 175–187. [https://doi.org/10.1016/S0378-5173\(03\)00091-7](https://doi.org/10.1016/S0378-5173(03)00091-7)
- Duret, C., Wauthoz, N., Sebti, T., Vanderbist, F., Amighi, K., 2012. Solid dispersions of itraconazole for inhalation with enhanced dissolution, solubility and dispersion properties. *Int. J. Pharm.* 428, 103–113. <https://doi.org/10.1016/j.ijpharm.2012.03.002>
- Farias, G., Ganley, W., Deddie, H.-J., Kippax, P., Shur, J., Price, R., 2017. Investigating the microstructure of dry powder inhalers using orthogonal analytical approaches, in: *Drug Delivery to the Lungs*. The Aerosol Society, Edinburg, UK, pp. 262–265.
- Fernandes, B., Paiva, A.M., Corvo, M.L., Costa, E., Maia, F.M., 2016. Paddle Over Disk as a Dissolution Test for Orally Inhaled Fluticasone Propionate: Impact of Temperature, Dose and Formulation, in: *Respiratory Drug Delivery Europe 2017 Book 2*. Nice, France, p. 215.
- Floroiu, A., Klein, M., Krämer, J., Lehr, C.M., 2018. Towards standardized dissolution techniques for in vitro performance testing of dry powder inhalers. *Dissolution Technol.* 25, 6–18. <https://doi.org/10.14227/DT250318P6>
- Grady, H., Elder, D., Webster, G.K., Mao, Y., Lin, Y., Flanagan, T., Mann, J., Blanchard, A., Cohen, M.J., Lin, J., Kesisoglou, F., Hermans, A., Abend, A., Zhang, L., Curran, D., 2018. Industry's View on Using Quality Control, Biorelevant, and Clinically Relevant Dissolution Tests for Pharmaceutical Development, Registration, and Commercialization. *J. Pharm. Sci.* 107, 34–41. <https://doi.org/10.1016/j.xphs.2017.10.019>
- Grainger, C.I., Saunders, M., Buttini, F., Telford, R., Merolla, L.L., Martin, G.P., Jones, S.A., Forbes, B., 2012. Critical characteristics for corticosteroid solution metered dose inhaler bioequivalence. *Mol. Pharm.* 9, 563–569. <https://doi.org/10.1021/mp200415g>
- Heng, D., Cutler, D.J., Chan, H.-K., Yun, J., Raper, J.A., 2008. What is a Suitable Dissolution Method for Drug Nanoparticles? *Pharm. Res.* 25, 1696–1701. <https://doi.org/10.1007/s11095-008-9560-0>
- Human Metabolome Database, n.d. Showing metabocard for Raffinose (HMDB0003213) [WWW Document]. URL <http://www.hmdb.ca/metabolites/HMDB0003213> (accessed 12.3.21).
- International Conference Harmonisation, 2020. ICH guideline Q12 on technical and regulatory

- considerations for pharmaceutical product lifecycle management.
- International Conference Harmonisation, 2012. ICH Guideline Q11 on Development and Manufacture of Drug Substances, European Medicines Agency.
- International Conference Harmonisation, 2005. ICH Guideline Q9 on quality risk management, European Medicines Agency.
- International Council for Harmonisation, 2015. ICH guideline Q10 on Pharmaceutical Quality System, European Medicines Agency.
- International Council for Harmonisation, 2009. ICH Topic Q8 (R2) Pharmaceutical Development, Step 5: Note for Guidance on Pharmaceutical Development, European Medicines Agency.
- Jain, N.K., Roy, I., 2008. Effect of trehalose on protein structure. *Protein Sci.* NA-NA. <https://doi.org/10.1002/pro.3>
- Kwon, M.J., Bae, J.H., Kim, J.J., Na, K., Lee, E.S., 2007. Long acting porous microparticle for pulmonary protein delivery. *Int. J. Pharm.* 333, 5–9. <https://doi.org/10.1016/j.ijpharm.2007.01.016>
- Langenbucher, F., 1972. Letters to the Editor: Linearization of dissolution rate curves by the Weibull distribution. *J. Pharm. Pharmacol.* 24, 979–981. <https://doi.org/10.1111/j.2042-7158.1972.tb08930.x>
- Mangal, S., Nie, H., Xu, R., Guo, R., Cavallaro, A., Zemlyanov, D., Zhou, Q., 2018. Physico-Chemical Properties, Aerosolization and Dissolution of Co-Spray Dried Azithromycin Particles with L-Leucine for Inhalation. *Pharm. Res.* 35, 28. <https://doi.org/10.1007/s11095-017-2334-9>
- Marple, V.A., Olson, B.A., Santhanakrishnan, K., Mitchell, J.P., Hudson-Curtis, B.L., Murray, S.C., Hudson-Curtis, B.L., 2003. Next Generation Pharmaceutical Impactor (a new impactor for pharmaceutical inhaler testing). Part II: Archival calibration. *J. Aerosol Med. Depos. Clear. Eff. Lung* 16, 301–324. <https://doi.org/10.1089/089426803769017668>
- May, S., Jensen, B., Weiler, C., Wolkenhauer, M., Schneider, M., Lehr, C.-M.M., 2014. Dissolution Testing of Powders for Inhalation: Influence of Particle Deposition and Modeling of Dissolution Profiles. *Pharm. Res.* 31, 3211–3224. <https://doi.org/10.1007/s11095-014-1413-4>
- May, S., Jensen, B., Wolkenhauer, M., Schneider, M., Lehr, C.M., 2012. Dissolution Techniques for In Vitro Testing of Dry Powders for Inhalation. *Pharm. Res.* 29, 2157–2166. <https://doi.org/10.1007/s11095-012-0744-2>
- Moura, C., Neves, F., Costa, E., 2015. Optimized Composite Particles for API-independent Formulations with Enhanced Performance, in: Dalby, R., Byron, P., Peart, J., Suman, J., Young, P., Traini, D. (Eds.), *Respiratory Drug Delivery*. DHI Publishing, River Grove, IL, USA, pp. 165–176.
- Murdande, S.B., Pikal, M.J., Shanker, R.M., Bogner, R.H., 2010. Solubility advantage of amorphous pharmaceuticals: I. A thermodynamic analysis. *J. Pharm. Sci.* 99, 1254–1264. <https://doi.org/10.1002/jps.21903>
- Musters, J., van den Bos, L., Kellenbach, E., 2013. Applying QbD Principles To Develop a Generic UHPLC Method Which Facilitates Continual Improvement and Innovation Throughout the Product Lifecycle for a Commercial API. *Org. Process Res. Dev.* 17, 87–96. <https://doi.org/10.1021/op300292a>
- Nichols, S.C., Mitchell, J.P., Sandell, D., Andersson, P.U., Fischer, M., Howald, M., Pengilly, R., Krüger, P., 2016. A Multi-laboratory in Vitro Study to Compare Data from Abbreviated and

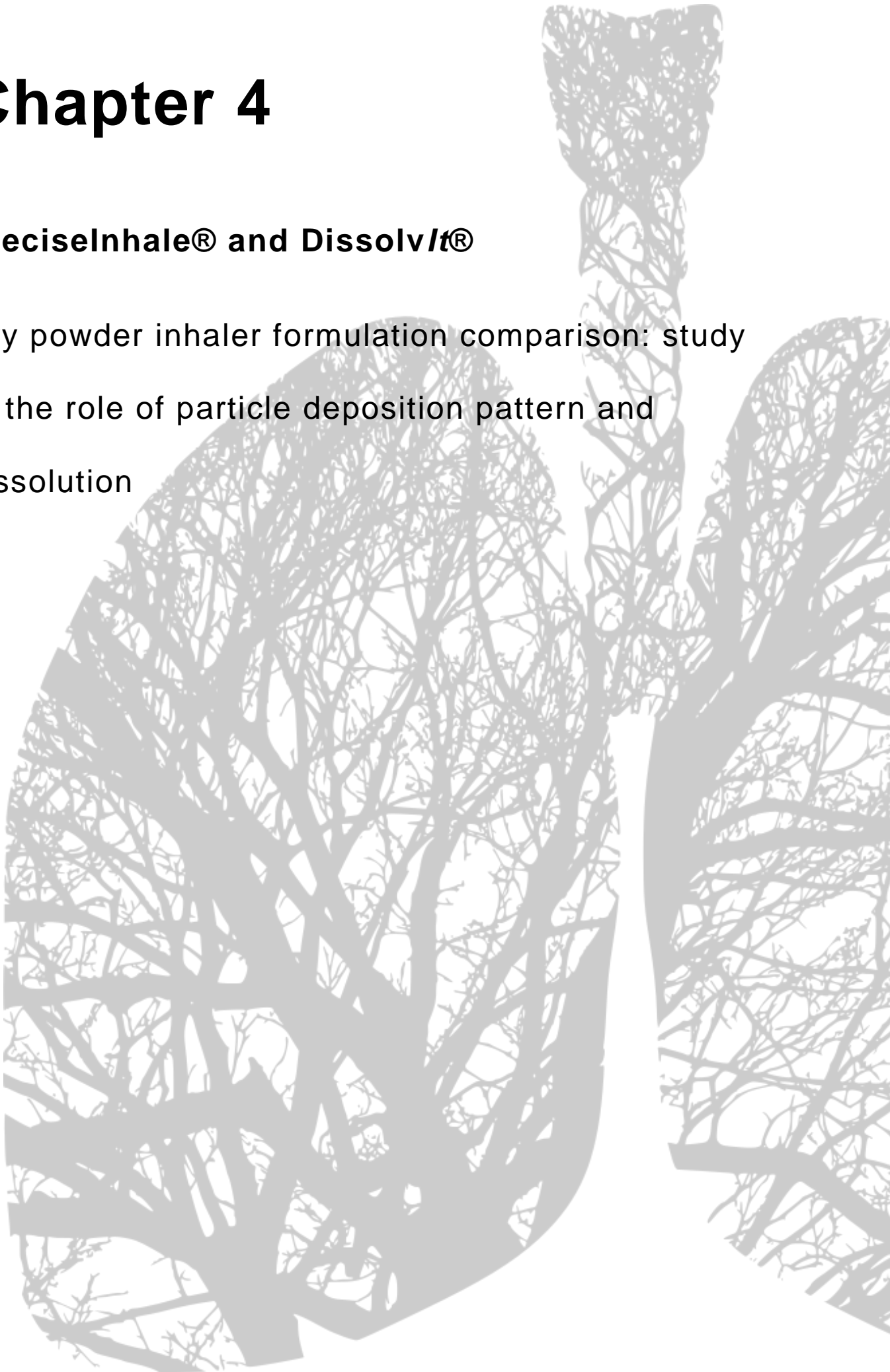
- Pharmacopeial Impactor Measurements for Orally Inhaled Products: a Report of the European Aerosol Group (EPAG). *AAPS PharmSciTech* 17, 1383–1392. <https://doi.org/10.1208/s12249-015-0476-9>
- Noriega, B., Paiva, A.M., Corvo, M.L., Costa, E., 2018. Dissolution of Orally Inhaled Drugs Using Paddle Over Disk Apparatus A Deposition Study, in: *Respiratory Drug Delivery*. Tucson, Arizona, pp. 411–416. <https://doi.org/10.15713/ins.mmj.3>
- Peraman, R., Bhadraya, K., Padmanabha Reddy, Y., 2015. Analytical Quality by Design: A Tool for Regulatory Flexibility and Robust Analytics. *Int. J. Anal. Chem.* 2015, 1–9. <https://doi.org/10.1155/2015/868727>
- Pilcer, G., Rosière, R., Traina, K., Sebti, T., Vanderbist, F., Amighi, K., 2013. New Co-Spray-Dried Tobramycin Nanoparticles-Clarithromycin Inhaled Powder Systems for Lung Infection Therapy in Cystic Fibrosis Patients. *J. Pharm. Sci.* 102, 1836–1846. <https://doi.org/10.1002/jps.23525>
- Price, R., Shur, J., 2017. Apparatus and method for determination of the fine particle dose of a powder inhalation formulation. WO2017051180A1.
- Price, R., Shur, J., Ganley, W., Farias, G., Fotaki, N., Conti, D.S., Delvadia, R., Absar, M., Saluja, B., Lee, S., 2020. Development of an Aerosol Dose Collection Apparatus for In Vitro Dissolution Measurements of Orally Inhaled Drug Products. *AAPS J.* 22, 1–9. <https://doi.org/10.1208/s12248-020-0422-y>
- Radivojev, S., Zellnitz, S., Paudel, A., Fröhlich, E., 2019. Searching for physiologically relevant in vitro dissolution techniques for orally inhaled drugs. *Int. J. Pharm.* 556, 45–56. <https://doi.org/10.1016/j.ijpharm.2018.11.072>
- Raula, J., Rahikkala, A., Halkola, T., Pessi, J., Peltonen, L., Hirvonen, J., Järvinen, K., Laaksonen, T., Kauppinen, E.I., 2013. Coated particle assemblies for the concomitant pulmonary administration of budesonide and salbutamol sulphate. *Int. J. Pharm.* 441, 248–254. <https://doi.org/10.1016/j.ijpharm.2012.11.036>
- Riley, T., Christopher, D., Arp, J., Casazza, A., Colombani, A., Cooper, A., Dey, M., Maas, J., Mitchell, J., Reiners, M., Sigari, N., Tougas, T., Lyapustina, S., 2012. Challenges with Developing In Vitro Dissolution Tests for Orally Inhaled Products (OIPs). *AAPS PharmSciTech* 13, 978–989. <https://doi.org/10.1208/s12249-012-9822-3>
- Rohrschneider, M., Bhagwat, S., Krampe, R., Michler, V., Breikreutz, J., Hochhaus, G., 2015. Evaluation of the Transwell System for Characterization of Dissolution Behavior of Inhalation Drugs: Effects of Membrane and Surfactant. *Mol. Pharm.* 12, 2618–2624. <https://doi.org/10.1021/acs.molpharmaceut.5b00221>
- Russell-Graham, D., Cooper, A., Stobbs, B., McAulay, E., Bogard, H., Heath, V., Monsallier, E., 2010. Further evaluation of the fast-screening impactor for determining fine particle fraction of dry powder inhalers, in: Mitchell, J., Nichols, S.C. (Eds.), *Drug Delivery to the Lungs-21*. The Aerosol Society, Edinburgh, pp. 374–377.
- Salama, R.O., Traini, D., Chan, H.K., Young, P.M., 2008. Preparation and characterisation of controlled release co-spray dried drug-polymer microparticles for inhalation 2: Evaluation of in vitro release profiling methodologies for controlled release respiratory aerosols. *Eur. J. Pharm. Biopharm.* 70, 145–152. <https://doi.org/10.1016/j.ejpb.2008.04.009>

- Sdraulig, S., Franich, R., Tinker, R.A., Solomon, S., O'Brien, R., Johnston, P.N., 2008. In vitro dissolution studies of uranium bearing material in simulated lung fluid. *J. Environ. Radioact.* 99, 527–538. <https://doi.org/10.1016/j.jenvrad.2007.08.009>
- Shah, V.P., Tsong, Y., Sathe, P., Williams, R.L., 1999. Dissolution profile comparison using similarity factor, *f*₂. *Dissolution Technol.* <https://doi.org/10.14227/DT060399P15>
- Sievens-Figueroa, L., Pandya, N., Bhakay, A., Keyvan, G., Michniak-Kohn, B., Bilgili, E., Davé, R.N., 2012. Using USP I and USP IV for Discriminating Dissolution Rates of Nano- and Microparticle-Loaded Pharmaceutical Strip-Films. *AAPS PharmSciTech* 13, 1473–1482. <https://doi.org/10.1208/s12249-012-9875-3>
- Son, Y.-J., McConville, J.T., 2012. Preparation of sustained release rifampicin microparticles for inhalation. *J. Pharm. Pharmacol.* 64, 1291–1302. <https://doi.org/10.1111/j.2042-7158.2012.01531.x>
- Son, Y.J., Horng, M., Copley, M., McConville, J.T., 2010. Optimization of an in vitro dissolution test method for inhalation formulations. *Dissolution Technol.* 17, 6–13. <https://doi.org/10.14227/DT170210P6>
- Son, Y.J., McConville, J.T., 2009. Development of a standardized dissolution test method for inhaled pharmaceutical formulations. *Int. J. Pharm.* 382, 15–22. <https://doi.org/10.1016/j.ijpharm.2009.07.034>

Chapter 4

PreciseInhale® and DissolvIt®

Dry powder inhaler formulation comparison: study of the role of particle deposition pattern and dissolution



This chapter has been published as:

Noriega, B., Malmlöf, M., Costa, E., Corvo, M.L., Gerde, P., Maia F. M., 2017. Dissolution of Orally Inhaled Drugs using DissolvIt®: Influence of a Newly Designed Pre-Separator for Particle Collection. In Drug Delivery to the Lungs 28. The Aerosol Society. Bristol. pages 190-4.

Noriega, B., Malmlöf, M., Corvo, M.L., Gerde, P., Costa, E, Collecting the Biorelevant Aerosol Fraction for Dissolution Testing of Orally Inhaled Drugs: Adding a Newly Designed Pre-Separator to PreciseInhale®. In In Respiratory Drug. Delivery 2018, Book 2. Pages 405-10

Noriega-Fernandes, B., Malmlöf, M., Nowenwik, M., Gerde, P., Corvo, M.L., Costa, E., 2021. Dry powder inhaler formulation comparison: Study of the role of particle deposition pattern and dissolution. Int. J. Pharm. 607:121025. <https://doi.org/10.1016/j.ijpharm.2021.121025>

4.1 SUMMARY

The composition, morphology and dissolution profile of particles and formulation micro-sized agglomerates delivered upon inhalation may have a significant impact on the product clinical effect. However, although several efforts are ongoing, a methodology that considers deposition structure and dissolution performance evaluation in a biorelevant set-up is not yet standardized. The goal of this work is to apply a collection and dissolution methodology able to discriminate dry powder inhaler formulations in terms of deposition structures and dissolution profile *in vitro*. Hence, initially an existent dissolution and absorption system was optimized for DPI characterization by implementing a pre-separator to collect the respirable fraction. Afterward, Fluticasone Propionate (FP) engineered particles and formulated products (used as a case study) were collected employing a breath simulator and characterized regarding (i) aerodynamic particle size distribution; (ii) deposited microstructures; and (iii) dissolution/absorption profiles using the DissolvIt® bio-relevant dissolution equipment. The results indicated that the particle engineering technology had an impact on the generated and deposited microstructures, here associated to the differences on surface properties of jet milled and wet polished particles as quantified by the specific surface area. Differences on surface properties modulate particle interactions, resulting in agglomerates of drug substance and excipient upon actuation with significant different morphologies, observed by microscope, as well as quantified by Marple cascade impactor. These observations allow for a further understanding of the DPI aerosolization and deposition mechanisms. The dissolution and absorption assessment indicates that the presence of lactose may accelerate the drug substance dissolution kinetics, and the FP dissolution can be significantly enhanced when formulated as a spray-dried dispersion particle. Ultimately, the results suggest dissolution testing can be an essential tool to both optimize an innovator DPI and de-risk generics development.

4.2 INTRODUCTION

Due to the direct targeting of the surfaces to be acted upon, the large absorption area and the possibility to avoid first pass metabolism (Jennings et al., 1991; Lipworth, 1999), the inhalation route of administration has been used since ancient times (de Boer et al., 2017) not only for locally acting drugs but also, more recently, for the systemic delivery of biopharmaceuticals (Agu et al., 2001). To target the deep lung, DPIs were developed and popularized for overcoming many of the drawbacks of the other approaches (Mehta, 2016). DPI product development comprises the formulation design and the selection of a suitable device. The formulation is designed in order to optimize drug delivery to the lung with the selected device, and a number of approaches can be followed, from a more traditional physical mixture of micronized drug substance (DS) with carrier excipients, to a tailored particle design containing DS and suitable excipients using techniques such as spray-drying, spray freeze drying, emulsion-based and supercritical antisolvent (Chow et al., 2007), more suitable when high delivery efficiencies are required.

Although the most recent development strategies present numerous advantages (tailored particle for specific conditions, allowing for solubility/permeability enhancement, targeted deposition and one step process), the traditional approach is still the go to solution for low dosage products with a crystalline DS resistant to the high energy milling step. The formulation design most frequently comprise micronized DS, of 1 to 5 μm diameter, mixed with larger carrier particles, and are referred as carrier-based (CB) formulations (Jones and Price, 2006). The larger particles are responsible for (i) carrying the cohesive micronized DS particles from capsule/device to the upper airway and (ii) dispersing them as individual particles/small agglomerates during the inhalation maneuver: the cohesive agglomerates of the drug particles can be overcome by distributing and establishing stable adhesive interaction between drug and excipient. These phenomena enables an easier and reproducible aerosolization (de Boer et al., 2017).

Although DPI development requires clinical evaluation to test safety and efficacy and ultimate approval by regulatory agencies, *in vitro* performance characterization is employed to guide product development and is critical on de-risking this process. Aerodynamic performance of the product is evaluated by the formulation aerodynamic particle size distribution (APSD) profile. Considering this, an APSD classification test quantifies the emitted dose (ED) – total amount of DS emitted by the device during an actuation of a capsule/blister or other metered dose – and selected fractions such as the fine particle dose (FPD_{<5 μm}) – fraction of DS with an aerodynamic diameter (D_a) smaller than 5 μm , fraction

considered capable of reaching the deeper stages of the lung (Newman and Peart, 2009). APSD characterization allows for the optimization of the aerodynamic performance, while minimizing product variability by employing compendial impaction methods such as the Andersen Cascade Impactor (ACI), or more recently the Next Generation Impactor (NGI), which are described in the European and United States pharmacopeias (USP) (“Aerosols, Nasal Sprays, Metered-dose Inhalers and Dry Powder Inhalers,” 2014, “Preparations for inhalation: aerodynamic assessment of fine particles.,” 2014). The fast screening impactor (FSI) can also be used as an abbreviated method in an initial screening to determine if the product is fit for purpose. The impaction equipment separates the powder in stages with a defined D_a cut-offs (dependent on the actuation flow), including an USP induction port (IP), aiming to collect the particles deposited in the throat region, and a USP pre-separator (PS) to collect the coarse particles not deposited on the IP.

However, the aerodynamic characterization of a DPI goes only as far as suggesting where the DS will be deposited, leaving the formulation developer in the dark regarding the deposition pattern (agglomerate morphology and composition) and its dissolution and absorption profiles – factor which may have a significant impact on the DS action (Bosselmann and Williams, 2012; Radivojev et al., 2019). For a high solubility and high permeability DS (Biopharmaceutics Classification System class I), these factors are not as relevant; yet, for the remaining classes, dissolution and absorption performance may be critical for development decisions. A standard collection, dissolution and absorption methodology is not yet agreed upon, nevertheless several options are being explored in the literature. (Radivojev et al., 2019) - some proposals are direct outputs from a FDA initiative - FY2019 and FY2020 Generic Drug User Fee Amendments science and research program for Inhalation and Nasal - and several solutions are available in the market (May et al., 2012; Noriega et al., 2017). Overall, the methodologies focus on the following challenges:

1. the selection/development of the sample collection method which samples the DPI inhalable fraction in a biorelevant way, i.e. ensures low particle density (similarly to the powder deposition in the lung surface); and
2. to simulate the lung surface where the dissolution takes place, including the presence or not of mucus, its composition and its influence in the dissolution and permeation process, and the selection of an appropriate dissolution media.

With this in mind, the published strategies usually include a sample collection step using an impactor or impinger as it allows to collect a specific aerosol fraction, based on aerodynamic particle size. Some authors use the impactor as is, performing the dissolution on an impactor/impinger stage directly, combined with standardized dissolution methods such as Apparatus V, Franz cell or Transwell® system (Arora et al., 2010; Fernandes et al., 2016a; Riley et al., 2012; Rohrschneider et al., 2015a; Son et al., 2010). This strategy has the advantage of using an already standardized apparatus and collecting powder with an inhalable aerodynamic particle size. However, the powder is deposited in “hotspots” defined by the impactor nozzles for the stage being used, which has been shown to have an impact on the dissolution rate for poorly soluble DS due to the local saturation and poor wettability. Considering this limitation, other powder collecting strategies have been designed by adapting standard impactors (Price et al., 2020), aiming to ensure a homogenous distribution of the aerosolized dose, showing to minimize the dose influence on the dissolution profile. The impact of deposited agglomerates upon actuation has also been investigated in commercial combination products by Morphology-Directed Raman Spectroscopy (Farias et al., 2017) showing a correlation of the agglomerate composition and amount with the dissolution rate of drug substance. However, the mechanism governing the observed results are not clear, possibly due to the additional characterization, such as 3D morphology and aerodynamic particle size of the agglomerates. Although the collection systems are showing significant improvements regarding particle deposition and characterization, the dissolution stage is still limited by the standard apparatus available in the market – large dissolution volumes without mucus.

In the present work a newly designed dissolution and absorption methodology is employed to assess the impact of the formulation strategy on the DS release after particle deposition for a low solubility corticosteroid used as a model drug – fluticasone propionate (FP). The ultimate goals of this work are to:

- (i) optimize the PreciseInhale® collection system by implementing a pre-separator to collect the respirable fraction (section 4.3). For that, two commercial DPIs were tested with and without the pre-separator, evaluating the impact on deposition and dissolution profile.
- (ii) study the impact of the excipients in a carrier-based formulation on the dissolution and absorption profile. The addition of coarse and fine lactose as a carrier based excipient has been mostly studied regarding the impact on manufacturability and aerodynamic performance (Rahimpour and Hamishehkar, 2012), but its impact on DS dissolution when compared with the

DS alone requires further data aside from the published (Hochhaus et al., 2021; Noriega et al., 2019);

(iii) investigate the effect of the particle engineering technology used for DS milling on the microstructures generated upon formulation actuation and deposition, as well as on the dissolution and absorption profile – the high energy jet milling technology was compared with the more delicate wet polishing technology (size reduction in suspension followed by spray-drying (SD) for particle isolation);

(iv) lastly, compare the collection and dissolution profiles of the micronized DS with a carrier-free formulation manufactured by SD containing a similar DS load incorporated in composite particles consisting of trehalose and L-leucine. The described composite particles are engineered to optimize the aerodynamic performance of the DPI product (Moura et al., 2015).

Different DPI formulation strategies for a low solubility/low permeability DS were compared employing a novel collection, dissolution and absorption methodology, including a product on the market, in order to simulate generic development comparison.

4.3 INFLUENCE OF A NEWLY DESIGNED PRE-SEPARATOR FOR PARTICLE COLLECTION

4.3.1 Outline

Gerde et al. developed an *in vitro* model that simulates the dissolution and absorption of drugs from inhaled aerosols, mimicking clinical pharmacokinetic data - DissolvIt® (Gerde et al., 2017b). Prior to dissolution testing, products are aerosolized and collected on coverslips using the PreciseInhale® aerosol generator. PreciseInhale® comprises an induction port (IP), similar to typical cascade impaction apparatuses, but the IP upward instead of downwards to interface with the coverslip deposition chamber. However, in this configuration the set-up does not include a pre-separator (PS), resulting in the collection of coarse particles which would typically deposit on the upper airways, thereby decreasing the biorelevance of the succeeding dissolution test. Furthermore, it might be a limiting factor for successfully establishing correlations between cascade impaction and dissolution testing data.

The goal of the present section is to optimize the particle collection procedure for dissolution testing by including an extra impaction stage for coarse particles in the PreciseInhale®. Accordingly, a PS was designed for an upward- instead of downward directed flow as a component of PreciseInhale®, matching an actuation flow rate of 40 L/min. The two commercial products, Flixotide Diskus and Pulmicort Flexhaler, were actuated with and without the PS in the PreciseInhale® system to study the influence of the PS on powder deposition and dissolution.

4.3.2 Materials and methods

4.3.2.1 Materials

Flixotide Diskus 240 µg from GSK (UK) and Pulmicort Flexhaler 180 µg from AstraZeneca (UK). Alpha, alpha-trehalose dihydrate, L-leucine, polyethylene oxide (MW 5 000 000) and L-alpha phosphatidyl choline were purchased from Merck KGaA (Germany). Bovine serum albumin was purchased from Chem Cruz Biochemicals (USA). Microscope coverslips of 13 mm diameter (No. 2) were purchased from MenzelGläser, Histolab (Germany). Glass fiber filters grade A used for the Marple-8 stage cascade impactor (MCI) was purchased from GE Healthcare Life Sciences (USA) and manually cut to fit the impactor stages. All other chemicals were of analytical grade.,

4.3.2.2 Methods

4.3.2.2.1 Preciselnhale® actuation

Preciselnhale® exposure system from Inhalation Sciences (Sweden) was employed with a glass deposition holding chamber to aerosolize and collect the powders on circular microscope coverslips with 13 mm in diameter. The detailed description of the system was previously published (Gerde et al., 2017a). Briefly, the operation comprises two steps: the actuation/generation of the aerosol and the exposure/deposition of the aerosol. During the actuation phase, the inhalation was simulated with a flow rate of 40 L/min, leading to the powder being transported from the inhaler through the induction port and holding chamber.

The two commercial products, Flixotide Diskus, containing FP and lactose coarse lactose particles, and Pulmicort Flexhaler, containing budesonide (BD) and fine lactose particles, were actuated with and without the PS, with a pressure drop of 1.2 kPa and 2.0 kPa, respectively. For the tests with the newly design PS (Figure 4.1Figure 4.), it is assembled under the collecting chamber. After actuation, during the exposure phase, the aerosolized powder is deposited simultaneously on nine glass coverslips in the bottom of the chamber by setting an outlet flow of 400 mL/s, with the air entering from the top of the chamber. Three coverslips (out of the nine) was used for immediate quantification of the deposited dose on the coverslips, another for scanning electron microscopy (SEM) analysis, and the remaining for Dissolution testing. All coverslips are also analyzed by naked eye and by light microscope to detect variations in deposition patterns.

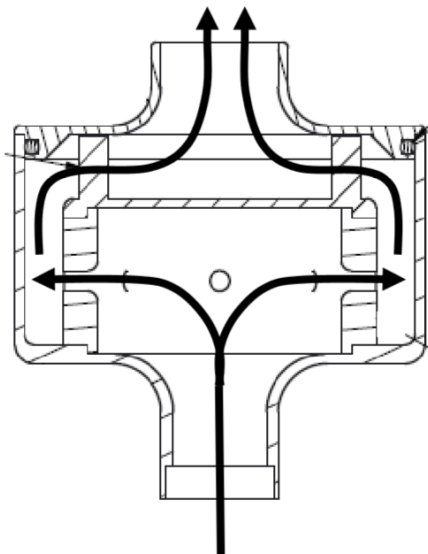


Figure 4.1 - Schematic of the newly designed PS. From (Noriega et al., 2018a).

4.3.2.2.2 Scanning electron microscopy

The microstructures generated after PreciseInhale[®] actuation were visualized by scanning electron microscope (SEM - Zeiss, Oberkochen, Germany). The coverslips and the collected particles were coated with 10 nm Platinum (Q150T ES, West Sussex, UK) and loaded into the SEM docking bay. The samples were analyzed in an Ultra 55 field emission SEM at 5 kV using the secondary electron detector. The images were captured at various magnifications.

4.3.2.2.3 APSD analysis by Marple Cascade Impactor

Marple cascade impactor (Chen et al., 2018) was employed to determine the APSD of the aerosol generated using the PreciseInhale[®], after actuation, aerosol expansion and transport to the bottom of the collection chamber. The relevance of using the MCI is to account for agglomerates generated during aerosol expansion and deposition.

To measure the APSD of the commercial DPI, a similar procedure to the powder collection using the PreciseInhale[®] system was followed, and the MCI was coupled to the coating chamber. The powder is expanded in the glass coating chamber and then displaced to the MCI at an exposure flow rate of 400 mL/min. At the top of the MCI ambient air was aspirated through the dilution port to reach the design flow rate of 2 L/min.

To quantify the amount of BD and FP deposited on each stage of the impactor each filter was immersed in 1.5 mL of mobile phase (80 % (v/v) methanol in water) and the FP was extracted for more than 15 min. Next the extraction solution was transferred to vials and centrifuged at 11 600 x g for at least 8 min. The solution, without pellet, was transferred to HPLC vials and analyzed with stable baseline using a C18 column (5 µm, 250 mm x 4.6 mm equipped with guard column) with an absorbance detection wavelength of 237 nm and an injection volume of 50 µL. The injection run time was 6.5 min and the retention time 4.8 for BD and 5.5 for FP.

4.3.2.2.4 Dissolution in the DissolvIt[®] system

Following the particle collection, the coated coverslips were used in the DissolvIt[®] apparatus from Inhalation Sciences (Sweden) to perform the dissolution test, previously described (Gerde et al., 2017b). For each experiment, three coated glasses from the same collection were analyzed. The dissolution took place in the dissolution chamber, from the coverslip glass to the pumped perfusate at 0.4 mL/min

through a 50 μm -thick layer of mucus simulant and a 10 μm -thick polycarbonate membrane (0.03 μm pore size), schematized in Figure 4.2. The system was maintained at 37 $^{\circ}\text{C}$. The described equipment was used to achieve a biorelevant characterization, as it allows for a biorelevant particle collection and dissolution (Selg et al., 2019).

The experiment was observed with an inverted light microscope and images were captured throughout the dissolution time. The perfusate exiting the dissolution chamber was collected in a 96-hole deep-well plate by using a custom-made fraction collector at 0, 4, 8, 15, 20, 30, 45, 60, 90, 120, 180 and 240 min for FP, and at 0, 20s, 40s, 1, 2, 3, 5, 8, 15, 30, 60, 120 min, for a total volume of 96 mL each.

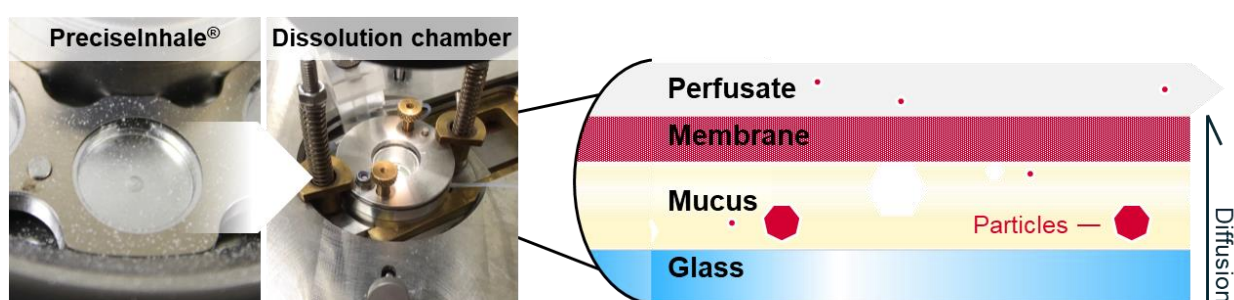


Figure 4.2 - Dissolution chamber set up. Left: coated coverslip on Preciselnhale® after actuation; right: dissolution chamber in place in the DissolvIt® equipment with zoom in to the dissolution chamber layers, from glass to perfusate. Adapted from (Noriega et al., 2019)

4.3.2.2.4.1 Dissolution quantification

The FP and BD from the sampled dissolution timepoints of the commercial Flixotide Diskus and Pulmicort Flexhaler was extracted from the perfusate and quantified using liquid chromatography mass spectrometry (LC-MS/MS), performed by Pharm-Analyt Labor GmbH (Austria), LOQ at 0.100 ng/mL for perfusate buffer samples.

For mass balance purposes, the FP and BD remaining in the dissolution system after the test was quantified for all the formulations. To that end 20 mL of 1:1 (v/v) DMSO:Methanol was added to the collected dissolution cell followed by 10 min ultrasound. These led to dissolution of the glue of the tape fixing the polycarbonate (membrane) and the cell, and to the separation of the glass disk from the membrane. After that samples were vortexed strongly for 5 min and then sampled in triplicate aliquots for chemical analysis (LC-MS/MS), performed by Pharm-Analyt Labor GmbH (Austria), with a LOQ of 20.0 ng total amount.

4.3.2.2.4.2 Data handling

The dissolution data was normalized to the total amount deposited in the coverslip during aerosol collection (M_{dep} , Equation 4.1), which was quantified as the sum of the DS dissolved in the perfusate during the dissolution test (M_{perf}) and the non-dissolved DS, extracted from the system and quantified once the dissolution experiment is finalized (M_{system}).

$$M_{dep} = M_{perf} + M_{system} \quad \text{Equation 4.1}$$

The cumulated dissolved dose was calculated by trapezoid integration (Equation 4.2)

$$M_{perf} = \sum_{n=1}^N (t_n - t_{n-1}) \times \left(M_{n-1} + \frac{M_n - M_{n-1}}{2} \right) \quad \text{Equation 4.2}$$

In which N is the number of collected timepoints, t_n and t_{n-1} are two consecutive timepoints, in minutes, and M_n and M_{n-1} are the masses of DS collected at those timepoints.

With the quantified amount of dissolved DS, the dissolution extent (Equation 4.3) can be calculated.

$$\text{Dissolution extent } (t) = \frac{M_c(t)}{M_{dep}} \quad \text{Equation 4.3}$$

In which M_c was the cumulative mass calculated with Equation 4.2 for each timepoint. To compare the dissolution profile of the manufactured formulations considering all timepoints (T_t) with the commercial product dissolution profile (R_t) the similarity factor, f_2 , was calculated as follows (Shah et al., 1999):

$$f_2 = 50 \cdot \log \left\{ \left[1 + \frac{1}{n} \sum_{t=1}^n (R_t - T_t)^2 \right]^{-0.5} \times 100 \right\} \quad \text{Equation 4.4}$$

4.3.2.2.5 Statistical analysis

To compare results, data were subjected to statistical analysis using unpaired T student analysis.

Differences were considered statistically significant at a level of $p < 0.05$.

4.3.3 Results and Discussion

4.3.3.1 Generated and deposited structure characterization

Table 4.1 summarizes the number of actuations for each collection and the obtained deposited dose of FP and BD (M_{dep}), with and without PS. The number of actuation was defined by a trial-and-error methodology. The deposited dose for the FP tests with and without the PS are statistically similar (p -value = 0.4), while the BD collected doses are statistically different (p -value = 0.02), with an overall relative standard deviation of 13%. The impact of the collected dose on the dissolution profile for BD using the DissolvIt® has been studied (Malmlöf et al., 2019), showing no significant impact of the dose for an RSD of 13% or lower. Hence, the BD dose is not expected to have a significant impact on the obtained dissolution profile for the studied range.

Table 4.1 – Summary of the number of actuations for each collection and the obtained deposited dose for the drug substances (DS) fluticasone propionate and budesonide (M_{dep}), with and without pre-separator (PS).

| Set up | Inhaler | Drug substance | M_{dep} (ng of DS) | Number of actuations |
|------------|---------------------|------------------------|----------------------|----------------------|
| Without PS | Flixotide Diskus | Fluticasone Propionate | 651 ± 293 | 1 |
| With PS | | | 618 ± 144 | 5 |
| Without PS | Pulmicort Flexhaler | Budesonide | 587 ± 51 | 7 |
| With PS | | | 739 ± 62 | 3 |

To assess the morphology of the generated and deposited structures with and without the PS, light microscope and SEM analysis were performed to the coverslip glasses after actuation. The light microscope images of the deposited particles on the coverslips using the PreciseInhale® and previous to dissolution are presented in Figure 4.3, for the Flixotide Diskus (Figure 4.3, A, B) and Pulmicort Flexhaler (Figure 4.3, C, D). With this image the overall deposition pattern can be evaluated, and different deposited microstructures can be observed. The Flixotide Diskus deposition structures are completely different when actuated in the presence (Figure 4.3, A) or absence (Figure 4.3, B) of the PS. Without the PS the powder deposits as mainly coarse lactose particles with adhered DS finer particles, while the presence of the PS leads to a homogenous distribution of finer particles. For the Pulmicort

Flexhaler, an apparent lower particle density is observed, however, that difference may be a consequence of the variability of powder deposition between glasses, thus no significant differences can be observed.

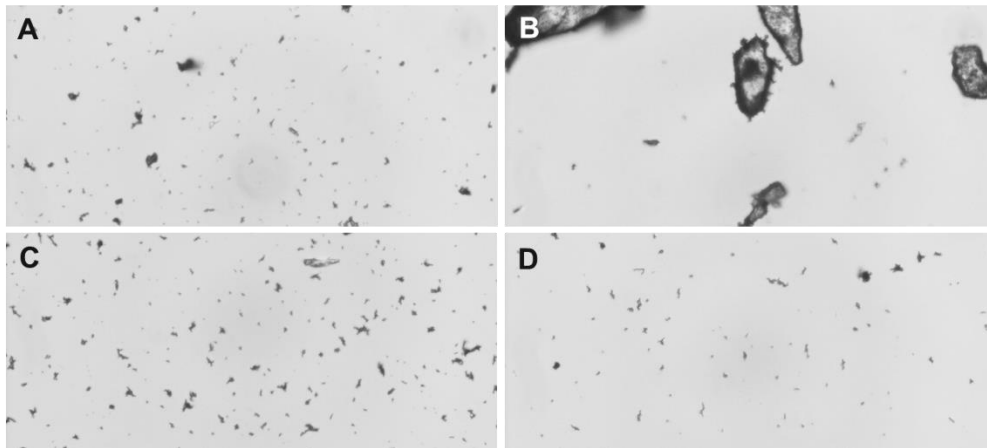


Figure 4.3 - Deposition pattern on coverslips of the Flixotide Diskus without (A) and with (B) the pre-separator (PS), and Pulmicort Flexhaler without (C) and with the PS (D), after actuation using the PreciseInhale®, obtained by light microscopy with a x20 objective

In Figure 4.4 the images obtained from SEM are presented, showing a significant difference between formulations. The deposited powder from Flixotide Diskus contains particles with a size range varying from 1 to 30 μm , with agglomerates of the fine particles and adhesion of the fines to the coarse particles. The particles from Pulmicort Flexhaler present a narrower size range and more fine agglomerates, with the larger particles being smaller than 10 μm . It is also possible to observe differences in the agglomerate morphology, as the Pulmicort's are filamentous, which influences the aerodynamic performance and may also influence dissolution. Comparing the images with and without PS, no significant difference can be observed regarding particle size in the case of Pulmicort Flexhaler, which could be expected as this formulation does not contain a significant coarse particles fraction according to literature (Sahib et al., 2010). However, the use of the PS facilitated the particle collection on the coverslip glasses, possibly due to a better aerosol mixing inside of the coating chamber, resulting in similar amount of DS deposited on the different glasses, and a more even deposition and better powder dispersion, as observed by a decrease of coarse agglomerates of particles visible to the naked eye (although not visible on the SEM micrographs). For Flixotide Diskus experiments, the images show a

significant difference regarding the amount of powder deposited, which is a result of the difference in the number of actuations required. Considering the deposited doses as presented in Table 4.1, it can be also concluded that for this formulation the amount of deposited powder is not directly proportional to the amount of DS, as the DSI load is similar with and without the PS. With this in mind, it is reasonable to believe that the PS captures a significant part of the DS, possibly due to the low pressure drop achieved in the inhaler, which may favor attachment to coarse particles or agglomerates.

Future work should include a separation step for the PS designed for a 60 L/min flow rate, to achieve optimal pressure drops for studied inhalers, and analyze the influence on the DS load on the glasses.

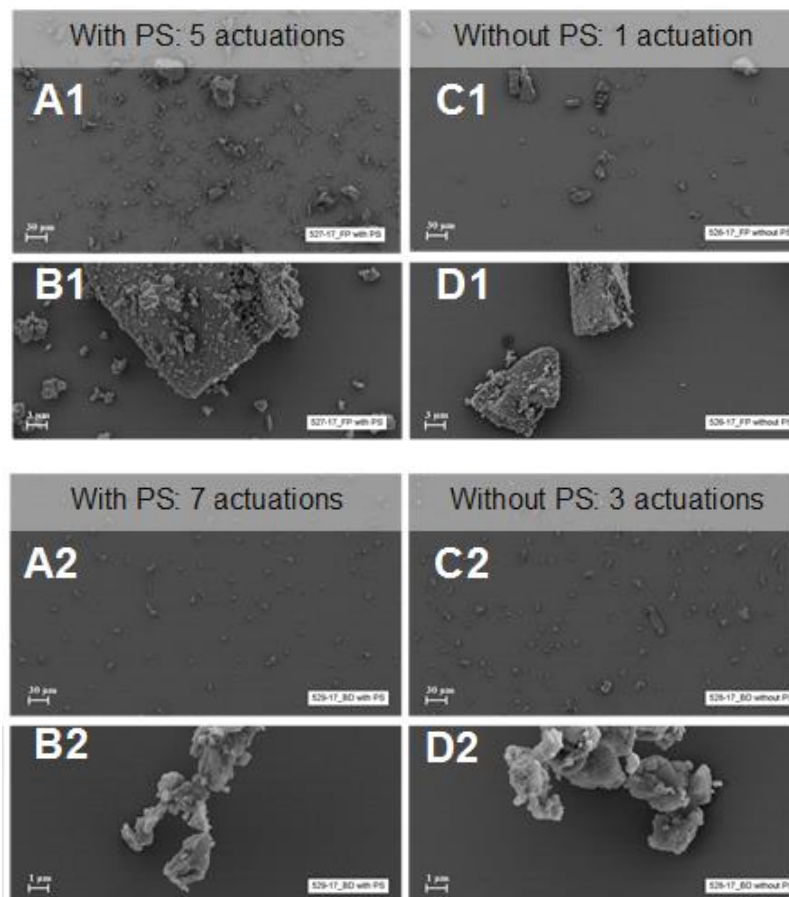


Figure 4.4 – Scanning electron microscopy images of the deposited aerosols from Flixotide Diskus (1), with pre-separator after 5 actuations (A1,B1) and without after 1 (C2,D2); and from Pulmicort Flexhaler (2), with pre-separator after 7 actuations (A2,B2) and without after 3 actuations (C2,D2). The scale represents 30 µm for figures A1, C1, A2 and C2, and 1 µm for figures B1, D1, B2 and D2.

4.3.3.2 Aerodynamic characterization

Regarding the APSD analysis, the use of the PS has a significant impact when actuating the Flixotide Diskus inhaler (MMAD decreases from 4.52 ± 0.09 to 4.21 ± 0.13 μm , $p\text{-value} = 0.03 < 0.05$, and the GSD from 1.71 ± 0.03 to 1.84 ± 0.05), as expected, because this formulation, contrary to the Pulmicort Flexhaler (from 3.37 ± 0.30 μm to 3.33 ± 0.04), contains a higher percentage of coarse particles. These results indicate the presence of the PS is capable to minimize coarse particle deposition on the coverslips, previous to dissolution, thus leading to a more biorelevant assessment.

Table 4.2 - Particle-size distribution as normalized mass frequency determined by Marple Cascade Impactor for Flixotide Diskus and Pulmicort Flexhaler, with and without the pre-separator (PS). Data expressed as mean \pm SD (n=3). MMAD - Median mass aerodynamic diameter, GSD – Geometric standard deviation.

| Device | Flixotide Diskus | | Pulmicort Flexhaler | |
|------------------------|------------------|-----------------|---------------------|-----------------|
| | With PS | Without PS | With PS | Without PS |
| Set-up | | | | |
| MMAD (μm) | 4.21 ± 0.13 | 4.52 ± 0.09 | 3.33 ± 0.04 | 3.37 ± 0.30 |
| GSD | 1.71 ± 0.03 | 1.84 ± 0.05 | 1.74 ± 0.08 | 1.73 ± 0.01 |

4.3.3.3 Dissolution profiles

The results of the dissolution test are presented in Figure 4.5. By observing the dissolution process through the inverted microscope, it was possible to see the BD powder completely dissolve during the test, and the FP powder remain in the mucus after 4 h. Accordingly, comparing the fraction retained of the two DS (Figure 4.5, A and B for FP and BD, respectively), a clear difference can be seen in the extent of dissolution between them, as BD release increases to 85% in 2 h, while FP does not reach 20% in 4 h. As it has been documented in previous work, a similar behavior can be observed in clinical trials of the studied drugs (Gerde et al., 2017b).

In Figure 4.5, C, the comparison of the dissolution profiles of FP collected with and without PS shows a similar profile, but given the higher standard deviation of the glass deposition data in the absence of the PS (651 ± 293 ng for FP), the results were not significantly different with or without the use of the PS. Surprisingly, the BD profiles (Figure 4.5, D) showed a great difference between the powder collected

with and without the PS ($f_2=38<50$). The fraction retained in the dissolution cell at the end of the test was 3-fold higher when the PS was not present during particle deposition, showing a slower dissolution in this case, which may be explained by the presence of larger agglomerates of particles on the glass coverslips visible to the naked eye, and therefore a reduced dissolution area (according to Fick's law). The maximum concentration of the pharmacokinetic profile was doubled in the presence of the PS, and the half-life time was reduced by 80%, however, the time of maximum concentration was not influenced. If this is the case, it can be concluded that even using the same powder formulation and inhaler, minor differences on powder behavior flow, due to for example changes in adhesion forces or in respiratory flow rates, will result in significant alterations of the drug pharmacokinetic profile, therefore the selection of an appropriate particle collection method is crucial to achieve a suitable *in vitro* / *in vivo* correlation result.

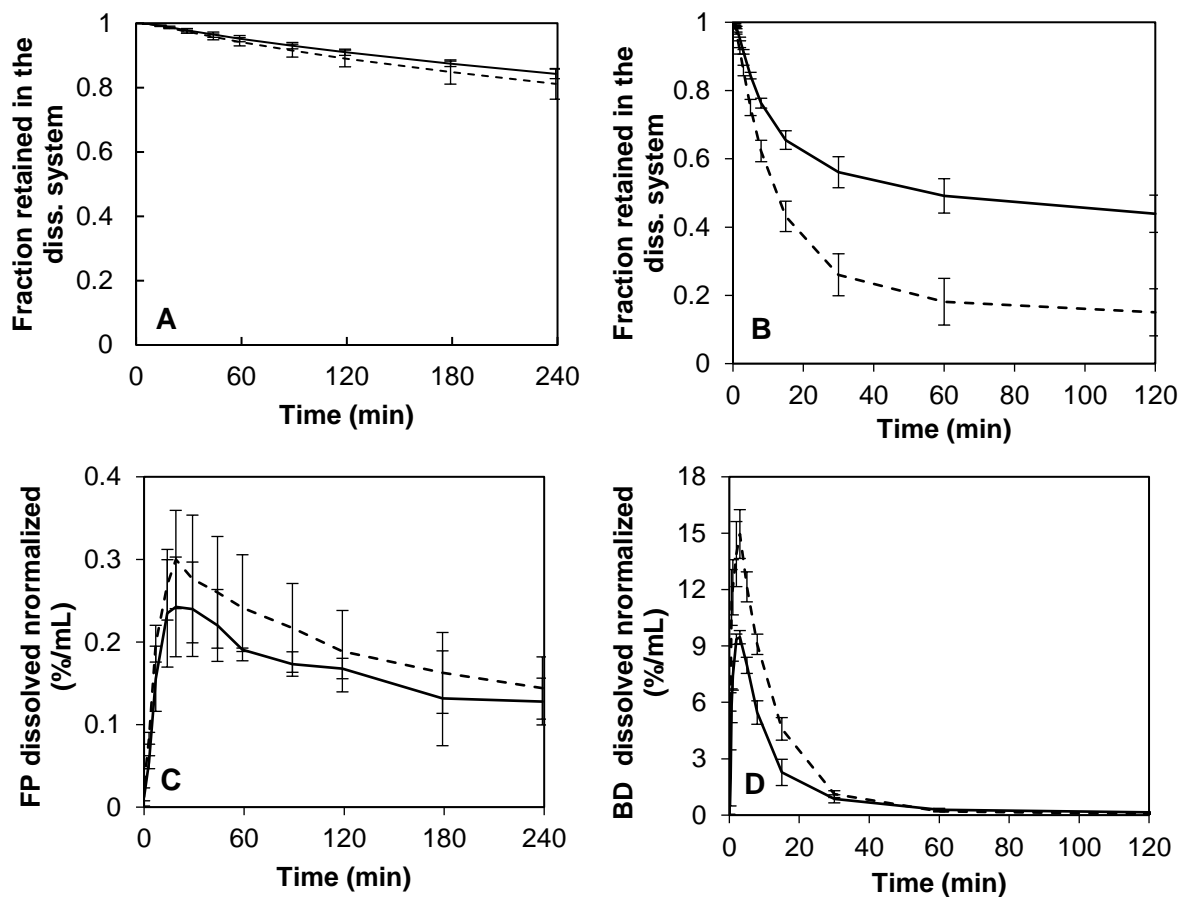


Figure 4.5 - Dissolution profiles obtained using DissolvIt[®] (n=3), as a fraction retained in the dissolution system for (A) the Flixotide Diskus containing fluticasone propionate (FP) and (B) the Pulmicort Flexhaler containing budesonide (BD); and as a fraction of total recovered (%/mL) for (C) the Flixotide Diskus and (D) the Pulmicort Flexhaler, with (dotted line) and without (full line) the pre-separator. All results normalized to the total deposited dose. Data expressed as mean \pm SD (n=3).

4.3.4 Conclusions

The influence of the presence of a newly designed PS in the collection of dry powders for dissolution testing was analyzed. Two commercial dry powders, Flixotide Diskus and Pulmicort Flexhaler were deposited on cover slip glasses using the PreciseInhale® apparatus, with and without PS, and characterized with SEM, MCI, and the DissolvIt® apparatus, which was used to obtain the respective dissolution profiles. The PS proved to have an influence on the powder aerodynamic profile and the DS load collected on the coverslips. The dissolution results were not significantly different for Flixotide Diskus, but for Pulmicort Flexhaler, the powder collected using the PS showed a higher dissolution rate, possibly due to the deposition of smaller agglomerates, pointing to the importance of particle deagglomeration on DS dissolution behavior. Future work includes testing the inhalers with higher flowrates and a new pre-separator appropriately designed for said flowrates, to increase powder deagglomeration and to better mimic the deposition of a fine particle fraction of a DS in the real lung.

4.4 DRY POWDER INHALER FORMULATION COMPARISON: STUDY OF THE ROLE OF PARTICLE DEPOSITION PATTERN AND DISSOLUTION

4.4.1 Outline

Following the optimization of the PreciseInhale® breath simulator in order to collect a more biorelevant fraction that is similar to the fine particle dose collected in a cascade impactor, in the present section the PreciseInhale® and DissolvIt® was used to evaluate differences on particle deposition, dissolution, and absorption for a low solubility DS (FP), by comparing manufactured formulations with the commercial Flixotide Diskus. For that, two particle engineering technologies (jet milling and wet polishing) were applied to micronize the crystalline DS, followed by a carrier-based formulation approach by blending the micronized material with coarse and fine lactose. Additionally, the spray-drying was used to manufacture a carrier-free formulation with optimized performance. All manufactured formulations were characterized according to standard characterization approaches (particle size distribution, specific surface area, aerodynamic performance, and particle morphology). The main goal of the present work is to understand the impact of the formulation strategy not only on the aerodynamic performance, but also on structured of the deposited structures of agglomerated material and on the dissolution and absorption profile.

4.4.2 Materials and methods

4.4.2.1 Materials

Flixotide Diskus 240 µg from GSK (UK). Crystalline fluticasone propionate (FP; $C_{25}H_{31}F_3O_5S$; Mw = 500.6) micronized by jet milling (JM) and wet polishing (WP) was supplied by Hovione S.A. (Portugal). Lactose micronized powders were purchased from DFE Pharma (Germany) - Lactohale 230 and Respitose SV003 - and from Meggle Pharma (Germany) - Inhalac 400. Capsules size 3 were purchased from Capsugel (France). Dissolution material were used as per described in section 4.3.2.1.

4.4.2.2 Methods

4.4.2.2.1 Preparation of DPI formulations

Homogeneous mixtures of 150 g of coarse and fine lactose with 1% w/w of micronized FP were prepared in a high shear mixer from Diosna (Germany) and a low shear mixer from Turbula® GlenMills (USA), following geometric dilution. Content of fine excipient in the prepared blends is described in Table 4.3. The mixtures were filled in size 3 capsules using a Quantos unit from Mettler Toledo AG (Spain) with a target fill weight of 20 mg, with acceptance limits of +/- 0.5 mg.

To prepare carrier-free powders, a solution with 2% (w/w) of solids in a water/ethanol (50/50, % w/w) solvent mixture was prepared, with 20% L-Leucine (w/w_{solids}), 79% Trehalose (w/w_{solids}) and 1% FP (w/w_{solids}). The solution was spray-dried at an outlet temperature of 95 °C, a feed flow of 7 g/min, atomization pressure of 8 bar and atomization gas flow at 50 mm in the rotameter, using a Büchi model B-290 Advanced unit (Switzerland) (Moura et al., 2015). The inlet temperature of the drying gas was adjusted to obtain the target outlet temperature. Hydroxypropyl methylcellulose (HPMC) size 3 capsules were hand filled with a target fill weight of 20 mg, with acceptance limits of +/- 1 mg.

Table 4.3 – Summary of the manufactured carrier-based formulations. FPJ blend – carrier-based formulation containing jet milled fluticasone propionate; FPW blend – carrier-based formulation containing wet polished fluticasone propionate.

| Formulation | Micronization technology | Mixing technology | Fine lactose | Coarse lactose | Fine lactose (%) |
|--------------------|---------------------------------|--------------------------|---------------------|-----------------------|-------------------------|
| FPJ blend | Jet Milling | High shear | Lactohale 230 | Respitose SV003 | 5 |
| FPW blend | Wet Milling | Low shear | Inhalac 400 | | 10 |

4.4.2.2.2 PreciseInhale® actuation

PreciseInhale® exposure system from Inhalation Sciences (Sweden) was employed with a glass deposition holding chamber to aerosolize and collect the powders on circular microscope coverslips with 13 mm in diameter. The detailed description of the system was previously published (Gerde et al., 2017a) and the set-up with the PS is schematized in Figure 4.6. A brief description can be found in section 4.3.2.2.1. After actuation, during the exposure phase (III in Figure 4.6) the aerosolized powder

is deposited simultaneously on nine glass coverslips in the bottom of the chamber by setting an outlet flow of 400 mL/s, with the air entering from the top of the chamber. Three coverslips (out of the nine) was used for immediate quantification of the deposited dose on the coverslips, another for SEM analysis, and the remaining for dissolution testing. All coverslips are also analyzed by naked eye and by light microscope to detect variations in deposition patterns. To aerosolize and collect the formulations, different set-ups and settings were used, as described in the following sections.

Aerosolization and collection of DPIs

The aerosolization and collection of the DPI formulations was achieved by adapting the PreciseInhale® system to the DPI actuation (Figure 4.6). The main goals with the PreciseInhale® tests are:

- To achieve a target dose of DS on the coverslip surface.
- To minimize the variability of the DS dose deposited on the different coverslips.
- To achieve a homogenous distribution of powder.

These three aspects are essential to achieve a reproducible dissolution.

For that purpose, the glass deposition chamber was connected to a newly designed pre-separator and induction port, that keep the DPI coarse particles from aerosolizing into the coating chamber (Noriega et al., 2018a). The DPI was fitted to the IP with mouthpiece adaptor (MPA). The DPIs were actuated at 40 L/min. After actuation, the powder aerosolizes and flows through the IP and PS, where the larger non-respirable particles and agglomerates deposit by sedimentation and impaction mechanisms. The finer particles and smaller agglomerates enter the coating chamber as the aerosol expands during the inhaler actuation cycle, and are subsequently pulled down by a vacuum source, depositing on the glass coverslips.

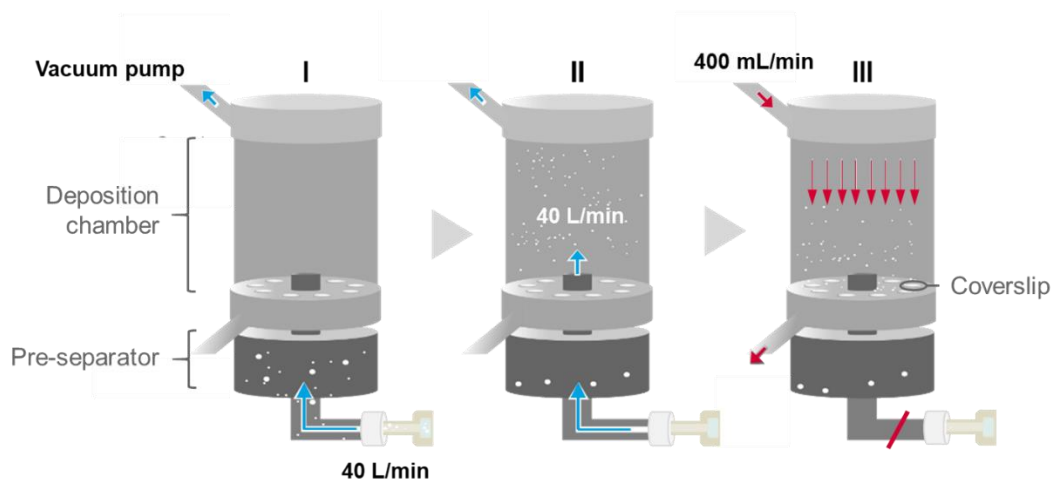


Figure 4.6 - Schematic of Preciselnhale[®] actuation- and glass deposition cycles. I – the DPI is actuated with a flow rate of 40 L/min, passing through the induction port (IP) and the pre-separator (PS); II – the coarser particles impact and deposit on the IP and PS, the finer particles expand in the glass deposition chamber; III – the finer particles are collected on the coverslips. Adapted from (Noriega et al., 2018a).

4.4.2.2.3 Aerosolization and collection of micronized drug substance

To aerosolize DS micronized by jet milling and wet polishing, the DustGun aerosol generator of the Preciselnhale[®] system was used: portions of highly compressed air (50 bar) were used to deagglomerate the micronized DS into highly concentrated respirable aerosols. The generated aerosols are then deposited on the coverslips. The amount of loaded DS to generate the aerosol and the DustGun generation pressure were optimized to achieve an uniform DS distribution on the 9 coverslips, as well as a similar deposited dose for both micronized material. The amount of DS deposited on the coverslips was quantified by HPLC during actuation parameters optimization. For the presented results, 0.55 mg of the jet milled FP and 0.52 mg of the wet polished FP were respectively loaded to the powder chamber of the DustGun generator.

For the carrier-based formulations 3 capsules were actuated, for the composite particles 1 capsule, and for the Flixotide Diskus, 4 blisters were actuated.

4.4.2.2.4 Milled fluticasone propionate and formulation characterization

4.4.2.2.4.1 *Particle size analysis and specific surface area determination*

The particle size distribution of micronized FP and of the carrier-free particles was measured as dry powder by laser diffraction using a HELOS laser diffraction instrument (Sympatec GmbH, Germany).

The particle size distribution data was presented as Dv10, Dv50 and Dv90 (particle size below which 10 %, 50 % and 90 % of the volume of particles exist).

The specific surface area was determined by multipoint Brunauer-Emmett-Teller (BET). Nitrogen (purity N99.8 %) was used as adsorbate and the BET surface area was determined in the relative pressure range of 0.05 to 0.35.

4.4.2.2.4.2 Scanning electron microscopy

Same procedure as per described in section 4.3.2.2.2.

4.4.2.2.4.3 APSD analysis by Next Generation Impactor and Fast Screening Impactor

NGI and FSI were used as an APSD characterization technique for manufactured capsules, using the standard apparatus at 4kPa. Both equipment were used as information provided was suited for formulation comparison, as proven in the literature (Mohan et al., 2017).

The APSD of the prepared carrier-based formulations was assessed by NGI from Copley Scientific (UK) at an airflow rate of 40 L/min with a total air volume of 4 L. Tests were performed using a RS01 Ultra High Resistance 2 device from Plastiapè (Italy). All impactor stages were coated using a coating agent solution (1 % glycerol in ethanol) to minimize particle bouncing. All formulations were assessed in triplicate, actuating five capsules in each test. FP was recovered from the IP, PS, stages 1 to 7, micro-orifice collector (MOC) and the actuated capsules, with a mixture of milli-Q water and acetonitrile (50:50, v/v) with 0.05 % (v/v) of 85% phosphoric acid (w/w). The FP was quantified using a waters HPLC system with UV detection (Waters 717 plus Autosampler; Waters 1525 binary HPLC Pump; Waters Jet Stream 2 Plus incubator) equipped with a C18 column (5 µm, 250 mm x 4.6 mm) at 35 ± 5 °C with a mobile phase of 35:35:30 ACN:MetOH:Sodium acetate 0.01M pH=4 (v/v/v), an absorbance detection wavelength of 240 nm and an injection volume of 20 µL. The injection run time was 10 min and the FP retention time 7.2 min. The data was analyzed using Copley Inhaler Testing Data Analysis Software version 3.10, according to pharmacopoeia requirements.

For the composite formulation, the APSD was assessed by FSI from Copley Scientific (Switzerland) with a similar inhaler and set-up. The FPF was collected in a glass microfiber filter from Whatman (UK), and quantified by weighing the filter before and after actuation in controlled conditions. The emitted dose is determined by weighing the capsule before and after actuation.

4.4.2.2.4.4 *APSD analysis by Marple Cascade Impactor*

Marple cascade impactor (Chen et al., 2018) was employed to determine the APSD of the aerosol generated using the PreciseInhale®, after actuation, aerosol expansion and transport to the bottom of the collection chamber. The relevance of using the MCI is to account for agglomerates generated during aerosol expansion and deposition.

The followed procedure is as per described in section 4.3.2.2.3.

4.4.2.2.5 Dissolution in the DissolvIt® system

Following the particle collection, the coated coverslips were used in the DissolvIt® apparatus from Inhalation Sciences (Sweden) to perform the dissolution test, previously described (Gerde et al., 2017b).

The system is described in section 4.3.2.2.4.

4.4.3 Results

4.4.3.1 Characterization of engineered particles

Jet milled, wet polished and spray-dried particles used in the present work were characterized for particle size and specific surface area (SSA) by was assessed by Brunauer-Emmet-Teller (BET) adsorption method. The results are presented in Table 4.4.

All particles are within the inhalation size range of 0.5 to 5 μm (Newman and Peart, 2009), with a Dv50 of 1.9 μm . The micronized particles present a smaller span than the spray-dried particles. Although the particle size does not vary significantly, the SSA shows a variation (jet milled particles present a 50% increase from the wet polished particles, and an almost double SSA than the spray-dried particles), indicating the variation observed in SSA is not related with PSD differences. These results are in accordance with previous observations (Moura et al., 2016).

Table 4.4 - Particle size distribution characterization of the micronized material and the spray-dried particles.

| | Dv10 (μm) | Dv50 (μm) | Dv90 (μm) | Span | SSA by BET (m^2/g) |
|-----------------------|------------------------|------------------------|------------------------|------|--------------------------------------|
| Jet milled | 0.9 | 1.9 | 3.6 | 1.4 | 6.5 |
| Wet polished | 1.1 | 1.9 | 3.2 | 1.1 | 4.3 |
| Spray-dried composite | 0.7 | 1.9 | 4.8 | 2.2 | 3.5 |

Dv10, Dv50 and Dv90: Particle size below which 10 %, 50 % and 90 % of the volume of particles exist; SSA: specific surface area; BET: Brunauer–Emmett–Teller.

4.4.3.2 Aerodynamic characterization

The NGI coupled with a flow controller and an MCI coupled with the PreciseInhale[®] system were used to characterize the aerodynamic performance of the manufactured formulations.

The aerodynamic profiles of the prepared carrier-based formulations with jet milled FP and wet polished FP determined by NGI are presented in Figure 4.7. The formulations have an ED of $173 \pm 8 \mu\text{g}/\text{capsule}$ and $176 \pm 10 \mu\text{g}/\text{capsule}$, a fine particle dose of $36 \pm 1 \mu\text{g}/\text{dose}$ and $60 \pm 7 \mu\text{g}/\text{dose}$, and a MMAD of $3.2 \pm 0.2 \mu\text{m}$ and $3.12 \pm 0.1 \mu\text{m}$, respectively for jet milled and wet polished formulations. In order to compare the model manufactured formulations with the commercial product, literature data was

considered. Literature results obtained using the ACI and NGI at 60 L/min are similar, indicating that this reference ACI data at lower flow rates can be benchmarked against the model manufactured formulations NGI data. In literature, the Flixotide Diskus 250 µg product is characterized for a flow rate of 60 L/min with an NGI (Hill and Slater, 1998) and for a range of 28.3 to 60 L/min using the ACI (Taki et al., 2011) with an ED of 87 to 93 % of the label claim (217 to 233 µg/dose) and a FPF of 15 to 22 % of the label claim (40 – 53 µg/dose).

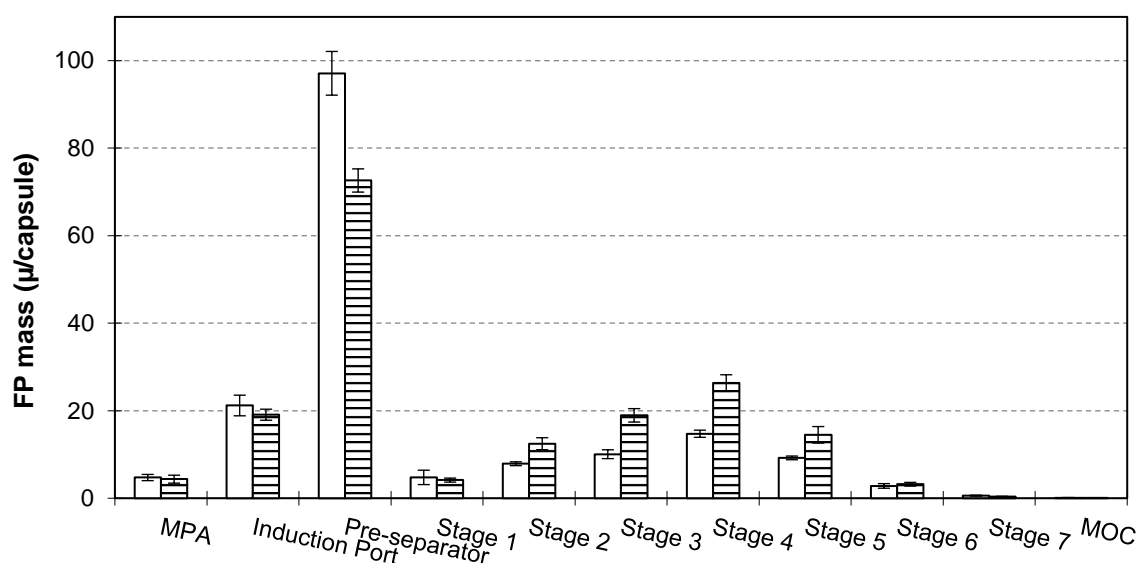


Figure 4.7 - Aerodynamic characterization of the fluticasone propionate formulations containing jet milled particles (white) and wet polished particles (stripes), determined by Next Generation Impactor. Data expressed as mean \pm SD (n=3). MPA: mouth piece adapter; MOC: micro-orifice collector.

Additionally, the MCI was used to characterize the APSD not only of the commercial and manufactured model products, but also of the micronized drug substance when aerosolized by the PreciseInhale® equipment. The goal of this step is to characterize the aerosol effectively being assessed by dissolution in the DissolvIt® apparatus. The results are presented in Figure 4.8 as APSD profiles and summarized in Table 4.5. The carrier-based formulations are compared in Figure 4.8.A, showing that a significant difference was observed between the measured MMAD of the manufactured formulations and the commercial DPI (p-value < 0.04 for the jet milled FP blend and p-value < 0.01 for the wet polished FP blend). The APSD of the milled drug substance are compared in Figure 4.8.B, showing the presence of significant more fine particles for the jet milled FP material (p-value < 0.03). Lastly, the commercial DPI

was compared with the composite formulation in Figure 4.8.C, showing a population of larger agglomerates (cut diameter > 10 µm) for the latter, not present in the remaining results, and a broader geometric standard deviation (GSD).

Table 4.5 - Aerodynamic performance parameters of the carrier-based formulations with jet milled fluticasone (FPJ blend) and wet polished fluticasone (FPW blend); of the composite formulation (comp. particles); and the commercial Flixotide Diskus. n=3.

| Parameter | FPJ blend | FPW blend | Comp. particles | Flixotide Diskus | |
|---------------------------------------|-------------|-------------|-----------------|------------------------------|-----------------------|
| Impactor equipment (flow rate, L/min) | NGI (40) | NGI (40) | FSI (40) | ACI ¹ (28.3 - 60) | NGI ² (60) |
| ED (µg/dose) | 173 ± 8 | 176 ± 10 | 211 ± 7 | - | 234 ± 2 |
| FPD (µg/dose) | 36 ± 1 | 60 ± 7 | 167 ± 10 | 40 ± 3 – 53 ± 2 | 50 ± 4 |
| FPF _{label claim} (%) | 18 ± 1 | 30 ± 1 | 79 ± 2 | 16 ± 1 – 21 ± 1 | 20 ± 1 |
| MMAD (µm) | 3.2 ± 0.2 | 3.2 ± 0.1 | - | - | 4.1 ± 0.1 |
| GSD - | 1.99 ± 0.02 | 2.40 ± 0.20 | - | - | 1.97 ± 0.02 |

¹ Results adapted from (Hill and Slater, 1998)

² Results adapted from (Taki et al., 2011)

ED: emitted dose; FPD: fine particle dose; FPF_{label claim}: fine particle fraction over lable claim; MMAD: mass mediam aerodynamic diameter; GSD: geometric standard deviation; NGI: next generation impactor; FSI: fast screening impactor; ACI: andersen cascade impactor.

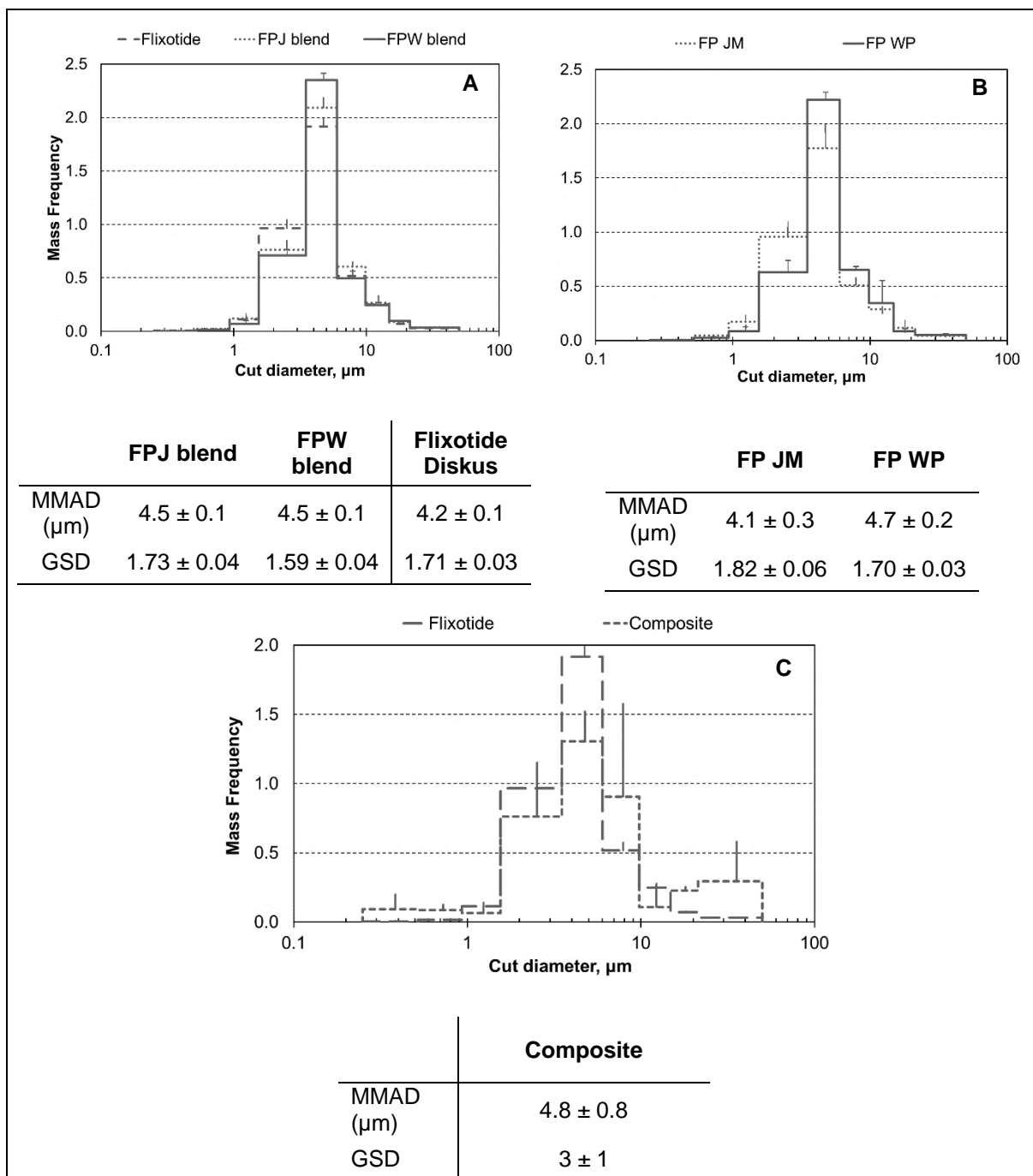


Figure 4.8 - Particle-size distribution as normalized mass frequency determined by Marple Cascade Impactor A –carrier-based formulations with jet milled fluticasone (FPJ blend), wet polished fluticasone (FPW blend) and commercial Flixotide Diskus; B – particle micronized by jet milling (FP JM) and wet polishing (FP WP); C – Composite formulation and the commercial Flixotide Diskus. Data expressed as mean \pm SD (n=3). MMAD - Median mass aerodynamic diameter, GSD – Geometric standard deviation

4.4.3.3 Generated and deposited structure characterization

To assess the morphology of the generated and deposited structures, which may have an impact on the dissolution profiles, a light microscope and a SEM analysis are performed to the coverslip glasses after actuation. The light microscope images of the deposited particles on the coverslips using the Preciselnhale® and previous to dissolution are presented in Figure 4.9, for the micronized drug substance by jet milling (A) and wet polishing (B), for the carrier-based formulations with jet milled FP (C) and wet polished (D), as well as the spray-dried particles (E) and the commercial Flixotide Diskus (F).

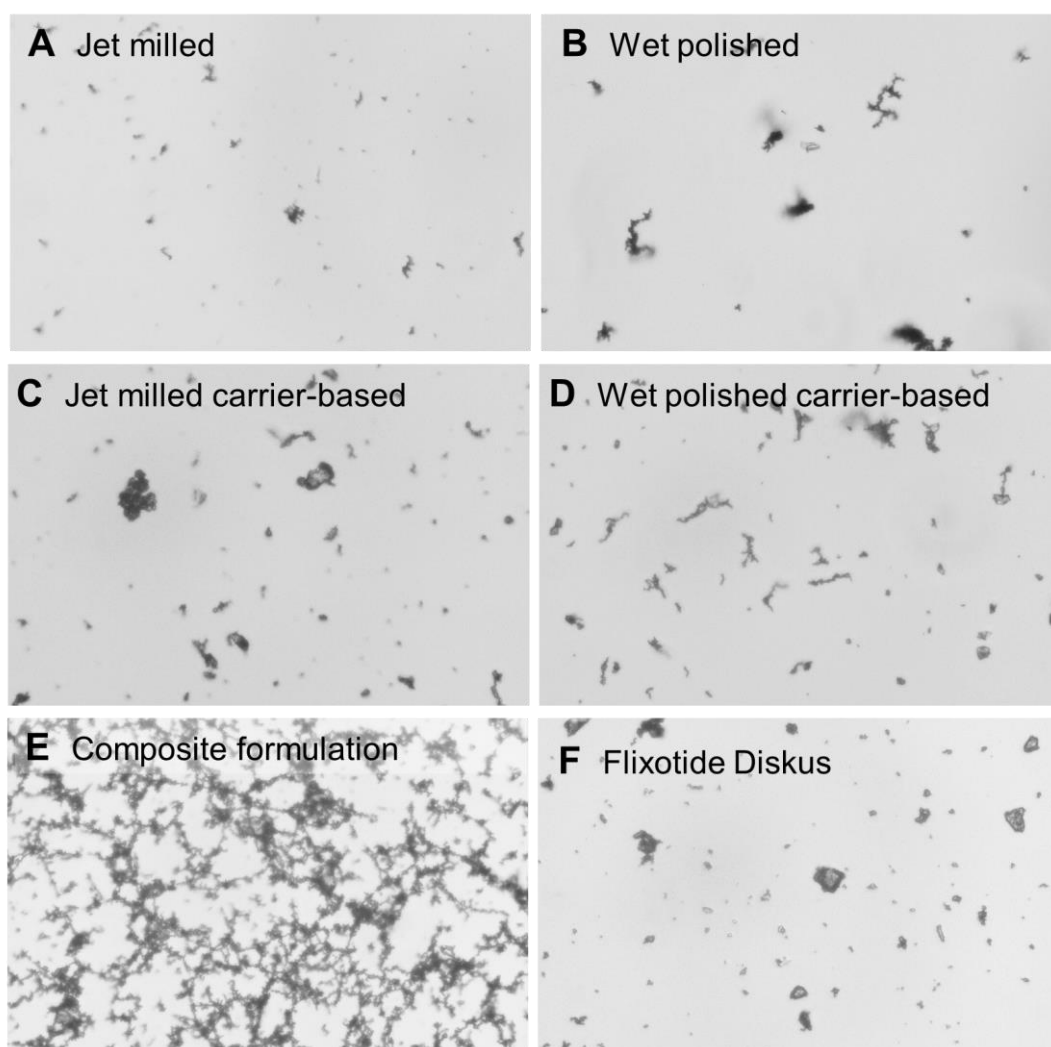


Figure 4.9 - Deposition pattern on coverslips of the jet milled fluticasone propionate (FP) particles (A) and wet polished FP particles (B); and carrier-based formulation containing jet milled FP (C), carrier-based formulation containing wet polished FP (D), and composite formulation (E) and the commercial Flixotide Diskus (F), after actuation using the Preciselnhale®, obtained by light microscopy with a x20 objective.

With this image the overall deposition pattern can be evaluated, and different deposited microstructures can be observed. The wet polished particles as well as the formulation containing those micronized particles deposited as larger filamentous structures, when compared with the jet milled micronized particles and respective carrier-based formulation. The spray-dried formulation deposited as a network of particles.

The SEM images of the deposited micronized particles after actuation using the PreciseInhale® are presented in Figure 4.10. This analysis allows for a more detailed structure evaluation. Regarding the particles obtained by jet milling and wet polishing (A and B), the images show the presence of individual filamentous agglomerates of different sizes, composed by very fine (from $<1\ \mu\text{m}$ to $3\ \mu\text{m}$) micronized particles. The individual particles are non-spherical, irregular with a crumpled surface. The images of the carrier-based deposited formulation particles (C and D) show the presence of coarse particles ($> 5\ \mu\text{m}$) with fine particles adhered to the surface. Additionally, the finer particles not adhered to the coarse lactose surface create agglomerates of micronized FP and fine lactose. A similar agglomerate structure is observed for the commercial formulation (F). Regarding the composite particles (E), the SEM images show a layer composed by a network of very fine particles (from $<1\ \mu\text{m}$ to $3\ \mu\text{m}$). Spherical particles with crumpled surface can be observed, as well as hollow particles.

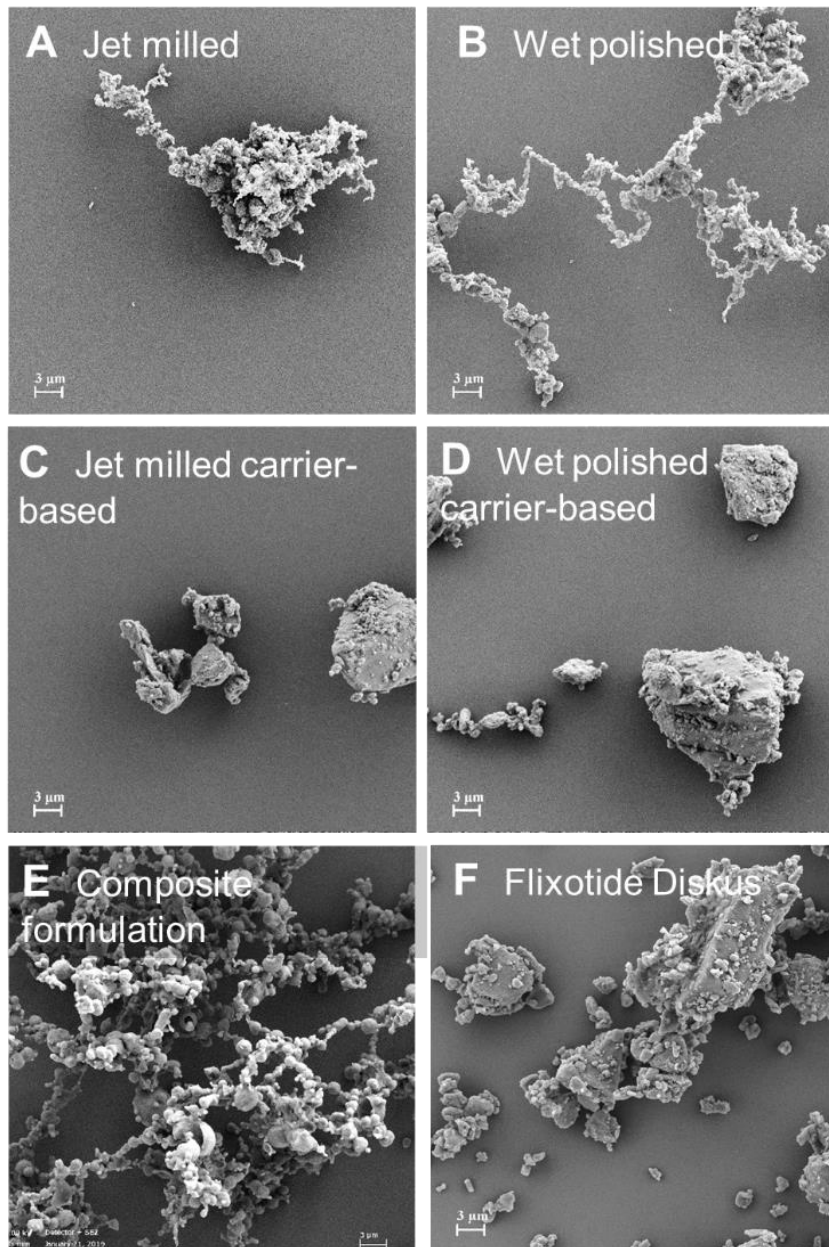


Figure 4.10 – SEM images of the of the jet milled fluticasone propionate (FP) particles (A) and wet polished FP particles (B); and carrier-based formulation containing jet milled FP (C), carrier-based formulation containing wet polished FP (D), and composite formulation (E), and the commercial Flixotide Diskus (F), after actuation using the PreciseInhale®.

4.4.3.4 Dissolution profiles

The dissolution profiles obtained with the DissolvIt® equipment for the manufactured formulations, micronized drug substance and the commercial DPI are presented in Figure 4.11. The profiles are presented as perfusate concentration normalized to the total amount of DS on the coverslips used in the dissolution test (M_{dep} presented in Table 4.6). The impact of DS deposition density on the dissolution

profile was previously studied (Malmlöf et al., 2019), indicating that the dose normalized C_{max} is inversely proportional to the deposited dose for FP in the studied range (300 to 700 ng per glass), and that a 100 ng difference in FP dose most likely does not affect the dissolution profile. Thus, the statistical significance of the deposited dose on the coverslips was considered (p-value by one-way student's t-Test) when comparing the different formulations.

The profiles of the carrier-based formulations are presented in Figure 4.11.A. It can be observed that the formulation containing jet-milled FP (FPJ blend) presents a dissolution profile similar to the commercial DPI, Flixotide Diskus, confirmed by the similarity factor, f_2 , of 99 %. Additionally, the formulation containing wet milled FP (FPW form) shows a lower C_{max} (p-value < 0.02) and a f_2 of 79 % when compared with the commercial DPI. All results were normalized to the total deposited dose of DS.

The DS alone profiles are presented in Figure 4.11.B, showing that both particle engineering technologies have a similar C_{max} (p-value > 0.05) and different from the commercial DPI (p-value < 0.02 and 0.07 for the jet milled material (FP JM) and the wet polished (FP WP), respectively), and f_2 of 71 % and 69 % FP JM and FP WP, respectively.

The composite formulation dissolution profile can be compared with the FPJ blend in Figure 4.11.C (both with similar deposited doses), showing a significantly different C_{max} (p-value < 0.02), and a f_2 of 54 %.

The t_{max} does not vary significantly for the different formulations.

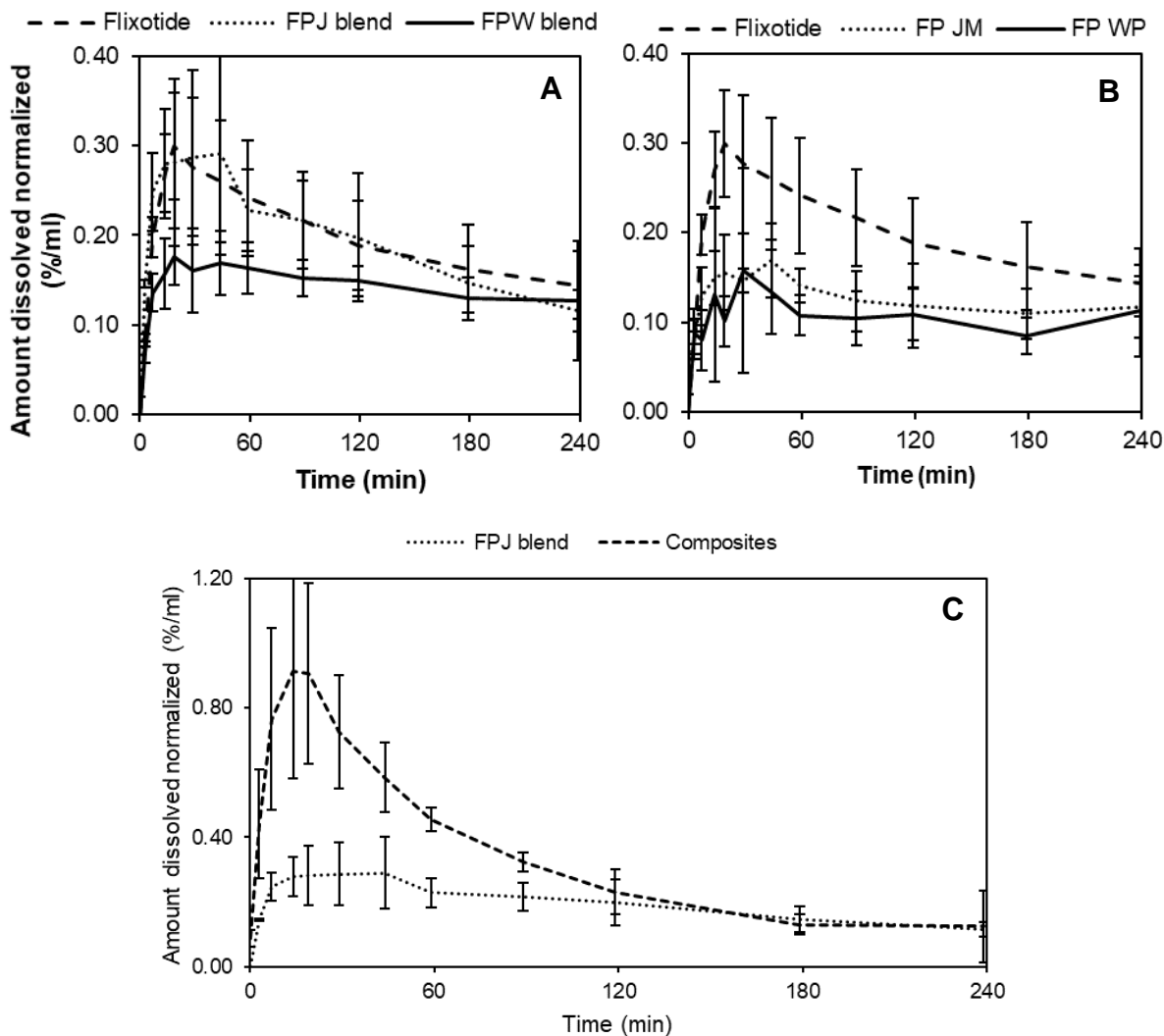


Figure 4.11 - Dissolution profiles obtained using DissolvIt® (n=3), as a fraction of total recovered (%/mL). A – comparison of the prepared carrier-based formulations with jet milled fluticasone (FPJ blend) and wet polished fluticasone (FPW blend) with the commercial carrier-based product Flixotide Diskus; B - comparison of the micronization technologies jet milling (FP JM) and wet polishing (FP WP) with the commercial Flixotide Diskus; C – Comparison of the composite formulation with the FPJ blend formulation. All results normalized to the total deposited dose. Data expressed as mean \pm SD (n=3).

For each dissolution profile the maximum concentration, C_{max} , the time of maximum concentration, t_{max} , and dissolution extent (as a percentage of the deposited dose) were determined, as well as the f_2 calculated, and are all summarized in Table 4.6. Additionally, the C_{max} and the dissolution extent are represented in Figure 4.12 for a more clear comparison. The Flixotide Diskus presents significant different C_{max} from the jet milled FP and the wet polished FP blend (0.30 ± 0.06 %/mL, 0.17 ± 0.04 %/mL and 0.18 ± 0.03 %/mL, respectively). The deposited dose for these tests is statistically similar (p -value > 0.05), therefore an impact of DS deposited density is not expected. The composite formulation also

presents a superior C_{max} (0.94 ± 0.26 , p-value < 0.02), and although the deposited dose is significantly lower, previous studies show the 3 fold increase is not explained by that difference (Malmjöf et al., 2019).

In regards to dissolution extent at 4 h (% of deposited dose), a significant difference was obtained from both milled DS (p-value < 0.02) and the composite formulation (p-value < 0.008).

Table 4.6 - The dissolution performance parameters for the fluticasone micronized by jet milling (FP JM) and wet polishing (FP WP), for the carrier-based formulations with jet milled fluticasone (FPJ blend), wet polished fluticasone (FPW blend), for the composite formulation and for the commercial Flixotide Diskusand using the DissolvIt® equipment and the deposited doses using Preciselnhale®. Data expressed as mean \pm SD (n=3). p-value by one-way student's t-Test.

| | FP JM | FP WP | FPJ blend | FPW blend | Composite | Flixotide Diskus |
|--|-----------------|-----------------|---------------------|---------------------|-----------------|------------------|
| M_{dep} (ng of FP) | 523 \pm 148 | 405 \pm 133 | 367 \pm 106 | 540 \pm 139 | 337 \pm 140 | 618 \pm 144 |
| p-value | > 0.1 | > 0.08 | > 0.07 ¹ | > 0.05 ² | | |
| C_{max} (fraction of total recovered) (%/mL) | 0.17 \pm 0.04 | 0.17 \pm 0.11 | 0.32 \pm 0.09 | 0.18 \pm 0.03 | 0.94 \pm 0.26 | 0.30 \pm 0.06 |
| t_{max} (min) | 34 \pm 17 | 31 \pm 13 | 32 \pm 21 | 27 \pm 14 | 17 \pm 3 | 19 \pm 0 |
| f_2 (%) ³ | 71 | 69 | 99 | 79 | 54 | 100 |
| Dissolution extent at 4h (% of deposited dose) | 11 \pm 1 | 10 \pm 3 | 19 \pm 5 | 14 \pm 3 | 30 \pm 1 | 19 \pm 5 |

¹ For all formulations except Flixotide Diskus

² For FP JM, FP WP and FPW blend

³ Calculated according to Equation 4, in comparison with the Flixotide Diskus dissolution curve.

C_{max} : Maximum concentration achieved by the DS during the dissolution test ; t_{max} : Time of C_{max} during the dissolution test ; f_2 : similarity factor; M_{dep} : Amount of DS deposited on the coverslip.

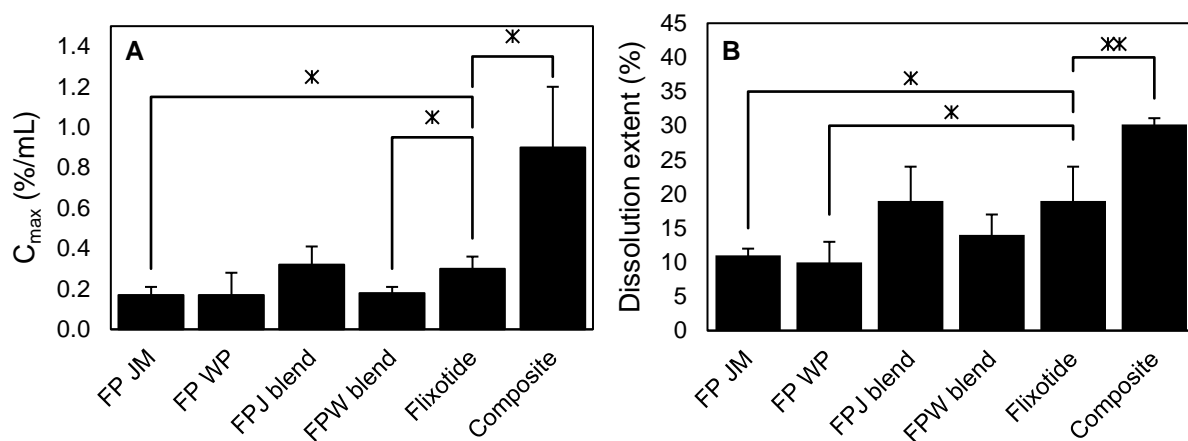


Figure 4.12 – Dissolution performance parameters. A - Maximum concentration (C_{max}) as a fraction of total recovered (%/mL) and B – Dissolution extent (% of total recovered), for each formulation compared with the commercial Flixotide Diskus (one-way student's t-Test* $p < 0.02$ and ** $p < 0.008$). Data expressed as mean \pm SD ($n=3$).

4.4.4 Discussion

In the present work, different DPI formulations containing FP are compared, including the commercial Flixotide Diskus, manufactured standard carrier-based formulations and a carrier-free spray-dried formulation with optimized aerodynamic performance. FP was selected as a model drug with low solubility and high permeability, thus a good testing candidate for discriminative dissolution and absorption studies.

With that in mind, the exercise of the present work started with a standard characterization approach in order to compare the manufactured carrier-based formulations with the commercial DPI, Flixotide Diskus, by measuring the PSD and SSA of the micronized FP prior to blending and of the composite particles manufactured by spray-drying (Table 4.4), as well as determining the aerodynamic performance of the manufactured formulations by NGI - Figure 4.7 and Table 4.5. Although the PSD of the micronized FP and of the composite particles were similar, these results showed how the final FPD determined by impactor was significantly different (Table 4.5), showcasing how the formulation strategy, such as the particle engineering technology, blending mechanism and the amount of fine lactose, has an impact on the drug product final performance, which is in accordance with the literature (Jones et al., 2010; Kaialy, 2016; Kinnunen et al., 2014). In specific, the lower SSA of the wet polished material and the higher fines content of the formulation can lead to lower coarse lactose adhesion and higher fines interaction (as observed in the SEM images), resulting in a higher fine particle fraction. When comparing with the literature data for the Flixotide Diskus (FPD of 40 ± 3 to 53 ± 2 $\mu\text{g}/\text{act}$ for 38.3 to 60 L/min flow rate), the manufactured carrier-based formulations over- and underperform the commercial DPI (for the wet polished and the jet milled formulations, respectively), which is due not only to differences in the formulation, but also in the used device, which has a significant impact on the formulation performance (Islam and Gladki, 2008). However, the commercial product was more similar to the formulation prepared with jet milled DS (FPD of 36 ± 1 $\mu\text{g}/\text{act}$ for 40 L/min) than the one prepared with the wet polished DS (FPD of 60 ± 7 $\mu\text{g}/\text{act}$ for 40 L/min). The carrier-free spray-dried formulation comprises particles previously designed (Moura et al., 2015) in order to achieve an optimized aerodynamic performance for pulmonary delivery (particles coated with L-leucine as a force control agent, optimizing powder dispersion upon actuation, and a controlled particles size within the inhalation range), resulting in a much higher FPD when compared with the carrier-based formulations. Although the considered formulations present differences regarding aerodynamic performance, expected considering the

formulation strategies, in the present work the impact of the formulation on the dissolution and absorption wants to be understood, independently to the aerodynamic performance. Therefore, to evaluate the dissolution and absorption profile the dose collected is normalized when collecting the formulations and micronized particles.

Aside from the standard aerodynamic characterization, the generated and deposited microstructures were evaluated after actuation and collection with the PreciseInhale[®] breath simulator, followed by a dissolution/absorption assessment with the biorelevant dissolution apparatus DissolvIt[®], as previously described. The non-formulated milled FP obtained by two particle engineering technologies with a similar PSD were also aerosolized using the PreciseInhale[®] DustGun aerosol generator in order to be similarly analyzed and better understand the formulation impact on deposition and dissolution/absorption. At this stage, the analysis was targeted to the aerosol after expansion and slow deposition, excluding the coarse fraction for the aerosol (retained in the IP and PS).

The qualitative analysis of the deposited aerosol (light microscope images of the deposited patterns (Figure 4.9) and SEM micrographs of the deposited agglomerates structure (Figure 4.10)) showed differences in deposition. An impact of the particle engineering technology was observed – larger filamentous agglomerates are generated for the wet polished material during powder expansion and deposition when compared with the jet milled material. Considering the morphology and particle size of the collected particles appears similar, the size of the agglomerates can be related with the surface area of the particles. These observations are in accordance with the literature data on cohesive forces of the jet milled and wet polished FP particles - the WP FP has stronger cohesion forces than the JM FP (Moura et al., 2016), which may lead to larger agglomerates formed during the expansion and deposition. Additionally the SSA results are not correlated with the PSD, which has been previously observed as well (Moura et al., 2016), further indicating an impact of the particle engineering technology on the particle surface. Overall, these results illustrate the impact of the particle engineering technology on the DS particle morphology, surface area and agglomerate structure, which will ultimately have an impact on the final drug product performance. Although previous experimental data indicated the particle engineering has an impact of particle surface, the present results show how that surface variations have an impact not only in the interactions previous and during powder actuation, but also on the size and shape of the resulting agglomerates following powder aerosolization – not previously observed. In

specific, the DS alone results are relevant on the development of high dose DPIs in which the DS particle interaction is especially relevant.

The carrier-based formulations showed the presence of individual particles, fine particle agglomerates and lactose-DS agglomerates (qualitatively identified by the particle size of the lactose), with DS adhered to the carrier surface. This indicates the actuation energy was not capable of breaking all the adhesion forces between DS to the lactose carrier generated during the mixing, more significantly for the formulation containing jet milled DS (Figure 4.9.C). These observations are in accordance with the impactor FPF results (lower FPF for the jet milled formulation) indicating a qualitative analysis after aerosolization can be relevant for impactor results understanding, which are still a “black box” with no clear single mechanisms underlying the performance obtained (Jones and Price, 2006; Kaialy, 2016; Shalash and Elsayed, 2017). Variations on deposition among formulations are also observed, with larger filamentous particles being generated for the carrier-based formulation containing the wet polished material. This may be related with the already described DS behavior or to the lactose fines being in a higher amount (10 % of Inhalac 400) in this formulation. For the commercial product Flixotide Diskus filamentous agglomerates could not be observed – they deposit as globular agglomerates. When comparing the deposition patterns, the formulation containing jet milled FP appears more similar to the commercial DPI. Interestingly enough, these results are aligned with the aerodynamic performance results ($FPF_{label\ claim}$ of Flixotide Diskus similar to the blend containing jet milled DS). However, more data would be necessary to confirm the observed relationship.

Following the qualitative analysis, the quantitative analysis of the aerosol in the coating chamber considers the APSD results obtained using the MCI with low flow rate (Figure 4.8). When comparing the commercial DPI to the carrier-based formulations - Figure 4.8.A – the manufactured formulations (MMAD of $4.5\pm 0.1\ \mu\text{m}$ and $4.5\pm 0.1\ \mu\text{m}$, for the jet milled FP blend and the wet polished FP blend, respectively) had a larger aerodynamic particle size ($p\text{-value} < 0.03$) than the commercial DPI (MMAD of $4.2\pm 0.1\ \mu\text{m}$), being this difference more significant for the WP blend. When compared to the NGI results, a significant increase of the measured MMAD was obtained for the manufactured formulations while the value for the commercial DPI was not greatly affected. These results are in accordance with the previously described qualitative results, as the manufactured formulations appear to generate filamentous structures prior to deposition, increasing the overall aerodynamic particle size of the aerosol

collected at low flow-rates, while the commercial formulation does not - the agglomerates responsible for aerodynamic particle size increase are globular and present previous to aerosol expansion.

The results of the micronized DS confirm this statement, as the wet polished FP has had a significantly larger (p-value = 0.03) aerodynamic particle size (MMAD of $4.7 \pm 0.2 \mu\text{m}$) than the jet milled FP (MMAD of $4.1 \pm 0.3 \mu\text{m}$), for particles with a similar PSD and morphology, indicating that the quantified difference is related with the observed larger agglomerates generated for the WP FP. Lastly, the composite formulation Figure 4.8.C) displays a profile with a bimodal distribution – one population centered on the 3.5 to 6.0 μm range, similarly to the remaining populations, and an additional one with a APSD larger than 14.8 μm – as well as smaller particle sizes (APSD < 1.55 μm) also being quantified. These results can be explained on the one hand by the high powder density on the coating chamber (detected on the glass microscopic analysis (Figure 4.9, Figure 4.10)) promoting the collection of large agglomerates on the first MCI stages; and on the other hand the engineered particles with optimized aerodynamic performance are able to reach the deeper stages. Overall, the MCI results indicate this is a good quantitative method to characterize and compare the aerosol fraction expanded in the collecting chamber and collected on the coverslips, capable of detecting structures generated during the coating experiments. In combination, the qualitative and quantitative analysis of the particles actuated and collected using the PreciseInhale[®] system allow for a more in depth characterization of DPI formulations following actuation, leading to a better understanding of the impact of formulation on powder dispersion and generated agglomerates.

The collected and characterized aerosols were assessed for dissolution and absorption with the Dissolv//[®] equipment. The dissolution results of the DS alone tests (Figure 4.11.B) showed that although the particle engineering technology had an impact on the morphology of the collected structures, those do not appear to affect the dissolution rate. According to the Noyes-Whitney equation (Wauthoz and Amighi, 2015), the dissolution in mucus is governed by the surface area of the drug solid in contact with the dissolution medium, by the diffusion coefficient of the DS in the medium (determined by the Stokes–Einstein equation, which does not change for the two tests) and by the saturation solubility. Thus, based on the Noyes-Whitney equation, it can be observed that the surface area variations caused by the different size agglomerates was not significantly enough to affect the FP dissolution rate on the mucus for the powders with only DS.

When compared to the commercial DPI, both micronized DS had a slower dissolution rate which can be observed in an overall inferior amount dissolved per mL (Figure 4.11.B), and quantified by the lower dissolution extent (p-value < 0.02 for both) and lower C_{max} (p-value <0.02 for the jet milled material), summarized in Table 4.6 and compared in Figure 4.12.B. Additionally, DS alone particles present an overall slower dissolution than the formulated powders with lactose (although not statistically significant for formulation with wet polished FP, the average values are lower). This indicates that the presence of lactose may have an impact on the dissolution performance in the used set-up. Considering again the Noyes-Whitney equation, the presence of lactose would have an impact on the diffusion coefficient by affecting the mucus simulant viscosity – diffusion coefficient is inversely proportional to medium viscosity. Additionally, the presence of lactose in the agglomerates (in substitution to the drug substance particles) decreases the local concentration of FP, leading to faster dissolution (dependence of difference between local concentration and saturation). Thus, for low solubility DS, the deposition on the lung surface in the presence of absence of a fast-dissolving excipient such as lactose may have a significant impact on the DS dissolution rate. Knowing this, the previously discussed analysis on the deposited powder (qualitative and quantitative) is not only relevant to understand aerosol performance, but also on DS dissolution.

Figure 4.11.A shows a comparison of the two carrier-based formulations with the commercial DPI – it indicates that formulation manufactured with the jet milled material had a dissolution- and absorption profile similar to the commercial DPI, while the formulation manufactured using the wet polished DS had a significantly different profile as it shows to have a faster dissolution (p-value<0.02 for C_{max}). These results may be an indication of the impact of the microstructure of the deposited agglomerates for the two formulations, observed in Figure 4.9, as it has been previously described using a morphology directed Raman spectroscopy approach (Farias et al., 2017) that the presence of different amounts of other components of the formulation in the generated microstructure impact the dissolution kinetics of FP. Here, the globular lactose agglomerates are not observed on the optic microscope analysis for the formulation containing wet polished DS (Figure 4.9.D), indicating they are less present for this formulation, and its absence can be hindering the DS dissolution rate (as previously theorized). Overall, the results indicate that for carrier-based FP formulations, the fine-tuning of the formulation should not only consider the APSD but also the impact of the selected strategy (blending technology, type and amount of fines) on the generated structures during aerosolization and their impact on dissolution kinetics.

Lastly, the formulation of composite particles showed completely different behavior regarding the deposited particles (particle density and agglomerate structure) - Figure 4.9.E and Figure 4.10.E. The particles are spherical and slightly wrinkled, comprising 1 % of DS, trehalose and L-leucine. The particle density increase for the composite particles is expected as 99 % of the deposited material was excipient, while in the carrier-based formulations most of the coarse excipient was retained by the IP and the PS, and, thus, did not reach the coverslips. The dissolution profile for this formulation, presented in Figure 4.11.C, showed a 3 to 4 times faster dissolution and absorption of the FP, when compared with all the other tests, and specifically with the commercial DPI (p-value < 0.02 for C_{max} and p-value < 0.008 for dissolution extent). Previous work (Fernandes et al., 2015) showed that for this formulation the L-leucine is in the crystalline state and the trehalose is in the amorphous state, while the solid state of the FP could not be determined due to the low DS percentage on the formulation, therefore it is not clear if the dissolution kinetic is influenced by the solid state of the DS. On the other hand, the drug substance is expected to be uniformly dispersed in the spray-dried powder, thus ensuring a uniform distribution on the mucus surface and minimizing high concentration spots. Additionally, as previously discussed, the presence of high amounts of excipient can also have an impact on the medium viscosity, and therefore on the dissolution. Nevertheless, these results show how a carrier-free formulation strategy containing trehalose and L-leucine can be used not only for aerodynamic performance optimization, but also for solubility enhancement for inhalation formulations of low solubility DS.

4.4.5 Conclusion

The impact of the particle engineering technology on the micronized particle surface assessed by the SSA proved to generate deposited agglomerate structures with different sizes and morphologies, upon actuation and collection with the PreciseInhale® breath simulator. For the non-formulated micronized particles, the differences observed did not have an impact on the dissolution and absorption profile of a poorly soluble drug substance, indicating particle engineering can be applied to optimize aerodynamic performance of high dosage formulations (low to no excipient present) of poorly soluble drugs without a negative impact on bioavailability.

For the carrier-based formulations, the higher SSA of the jet milled particles led to a stronger adhesion to the coarse carrier particles, observed by microscope, resulting in poorer aerodynamic performance but significantly faster dissolution due to the presence of lactose on the agglomerates, when compared

with wet polished particles. For the commercial Flixotide Diskus, a similar correlation was found. Lastly, a composite formulation containing trehalose and L-leucine was compared with the carrier-based approach, showing a significant solubility enhancement. In conclusion, to both optimize an innovator DPI and de-risk generics development of poorly soluble drugs, particle engineering and lactose addition should be considered not only on aerodynamic performance, but also on deposition and dissolution, in order to find the right balance, applying a strategy including deposition, absorption and dissolution assessment.

4.5 REFERENCES

- Agu, R.U., Ugwoke, M.I., Armand, M., Kinget, R., Verbeke, N., 2001. The lung as a route for systemic delivery of therapeutic proteins and peptides. *Respir. Res.* 2, 198–209. <https://doi.org/10.1186/rr58>
- Arora, D., Shah, K.A., Halquist, M.S., Sakagami, M., 2010. In Vitro aqueous fluid-capacity-limited dissolution testing of respirable aerosol drug particles generated from inhaler products. *Pharm. Res.* 27, 786–795. <https://doi.org/10.1007/s11095-010-0070-5>
- Bosselmann, S., Williams, R.O.I., 2012. Route-Specific Challenges in the Delivery of Poorly Water-Soluble Drugs, in: Williams, R.O.I., Watts, A.B., Miller, D.A. (Eds.), *Formulating Poorly Water Soluble Drugs*. Springer Science+Business Media, New York, pp. 1–28. <https://doi.org/10.1007/978-1-4614-1144-4>
- Chen, M., Romay, F.J., Marple, V.A., 2018. Design and evaluation of a low flow personal cascade impactor. *Aerosol Sci. Technol.* 52, 192–197. <https://doi.org/10.1080/02786826.2017.1388498>
- Chow, A.H.L., Tong, H.H.Y., Chattopadhyay, P., Shekunov, B.Y., 2007. Particle engineering for pulmonary drug delivery. *Pharm. Res.* 24, 411–437. <https://doi.org/10.1007/s11095-006-9174-3>
- de Boer, A.H., Hagedoorn, P., Hoppentocht, M., Buttini, F., Grasmeyer, F., Frijlink, H.W., 2017. Dry powder inhalation: past, present and future. *Expert Opin. Drug Deliv.* 14, 499–512. <https://doi.org/10.1080/17425247.2016.1224846>
- Farias, G., Ganley, W., Deddie, H.-J., Kippax, P., Shur, J., Price, R., 2017. Investigating the microstructure of dry powder inhalers using orthogonal analytical approaches, in: *Drug Delivery to the Lungs*. The Aerosol Society, Edinburg, UK, pp. 262–265.
- Fernandes, B., Maia, F., Paiva, A., Corvo, M., Costa, E., 2016. Paddle over disk as a dissolution test for orally inhaled drugs: discriminating composite from carrier-based formulations., in: *Drug Delivery to the Lungs*. The Aerosol Society, Bristol, UK, pp. 308–312.
- Fernandes, D.A., Moura, C., Campos, S., Costa, E., Neves, F., 2015. Impact of the API Concentration on the Solid State Properties and Aerodynamic Performance of Composite Particles for DPIs., in: Dalby, R., Byron, P., Peart, J., Suman, J., Young, P., Traini, D. (Eds.), *Respiratory Drug Delivery*. DHI Publishing, Nice, pp. 165–176.
- Gerde, P., 2013. Exposure system. US8555873 B2.
- Gerde, P., Malmlöf, M., Havsborn, L., Sjöberg, C.-O., Ewing, P., Eirefelt, S., Ekelund, K., 2017a. DissolvIt: An In Vitro Method for Simulating the Dissolution and Absorption of Inhaled Dry Powder Drugs in the Lungs. *Assay Drug Dev. Technol.* 15, 77–88. <https://doi.org/10.1089/adt.2017.779>
- Hill, L.S., Slater, A.L., 1998. A comparison of the performance of two modern multidose dry powder asthma inhalers. *Respir. Med.* 92, 105–110. [https://doi.org/10.1016/S0954-6111\(98\)90040-3](https://doi.org/10.1016/S0954-6111(98)90040-3)
- Hochhaus, G., Chen, M.J., Kurumaddali, A., Schilling, U., Jiao, Y., Drescher, S.K., Amini, E., Kandala, B., Tabulov, C., Shao, J., Seay, B., Abu-Hasan, M.N., Baumstein, S.M., Winner, L., Shur, J., Price, R., Hindle, M., Wei, X., Carrasco, C., Sandell, D., Oguntimein, O., Kinjo, M., Delvadia, R., Saluja, B., Lee, S.L., Conti, D.S., Bulitta, J.B., 2021. Can Pharmacokinetic Studies Assess the Pulmonary Fate of Dry Powder Inhaler Formulations of Fluticasone Propionate? *AAPS J.* 23, 1–14. <https://doi.org/10.1208/s12248-021-00569-x>
- Islam, N., Gladki, E., 2008. Dry powder inhalers (DPIs)—A review of device reliability and innovation.

- Int. J. Pharm. 360, 1–11. <https://doi.org/10.1016/j.ijpharm.2008.04.044>
- Jennings, B.H., Andersson, K.-E., Johansson, S., 1991. Assessment of systemic effects of inhaled glucocorticosteroids: comparison of the effects of inhaled budesonide and oral prednisolone on adrenal function and markers of bone turnover. *Eur. J. Clin. Pharmacol.* 40, 77–82. <https://doi.org/10.1007/BF00315143>
- Jones, M.D., Price, R., 2006. The influence of fine excipient particles on the performance of carrier-based dry powder inhalation formulations. *Pharm. Res.* 23, 1665–1674. <https://doi.org/10.1007/s11095-006-9012-7>
- Jones, M.D., Santo, J.G.F., Yakub, B., Dennison, M., Master, H., Buckton, G., 2010. The relationship between drug concentration, mixing time, blending order and ternary dry powder inhalation performance. *Int. J. Pharm.* 391, 137–147. <https://doi.org/10.1016/j.ijpharm.2010.02.031>
- Kaijaly, W., 2016. On the effects of blending, physicochemical properties, and their interactions on the performance of carrier-based dry powders for inhalation ??? A review. *Adv. Colloid Interface Sci.* 235, 70–89. <https://doi.org/10.1016/j.cis.2016.05.014>
- Kinnunen, H., Hebbink, G., Peters, H., Shur, J., Price, R., 2014. An Investigation into the Effect of Fine Lactose Particles on the Fluidization Behaviour and Aerosolization Performance of Carrier-Based Dry Powder Inhaler Formulations 15, 898–909. <https://doi.org/10.1208/s12249-014-0119-6>
- Lipworth, B.J., 1999. Systemic Adverse Effects of Inhaled Corticosteroid Therapy. *Arch. Intern. Med.* 159, 941. <https://doi.org/10.1001/archinte.159.9.941>
- Malmlöf, M., Nowenwik, M., Meelich, K., Rådberg, I., Selg, E., Burns, J., Mascher, H., Gerde, P., 2019. Effect of particle deposition density of dry powders on the results produced by an in vitro test system simulating dissolution- and absorption rates in the lungs. *Eur. J. Pharm. Biopharm.* 139, 213–223. <https://doi.org/10.1016/j.ejpb.2019.03.005>
- May, S., Jensen, B., Wolkenhauer, M., Schneider, M., Lehr, C.M., 2012. Dissolution Techniques for In Vitro Testing of Dry Powders for Inhalation. *Pharm. Res.* 29, 2157–2166. <https://doi.org/10.1007/s11095-012-0744-2>
- Mehta, P., 2016. Dry Powder Inhalers: A Focus on Advancements in Novel Drug Delivery Systems. *J. Drug Deliv.* 2016, 1–17. <https://doi.org/10.1155/2016/8290963>
- Mohan, M., Lee, S., Guo, C., Peri, S.P., Doub, W.H., 2017. Evaluation of Abbreviated Impactor Measurements (AIM) and Efficient Data Analysis (EDA) for Dry Powder Inhalers (DPIs) Against the Full-Resolution Next Generation Impactor (NGI). *AAPS PharmSciTech* 18, 1585–1594. <https://doi.org/10.1208/s12249-016-0625-9>
- Moura, C., Neves, F., Costa, E., 2016. Impact of jet-milling and wet-polishing size reduction technologies on inhalation API particle properties. *Powder Technol.* 298, 90–98. <https://doi.org/10.1016/j.powtec.2016.05.008>
- Moura, C., Neves, F., Costa, E., 2015. Optimized Composite Particles for API-independent Formulations with Enhanced Performance, in: Dalby, R., Byron, P., Peart, J., Suman, J., Young, P., Traini, D. (Eds.), *Respiratory Drug Delivery*. DHI Publishing, River Grove, IL, USA, pp. 165–176.
- Newman, S., Peart, J., 2009. Dry Powder Inhalers, in: Newman, S. (Ed.), *Respiratory Drug Delivery: Essential Theory and Practice*. Respiratory Drug Delivery Online, R, pp. 257–307.
- Noriega, B., Malmlöf, M., Corvo, M.L., Gerde, P., Costa, E., 2018. Collecting the Biorelevant Aerosol

- Fraction for Dissolution Testing of Orally Inhaled Drugs: Adding a Newly Designed Pre-separator to PreciseInhale®, in: Respiratory Drug Delivery. Tucson, Arizona.
- Noriega, B., Malmjöf, M., Costa, E., Corvo, M.L., Gerde, P., Maia, F.M., 2017. Dissolution of Orally Inhaled Drugs using DissolvIt®: Influence of a Newly Designed Pre-Separator for Particle Collection, in: Drug Delivery to the Lungs 28. Aerosol Society, Bristol, UK, p. 190.
- Noriega, B., Malmjöf, M., Nowenwik, M., Gerde, P., Corvo, M.L., Costa, E., 2019. Biorelevant dissolution to differentiate formulation performance for inhalation, in: Drug Delivery to the Lungs. The Aerosol Society, Edinburg, UK, pp. 303–306.
- Preparations for inhalation: aerodynamic assessment of fine particles., 2014. , in: European Pharmacopoeia. European Directorate for the Quality of Medicines, Council of Europe, Strasbourg, France, pp. 309–320.
- Price, R., Shur, J., Ganley, W., Farias, G., Fotaki, N., Conti, D.S., Delvadia, R., Absar, M., Saluja, B., Lee, S., 2020. Development of an Aerosol Dose Collection Apparatus for In Vitro Dissolution Measurements of Orally Inhaled Drug Products. *AAPS J.* 22, 1–9. <https://doi.org/10.1208/s12248-020-0422-y>
- Radivojev, S., Zellnitz, S., Paudel, A., Fröhlich, E., 2019. Searching for physiologically relevant in vitro dissolution techniques for orally inhaled drugs. *Int. J. Pharm.* 556, 45–56. <https://doi.org/10.1016/j.ijpharm.2018.11.072>
- Rahimpour, Y., Hamishehkar, H., 2012. Lactose engineering for better performance in dry powder inhalers. *Adv. Pharm. Bull.* 2, 183–187. <https://doi.org/10.5681/apb.2012.028>
- Riley, T., Christopher, D., Arp, J., Casazza, A., Colombani, A., Cooper, A., Dey, M., Maas, J., Mitchell, J., Reiners, M., Sigari, N., Tougas, T., Lyapustina, S., 2012. Challenges with Developing In Vitro Dissolution Tests for Orally Inhaled Products (OIPs). *AAPS PharmSciTech* 13, 978–989. <https://doi.org/10.1208/s12249-012-9822-3>
- Rohrschneider, M., Bhagwat, S., Krampe, R., Michler, V., Breitreutz, J., Hochhaus, G., 2015. Evaluation of the Transwell System for Characterization of Dissolution Behavior of Inhalation Drugs: Effects of Membrane and Surfactant. *Mol. Pharm.* 12, 2618–2624. <https://doi.org/10.1021/acs.molpharmaceut.5b00221>
- Selg, E., Radivojev, S., Hassoun, M., Bansal, S., Scheibelhofer, O., Forbes, B., Paudel, A., Malmjöf, M., Nowenwik, M., Kumar, A., Gerde, P., Arora, S., 2019. Use of PBPK modelling to evaluate the performance of DissolvIt, a biorelevant dissolution assay for orally inhaled drug products. *Mol. Pharm.* <https://doi.org/10.1021/acs.molpharmaceut.8b01200>
- Shah, V.P., Tsong, Y., Sathe, P., Williams, R.L., 1999. Dissolution profile comparison using similarity factor, f2. *Dissolution Technol.* <https://doi.org/10.14227/DT060399P15>
- Shalash, A.O., Elsayed, M.M.A., 2017. A New Role of Fine Excipient Materials in Carrier-Based Dry Powder Inhalation Mixtures: Effect on Deagglomeration of Drug Particles During Mixing Revealed. *AAPS PharmSciTech* 18, 2862–2870. <https://doi.org/10.1208/s12249-017-0767-4>
- Son, Y.J., Horng, M., Copley, M., McConville, J.T., 2010. Optimization of an in vitro dissolution test method for inhalation formulations. *Dissolution Technol.* 17, 6–13. <https://doi.org/10.14227/DT170210P6>
- Taki, M., Ahmed, S., Marriott, C., Zeng, X.M., Martin, G.P., 2011. The “stage-by-stage” deposition of

- drugs from commercial single-active and combination dry powder inhaler formulations. *Eur. J. Pharm. Sci.* 43, 225–235. <https://doi.org/10.1016/j.ejps.2011.04.014>
- United States Pharmacopoeia XXXV, 2012. Rockville, MD, USA. Aerosols, Nasal Sprays, Metered-dose Inhalers and Dry Powder Inhalers (601).
- Verma, R., Ibrahim, M., Garcia-Contreras, L., 2015. Lung anatomy and physiology and their implications for pulmonary drug delivery, in: Nokhodchi, A., Martin, G.P. (Eds.), *Pulmonary Drug Delivery: Advances and Challenges Advances in Pharmaceutical Technology*. John Wiley & Sons, Ltd, pp. 1–17.
- Wauthoz, N., Amighi, K., 2015. Formulation strategies for pulmonary delivery of poorly soluble drugs, in: Nokhodchi, A., Martin, G.P. (Eds.), *Pulmonary Drug Delivery Advances and Challenges*. John Wiley & Sons, Ltd, Chichester, pp. 87–122.

Chapter 5

Dissolution method comparison and validation with
salmeterol xinafoate



5.1 SUMMARY

As frequently pointed out throughout the present thesis, there is not a performance characterization test for orally inhaled drugs aside from the cascade impaction assessment, which is limited to aerosolization performance – quantification of the amount of drug substance (DS) capable to reach the lung. In the present chapter two previously tested strategies for collection and dissolution assessment, the paddle over disk (POD) combined with a cascade impactor for particle collection, and the DissolvIt® system coupled with the PreciseInhale® equipment will be validated by testing a second model drug substance with a higher water solubility than fluticasone propionate (FP), salmeterol xinafoate (SX). Both systems were previously successfully applied to differentiate DPI formulations of FP, more significantly with the DissolvIt® system.

Firstly, the manufactured formulations were characterized by standard methodologies – the micronized particles were assessed for geometric particle size distribution and the manufactured formulations for aerodynamic particle size distribution (APSD). For the POD system, the dose collection strategy repeatability was confirmed and the independence of the dissolution rate to the dose collected was proven. Moreover, the effect of dissolved finer particles collected using the next generation impactor (NGI) versus the total fine particle fraction collected using the fast screening impactor (FSI) was observed when obtaining faster dissolution profiles.

For the DissolvIt® system, the impact of the particle engineering technology on the generated and deposited microstructures was confirmed by microscopy and Marple cascade impactor for the DS with higher solubility tested and correlated with cohesion and adhesion forces available in the literature. In regard to dissolution and absorption assessment, dissolution rate acceleration by the presence of lactose was confirmed, validating dissolution testing as an essential tool to both optimize an innovator DPI and de-risk generics development. Furthermore, these dissolution results can then provide input parameters for physiologically based pharmacokinetic (PBPK) modelling of the tested drug substances, towards establishing *in vitro* / *in vivo* predictive performance correlations.

5.2 INTRODUCTION

Throughout the present thesis several dissolution strategies were applied for the dissolution assessment of a very low solubility corticosteroid largely used as an inhalation product, fluticasone propionate (FP). FP was selected as a model drug not only for being a well-studied molecule largely used for inhalation studies, but also due to its low solubility which is expected to determine the dissolution kinetics and thus its therapeutic efficacy. Although solubility is regarded as a critical parameter in determining drug bioavailability (Tambosi et al., 2018), academia and industry are currently working on the design of an inhalation biopharmaceutical classification system (iBCS) which besides from the standard solubility and permeation considered for oral delivery, will also contemplate parameters such as the regional surface area, local activity (affected by the formulation and used device) and physicochemical properties of the drug product (Gallegos-Catalán et al., 2021; Hastedt et al., 2016). Bearing in mind the relevance of more than solubility and permeability in a drug substance dissolution kinetics, it becomes clear a collection and dissolution/absorption testing strategy for inhalation should be capable of characterizing and differentiate drug products in a range of values of solubility/permeability. Hence, in the present chapter two of the previously presented collection and dissolution/absorption systems will be validated by testing with a high solubility drug substance.

The paddle over disk (POD) apparatus consists of a vessel containing stirring medium and a disk containing an aerosol sample covered by a membrane. Its principal advantage is the use of the standard USP apparatus II, with the possibility of conjugating it with various aerosol collection strategies, such as impactor, impingers, or adaptations thereof, which are standardized methods for aerosol performance assessment. The main disadvantage of this strategy is the selection or development of a suitable aerosol collection set-up – it should be reproducible, allow for a simple sample transfer from the collection to the dissolution system, applicable to different formulations and DS, and finally it should ensure the particle deposition pattern on the collection surface does not have an impact on the dissolution dynamics. A more in-depth analysis of the system and proposed collection strategies are presented in the previous Chapters 2 (section 2.2.4) and 3. In short, the use of the NGI as a collection strategy resulted significant limitations regarding the impact of collected dose on the dissolution dynamics for a low solubility DS, FP, thus the FSI was successfully applied. Comparing with the literature and the commercially available options, the use of the FSI as a sample collection strategy bring the great benefit of using an already available and tested impactor equipment without the need for additional equipment design. The next

step on the method development is to test the FSI and POD strategy with a second drug substance with different characteristics (higher solubility) to validate the observed results.

The DissolvIt® dissolution equipment combined with the PreciseInhale® breath simulator as a collection system consists of diffusion system cell aiming to achieve a more biorelevant collection, dissolution, diffusion, and absorption. Using a breath simulator as a collection method has the advantage of ensuring particle interaction and agglomeration during collection, meaning the obtained dissolution profile accounts for a biorelevant particle deposition and interaction - the slow deposition allows the formation of powder microstructures which may have a significant influence in the dissolution behavior, as discussed in the previous Chapter 4. The DissolvIt® simulates dissolution, diffusion through mucus simulatant and diffusion through membrane to a blood simulatant, with flow tangential to the powder particles, as it is the case for blood vessels in the alveoli (Gerde et al., 2017a). The combined system has been studied in the literature (Gerde et al., 2017a; Hassoun et al., 2019; Malmlöf et al., 2019; Noriega-Fernandes et al., 2021; Noriega et al., 2017) and in the Chapter 4 of the present thesis, proving to be one of the stronger approximations to the *in vivo* environment. The capability to differentiate between different DPI formulations of a low solubility DS, FP, has been proven, but to ensure the range of applicability, a validation study is still required by evaluation different formulations of a high solubility DS.

Salmeterol is a LABA (long-acting β 2-agonists) classified as BCS class III, meaning its absorption to the blood stream may be limited by permeation and not dissolution. Nonetheless, salmeterol is a classical inhalation DS with a significant amount of available literature on inhalation delivery. For that reason, it was selected as the high solubility drug molecule, in comparison to the previously tested FP - 2.3 $\mu\text{g}/\text{mL}$ or water for SX (Wishart et al., 2022) in contrast with a solubility of 0.1 $\mu\text{g}/\text{mL}$ of water for FP (Tokumura et al., 2014). Salmeterol was prepared for inhalation delivery by micronization using two particle engineering technologies, jet milling (JM) and wet polishing (JM) and formulated with a carrier-based approach with lactose monohydrate as an excipient. Using salmeterol, the present chapter aims answer two main questions:

1. Are the developed collection and dissolution/absorption methods (Chapter 3 and Chapter 4) suitable for a high solubility DS, and are they capable to differentiate between formulations?
2. Should any differences in the methodology be considered for the high solubility drug substances?

5.3 MATERIALS AND METHODS

5.3.1 Materials

Crystalline salmeterol xinafoate (SX; C₃₆H₄₅NO₇; Mw = 603.7) micronized by jet milling (JM) and wet polishing (WP) was supplied by Hovione S.A. (Portugal). Lactose micronized powders Lactohale 230 and Respitose were purchased from DFE Pharma (Germany). Transparent capsules size 3 Vcaps were purchased from Capsugel (France). Polyethylene oxide (MW 5 000 000) and L-alpha phosphatidyl choline were purchased from Merck KGaA (Germany). Bovine serum albumin (BSA) was purchased from Chem Cruz Biochemicals (USA). Microscope coverslips of 13 mm diameter (No. 2) were purchased from MenzelGläser, Histolab (Germany). Glass fibre filters grade A of 76 mm used for the fast screening impactor was purchased from GE Healthcare Life Sciences (USA). Glass fibre filters grade A used for the Marple-8 stage cascade impactor (MCI) was purchased from GE Healthcare Life Sciences (USA) and manually cut to fit the impactor stages. Sodium dodecyl sulfate and phosphate buffer saline tablets were purchased from Sigma-Aldrich (USA). Polycarbonate membranes with a 76 mm diameter and 0.05 µm pore size were purchased from Whatman (USA). All other reagents were of analytical grade.

5.3.2 Formulation manufacture

Homogeneous mixtures of 150 g of coarse and fine lactose with 0.5% (w/w) of micronized SX as a ternary mixture were prepared in a high shear mixer from Diosna model P1-6 (Germany) following geometric dilution in a 0.5 L bowl. Content of fine excipient in the prepared blends is describes in Table 5.1. The mixtures were filled in size 3 capsules using a Quantos unit from Mettler Toledo AG (Spain) with a target fill weight of 20 mg, with acceptance limits of +/- 0.5 mg.

Table 5.1 - Summary of the manufactured carrier-based formulations. SXJ blend – carrier-based formulation containing jet milled salmeterol xinafoate; SXW blend – carrier-based formulation containing wet polished salmeterol xinafoate.

| Formulation | Micronization technology | Mixing technology | Fine lactose | Coarse lactose | fine lactose (%) |
|--------------------|---------------------------------|--------------------------|---------------------|-----------------------|-------------------------|
| SXJ blend | Jet Milling | High shear | Lactohale 230 | Respitose SV003 | 15 |
| SXW blend | Wet Milling | | | | |

5.3.3 Solubility assessment

The solubility of SX was determined in a dissolution medium consisted of 0.1M PBS with 0.04 % (w/v) SDS, pH 7.4. The saturation shake-flask method (Langenbucher, 1972) was used (n=3) with an excess of API (~20 mg) to the dissolution medium (~20 mL) in a glass vial, placed in an incubator at 37 °C and 100 rpm. Samples were collected after 24 h, centrifuged (11.600 x g) and quantified. The SX was quantified using a Waters HPLC system with UV detection (Waters 717 plus Autosampler; Waters 1525 binary HPLC Pump; Waters Jet Stream 2 Plus incubator) equipped with a C18 column (5 µm, 250 mm x 4.6 mm) at 35 ± 5 °C with a mobile phase of 35:35:30 ACN:Metanot:Amonium formate 0.01 M (v/v/v), pH 4, an absorbance detection wavelength of 216 nm and an injection volume of 20 µL. The injection run time was 8.0 min and the SX retention time 5.0 min.

5.3.4 Milled salmeterol xinafoate and formulation characterization

5.3.4.1 Particle size analysis

The particle size distribution of micronized SX was measured by laser diffraction (LD) as a wet dispersion using a Mastersizer 2000 from Malvern Instruments Ltd. (UK) equipped with the Hydro 2000S sample dispersion unit. The micronized SX was suspended in an appropriate anti-solvent containing a surfactant at a low concentration (proprietary method from Hovione S.A., undisclosed data). The sample in suspension was then mixed using a vortex and added to the dispersion targeting a stable obscuration limit. Continuous stirring and ultrasounds were applied to ensure adequate dispersion into primary particles. The particle size distribution data was presented as Dv10, Dv50 and Dv90 (particle size below which 10 %, 50 % and 90 % of the volume of particles exist).

5.3.4.2 Scanning electron microscopy

The micronized particles were visualized by scanning electron microscope (SEM - Zeiss, Oberkochen, Germany) after collection with the PreciseInhale® system. The samples were coated with 10 nm Platinum (Q150T ES, West Sussex, UK) and loaded into the SEM docking bay and analyzed in an Ultra 55 field emission SEM at 5 kV using the secondary electron detector. The images were captured at various magnifications.

5.3.4.3 Aerodynamic particle size distribution by Next Generation Impactor

Similarly to previous chapters, NGI was used as an APSD characterization technique for manufactured capsules, using the standard apparatus at 4kPa.

The APSD of the prepared carrier-based formulations was assessed by NGI from Copley Scientific (UK) at an airflow rate of 40 L/min with a total air volume of 4 L. Tests were performed using a RS01 Ultra High Resistance device from Plastiapae (Italy). All impactor stages were coated using a coating agent solution (1% glycerol in ethanol) to minimize particle bouncing. All formulations were assessed in triplicate, actuating five capsules in each test. SX was recovered from the IP, PS, stages 1 to 7, micro-orifice collector (MOC) and the actuated capsules, with a mixture of milli-Q water and acetonitrile (50:50, v/v) with 0.05 % (v/v) 85% phosphoric acid (w/w). The samples were quantified according to section 5.3.3. The data was analyzed using Copley Inhaler Testing Data Analysis Software version 3.10, according to pharmacopoeia requirements ("General Chapter <601> Physical tests and determinations: Aerosols. Nasal sprays, Metered-dose inhalers, and dry powder inhalers," 2012).

5.3.4.4 Aerodynamic particle size distribution analysis by Marple Cascade Impactor

Marple cascade impactor (Chen et al., 2018) was employed to determine the APSD of the aerosol generated using the PreciseInhale®, after actuation, aerosol expansion and transport to the bottom of the collection chamber. As stated in previous chapters, the relevance of using the MCI is to account for agglomerates generated during aerosol expansion and deposition.

To measure the APSD of the micronized SX and the prepared formulations the MCI was coupled to the PreciseInhale® coating chamber. The detailed method description can be found in Chapter 4, section 4.3.2.2.3. To quantify the amount of SX deposited on each stage of the impactor each filter was immersed in 1.5 mL of mobile phase (80 % (v/v) methanol in water) and the SX was extracted for more than 15 min. Next the extraction solution was transferred to vials and centrifuged at 11 600 x g (13 000 rpm) for at 8 min. The supernatant was transferred to HPLC vials and analysed with stable baseline using Agilent Eclipse XDB-C18, 5 µm, 4.6 x 250 mm) with an absorbance detection wavelength of 216 nm and an injection volume of 50 µL. The injection run time was 6.5 min and the SX retention time 3.0 min.

5.3.5 Dissolution testing

The manufactured formulations were analysed for dissolution using the previously described methodologies – paddle over disk (POD) combined with an aerodynamic particle size determination system for particle collection (Chapter 3, section 3.5.4); and DissolvIt® coupled with the PreciseInhale® breath simulation for particle collection (Chapter 4).

5.3.5.1 Paddle over disk apparatus

The POD apparatus methodology for dissolution assessment coupled with the NGI or the FSI for DPI sampled collection was previously developed and optimized as detailed in Chapter 2. In summary, using the NGI as sample collection, the DPI formulations were actuated in an NGI following with the conditions previously described for aerodynamic profile determination (Section 5.3.4.3) to obtain particle separation and collect a known amount of formulation with a known aerodynamic particle size distribution. The collection was conducted by placing a dissolution cup assembled with an impactor insert in stage 4 of the NGI - stage with higher amount of deposited DS. Using the FSI, the formulations were actuated at similar conditions to the NGI and the fine particle fraction (FPF) was collected on a on a micro glass fibre filter. The filter was then punched prior to transfer to the stainless-steel collector. Finally, 1 mL of dissolution media was added to the collector surface and the filter was placed on top.

For dissolution assessment, following the impaction with the NGI or FSI, the stainless-steel collector with the sampled formulation was covered with a pre-soaked polycarbonate membrane with a 76 mm diameter and 0.05 µm pore size, which was sealed in place with the securing ring of the membrane holder, to be finally placed inside a dissolution vessel (Tablet Dissolution Tester DIS 6000 from Copley Scientific was employed). The apparatus consisted of vessels containing 350 mL of dissolution medium maintained at a controlled temperature and stirred with paddles at 75 rpm, placed 25 ± 2 mm above the membrane holder.

5.3.5.2 DissolvIt® and PreciseInhale® systems

The DissolvIt® and PreciseInhale® systems were described in detail in Chapter 4 (sections 4.3.2.2.1 and 4.3.2.2.4, respectively). In summary, the Plastiape Monodose inhaler (40L/min at 4 kPa pressure drop) was actuated at 40 L/min using the PreciseInhale® system with the newly designed per-separator. After actuation, the powder aerosolizes and the finer particles and smaller agglomerates (not retained

in the induction port and pre-separator) enter the coating chamber and are pulled down by a vacuum source, depositing on glass coverslips. For the jet milled and wet polished SX, the DustGun aerosol generator system was used, where portions of highly compressed air (50 bar) are employed to deagglomerate powder into highly concentrated respirable aerosols. Likewise, after entering the coating chamber, the aerosols are pulled down by the vacuum source and deposit on glass coverslips.

Following the particle collection, three coated coverslips for each experiment were used in the DissolvIt® apparatus. The dissolution took place at a controlled temperature in the dissolution chamber, from the coverslip glass to the pumped perfusate through a 50 µm-thick layer of mucus simulant and a 10 µm-thick polycarbonate membrane (0.03 µm pore size).

5.3.5.3 Extraction and quantification

The SX from the sampled dissolution timepoints was extracted from the perfusate by liquid-liquid extraction. 100 µL of dissolution sample was added to 100 µL of NH₄OH 0.5 M and vortexed for 30 seconds. The mixture was transferred to a solid-supported liquid/liquid extraction vessel of 200 µL, followed by the addition of 1 mL of ethyl acetate. The samples were evaporated overnight until dry using a hotte and a 40 °C bath, and reconstituted in 100 µL of methanol

All the extracted samples were quantified in triplicate by the Structural Analysis Lab, Faculdade de Farmácia, Universidade de Lisboa (Portugal), employing LC-MS/MS Waters (Ireland) equipment with a Mediterranea Sea 18 5 µm column (15 x 0.21 cm) at 35 °C, with a mobile phase of acetonitrile-0.5 M formic acid + 0.1% formic acid in water (70:30, 6 min / 10:90, 0.1 min / 70:30, 8.9 min v/v), at a flow rate of 0.3 mL/min and an injection volume of 10 µL. For the detection, the MicroMass QuattroMicro® API triple quadrupole mass spectrometer from Waters (Ireland) was used equipped with an electrospray source in a positive mode. Capillary and cone voltages were set to 3.0 kV and 20 V, respectively.

For mass balance purposes, the SX remaining in the dissolution system after the test was quantified for all the tests. To that end, 20 mL of DMSO:Methanol (1:1, v/v) was added to the collected dissolution cell followed by 10 min ultrasound. These led to dissolution of the glue of the tape fixing the polycarbonate (membrane) and the cell, and to the separation of the glass disk from the membrane. Subsequently, samples were vortexed strongly for 5 min and then sampled, in triplicate aliquots, for chemical analysis (LC-MS/MS), performed by Pharm-Analyt Labor GmbH (Austria), with a LOQ of 20.0 ng total amount.

5.3.5.4 Data analysis

To interpret the dissolution rate data, the obtained dissolution profiles were fitted to the Weibull model, a general mathematical expression used to describe the curve in terms of mathematical parameters (Langenbucher, 1972). The Weibull model (Equation 3.) expresses the accumulated fraction of the material in a solution, m , at time t , and a and b define the time scale and curve. It has been reported in the literature as a reasonable description of the dissolution of orally inhaled drugs (Riley et al., 2012). The dissolution time (Equation 3.2), T_d , corresponds to the time necessary to dissolve 63.2 % of the totally released drug.

$$m = 1 - \exp\left[\frac{-t^b}{a}\right] \quad \text{Equation 5.1}$$

$$a = (T_d)^b \quad \text{Equation 5.2}$$

For the DissolvIt® samples, the dissolution data was normalized to the total amount deposited in the coverslip during aerosol collection (M_{dep} , Equation 5.3), which was quantified as the sum of the DS dissolved in the perfusate during the dissolution test (M_{perf}) and the non-dissolved DS, extracted from the system and quantified once the dissolution experiment is finalized (M_{system}).

$$M_{dep} = M_{perf} + M_{system} \quad \text{Equation 5.3}$$

The cumulated dissolved dose was calculated by trapezoid integration (Equation 5.4)

$$M_{perf} = \sum_{n=1}^N (t_n - t_{n-1}) \times \left(M_{n-1} + \frac{M_n - M_{n-1}}{2} \right) \quad \text{Equation 5.4}$$

In which N is the number of collected timepoints, t_n and t_{n-1} are two consecutive timepoints, in minutes, and M_n and M_{n-1} are the masses of DS collected at those timepoints.

With the quantified amount of dissolved DS, the dissolution extent (Equation 5.5) can be calculated.

$$\text{Dissolution extent } (t) = \frac{M_c(t)}{M_{dep}} \quad \text{Equation 5.5}$$

In which M_c was the cumulative mass calculated with Equation 2 for each timepoint.

5.3.6 Statistical analysis

To compare results, data were subjected to statistical analysis using unpaired T student analysis.

Differences were considered statistically significant at a level of $p < 0.05$

5.4 SALMETEROL CARRIER-BASED FORMULATIONS

CHARACTERIZATION

In the present section, the standard formulation characterization for the two manufactured carrier-based salmeterol xinafoate (SX) formulations is summarized. The SX formulations consisted of one containing jet milled DS particles and another wet polished particles. Standard characterization includes the particle size of the micronized material and the aerodynamic performance determined by impactor equipment, similarly to the previous chapters.

5.4.1 Particle size distribution by laser diffraction

Jet milled and wet polished particles used in the present section were characterized for particle size. The results are presented in Table 5.2. All particles are within the inhalation size range of 0.5 to 5 μm (Newman and Peart, 2009). The jet milled particles are larger than the wet polished particles (Dv90 of 4.9 μm to 3.9 μm , respectively), which can have an impact on the aerodynamic performance and on the dissolution profile obtained. The impact of this variable will be discussed in the following sections.

Table 5.2 - Particle size distribution characterization of the micronized salmeterol xinafoate (SX) particles.

| SX | Dv10 (μm) | Dv50 (μm) | Dv90 (μm) | Span |
|--------------|------------------------|------------------------|------------------------|------|
| Jet milled | 1.2 | 2.6 | 4.9 | 1.4 |
| Wet polished | 0.6 | 1.5 | 3.9 | 2.2 |

Dv10, Dv50 and Dv90: Particle size below which 10 %, 50 % and 90 % of the volume of particles exist;

5.4.2 Aerodynamic characterization by Next Generation Impactor

The NGI coupled with a flow controller was used to characterize the aerodynamic performance of the manufactured formulations containing jet milled SX and wet polished SX. The aerodynamic profiles are presented in Figure 5.2 and the performance parameters are summarized in Table 5.3.

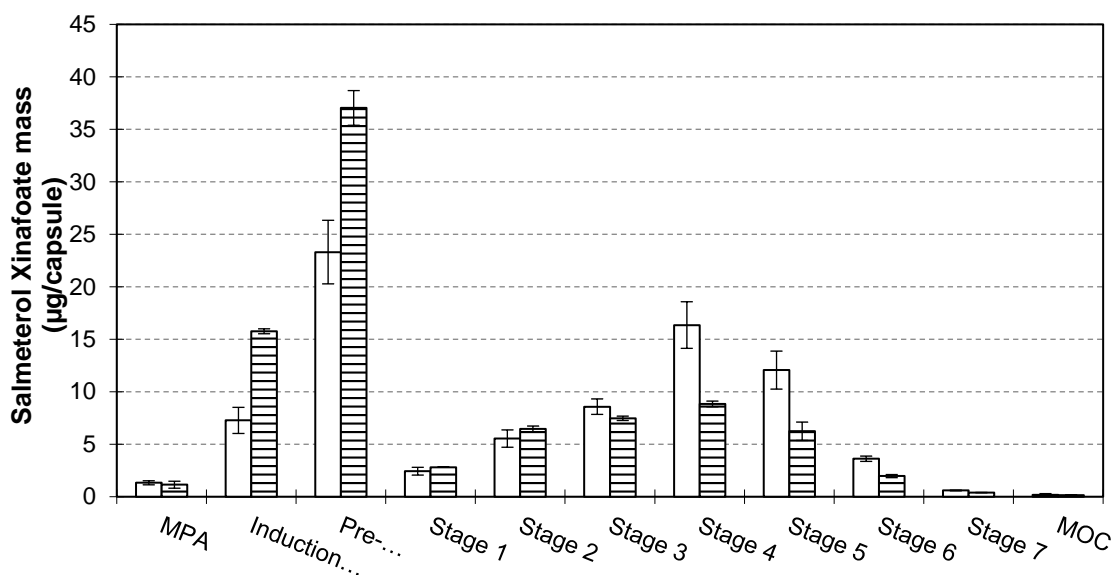


Figure 5.1 - Aerodynamic characterization of the salmeterol xinafoate formulations containing jet milled particles (white) and wet polished particles (stripes), determined by Next Generation Impactor. Data expressed as mean \pm SD (n=3). MPA: mouthpiece adapter; MOC: micro-orifice collector.

Table 5.3 - Aerodynamic performance parameters of the carrier-based formulations with jet milled salmeterol xinafoate (jet milled SX blend) and wet polished salmeterol (wet polished SX blend) determines by Next generation impactor (NGI), n=3.

| | Jet milled SX blend | Wet polished SX blend |
|---------------------------------------|---------------------|-----------------------|
| Impactor equipment (flow rate, L/min) | NGI (40) | NGI (40) |
| ED ($\mu\text{g}/\text{dose}$) | 81 ± 7 | 88 ± 2 |
| FPD ($\mu\text{g}/\text{dose}$) | 40 ± 1 | 24 ± 1 |
| Stage 4 ($\mu\text{g}/\text{dose}$) | 16 ± 2 | 8.8 ± 0.3 |
| MMAD (μm) | 2.6 ± 0.2 | 3.3 ± 0.2 |
| GSD | 2.1 ± 0.1 | 2.2 ± 0.1 |

ED: emitted dose; FPD: fine particle dose; MMAD: mass median aerodynamic diameter; GSD: geometric standard deviation.

The two formulation present significantly different aerodynamic performances, with the jet milled material generating a formulation with a smaller mass median aerodynamic diameter (MMAD). These results are not in accordance with the particle sizes obtained by laser diffraction, as the jet milled material was composed of larger particles and thus it is expected to have a larger MMAD. However, the difference can be easily explained by the impact of other physical properties, as it is expected that different particle

engineering technologies will produce particles with different properties (Moura et al., 2016; Noriega-Fernandes et al., 2021).

One parameter identified in the literature as critical for the carrier-based DPI aerodynamic performance is the cohesion/adhesion balance ratio (CAB_{ratio}) of the micronized DS. CAB_{ratio} is an approach to the quantification of interparticulate forces by colloidal probe atomic force microscopy by enabling the measurement of the ratio between the cohesion of one material and its adhesion to another material for an equivalent contact geometry (Begat et al., 2004). For instance, an increase in cohesive strength has shown to lead to a higher FPF in various studies (Begat et al., 2004; Jones et al., 2008a, 2008b). Furthermore, a linear correlation was observed between the FPF and CAB_{ratio} for different carriers (Hooton et al., 2006), and the crystallization conditions were found to have an impact in CAB_{ratio} and showed a correlation with aerodynamic performance (Kubavat et al., 2012a, 2012b). Specifically for SX prepared by jet milling and wet polishing, literature data indicates that the jet milled particles are more adhesive to lactose ($CAB_{ratio} \sim 0.9$) than the in the wet polished powders, which showed to be slightly cohesive ($CAB_{ratio} > 1$; $CAB_{ratio}=1.18$) (Moura et al., 2014), also leading to a higher FPF.

Thus, considering the listed literature data and the observed results, the jet milled and wet polished SX are expected to have different cohesion/adhesion balances, and that difference is expected to have an impact on the formulation performance – for instance higher cohesiveness of the wet polished material leads to stronger DS agglomerates, more challenging to deagglomerate and mix with the carrier in the blending step, which can lead to a deposition of large SX agglomerates on the earlier stages of the impactor during the powder actuation. Low cohesiveness of the jet milled material, on the other hand, allows for an easier interaction with the carrier (by interaction with coarse lactose surfaces and lactose fines, in both cases leading to easier release of DS particles (Jones and Price, 2006) – see detailed description of carrier-based mechanism in Chapter 2, section 2.3.1, for a detailed explanation of the mechanism of action of ternary components within dry powder aerosols.). Herein, the same formulation composition and manufacturing procedure was used for both micronized DS. The NGI and CAB data suggest that adjustments might have been needed to successfully overcome the relative cohesive forces of one micronized drug substance over the other for the benefit of maximizing performance.

5.4.3 Aerodynamic characterization by Marple Cascade Impactor

The Marple cascade impactor (MCI) coupled with the PreciseInhale® was used to assess the aerodynamic performance of the generated agglomerates during powder deposition to the cover glasses, for the micronized SX and the prepared formulations. The possible particle interactions during the powder deposition stage can determine the microstructure of the collected agglomerates used for dissolution (Noriega-Fernandes et al., 2021), thus the MCI is essential in the understanding of the dissolution results as it characterizes particles following the passage on the deposition chamber after aerosol expansion and deposition at a slow flowrate of 400 mL/min. The results may differ from the NGI analysis as it characterizes the formulation as it leaves the inhaler without an aerosol expansion and slow deposition stage. The obtained results are presented in Figure 5.2 and summarized in Table 5.4.

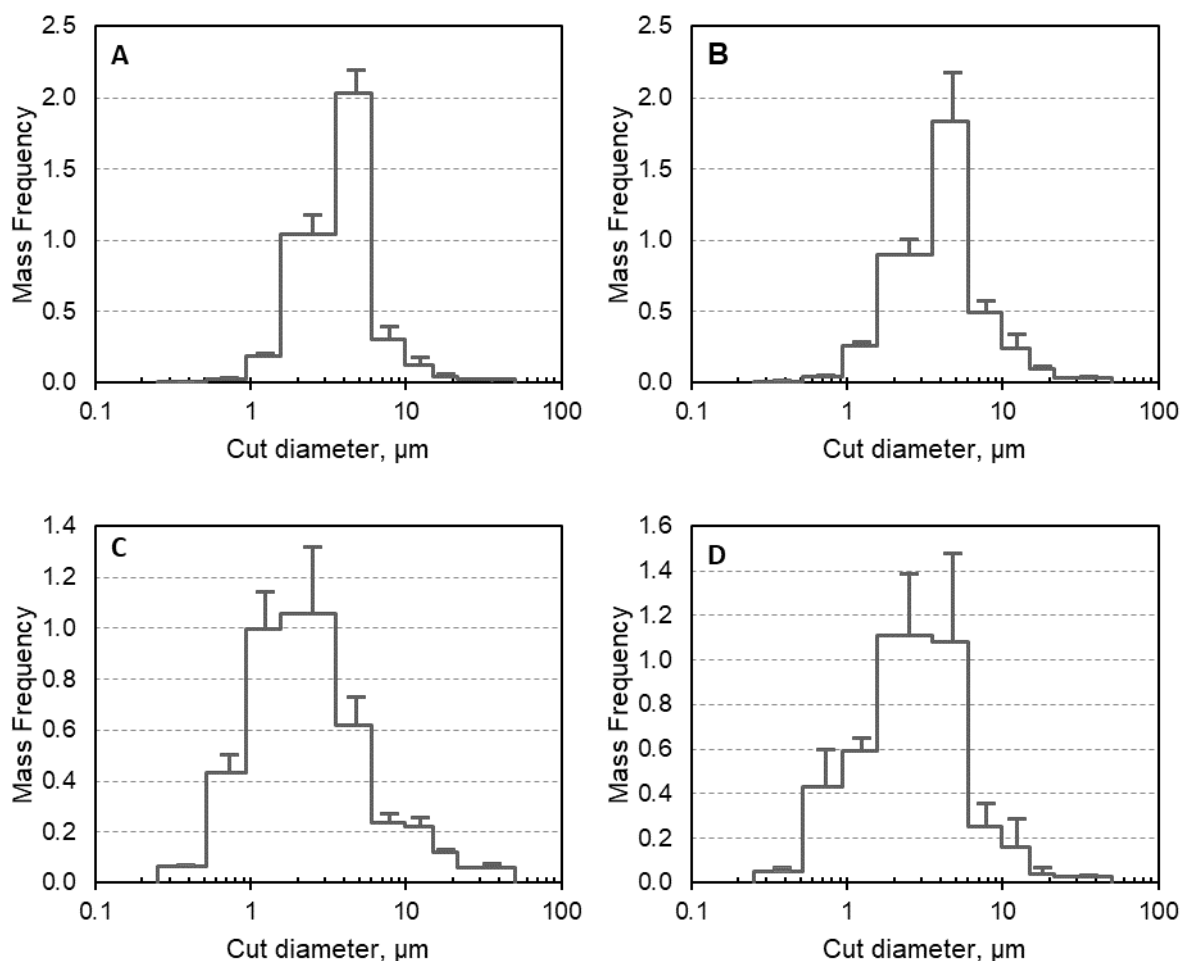


Figure 5.2 – Particle-size distribution as normalized mass frequency determined by Marple Cascade Impactor A – jet milled salmeterol xinafoate; B - wet polished salmeterol xinafoate; C – carrier-based formulations jet milled salmeterol xinafoate; and D - carrier-based formulations with wet polished salmeterol xinafoate, n=3.

Table 5.4 - Particle-size distribution parameters determined by Marple Cascade Impactor. Jet milled SX blend - carrier-based formulations with jet milled salmeterol xinafoate; wet polished SX blend - carrier-based formulations with wet polished salmeterol xinafoate; jet milled SX –salmeterol; and wet polished SX – wet polished salmeterol xinafoate. Data expressed as mean \pm SD (n=3).

| Exposure material | MMAD (μm) | GSD |
|-----------------------|------------------------|---------------|
| Jet milled SX blend | 3.9 \pm 0.2 | 1.6 \pm 0.1 |
| Wet polished SX blend | 4.1 \pm 0.1 | 1.8 \pm 0.1 |
| Jet milled SX | 2.3 \pm 0.1 | 2.3 \pm 0.2 |
| Wet polished SX | 2.8 \pm 0.2 | 2.2 \pm 0.2 |

MMAD - Mass median aerodynamic diameter, GSD – Geometric standard deviation.

The presented results show an overall tendency for a larger MMAD for the formulations and a broader distribution for the DS alone micronized powders. The broader APSD profile for the DS alone powders is possibly due to the presence of SX agglomerates which are eliminated in the process to obtain the formulation, namely by sieving and blending procedures. During the blending, the DS particles are homogeneously distributed on the carrier surface and as DS-lactose agglomerates, leading to the release of fine DS particles upon actuation. The described effect is well known and described in the literature (Jones and Price, 2006).

Jet milled and wet polished SX present significant differences in terms of aerodynamic size ($2.3 \pm 0.1 \mu\text{m}$ to $2.8 \pm 0.2 \mu\text{m}$, respectively), which is contrary to the PSD results obtained by laser diffraction, indicating the APSD is mostly influenced by the presence of agglomerates (eliminated during laser diffraction analysis) and their interparticle forces upon powder dispersion. Based on these results, the wet polished material appears to have more agglomerates of particles in the deposition chamber, which can be a result already existent agglomerates on the DS powder (in accordance with the high cohesion forces determined for wet polished SX (Moura et al., 2014)), or of the generation of agglomerates during the aerosol expansion and deposition (due to electrostatic interactions, for example). However, upon formulation the differences observed are not significant, showcasing the importance of formulation for product performance.

Nonetheless, the formulation containing jet milled SX presents a lower average MMAD and GSD (Table 5.4). When comparing these results with the APSD determined by NGI (Table 5.3), the tendencies are aligned. Moreover, the MMAD results determined by MCI were significantly larger ($3.9 \pm 0.2 \mu\text{m}$ and $4.1 \pm 0.1 \mu\text{m}$ for the jet milled and the wet polish particle engineering technology, respectively, versus $2.6 \pm 0.2 \mu\text{m}$ and $3.3 \pm 0.2 \mu\text{m}$), tendency previously observed for the FP formulations (Table 4.5, Chapter 4) (Noriega-Fernandes et al., 2021), and caused by the agglomerates generated in the deposition chamber and observed in the microscopic images. For the salmeterol formulations, a similar effect is expected to occur, and will be discussed in the deposition results section of the PreciseInhale® and DissolvIt® dissolution system below.

5.5 PADDLE OVER DISK METHODOLOGY VALIDATION FOR A HIGH SOLUBILITY DRUG SUBSTANCE: SALMETEROL XINAFOATE

5.5.1 Outline

The development of the paddle over disk (POD) apparatus dissolution methodology for orally inhaled and nasal products (OINDP) as well as the identification of the method critical parameters was presented in Chapter 3. In the present section the POD will be applied to a second DS, salmeterol xinafoate, with a significantly higher water solubility. The main goals of the present section are:

1. To validate the POD methodology by applying it to a second model drug with different solubility characteristics. For that the two explored particle collection techniques (NGI and FSI) were used and compared, and the impact of collected DS dose was assessed for the FSI collection.
2. To evaluate the differentiation capabilities of the POD apparatus for two carrier-based formulation with a similar DS dose. For that, the dissolution media composition was varied to maximize differentiation power.

5.5.2 Experimental design

The two manufactured SX formulations were used in a number of tests using the POD apparatus (Table 5.5). The following variables were evaluated:

- Collection method: for both formulations tests were performed using the NGI and the FSI as collection method. The goal of this assessment was to evaluate if the impact of the collection strategy observed for fluticasone (low solubility DS) in Chapter 3, section 3.5.4 is maintained for a higher solubility DS, and thus if it should be considered in these cases.
- Number of actuations: number of actuations was varied for the same formulation (from 96 to 120 µg for the formulation containing wet polished DS) to assess the impact of collected dose on the dissolution profile after FSI collection and thus confirm the developed methodology overcomes the dose dependency limitation described in the literature (Noriega et al., 2018b; Son et al., 2010) and previous chapters.
- Dissolution media composition: for SX the dissolution rate is much faster than for FP , consequence of the solubility difference, and for that reason, the formulation differentiation is

more challenging. Sodium dodecyl sulphate (SDS), the dissolution media surfactant, concentration was varied from 0.4 to 0 % (w/v), as the surfactant content has been proven to have an impact on the dissolution rate of the POD apparatus (May et al., 2012; Son et al., 2010; Son and McConville, 2009).

Table 5.5 - Summary of dissolution tests the carrier-based formulations with jet milled salmeterol xinafoate (jet milled SX blend) and wet polished salmeterol xinafoate (wet polished SX blend) performed using the paddle over disk apparatus (POD) after collection using the fast screening impactor (FSI) and the next generation impactor (NGI). Grey lines correspond to the formulation containing jet milled SX.

| Test | Formulation | Collection method | Number of actuations | Replicates | % SDS (w/v) |
|-------------|-----------------------|--------------------------|-----------------------------|-------------------|--------------------|
| 1 | Jet milled SX blend | FSI | 3 | 2 | 0.4 |
| 2 | Wet polished SX blend | FSI | 4 | 2 | 0.4 |
| 3 | Wet polished SX blend | FSI | 5 | 2 | 0.4 |
| 4 | Jet milled SX blend | FSI | 3 | 3 | 0.1 |
| 5 | Wet polished SX blend | FSI | 5 | 3 | 0.1 |
| 6 | Jet milled SX blend | FSI | 3 | 3 | 0.0 |
| 7 | Jet milled SX blend | NGI | 7 | 3 | 0.4 |
| 8 | Wet polished SX blend | NGI | 12 | 3 | 0.4 |

SDS: sodium dodecyl sulphate

5.5.3 Results and discussion

5.5.3.1 Dissolution profiles after collection with fast screening impactor

In order to evaluate the homogeneity of the collected product, as well as the repeatability of the FSI as a collection strategy, an additional control measurement was implemented for the dissolution tests applying the FSI as a collection strategy. Hence, for all tests, the total amount of SX deposited on the FSI filter (w_{total}) was determined by summing the total placed in the dissolution media (w_{diss}) with the amount remaining in the outer filter following punching ($w_{outer\ ring}$) - Equation 3.5. Additionally, the total amount of collected powder (SX and lactose) was determined by weight difference of the filter before and after actuation (w_{powder}). Finally, the percentage of SX in the deposited powder was calculated. The listed data are summarized in Table 5.6.

$$w_{total} = w_{diss} + w_{outer\ ring} \quad \text{Equation 5.6}$$

Table 5.6 - Summary of collected doses of salmeterol xinafoate (SX) and total powder (SX and lactose) for all the paddle over disk (POD) dissolution tests using fast screening impactor (FSI) as a collection method, n=3. The SX in FPF (%) is the percentage of SX in the total amount of collected powder. Grey lines (test 1, 4 and 6) correspond to the formulation containing jet milled SX.

| Test | No. act. | Expected dose (μg) ¹ | w_{diss} (μg) | $w_{outer\ ring}$ (μg) | w_{total} (μg) | w_{powder} (mg) | SX in FPF (%) |
|----------------|----------|--|------------------------------|-------------------------------------|-------------------------------|-------------------|---------------|
| 1 | 3 | 120 | 68 ± 3 | 31 ± 1 | 103 ± 3 | 2.68 ± 0.03 | 3.8 ± 0.1 |
| 2 | 4 | 96 | 62 ± 5 | 32 ± 2 | 94 ± 7 | 3.65 ± 0.03 | 2.6 ± 0.2 |
| 3 | 5 | 120 | 72 ± 1 | 42 ± 1 | 114 ± 3 | 4.3 ± 0.1 | 2.6 ± 0.1 |
| 4 ² | 3 | 120 | 69 ± 5 | 36 ± 2 | 105 ± 5 | 3.1 ± 0.1 | 3.4 ± 0.1 |
| 5 | 5 | 120 | 77 ± 3 | 40 ± 1 | 117 ± 3 | 4.6 ± 0.1 | 2.6 ± 0.1 |
| 6 | 3 | 120 | 69 ± 3 | 38 ± 2 | 107 ± 5 | 2.9 ± 0.2 | 3.7 ± 0.1 |

¹ Calculated based on the fine particle dose. ² Based on 2 samples. w_{diss} - total amount of DS placed in the dissolution media (after cutting the filter), in μg ; $w_{outer\ ring}$ - DS remaining in the outer ring after cutting the FSI filter, in μg ; w_{total} - total amount of DS collected (Equation 3.5) in μg ; w_{powder} - the total amount of powder collected, in mg;

Evaluating the values of expected and total collected doses collected using the FSI prior to dissolution assessment, slight variations can be observed – for the formulation containing jet milled SX (shaded grey in Table 5.6, Test 1, 4 and 6) the expected dose of 120 μg was not achieved, however the observed

delta is explained by various reasons: (i) the expected dose is calculated with the FPD value determined by NGI, while the samples of tests 1 to 6 was collected with the FSI equipment, and variations between equipment are expected (Mohan et al., 2017); and (ii) small product losses are expected on the sample preparation due to the required steps – removal of filter from the FSI holder, filter punching, placing of filter on dissolution holder and covering with membrane. Nonetheless, the total amount of DS placed in the dissolution media (after cutting the filter), w_{diss} , is similar for all tests with jet milled SX (68 ± 3 , 69 ± 5 and 69 ± 3 $\mu\text{g}/\text{test}$), indicating the FSI allows for a reproducible method. For the formulation containing wet polished SX, the collected amounts are in accordance with the expected values. The total amount of SX placed in the dissolution media after cutting the filter, w_{diss} , is slightly different for the same number of actuation (72 ± 1 and 77 ± 3 $\mu\text{g}/\text{test}$), however the SX fraction in the FPF is maintained for all the tests, indicating the variability may be due to formulation variability.

Overall, these results indicate a good repeatability and powder homogeneity for both the formulation containing jet milled SX and wet polished SX.

Following dose collection, the generated samples were used for dissolution assessment using the POD apparatus. The dissolution profiles of the listed tests 1 to 6 are presented in Figure 5.3 to Figure 5.5, and summarized in Table 5.7. The dissolution profiles comparing the impact of dose collection and formulation were fitter to the Weibull model to have more comparison parameters (Equation 3. and Equation 3.2). All the Weibull models fitted to the data present a R^2 larger than 0.9, indicating a good fit. In the Weibull model a denotes a scale parameter that describes the time dependence, while b describes the shape of the dissolution curve progression.

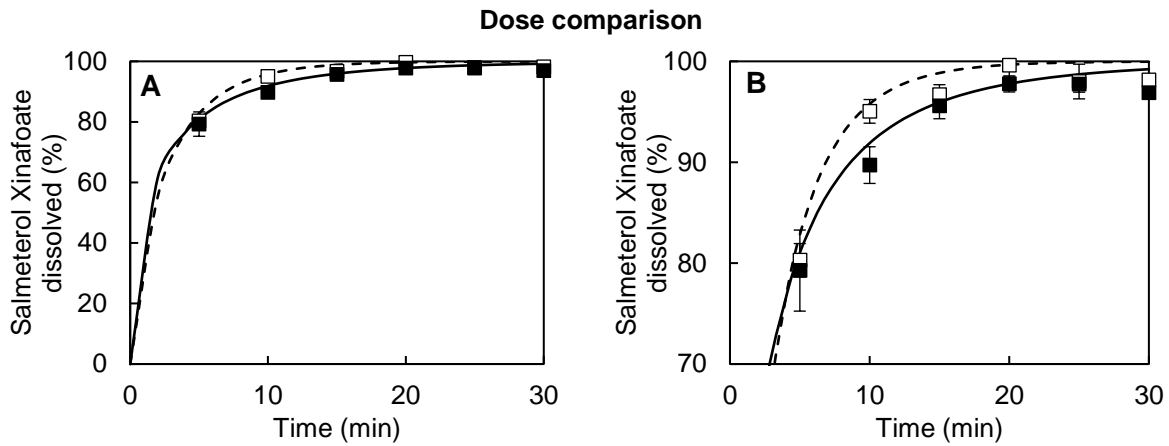


Figure 5.3 – A: Dissolution profile (salmeterol xinafoate dissolved) determined using the paddle over disk apparatus after collection, using the fast screening impactor of the carrier-based formulations containing wet polished salmeterol xinafoate after actuation 4 capsules, $62 \pm 5 \mu\text{g}$ (\square) and 5 capsules, $72 \pm 1 \mu\text{g}$ (\blacksquare). B is a zoom in (70 – 100% of dissolution). Each profile is given by two replicates. Lines were fitted with Weibull model, $R^2 > 0.9$.

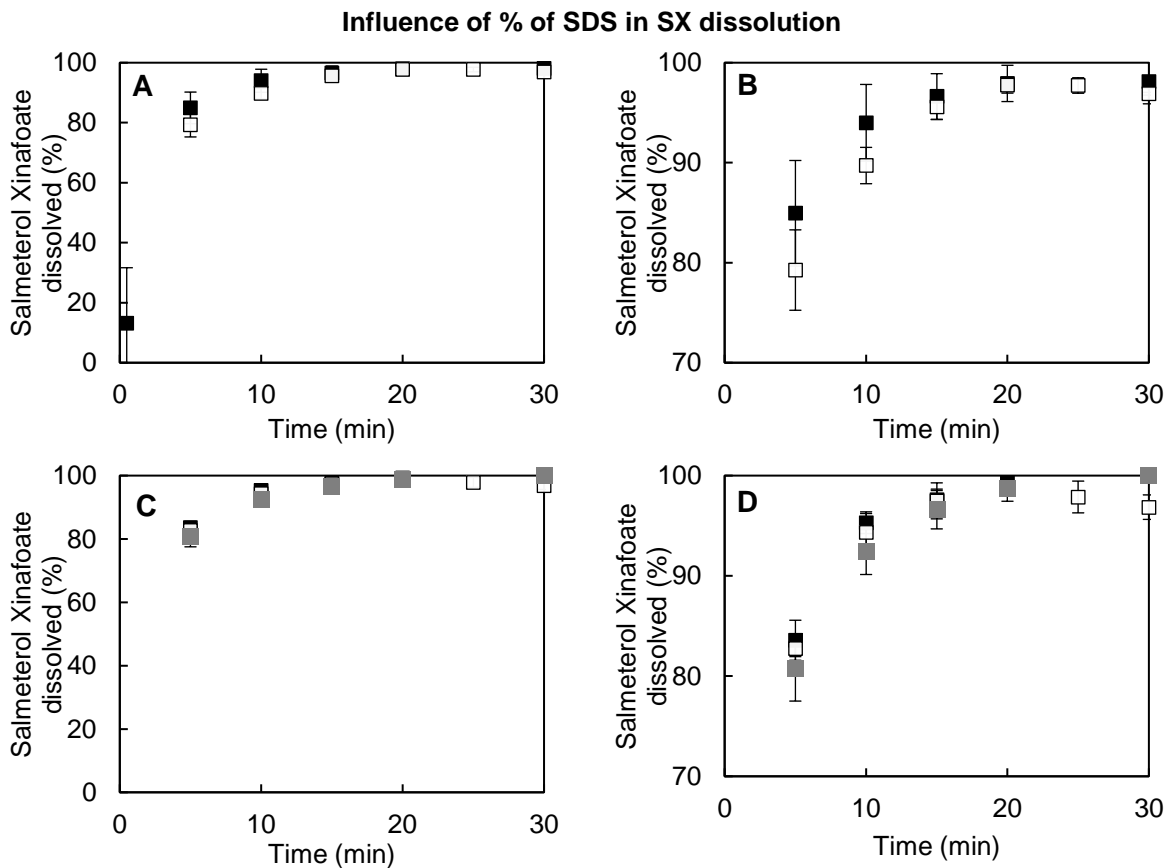


Figure 5.4 – Dissolution profile determined using the paddle over disk apparatus after collection using the fast screening impactor of the carrier-based formulations containing wet polished (5 capsules actuated, A) and jet milled (3 capsules actuated, C) salmeterol xinafoate in dissolution media containing 0.4% SDS (\square), $n=2$, 0.1% SDS (\blacksquare), $n=3$, and 0.0% SDS (\blacksquare), $n=3$. B and D is a zoom in (70 – 100% of dissolution).

Formulation comparison

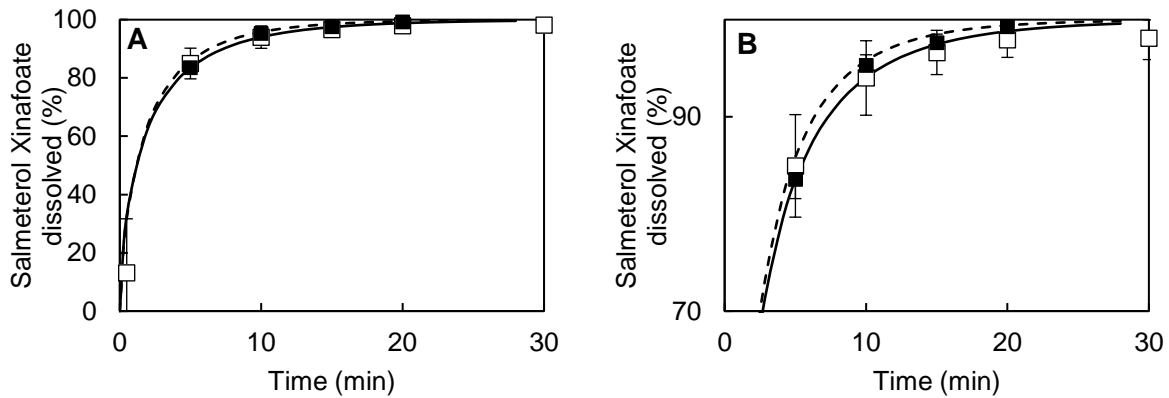


Figure 5.5 – A: Dissolution profile determined using the paddle over disk apparatus after collection using the fast screening impactor of the carrier-based formulations containing wet polished salmeterol xinafoate after actuation 5 capsules (□) and jet milled salmeterol xinafoate after actuating 3 capsules (■). B is a zoom in (70 – 100% of dissolution). Each profile is given by three replicates. Lines were fitted with Weibull model. $R^2 > 0.9$.

Table 5.7 - The dissolution performance parameters for the performed dissolution tests using the Paddle over disk apparatus couples with the fast screening impactor, for jet milled and wet polished formulations of salmeterol xinafoate (SX).

| | Test 2 | Test 3 | Test 4 | Test 5 |
|--------------------------|---|---|--|---|
| Short description | Wet polished SX 4 actuations 0.4% SDS | Jet milled SX 5 actuations 0.4% SDS | Wet polished SX 3 actuations 0.1% SD | Jet milled SX 5 actuations 0.1% SDS |
| a^2 | -0.35 | -0.20 | -0.20 | -0.20 |
| b^2 | 0.85 | 0.60 | 0.70 | 0.65 |
| T_d (min) ² | 2.58 | 2.15 | 1.93 | 2.82 |
| R^2 | 0.9864 | 0.9841 | 0.9895 | 0.9383 |

¹ Calculated according to Equation 4, compared with formulation with trehalose/raffinose

² Calculated according to Equations 1 and 2

SDS – sodium dodecyl sulfate

The collected dose impact on the SX dissolution profile (Figure 5.3), increased the collected dose from $62 \pm 5 \mu\text{g}$ to $72 \pm 1 \mu\text{g}$, by varying the number of actuated capsules from 4 to 5. The results showed that the profiles are not significantly different, indicating the SX dose collected for the dissolution profile assessment does not have an impact on the dissolution profile, once again confirming the FSI as a collection methodology that overcomes the dose dependency limitation, in the present case for a high

aqueous solubility DS. This result is relevant considering that literature data has shown a dependency on dose using the POD apparatus following collection using the NGI even for high solubility DS such as budesonide (May et al., 2012; Son et al., 2010) and hydrocortisone (Son and McConville, 2009), with an aqueous solubility of 14 µg/mL (Borgstrom et al., 1994) and 1800 µg/mL (El Maghraby, 2008), respectively.

When decreasing the surfactant content on the dissolution media to attempt a slower dissolution profile (solubility decrease from 798 ± 32 µg/mL on 0.4% (w/v) SDS in 0.1M PBS buffer, pH 7.4, to approximately water solubility (0.1M PBS), no significant impact of the SDS concentration was observed for both formulations (Figure 5.4), indicating the limiting step for the obtained profiles is not the solubility or wettability of the micronized SX. A second variable which could have an impact on the observed dissolution/permeation rate is the type and porous size of the used membrane (0.05 µm), as salmeterol is a high solubility/low permeability DS (Hochhaus, 2018) - this analysis should be considered in future studies.

Finally, when comparing the two manufactured formulations (test 4 versus test 5), with jet milled and wet polished SX (Figure 5.5), the dissolution kinetics are statistically similar, indicating the POD is not capable of differentiating between SX carrier-based formulations regarding dissolution kinetics.

5.5.3.2 Dissolution profiles after collection with NGI

When using the NGI as a collection strategy, the repeatability of the method is not expected to be a critical parameter as the equipment is used as per designed for APSD measurement (without stage coating), and thus the dose collected on each stage is expected to be repeatable (V. Marple et al., 2003; Virgil A. Marple et al., 2003b). Nonetheless, as the number of actuated capsules increased from the five used to assess the APSD, the total collected dose may vary from the expected due to particle bouncing and accumulation in the equipment interstage resulting from the lack of stage coating – previously observed for FP formulations (Fernandes et al., 2016a), and detailed in Chapter 3, Figure 3.6. Moreover, aiming for better dissolution profile analysis and comparison, similarly to the FSI collection, the amount of collected powder (SX and lactose) on the stage 4 of the NGI was weighed and the percentage of SX on the stage was calculated – Table 5.8.

Table 5.8 - Summary of collected doses of salmeterol xinafoate (SX) and total powder (SX and lactose) for the paddle over disk dissolution tests using next generation impactor (NGI) as a collection method, n=3. The SX in stage 4 (%) is the percentage of SX in the total amount of collected powder. Grey line correspond to the formulation containing jet milled SX.

| Test | No. act. | Expected dose (μg) ¹ | w_{diss} (μg) | w_{powder} (mg) | SX in stage 4 (%) |
|------|----------|--|-------------------------------------|--------------------------|-------------------|
| 7 | 7 | 112 | 92 ± 1 | 1.4 ± 0.1 | 6.8 ± 0.7 |
| 8 | 12 | 106 | 78 ± 5 | 2.1 ± 0.2 | 3.8 ± 0.1 |

¹ Calculated based on the fine particle dose. w_{diss} - total amount of XS placed in the dissolution media, in μg ; w_{powder} - the total amount of powder collected, in mg;

The determined values of collected dose at the end of dissolution assessment, w_{diss} , indicate an overestimation of approximately 20 % and 35 % for the formulation containing jet milled and wet polished SX, respectively. Consequently, the two formulations were tested with different doses in the dissolution media, which will be considered in the dissolution profile results discussion. As previously discussed, this effect is a possibly consequence of the increase of number of capsules actuated without stage coating leading to a non-linear relationship between the number of actuations and the deposited amount. In fact, coating the NGI stages has been found to reduce particle bounce and re-entrainment, and thus reduce bias and variability of the measurements, particularly for DPI formulations (Bonam et al., 2008). Furthermore, if the number of actuations used in the NGI test is too large, a stage overloading can be observed affecting the jet-to-plate distance, and thus lead to an apparent shift to finer particle sizes (Feddah and Davies, 2010; Kamiya et al., 2004; Nasr and Allgire, 1995).

Although the expected dose was not obtained, its variability remained low (relative standard deviation of 2 and 6 % for the formulation containing jet milled and wet polished SX, respectively), indicating the delta between the expected and obtained was maintained, and thus the collection method was repeatable. Considering the method development for new formulations, an initial assessment should be included to determine the dose to be collected prior to dissolution, considering the absence of stage coating and the total number of actuations.

When considering the last column (SX in stage 4 (%)) of Table 5.8, the percentage of SX on the deposited powder, a significant difference was detected between formulations, which is aligned with the similar analysis in the FSI (Table 5.6) – higher SX percentage for the formulation with a higher FPF determined by NGI. For a carrier-based formulation, these results showcase how the DS to excipient

ratio varies throughout the impactor stages, i.e., a higher amount of DS does not indicate a higher amount of excipient, unlike other formulations such as spray-dried composite formulations. Expanding these considerations to dissolution testing, the lactose percentage in the used stage can have an impact on the wettability and dissolution of the DS – as described in previous chapters and discussed in the literature (Noriega-Fernandes et al., 2021).

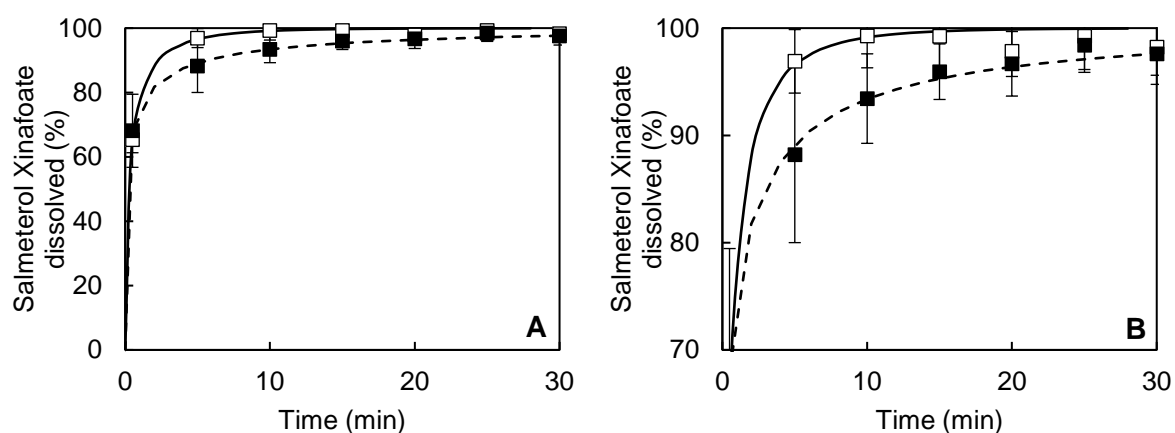


Figure 5.6 – A: Dissolution profile determined using the paddle over disk apparatus after collection using the next generation impactor, stage 4, of the carrier-based formulations containing wet polished salmeterol xinafoate after actuation 12 capsules, $78 \pm 5 \mu\text{g}$ (\square) and jet milled salmeterol xinafoate after actuating 7 capsules, $92 \pm 1 \mu\text{g}$ (\blacksquare). B is a zoom in (50 – 100% of dissolution). Each profile is given by three replicates. Lines were fitted with Weibull model.

Table 5.9 - The dissolution performance parameters for the performed dissolution tests using the Paddle over disk apparatus coupled with the next generation impactor, for jet milled and wet polished formulations of salmeterol xinafoate (SX).

| | Test 7 | Test 8 |
|--------------------------|---|--|
| Short description | Jet polished SX 7 actuations 0.4% SDS | Wet polished SX 12 actuations 0.4% SDS |
| a^2 | 0.18 | 0.14 |
| b^2 | 0.50 | 0.29 |
| T_d (min) ² | 0.44 | 0.32 |
| R^2 | 0.9963 | 0.9961 |

¹ Calculated according to Equation 4, compared with formulation with trehalose/raffinose

² Calculated according to Equations 1 and 2

Using the NGI as a collection method, a significantly faster dissolution profile was obtained (Figure 5.6), when compared with the samples collected using the FSI. It is important to note that the collected amounts using the FSI are similar or higher than the doses collected in the stage 4 of the NGI, eliminating the possibility of the difference observed being dose related – a limitation previously identified for the POD apparatus following NGI collection (in the literature and described in detail in Chapter 3). This can be explained by the smaller particle size of the fractions collected using the NGI (aerodynamic diameter between 3.5 μm and 2.1 μm for stage 4 (Virgil A Marple et al., 2003), while the FSI collects the fraction with an aerodynamic diameter below 5 μm). Additionally, these results confirm (in addition to Figure 5.3) for a high solubility DS such as SX, the particle packaging in hotspots due to the nozzles of the NGI stages does not have an impact on the dissolution profile obtained.

Comparing the dissolution profile of the two formulations, no statistically significant differentiation was detected, which is aligned with all the POD results obtained for SX in the present chapter. However, the average dissolution profiles suggest a faster dissolution rate the formulation containing wet polished material.

In general, the deposited dose dissolved at a fast rate for all dissolution tests, in accordance with the prompt effect of the drug as bronchodilator, despite it being classified sparingly soluble. Moreover, considering the overall results, the POD is possibly not the best method to differentiate formulation of high solubility DS as it appears to have close to no response to the critical parameters variations previously defined. Considering that, in the next section the dissolution and absorption profile of salmeterol will be assessed with the Dissolv*It*® system.

5.5.4 Conclusions

In the present section the POD apparatus used as an *in vitro* dissolution test for DPI was validated by testing a second model drug with a higher water solubility than the previous development tests. The validation was assessed firstly by proving the repeatability and uniformity of cascade impactors as a dose collection method, and secondly by evaluating the impact of the cascade impactor (NGI vs FSI), collected dose, formulation and dissolution media on the generated dissolution profiles.

In conclusion, when using the FSI as a collection strategy, the system showed no response to the variation of the selected critical parameters and was unsuccessful in the differentiation of carrier-based formulations. The observed lack of response, on the one hand suggest an unsuitability of the POD

apparatus to differentiate carrier-based high solubility crystalline drug substance. On the other hand, the proven independence of the collected dose validates one of the main limitations of the POD system is overcome. Moreover, the inability to differentiate carrier-based formulations was previously observed for a low solubility DS, with the differentiation capabilities being observed for carrier-based versus spray-dried formulation. Hence, future work on the POD system should include the stated comparison. Lastly, when comparing the two particle collection strategies, the use of the NGI led to a faster dissolution possibly due to the smaller particle size distribution being analyzed, and proving some differentiation capabilities.

5.6 DISSOLVIT® METHOD VALIDATION FOR A HIGH SOLUBILITY DRUG SUBSTANCE: SALMETEROL XINAFOATE

5.6.1 Outline

In the previous Chapter 4, the PreciseInhale® and DissolvIt® biorelevant methodology was used to evaluate differences on particle deposition, dissolution, and absorption for a low solubility DS (fluticasone propionate, FP). In the present section, a similar approach will be followed for a high solubility DS (salmeterol xinafoate, SX) in order to understand the impact for the DS solubility on the particle dissolution as well as on the dissolution and absorption profile. For that, two particle engineering technologies (jet milling and wet polishing) were applied to micronize the crystalline DS, followed by carrier-based formulation approach by blending the micronized material with coarse and fine lactose.

The application of the PreciseInhale® and DissolvIt® methodology to a high solubility DS is relevant in order to better understand the impact of formulation and particle engineering in a range of DS types. The data generated with SX show how the used methodology is capable to differentiate distinct particle engineering technologies and formulations, with a significant impact of the presence of lactose as a carrier excipient. These results confirm DPI formulation should be considered not only as a tool for aerodynamic performance targeting, but also as a dissolution and absorption modulator.

5.6.2 Experimental design

The two micronized SX powders (jet milled and wet polished) and manufactured SX formulations were used in a number of tests using the DissolvIt® dissolution system coupled with the PreciseInhale® breath simulator (Table 5.10). The number of actuations, amount of loaded powder on the DustGun pressure chamber and the used dispersing pressure were defined in order to target a similar dose on the collecting glass coverslips. The following variables were evaluated:

- Particle engineering technology: the impact of the particle engineering technology used to micronize the crystalline SX (jet milling and wet polishing) on the deposition, dissolution and absorption was investigated by generating deposition data and dissolution/absorption profiles for both the DS alone and the formulated carrier-based material.

- **Formulation:** The impact of formulating with lactose as a carrier excipient was evaluated by comparing the deposition structures and obtained profiles of DS alone powder to formulated mixtures.

Table 5.10 - Summary of dissolution tests of micronized salmeterol xinafoate (SX) (jet milled and wet polished) and the carrier-based formulations with jet milled SX (jet milled SX blend) and wet polished SX (wet polished SX blend) performed using the DissolvIt® after collection using the PreciseInhale®

| Test | Powder/ Formulation | Dispersion method | Number of actuations / Loaded powder (mg) | Dispersing pressure (bar) |
|------|--------------------------|--|--|---------------------------------|
| 1 | Jet milled SX | DustGun | 1.4 | 100 |
| 2 | Wet polished SX | | 1.1 | 100 |
| 3 | Jet milled SX blend | Inhaler aerosol generator with Plastiape Monodose inhaler | 4 | - |
| 4 | Wet polished SX blend | | 5 | - |

5.6.3 Results and discussion

5.6.3.1 Deposition

Following DPI actuation and micronized SX dispersion using the PreciseInhale® system with the exposure chamber, the collected particles were evaluated by light microscope (Figure 5.7) and by SEM analysis (Figure 5.8). As previously explained, the evaluation of morphology of the generated and deposited structures can be relevant for the interpretation of the dissolution and absorption profiles obtained using the DissolvIt® equipment.

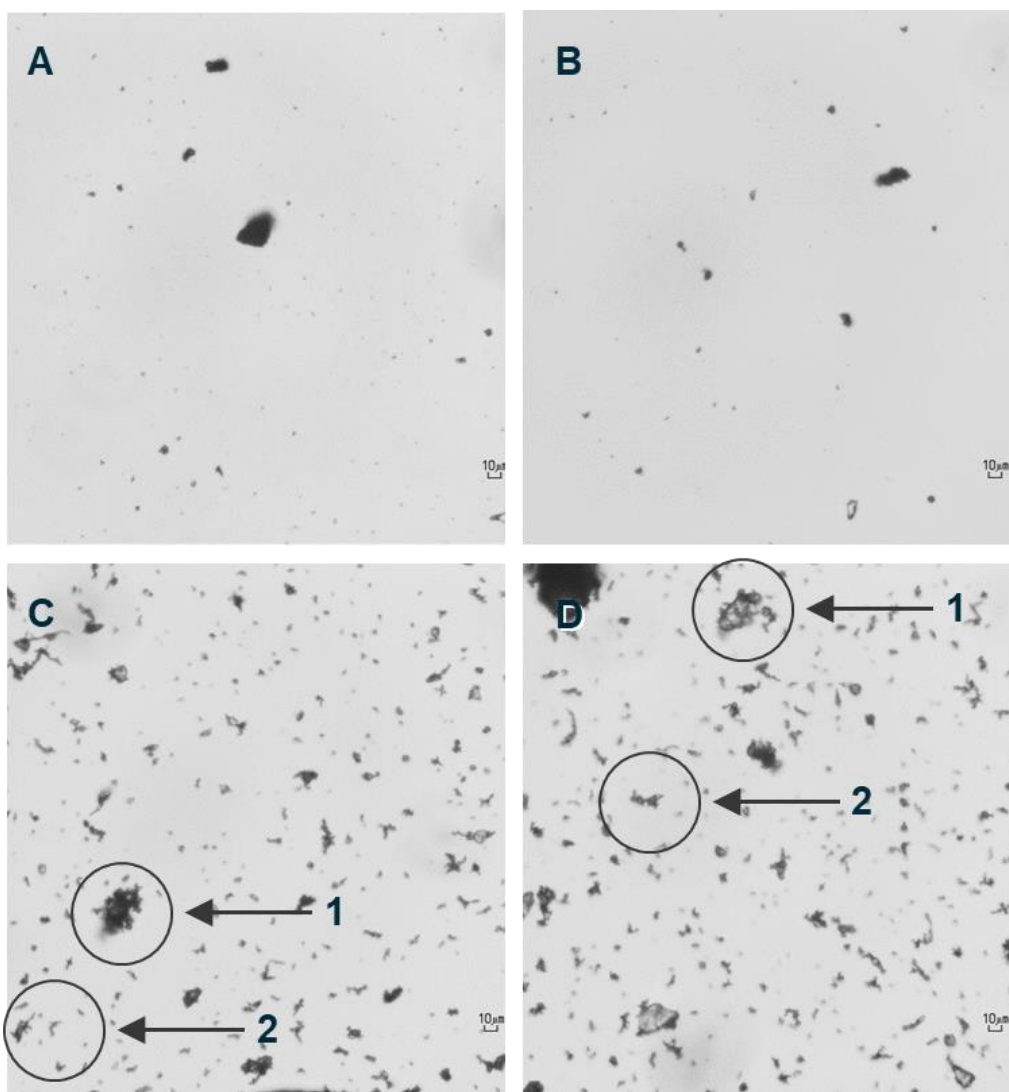


Figure 5.7 - Deposition pattern on coverslips of the jet milled salmeterol xinafoate (SX) particles (A) and wet polished SX particles (B); and carrier-based formulation containing jet milled SX (C), carrier-based formulation containing wet polished SX (D) after actuation using the PreciseInhale®, obtained by light microscopy with a x20 objective. 1 – agglomerates of coarse and fine particles; 2 – agglomerates of fine particles.

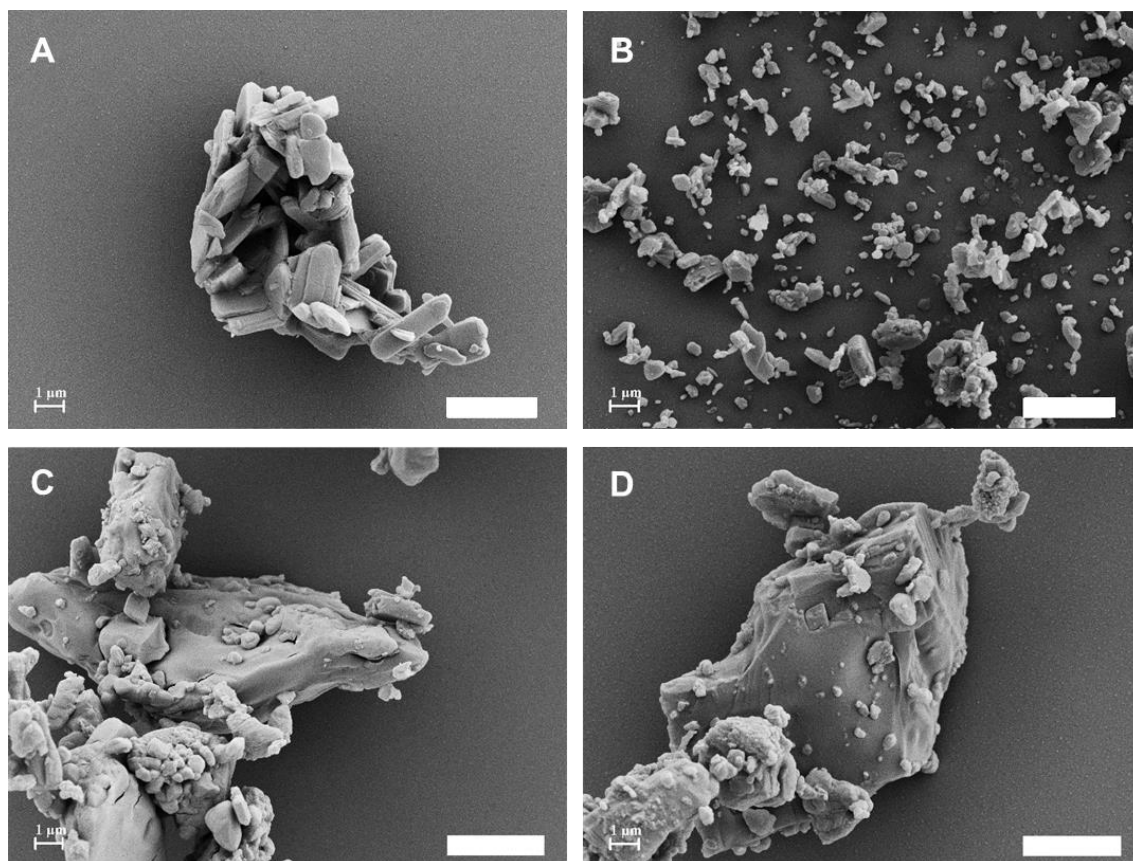


Figure 5.8 - SEM images of the of the jet milled salmeterol xinafoate (SX) particles (A) and wet polished SX particles (B); and carrier-based formulation containing jet milled SX (C) and carrier-based formulation containing wet polished SX (D) after actuation using the PreciseInhale®.

Unlike the FP micronized particles and formulations, the particle engineering technology does not appear to have a significant impact on the deposited structures' morphology, observed by both optical microscopy and SEM –pictures in Figure 5.7 and Figure 5.8. (A and C - jet milled SX alone and formulated) present similar morphology particles and structures to the pictures on the Figure 5.7.B and Figure 8. (B and D - wet polished SX alone and formulated).

SX alone powders appear to deposit as large globular agglomerates (Figure 5.7 and Figure 5.8, A and B), unlike the FP powders which showed a tendency for filamentous agglomerates (Noriega-Fernandes et al., 2021). This can be an indication of a more effective deagglomeration for the FP powders, which then re-agglomerate upon expansion in the deposition chamber, while de SX agglomerates may be a result of poor powder deagglomeration upon actuation with the DustGun mechanism. To ensure homogeneity between glasses when dispersing the micronized SX powders, a higher chamber pressure of the DustGun was required in comparison with the FP tests – pressure of 100 bar for the SX powders, while the FP were perfectly dispersed with 50 bar. The DustGun pressure is responsible for the

micronized powder dispersion (Gerde et al., 2004), and poor glass homogeneity usually requires higher pressures to overcome the strong particle cohesion forces and optimize homogeneity between cover glasses.

Interestingly enough, the formulated powders (Figure 5.7 and Figure 5.8, C and D) do not appear to deposit as the previously described globular agglomerates. Moreover, they show a tendency to deposit and filamentous agglomerates composed by fine particles and agglomerates as coarse and fine particles (identified as 1 and in Figure 5.7, respectively), as previously observed for the FP carrier-based formulations (Chapter 4, Noriega-Fernandes et al., 2021).

In summary, the main observation from the deposition analysis is the increased difficulty to deagglomerate the SX alone powders, in comparison with the FP powders, and how the presence of lactose added through blending appears to eliminate those agglomerates. This is especially relevant when considering high dosage formulations with a high drug load, as in those cases the DS characteristics will drive the deagglomeration mechanism and structure generation upon actuation and even for similar PSD, it can lead to completely different deposition tendencies. As excipients are included in the formulation, the DS dominance may be diluted. Still before assessing the dissolution results in the next subsection, the relevance of a deposition analysis in the understanding of DPI performance is here demonstrated.

5.6.3.2 Dissolution

The dissolution profiles obtained with the Dissolv^{IT}® equipment for the manufactured formulations and micronized drug substance are presented in Figure 5.9 and Figure 5.10, and the dissolution performance parameters are summarized in Table 5.11. The profiles are presented as perfusate concentration normalized to the total amount of DS on the coverslips used in the dissolution test (M_{dep} presented in Table 5.11). The impact of the SX deposition density on the dissolution profile was previously studied for the deposited dose range of the present work, 500 to 1300 ng per glass, within the studied range of 200 and 1600 ng per glass, (Malmlöf et al., 2019) with no significant impact on the dissolution profile determined parameters, C_{max} (%/mL), t_{max} (min) and fraction of retention. Thus, the differences observed in the obtained dissolution profiles are not caused by the impact of the deposited doses.

Formulation comparison

The dissolution profiles of the carrier-based formulations are presented in Figure 5.9, as the fraction of total recovered over time (Figure 5.9, A and B) and as the fraction retained in the dissolution system (Figure 5.9, C). The total amount of deposited SX on the coverslips for the two formulations is statistically similar (p -value > 0.06), presented in Table 5.11

The comparison of the carrier-based formulations dissolution and absorption profiles shows statistically similar profiles for the first minutes of dissolution (5 minutes, zoomed-in in Figure 5.9, C) which differentiate when the SX concentration peaks (C_{max} , %/mL), as it occurs at different times for the both studied formulations (p -value < 0.01 , Table 5.11), for statistically similar C_{max} values. Following the profile C_{max} , the fraction retained profiles showed one time point with a statistically different fraction values (at 8.5 min) and the remaining timepoints although with different averages indicating a faster dissolution/absorption for the formulation containing jet milled SX, are statistically similar (p -value > 0.05). Thus, overall, the differentiation between formulations is slight but existent. Moreover, these results showcase once again the relevance to including absorption/dissolution assessment in the formulation development stage to have a clear understanding of the DS fate once it reaches the deep lung, which can vary depending on slight formulation adjustments (in the present case, changes on the particle engineering technology).

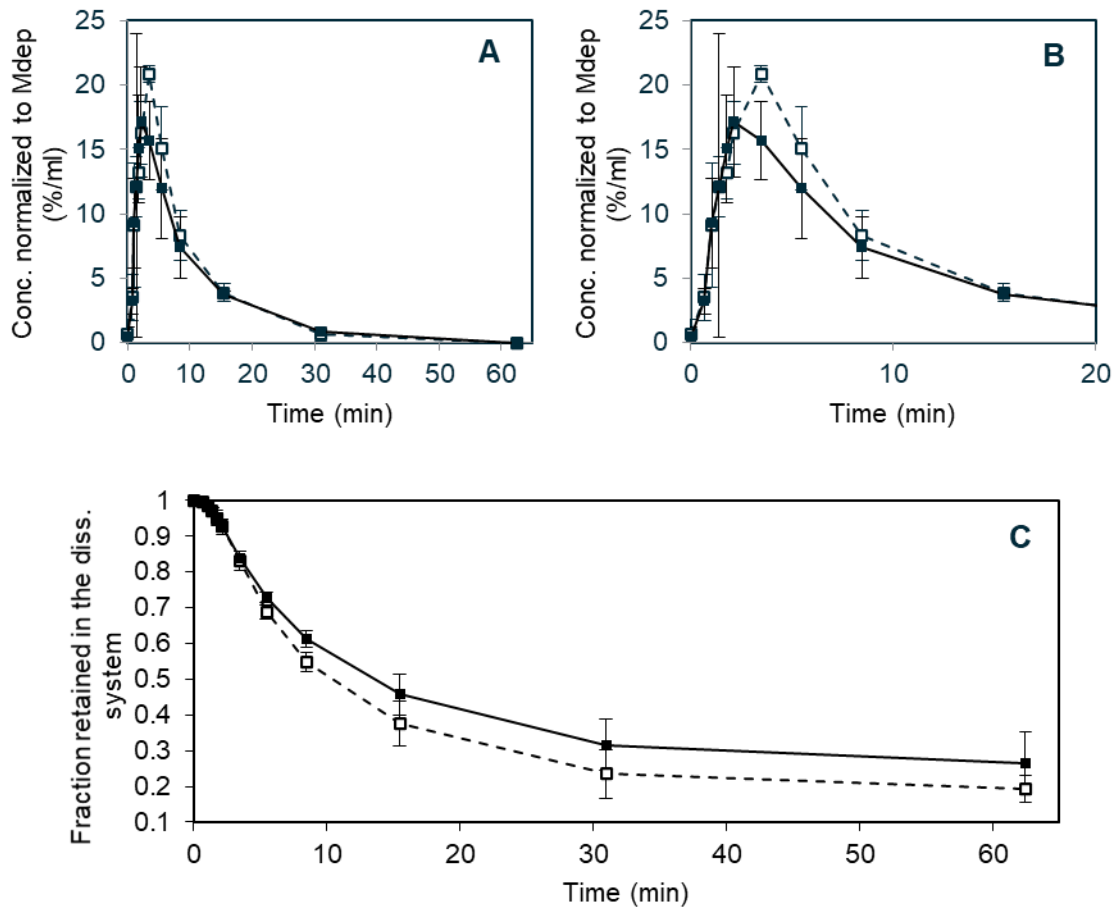


Figure 5.9 - Dissolution profiles obtained using DissolvIt®. A - Comparison of the prepared carrier-based formulations with jet milled salmeterol xinafoate (jet milled SX blend, □) and wet polished salmeterol xinafoate (wet polished SX blend, ■) as a fraction of total recovered (%/mL), B – zoom in to the first 20 minutes, C – fraction retained in the dissolution system. All results normalized to the total deposited dose. Data expressed as mean \pm SD (n=3). * p-value < 0.05.

To better understand if the difference is maintained for the DS (SX) alone powder, as well as the impact of the presence of lactose as an excipient, the dissolution/absorption profiles for the micronized material are presented in Figure 5.10.

Salmeterol xinafoate alone comparison

For the SX alone powders micronized by jet milling and wet polishing, the dissolution profiles are presented in Figure 5.9, as the fraction of total recovered over time (Figure 5.9, A and B), as the fraction retained in the dissolution system (Figure 5.9, C). The total amount of deposited SX on the coverslips for the two particle engineering technologies is statistically similar (p-value > 0.05), presented in Table 5.11

The two micronized powders present a similar C_{\max} (8 ± 3 %/mL and 9 ± 1 %/mL, for the jet milled and wet polished material, respectively), with the wet polished SX presenting a faster dissolution (t_{\max} of 4 ± 1 min, statistically lower than 7 ± 2 min for the jet milled material, p -value < 0.03 , Table 5.11). The faster initial dissolution of the wet polished material is confirmed by the fraction retained in the dissolution system over time (Figure 5.9, C). During the last 30 minutes, there is a shift as the wet polished material decreases its dissolution rate leading to a final retention significantly lower for the wet polished material (p -value < 0.05), and thus an overall faster dissolution for the jet milled material.

The jet milled material had a larger geometric PSD (Dv_{90} of $4.9 \mu\text{m}$ versus the $3.9 \mu\text{m}$ of the WP material), but a significantly smaller MMAD ($2.3 \pm 0.1 \mu\text{m}$ versus $2.8 \pm 0.2 \mu\text{m}$), indicating the presence of larger agglomerated for the wet polished material, as previously discussed. Considering these results and the Noyes-Whitney equation (Wauthoz and Amighi, 2015), an initial faster dissolution of the wet polished material can be a result of the finer individual particles with a larger surface area, and a slower final dissolution mainly driven by agglomerates with a smaller surface area.

These results indicate the particle engineering technology used has a significant impact on the dissolution profile of the SX alone particles, possibly due to the differences in particle dispersion and deposition.

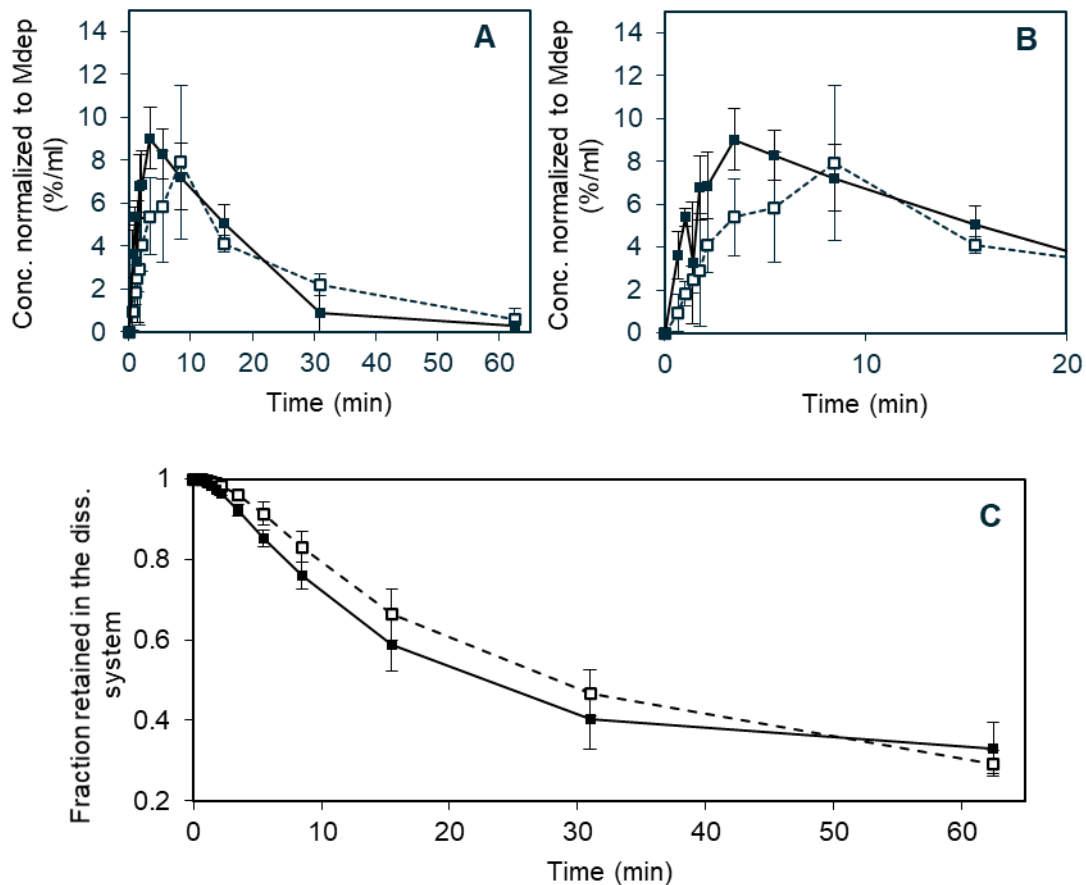


Figure 5.10 - Dissolution profiles obtained using Dissolv/It®. A - Comparison of the jet milled salmeterol xinafoate (jet milled SX, □) and wet polished salmeterol (wet polished SX, ■) as a fraction of total recovered (%/mL), B – zoom in to the first 20 minutes, C – fraction retained in the dissolution system with a zoom window in to the first 5 min. All results were normalized to the total deposited dose. Data expressed as mean ± SD (n=3). * p-value < 0.05.

Overall analysis

When comparing with the dissolution/absorption performance of the carrier-based formulation formulations with the SX alone, the results show a clear impact of the presence of lactose as a carrier in the measured profiles. The C_{max} , t_{max} and dissolution extent at 8.5 min values (Table 5.11) confirm this conclusion with statistical significance (p-value < 0.01 for C_{max} and p-value < 0.02 for the remaining parameters). These results confirm the obtained for the FP formulations – although not statistically significant for the formulation with wet polished FP, the average values of the dissolution/absorption profile were lower for the DS alone (Noriega-Fernandes et al., 2021).

As previously stated (Chapter 4), two hypothesis are presented to explain the impact of the lactose on solubility:

1. The presence of lactose, observed in the deposition images, has an impact on the diffusion coefficient of the Noyes-Whitney equation by affecting the mucus simulant viscosity – diffusion coefficient is inversely proportional to medium viscosity.
2. The presence of lactose in the agglomerates (in substitution to the drug substance particles) decreases the local concentration of DS, leading to faster dissolution (dependence of difference between local concentration and saturation). Additionally, the blending step eliminates the DS large agglomerates (Figure 5.7), possibly responsible for a slower dissolution, as mentioned in the discussion of Figure 5.9

The SX results led to the conclusion that the presence of lactose has a relevant impact not only for low solubility DS such as FP, but also for high solubility DS (SX). Although the two presented hypothesis can be considered in the dissolution/absorption assessment, their contribution may vary depending on the DS solubility. For a low solubility DS, the second hypothesis is possibly more relevant as the limiting step is the dissolution, thus the decrease of local saturation with a dissolution rate increase will be more relevant, while for a high solubility DS the increase of diffusion through the mucus may be the limiting step, thus the lactose dissolution and impact on mucus viscosity is possibly more relevant.

Table 5.11 - The dissolution performance parameters for the carrier-based formulations with jet milled salmeterol xinafoate (jet milled SX blend) and wet polished salmeterol xinafoate (wet polished SX blend), and for the jet milled SX and wet polished SX alone, using the DissolvIt® equipment and the deposited doses using PreciseInhale®. Data expressed as mean ± SD (n=3). p-value by one-way student's t-Test.

| | Jet milled SX blend | Wet polished SX blend | Jet milled SX | Wet polished SX |
|---|---------------------|-----------------------|---------------|-----------------|
| M _{dep} (ng of SX) | 671 ± 152 | 924 ± 166 | 1173 ± 254 | 782 ± 205 |
| C _{max} (fraction of total recovered) (%/mL) | 21 ± 1 | 21 ± 3 | 8 ± 3 | 9 ± 1 |
| p-value | <0.01 ¹ | <0.01 ² | - | - |
| t _{max} (min) | 3 ± 0 | 2 ± 0 | 7 ± 2 | 4 ± 1 |
| p-value | <0.01 | | <0.03 | |
| AUC (%/mL.h) | 3.4 ± 0.1 | 3.1 ± 0.3 | 2.9 ± 0.1 | 2.8 ± 0.2 |
| Dissolution extent at 8.5 min (% of deposited dose) | 46 ± 3 | 39 ± 2 | 16 ± 3 | 24 ± 3 |
| Dissolution extent at 1h (% of deposited dose) | 81 ± 3 | 73 ± 7 | 71 ± 3 | 67 ± 5 |

¹ in compassion with SX JM. ² in comparison with SX WP. C_{max}: Maximum concentration achieved by the DS during the dissolution test ; t_{max}: Time of C_{max} during the dissolution test ; M_{dep}: Amount of DS deposited on the coverslip.

5.6.4 Conclusions

Overall, the biorelevant actuation, collection and dissolution/absorption approach applied allowed not only to rank formulations in regard to their dissolution rate, but also to understand the underlying mechanisms. The development of new and generic inhalation drug products, in specific DPIs, is a complex and time consuming challenge, but the presented technology has the potential to minimize delays by empowering the development teams with information which can be significant to make the right decisions along the process. Also, pharmacokinetic parameters t_{max}, C_{max} and AUC could be used together with available clinical data for the model drug substances for establishing PBPK models that could then be leveraged for potentially anticipating if any differences in *in vitro dissolution* profiles have any impact on pharmacokinetic parameters.

5.7 BIBLIOGRAPHY

- Begat, P., Morton, D.A. V., Staniforth, J.N., Price, R., 2004. The Cohesive-Adhesive Balances in Dry Powder Inhaler Formulations II: Influence on Fine Particle Delivery Characteristics. *Pharm. Res.* 21, 1826–1833. <https://doi.org/10.1023/B:PHAM.0000045236.60029.cb>
- Bonam, M., Christopher, D., Cipolla, D., Donovan, B., Goodwin, D., Holmes, S., Lyapustina, S., Mitchell, J., Nichols, S., Pettersson, G., Quale, C., Rao, N., Singh, D., Tougas, T., Van Oort, M., Walther, B., Wyka, B., 2008. Minimizing Variability of Cascade Impaction Measurements in Inhalers and Nebulizers. *AAPS PharmSciTech* 9, 404–413. <https://doi.org/10.1208/s12249-008-9045-9>
- Borgstrom, L., Bondesson, E., Moren, F., Trofast, E., Newman, S.P., 1994. Lung deposition of budesonide inhaled via Turbuhaler®: A comparison with terbutaline sulphate in normal subjects. *Eur. Respir. J.* 7, 69–73. <https://doi.org/10.1183/09031936.94.07010069>
- El Maghraby, G.M., 2008. Transdermal delivery of hydrocortisone from eucalyptus oil microemulsion: Effects of cosurfactants. *Int. J. Pharm.* 355, 285–292. <https://doi.org/10.1016/j.ijpharm.2007.12.022>
- Feddah, M.R., Davies, N.M., 2010. Influence of single versus multiple actuations on the particle size distribution of beclometasone dipropionate metered-dose inhalers. *J. Pharm. Pharmacol.* 55, 1055–1061. <https://doi.org/10.1211/0022357021549>
- Fernandes, B., Maia, F., Paiva, A., Corvo, M., Costa, E., 2016. Paddle over disk as a dissolution test for orally inhaled drugs: discriminating composite from carrier-based formulations., in: *Drug Delivery to the Lungs*. The Aerosol Society, Bristol, UK, pp. 308–312.
- General Chapter <601> Physical tests and determinations: Aerosols. Nasal sprays, Metered-dose inhalers, and dry powder inhalers, 2012. , in: *United States Pharmacopeial (USP)*. Rockville (MD): The United States Pharmacopeial Convention, pp. 615–628.
- Gerde, P., Ewing, P., Låstbom, L., Ryrfeldt, Å., Waher, J., Lidén, G., 2004. A Novel Method to Aerosolize Powder for Short Inhalation Exposures at High Concentrations: Isolated Rat Lungs Exposed to Respirable Diesel Soot. *Inhal. Toxicol.* 16, 45–52. <https://doi.org/10.1080/08958370490258381>
- Gerde, P., Malmjöf, M., Havsborn, L., Sjöberg, C.-O., Ewing, P., Eirefelt, S., Ekelund, K., 2017. DissolvIt: An In Vitro Method for Simulating the Dissolution and Absorption of Inhaled Dry Powder Drugs in the Lungs. *Assay Drug Dev. Technol.* 15, 77–88. <https://doi.org/10.1089/adt.2017.779>
- Hassoun, M., Malmjöf, M., Scheibelhofer, O., Kumar, A., Bansal, S., Selg, E., Nowenwik, M., Gerde, P., Radivojev, S., Paudel, A., Arora, S., Forbes, B., Hassoun, M., Bansal, S., Scheibelhofer, O., Forbes, B., Paudel, A., Malmlof, M., Nowenwik, M., Kumar, A., Gerde, P., Arora, S., 2019. Use of PBPK modelling to evaluate the performance of DissolvIt, a biorelevant dissolution assay for orally inhaled drug products. *Mol. Pharm.* 16, 1245–1254. <https://doi.org/10.1021/acs.molpharmaceut.8b01200>
- Hastedt, J.E., Bäckman, P., Clark, A.R., Doub, W., Hickey, A., Hochhaus, G., Kuehl, P.J., Lehr, C., Mauser, P., McConville, J., Niven, R., Sakagimi, M., Weers, J.G., 2016. Scope and relevance of a pulmonary biopharmaceutical classification system AAPS/FDA/USP Workshop March 16-17th, 2015 in Baltimore, MD. *AAPS Open* 2, 1. <https://doi.org/10.1186/s41120-015-0002-x>
- Hochhaus, G., 2018. Predictive Dissolution Methods for OINDPs - Development of an Optimized

Dissolution Test System for OINDPs.

- Hooton, J.C., Jones, M.D., Price, R., 2006. Predicting the behavior of novel sugar carriers for dry powder inhaler formulations via the use of a cohesive–adhesive force balance approach. *J. Pharm. Sci.* 95, 1288–1297. <https://doi.org/10.1002/jps.20618>
- Jones, M.D., Harris, H., Hooton, J.C., Shur, J., King, G.S., Mathoulin, C.A., Nichol, K., Smith, T.L., Dawson, M.L., Ferrie, A.R., Price, R., 2008a. An investigation into the relationship between carrier-based dry powder inhalation performance and formulation cohesive–adhesive force balances. *Eur. J. Pharm. Biopharm.* 69, 496–507. <https://doi.org/10.1016/j.ejpb.2007.11.019>
- Jones, M.D., Hooton, J.C., Dawson, M.L., Ferrie, A.R., Price, R., 2008b. An Investigation into the Dispersion Mechanisms of Ternary Dry Powder Inhaler Formulations by the Quantification of Interparticulate Forces. *Pharm. Res.* 25, 337–348. <https://doi.org/10.1007/s11095-007-9467-1>
- Jones, M.D., Price, R., 2006. The influence of fine excipient particles on the performance of carrier-based dry powder inhalation formulations. *Pharm. Res.* 23, 1665–1674. <https://doi.org/10.1007/s11095-006-9012-7>
- Kamiya, A., Sakagami, M., Hindle, M., Byron, P.R., 2004. Aerodynamic sizing of metered dose inhalers: An evaluation of the andersen and next generation pharmaceutical impactors and their USP methods. *J. Pharm. Sci.* 93, 1828–1837. <https://doi.org/10.1002/jps.20091>
- Kubavat, H.A., Shur, J., Ruecroft, G., Hipkiss, D., Price, R., 2012a. Influence of primary crystallisation conditions on the mechanical and interfacial properties of micronised budesonide for dry powder inhalation. *Int. J. Pharm.* 430, 26–33. <https://doi.org/10.1016/j.ijpharm.2012.03.020>
- Kubavat, H.A., Shur, J., Ruecroft, G., Hipkiss, D., Price, R., 2012b. Investigation into the Influence of Primary Crystallization Conditions on the Mechanical Properties and Secondary Processing Behaviour of Fluticasone Propionate for Carrier Based Dry Powder Inhaler Formulations. *Pharm. Res.* 29, 994–1006. <https://doi.org/10.1007/s11095-011-0640-1>
- Langenbucher, F., 1972. Letters to the Editor: Linearization of dissolution rate curves by the Weibull distribution. *J. Pharm. Pharmacol.* 24, 979–981. <https://doi.org/10.1111/j.2042-7158.1972.tb08930.x>
- Malmlöf, M., Nowenwik, M., Meelich, K., Rådberg, I., Selg, E., Burns, J., Mascher, H., Gerde, P., 2019. Effect of particle deposition density of dry powders on the results produced by an in vitro test system simulating dissolution- and absorption rates in the lungs. *Eur. J. Pharm. Biopharm.* 139, 213–223. <https://doi.org/10.1016/j.ejpb.2019.03.005>
- Marple, V., Olson, B., Santhanakrishnan, K., Mitchell, J., Hudson-curtis, B.L., 2003. Next Generation Pharmaceutical Impactor Part II: Archival Calibration. *J. Aerosol Med.* 16, 301–324. <https://doi.org/10.1089/089426803769017668>
- Marple, Virgil A, Ph, D., Roberts, D.L., Ph, D., Romay, F.J., Ph, D., Miller, N.C., Ph, D., Truman, K.G., Sc, B., Oort, M.V.A.N., Ph, D., Olsson, B.O., Ph, D., Hochrainer, D., Phil, D., 2003. Next Generation Pharmaceutical Impactor (A New Impactor for Pharmaceutical Inhaler Testing). Part I : Design 16, 283–299.
- Marple, Virgil A., Roberts, D.L., Romay, F.J., Miller, N.C., Truman, K.G., Van Oort, M., Olsson, B.O., Holroyd, M.J., Mitchell, J.P., Hochrainer, D., Ph, D., Roberts, D.L., Ph, D., Romay, F.J., Ph, D., Miller, N.C., Ph, D., Truman, K.G., Sc, B., Oort, M.V.A.N., Ph, D., Olsson, B.O., Ph, D., Hochrainer,

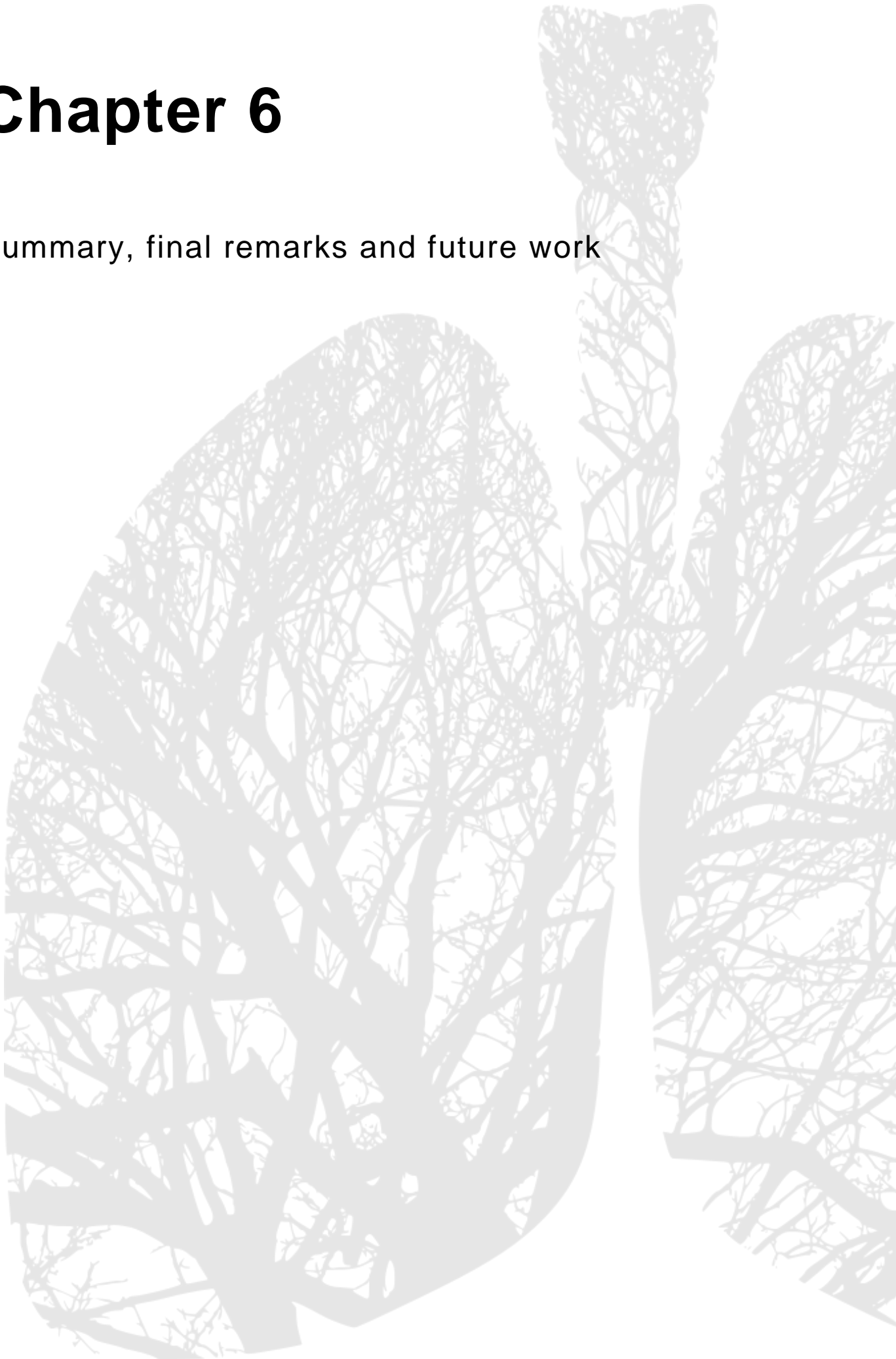
- D., Phil, D., 2003. Next generation pharmaceutical impactor (a new impactor for pharmaceutical inhaler testing). Part I: Design. *J. Aerosol Med.* 16, 283–299. <https://doi.org/10.1089/089426803769017659>
- May, S., Jensen, B., Wolkenhauer, M., Schneider, M., Lehr, C.M., 2012. Dissolution Techniques for In Vitro Testing of Dry Powders for Inhalation. *Pharm. Res.* 29, 2157–2166. <https://doi.org/10.1007/s11095-012-0744-2>
- Mohan, M., Lee, S., Guo, C., Peri, S.P., Doub, W.H., 2017. Evaluation of Abbreviated Impactor Measurements (AIM) and Efficient Data Analysis (EDA) for Dry Powder Inhalers (DPIs) Against the Full-Resolution Next Generation Impactor (NGI). *AAPS PharmSciTech* 18, 1585–1594. <https://doi.org/10.1208/s12249-016-0625-9>
- Moura, C., Neves, F., Aguiar-Ricardo, A., Shur, J., Price, R., Costa, E., 2014. Impact of Jet Milling and Wet Polishing Technologies on Particle Properties for Three Inhalation APIs . Part 2: DPI Formulation and Aerodynamic Performance. *Respir. Drug Deliv.* 595–600.
- Moura, C., Neves, F., Costa, E., 2016. Impact of jet-milling and wet-polishing size reduction technologies on inhalation API particle properties. *Powder Technol.* 298, 90–98. <https://doi.org/10.1016/j.powtec.2016.05.008>
- Nasr, M.M., Allgire, J.F., 1995. Loading Effect on Particle Size Measurements by Inertial Sampling of Albuterol Metered Dose Inhalers. *Pharm. Res. An Off. J. Am. Assoc. Pharm. Sci.* <https://doi.org/10.1023/A:1016253303206>
- Newman, S., Peart, J., 2009. Dry Powder Inhalers, in: Newman, S. (Ed.), *Respiratory Drug Delivery: Essential Theory and Practice*. *Respiratory Drug Delivery Online*, R, pp. 257–307.
- Noriega-Fernandes, B., Malmlöf, M., Nowenwik, M., Gerde, P., Corvo, M.L., Costa, E., 2021. Dry powder inhaler formulation comparison: Study of the role of particle deposition pattern and dissolution. *Int. J. Pharm.* 607. <https://doi.org/10.1016/j.ijpharm.2021.121025>
- Noriega, B., Malmlöf, M., Costa, E., Corvo, M.L., Gerde, P., Maia, F.M., 2017. Dissolution of Orally Inhaled Drugs using DissolvIt®: Influence of a Newly Designed Pre-Separator for Particle Collection, in: *Drug Delivery to the Lungs 28*. Aerosol Society, Bristol, UK, p. 190.
- Noriega, B., Paiva, A.M., Corvo, M.L., Costa, E., 2018. Dissolution of Orally Inhaled Drugs Using Paddle Over Disk Apparatus A Deposition Study, in: *Respiratory Drug Delivery*. Tucson, Arizona, pp. 411–416. <https://doi.org/10.15713/ins.mmj.3>
- Riley, T., Christopher, D., Arp, J., Casazza, A., Colombani, A., Cooper, A., Dey, M., Maas, J., Mitchell, J., Reiners, M., Sigari, N., Tougas, T., Lyapustina, S., 2012. Challenges with Developing In Vitro Dissolution Tests for Orally Inhaled Products (OIPs). *AAPS PharmSciTech* 13, 978–989. <https://doi.org/10.1208/s12249-012-9822-3>
- Son, Y.J., Horng, M., Copley, M., McConville, J.T., 2010. Optimization of an in vitro dissolution test method for inhalation formulations. *Dissolution Technol.* 17, 6–13. <https://doi.org/10.14227/DT170210P6>
- Son, Y.J., McConville, J.T., 2009. Development of a standardized dissolution test method for inhaled pharmaceutical formulations. *Int. J. Pharm.* 382, 15–22. <https://doi.org/10.1016/j.ijpharm.2009.07.034>
- Tambosi, G., Coelho, P.F., Luciano, S., Lenschow, I.C.S., Zétola, M., Stulzer, H.K., Pezzini, B.R., 2018.

Challenges to improve the biopharmaceutical properties of poorly water-soluble drugs and the application of the solid dispersion technology. *Matéria (Rio Janeiro)* 23. <https://doi.org/10.1590/s1517-707620180004.0558>

- Tokumura, T., Miyazaki, E., Isaka, H., Kaneko, N., Kanou, M., 2014. Solubility of fluticasone propionate in aqueous solutions measured by a method avoiding its adsorption to experimental tools. *Int. Res. J. Pharm. Appl. Sci.* 4, 19–24.
- Wauthoz, N., Amighi, K., 2015. Formulation strategies for pulmonary delivery of poorly soluble drugs, in: Nokhodchi, A., Martin, G.P. (Eds.), *Pulmonary Drug Delivery Advances and Challenges*. John Wiley & Sons, Ltd, Chichester, pp. 87–122.
- Wishart, D.S., Guo, A., Oler, E., Wang, F., Anjum, A., Peters, H., Dizon, R., Sayeeda, Z., Tian, S., Lee, B.L., Berjanskii, M., Mah, R., Yamamoto, M., Jovel, J., Torres-Calzada, C., Hiebert-Giesbrecht, M., Lui, V.W., Varshavi, Dorna, Varshavi, Dorsa, Allen, D., Arndt, D., Khetarpal, N., Sivakumaran, A., Harford, K., Sanford, S., Yee, K., Cao, X., Budinski, Z., Liigand, J., Zhang, L., Zheng, J., Mandal, R., Karu, N., Dambrova, M., Schiöth, H.B., Greiner, R., Gautam, V., 2022. HMDB 5.0: the Human Metabolome Database for 2022. *Nucleic Acids Res.* 50, D622–D631. <https://doi.org/10.1093/nar/gkab1062>

Chapter 6

Summary, final remarks and future work



The present PhD thesis aims to develop and optimize collection and dissolution systems for orally inhaled drug products, both in a quality control (QC) perspective, with strategies based on pre-existing compendial methodologies, and in a biorelevant performance prediction perspective, with the application of a newly developed breath simulator coupled with a biorelevant dissolution system. The main conclusions of this work are presented in the present section by addressing the two thesis objectives stated in Chapter 1:

- i) Evaluating the differentiation capability and applicability of dissolution compendial methods designed to other dosage forms in combination to cascade impactors as possible QC or screening tools.

Within the strategies based on pre-existing compendial methodologies, the paddle over disk apparatus (USP apparatus II) coupled with the next generation impactor (NGI) for particle collection was considered as a starting point for method development. When applied, it successfully differentiated dissolution kinetics of carrier-free from carrier-based formulations of fluticasone propionate (FP), with the carrier-free formulation showing a significantly faster dissolution rate. The main limitation of the strategy was the dependency of the dissolution kinetics to the amount of collected FP – a decrease of dissolution rate was obtained for higher doses of collected FP, which is in accordance with the literature observations. The proposed explanation is a local concentration of FP in the dissolution media surrounding the collected powder, due to the disposition in powder hotspots caused by the NGI stage nozzles. To minimize the impact of local concentration, variations of NGI collection strategy were attempted, but ultimately the dose dependency limitation could not be eliminated while maintaining the dissolution set-up (selected medium and membrane). Although the obtained results render the methodology relevant for formulation screening as much as the identified critical method parameters are controlled, further work should be performed to better understand the system dynamics and minimize the dose limitation. These include studying the impact of the selected membrane, considering both the type and porosity, and the dissolution media, in specific, the type and concentration of surfactant. It is important to bear in mind the present strategy has the benefit of being simple and straightforward, but it is a far stretch from simulating lung environment, on both particle deposition and dissolution. Additionally, it is limited by the collection of powder fractions within an aerodynamic particle size (defined by the NGI stage), and thus requiring several dissolution assessments to have a complete picture of the totality of powder reaching the lung surface. In conclusion, it is well suited for formulation

screening at early stages of development or as a QC tool throughout manufacturing batches, but further development should be considered which can be specific for each drug substance (DS) and formulation.

The paddle over disk (POD) combined with the fast-screening impactor (FSI) as an alternative to the NGI was tested aiming to overcome the previously listed limitations. The FSI collects the totality of the fine particle dose as homogeneously dispersed powder on a glass fiber filter. The powder homogeneous disposition as well as the presence of the filter lead to better wettability and diffusion, thus eliminating dose dependency for carrier-based FP formulations in the studied ranges, while maintaining a sample preparation reproducibility. The methodology was validated by testing a second DS with a higher water solubility, salmeterol xinafoate (SX), aiming to assess the applicability of the method by proving the repeatability and uniformity of cascade impactors as a dose collection method, and by evaluating the impact of the cascade impactor (NGI vs FSI), collected dose, formulation, and dissolution media on the generated dissolution profiles. The results led to believe the POD apparatus is not suitable to differentiate carrier-based formulations of high solubility crystalline DS; but also proved one of the main limitations of the POD system was overcome by using the FSI – the dose dependency. This novel approach with the FSI as a collection method is an upgrade of the previous one, but being newly developed, requires significant and time-consuming sample handling (filter punching placement on the dissolution disk manually) which should be minimized in future work by the design of a more automated system for sample preparation. Moreover, although the use of the FSI as a collection method showed to be somewhat more biorelevant than the NGI, considering it collects the entirety of the fine particle fraction in a dispersed manner, the overall methodology can be further adapted towards a more biorelevant method, such as (i) the use of impactor inlets that simulate the human upper airway anatomy (e.g. Alberta Idealized Throat) to collect a more biorelevant powder fractions, or (ii) change dissolution medium composition to better mimic the *in vivo* lung fluid. It is important to note that the suggested alterations could lead to a more complex system slightly closer to the lung dissolution, but even to with a very different environment – significantly higher particle density due to the small dissolution area in comparison with the lung absorption surface (~100 m²), and a stirring fluid instead of a stagnant and thin lining fluid. Considering this, we also propose the use of the paddle over disk couples with the FSI as an initial screening and QC dissolution assessment.

An analytical quality by design (AQbD) approach was implemented to yet another new collection/dissolution combination - USP apparatus IV, flow-through system, with the FSI - allowing a

deeper and structured understanding of the system variables' impact on dissolution. The USP apparatus IV set-up promotes a direct contact between the DS and dissolution medium, eliminating the impact of membrane diffusion, thus having as output real dissolution kinetics. The flow-through system coupled with AQB approach proved itself a better QC solution, with easily controlled method parameters with a clear impact on dissolution profiles. However, local saturation phenomena might have impacted some of the dependencies observed, and the sample preparation can be further improved to ensure the dissolution cell is completely filled upon dissolution initiation. Moreover, future work should include testing the system with different formulations and DS to assess differentiation powder.

- i) Optimization and testing of a biorelevant collection and dissolution/absorption system with potential for IVIVC by differentiating micronized and formulated DS following different particle engineering and formulation approaches.

Considering the biorelevant performance prediction perspective, the breath simulator PreciseInhale® coupled with a biorelevant dissolution/absorption system, DissolvIt®, were studied. PreciseInhale® was optimized within the scope of the present thesis by adding a pre-separator (PS) impactor stage, intended to mimic the NGI PS aerodynamic particle size cut-off, and thus prevent coarser particles, expected to deposit in the upper respiratory tract to the dissolution system. The presence of the PS resulted in a significant impact on the particle deposited microstructures upon actuation, as on the dissolution results obtained, suggesting the importance of having a biorelevant particle collection system prior to dissolution. Future work should include the design of PSs calibrated for different flow-rates, at the moment only designed for 40 L/min, to achieve optimal pressure drops for different inhalers and thus increase powder de-agglomeration and to better mimic the deposition of a fine particle fraction of an DS in the real lung.

Following the collection system optimization, the application of the biorelevant collection and dissolution system to the characterization and comparison of carrier-based and carrier-free formulations with a commercial DPI showed how deposition characterization and dissolution testing can be an essential tool to both optimize an innovator DPI and de-risk generics development – the particle engineering technology employed to micronize the crystalline FP has a significant impact on the deposition structured generated upon actuation, and as a consequence on the dissolution kinetics obtained. Moreover, the presence of lactose in the generated microstructures increased dissolution rates of FP, and the formulation as a carrier-free solid dispersion led to a 3-fold faster dissolution rate. These

observations were validated doing a similar assessment for SX carrier-based formulations, proving to be a highly differentiating method even for fast dissolving DS. One of the main advantages of the DissolvIt® system is the generation of a pharmacokinetic-like dissolution profile, including parameters such as maximum perfusate concentration, time of maximum concentration and area under the curve, which have been used in the literature as input parameters for physiologically based pharmacokinetic (PBPK) modelling of the tested drug substances, towards establishing *in vitro* / *in vivo* predictive performance correlations. Therefore, the results and observations of the present PhD thesis render the PreciseInhale® and DissolvIt® systems suitable for (i) formulation selection in later stages of pre-clinical or early clinical development, aiming to adjust therapeutic effect based on biorelevant dissolution parameters, and (ii) for maximizing the chances of therapeutic equivalence during generic development. Following the present PhD work focused on biorelevant collection and dissolution/absorption systems, *in vivo* data should be generated with the tested formulations in order to confirm the predictability powder of the described methodologies.